A Multi-Faceted Approach to Carbon Mineralization Advancement

by

Caleb Michael Woodall

B.Sc., The University of Arkansas, 2017

A Dissertation Submitted in Partial Fulfillment of the Requirements for the Degree of

Doctor of Philosophy

in

Chemical Engineering

at

Worcester Polytechnic Institute

Worcester, Massachusetts, USA

By

March 2021

APPROVED

Dr Jennifer Wilcox, Academic Advisor
Department of Chemical Engineering,
Worcester Polytechnic Institute

Dr Nikolaos K. Kazantzis, Committee Member
Department of Chemical Engineering,
Worcester Polytechnic Institute

Dr David DiBiasio, Committee Member
Department of Chemical Engineering,
Worcester Polytechnic Institute

Dr Aaron Sakulich, Committee Member
Department of Civil & Environmental Engineering,
Worcester Polytechnic Institute

Dr Gregory Dipple, Committee Member
Department of Earth, Ocean, and Atmospheric Sciences
University of British Columbia

Dr Susan Roberts, Department Head
Department of Chemical Engineering,
Worcester Polytechnic Institute

This page intentionally left blank.

Dedication

This Dissertation is dedicated to my late brother Noah David Woodall, whom I love dearly and think about every day. May I move forward with my career with his same curiosity and enthusiasm, and have an impact on the world large enough for the both of us.

This page intentionally left blank.

Acknowledgements

First and foremost, none of this work would have been possible without the support of my advisor, Jennifer Wilcox. Four years ago, I could not have imagined the opportunities I would be given to meet incredible people in the climate mitigation field, travel to amazing locations around the world, and complete impactful research. What may prove to be even more valuable are the skills I gained in independent learning, taking initiative, public speaking, networking, productivity, and confidence. All of this is because of your leadership, guidance, and confidence in me, and I could not be more thankful.

Secondly, I must thank my family for their love and support during the past four years, which have certainly been the most challenging of my life. Always knowing you were available to talk and support me means a great deal. To my Dad, Mom, Aaron, Noah, Elizabeth, Becky – thank you and I love you dearly. This gratitude is extended to Katie, who has been a tremendous help with my mental health and stability in the last five months, which have truly brought sorrows deeper than I could have ever imagined with the loss of Noah.

I would like to recognize my lab-mates in the Clean Energy Conversions Lab. Dr. Cyrus Kian and Dr. Hélène Pilorgé, your support in and out of the workspace was invaluable; thank you for providing lifetime friendship. Noah McQueen, your unrivaled work ethic and productivity has consistently helped me push myself to surpass my own limits; thank you for your help and support in the work I've done with and without you. Dr. Simona Liguori, you helped me build the foundation of my research skills in the first year of my Ph.D., and continually provided support during some of the more challenging times of my experience – grazie! Dr. Pete Psarras, I truly enjoyed our conversations we had during the few times our work overlapped, and only wish we were provided more interaction; I wish you luck in your new position at UPenn. And to my lab-mates that joined later in my Ph.D. experience – Dr. Ben Kolosz, Dr. Dan Nothaft, Katherine Gomes, Max Pisciotta, Sam Layding – I enjoyed getting to know you, thank you for the intellectual support, and wish you the best in your continued work in our group.

To the remaining members of my Ph.D. Committee – each one of you proved critical in the completion of my work. Dr. Nikolaos Kazantzis, thank you for your enthusiasm with my work and help in teaching part of your process dynamics course. Dr. Aaron Sakulich, your course on cement chemistry and concrete corrosion was invaluable for my understanding of the intricacies involved with the construction industry. Dr. David DiBiasio, thank you for guiding me in developing youth education materials. And last but certainly not least, Dr. Greg Dipple, thank you for your support in all things related to mineralogy and mine tailings!

A big thank-you must be extended to the collaborators at University of British Columbia, who helped me establish a firm foundation in geochemistry and mineralogy, and helped me collect the experimental results in Chapter 2. Dr. Greg Dipple, thank you again for your guidance in my work throughout my Ph.D. Xueya Lu, Dr. Connor Turvey, Fran Jones, Katrin Steinpórsdóttir, and the rest of Greg's group, thank you so much for your help.

The experimental work in Chapter 3 was done with the help of Noah McQueen and Ethan Simmons at the Colorado School of Mines. Thanks to both of you for braving my first experience in leading research experiments and all the troubleshooting that came with it. Additionally, thanks to Community Energy, Inc. for funding work with Sibanye-Stillwater and for acquiring the tailings samples; namely David Richardson, with whom I really enjoyed conversating about work and life.

The work in Chapter 4 was done in Magdeburg, Germany, with the collaboration of the Max Planck Institute and Otto von Guericke University. Thank you to Professor Kai Sundmacher for your support and guidance, Dr. Andreas Voigt for your guidance and kindness in welcoming me to Germany, Martin Uxa for your help around the lab and arranging instrument times, and Anne Christin Reichelt for your patience in analyzing all of the ion chromatography samples I generated.

The technoeconomic analysis tool presented in Chapter 5 was funded by the Prime Coalition. Thanks to Johanna Wolfson for commissioning the tool and giving me this great learning opportunity, and to James DeCunzo for help in guiding the tool's functionality.

Another thank-you must be given to my lab-mates and co-authors of the utilization review presented in Chapter 6. Noah McQueen, thank you for your help in writing Section 2.1, and Dr. Hélène Pilorgé, thank you for support in proofreading, graphics, and concepts.

Perhaps my favorite chapter of this Dissertation, Chapter 7 would not be possible without the support of ClearPath Inc. Thank you to the ClearPath team for giving me the opportunity to be your first Summer Fellow, and allowing me to experience a different side of advancing climate mitigation technology in the policy sphere. A special thanks goes to Justin Ong, who acted as my mentor throughout my fellowship and gave me unyielding support and guidance.

The youth outreach portion of my Dissertation, Chapter 8, was ever-evolving due to complications with COVID-19 in 2020, but I'm happy with its final form in a paper published in "Frontiers for Young Minds." Thanks to Dr. David DiBiasio and Dr. Kristin Boudreau for your guidance in developing education materials, and to Bella Piccione and Michela Benazzi for your help in writing the paper – especially to Bella for the incredible illustrations you made!

Finally, I must give recognition to past instructors who helped build the foundation of my work ethic and education. I must start with those at North Little Rock High School – Karla Whisnant, Katie Vandiver, Lisa Doss, Mary Beth Cox, Bruce Maddox, Hannah Smith; all of you played an essential role in my early educational development. At the University of Arkansas College of Engineering, I must acknowledge Dr. Ed Clausen, Dr. Jeremy Herman, Dr. Christa Hestekin, Dr. Greg Thoma; my appreciation continues to grow for the chemical engineering "tool belt" you gave me, as new and unique applications continue to appear for the various tools I accumulated over the years from you. Erick Specking, your mentorship over three years of working for you is unmatched, and I cannot thank you enough. At the Colorado School of Mines, my instructors Dr. Carolyn Koh, Dr. Ning Wu, Dr. Diego Gomez-Gualdron, and Dr. Sumit Agarwal; you all gave me shinier, more advanced tools to add to my collection, and I am truly grateful. Finally, Dr. Kevin Cash – your introduction to research course was the most helpful course in all of my Ph.D. coursework. Thank you for giving me an excellent foundation of literature review, research presenting, and proposal writing.

Abstract

The levels of carbon emissions in our atmosphere due to a dependence on fossil energy calls for swift action to prevent potentially devastating impacts of climate change. Along with a transition away from fossil energy sources, climate models call for capture of CO_2, both at the source of emissions and directly from the ambient air. In both cases, a safe method to permanently store the CO_2 is required so that the CO_2 is not re-emitted.

Carbon mineralization can capture and permanently store CO_2 in the form of carbonate minerals by reacting it with alkalinity (i.e., Mg or Ca). The alkalinity can be found in abundant silicate minerals (e.g., olivine, serpentine, plagioclase feldspar), wastes from industrial or mining practices (e.g., steelmaking slags, mine tailings), or geologic formations (e.g., peridotite, basalt). Mine tailings are particularly promising because of their large reactive surface area and because their production is projected to grow by an order of magnitude in the coming century due to increased demand of metals like nickel and platinum for the global energy transition.

In this Dissertation, tailings are studied from Sibanye-Stillwater in Nye, Montana, which produces copper, nickel, and platinum group metals (PGM). The tailings were characterized, revealing that they contain alkalinity distributed in several silicate groups, including tecto-, ino-, and phyllo-silicates. Given this heterogeneous nature, it was determined that mineralization would be more effective if the alkalinity is extracted from the tailings prior to reaction with CO_2. Three methods were used to extract the alkalinity from the tailings. At ambient conditions, < 3% of Ca and < 1% Mg were extracted, indicating that a process with elevated conditions would be necessary to increase alkalinity extraction. Other processes used were the Alternative ÅA Route and the pH swing process, which extract alkalinity through a thermal reaction with ammonium sulfate and through acidic dissolution, respectively. Using these two processes, top extraction efficiency values ranged 40-81% for Mg and 4-14% for Ca. Extraction of Ca was limited primarily due to the restrictive tectosilicate structure of anorthite, which holds nearly 80% of the Ca in the tailings. Several suggestions for future work are made, which could increase the extraction of Ca while decreasing the consumption of reagents and cost of equipment.

A technoeconomic analysis tool was developed to evaluate and compare a variety of carbon mineralization processes. When the tool was used to compare the processes used in this Dissertation, the Alternative ÅA Route was revealed to be more economical than the pH swing at the conditions tested. Despite extracting more Mg, pH swing process economics suffered from high equipment costs, as mineral acids like sulfuric acid require corrosion-resistant equipment, and organic acids like citric acid require longer dissolution times and thus larger equipment volumes. The tool compared the processes optimized in this Dissertation, but removal of simplifying assumptions will be necessary to improve the tool's usability and robustness.

Products of carbon mineralization can be utilized as products in the construction industry. A review of the current state of product utilization reveals that up to three $GtCO_2$ could be avoided if all alkaline feedstock was converted. Further an analysis shows that more than two-thirds of emissions in the U.S. concrete industry could be avoided by decarbonization technologies and techniques, including the use of carbon mineralization products. However, additional research is still needed

to demonstrate reliability of the new, relatively unproven products, and government policies are needed to revise outdated regulations that limit innovation in construction materials. It is suggested that public funding should be allocated to researching these areas. To help motivate and enhance understanding of carbon mineralization for policymakers, along with the general public and our youth, a high-level description of the technology has been written.

Table of Contents

1. Introduction 1
- 1. Carbon Mineralization Problems Worth Solving 1
  - 1.1. Introducing Carbon Mineralization 1
  - 1.2. Sibanye-Stillwater Mine Tailings: A Model for Broad Impact 2
  - 1.3. Related Problems on Multiple Scales 2
- 2. Research Objectives 3
- 3. Organization of Dissertation 3
- References 4

2. Characterization and Reactivity Analysis of PGM Tailings 7
- Abstract 7
- 1. Introduction 8
- 2. Materials & Methods 9
  - 2.1. Samples 9
  - 2.2. Characterization Experiments 10
  - 2.3. Flow-Through Dissolution 10
  - 2.4. Disk Carbonation 12
- 3. Results 13
  - 3.1. Characterization Experiments 13
    - 3.1.1. Characteristics of mine tailings 13
    - 3.1.2. Composition of tailings ponds 15
  - 3.2. Flow-Through Dissolution 17
  - 3.3. Disk Carbonation 19
- 4. Discussion 21
  - 4.1. Significance of Results 21
  - 4.2. Opportunity for Climate Impact 22
- References 23

3. Optimizing Carbon Mineralization with PGM Tailings via Thermal Cation Extraction 27
- Abstract 27
- 1. Introduction 28
- 2. Materials & Methods 30
  - 2.1. Materials 30
  - 2.2. Methods 31
- 3. Results 32
  - 3.1. Standard Deviation of Initial Temperature Trials 32
  - 3.2. Effect of Reaction Temperature 32
  - 3.3. Effect of Heat Ramp 33
  - 3.4. Effect of Reaction Time 34
  - 3.5. Effect of Water Presence 34
  - 3.6. Effect of Reagent Ratio 35
- 4. Discussion 36
  - 4.1. Review of Results 36
  - 4.2. Recommendations for Future Work 38
- References 39

4. Optimizing Carbon Mineralization with PGM Tailings via Acidic Cation Extraction 41
Abstract 41
1. Introduction 42
2. Materials & Methods 43
2.1. Materials 43
2.2. Methods 44
3. Results 46
3.1. Comparison of Organic and Mineral Acids 45
3.2. Effect of Time in Organic Acid Dissolution 47
3.3. Effect of Solid/Liquid Ratio 50
3.4. Series and Parallel Dissolution for Increased Efficiency 52
3.4.1. Parallel dissolution with organic acids 53
3.4.2. Series dissolution with organic acids 54
3.4.3. Series dissolution with mineral acids 55
4. Discussion 57
4.1. Estimating Tail 2a Dissolution Rates 57
4.2. Relating Dissolution Mechanisms and Mineral Phases 58
4.3. Problems with Carbonation 60
5. Conclusions and Recommendations 62
5.1. Results Summary and Climate Context 62
5.2. Recommendations for Future Work 62
References 65
5. Technoeconomic Analysis of Alkalinity Extraction Methods 69
Abstract 69
1. Introduction 70
2. Methodology 70
3. Economic Analysis of Scenarios in Previous Dissertation Chapters 73
3.1. Thermal Alkalinity Extraction – Effect of Reaction Temperature on Costs 73
3.2. Acidic Alkalinity Extraction – Effect of Solid/Liquid Ratio on Costs 74
3.3. Acidic Alkalinity Extraction – Effect of Sulfuric Acid Concentration on Costs 75
3.4. Acidic Alkalinity Extraction – Citric vs Sulfuric Acid Solutions 76
3.5. Comparison of Thermal and Acidic Alkalinity Extraction 78
4. Discussion of Carbon Mineralization Methods for Sibanye-Stillwater Tailings 79
4.1. *Ex-situ* Methods – Performance and Improvements 79
4.2. Ex-situ vs Surficial Carbon Mineralization 80
5. Future Improvements to the Tool 80
References 82

6. Utilization of Carbon Mineralization Products – Current State and Potential 85
Abstract 85
1. The Role of Carbon Mineralization in Mitigating Climate Change 86
1.1. Carbon Mineralization and Market Potential 87
2. Overview of Carbon Mineralization Processes 88
2.1. Challenges with Alkalinity Extraction 88
2.1.1. Mechanical Activation 88
2.1.2. Chemical Activation – Acid Extraction 89
2.1.3. Chemical Activation – Salt Extraction 90
2.1.4. Thermal Activation 90
2.2. Challenges with the Carbonation Step 90
2.2.1. Considerations with CO_2 91
2.2.2. Passivating Product Layer 91
2.2.3. Product Selection 92
2.3. Areas for Further Research 93
3. Alkalinity Available for Carbon Mineralization 93
3.1. Industrial Alkalinity Sources 93
3.1.1. Current markets and potential growth 94
3.2. Mined Alkalinity Sources 95
4. Marketable Products of Carbon Mineralization 96
4.1. Analysis of Current Commercial Efforts 96
4.2. Proposing New Products 99
4.2.1. Precipitated Calcium Carbonate 99
4.2.2. Magnesia Cements 100
4.2.3. Flame-retardant Fillers 100
4.2.4. Utilization of Silica Byproduct 101
5. Outlook for CCUS with Carbon Mineralization 101
References 103
7. Policy Recommendations for Decarbonization in Concrete and Pavements 113
Abstract 113
Executive Summary 114
1. Introduction – Reducing Emissions from Concrete and Pavements 115
1.1. Concrete and Pavement Terms Defined 115
2. Decarbonization Opportunities 118
2.1. Carbon Capture at Cement Plants 118
2.2. Alterations to Concrete and Asphalt Mixtures 121
2.3. Synthesizing New Materials with Stored CO_2 123
3. Summary of Options 127
4. Recommendations 129
References 130
8. Description of Carbon Mineralization for Young Minds and Non-Scientists 133
Abstract 133
1. Why is CO_2 Harmful, and What Can Be Done? 134
2. What are Carbonate Minerals? 134
3. How Does Carbon Mineralization Work? 135
4. What Can We Do with the Carbonate Products? 136

5. How Developed is this Technology? 137
6. Carbon Mineralization in the Ocean 137
7. How Can You Get Involved? 137
Glossary 138
References 138
9. Conclusions and Recommendations for Future Work 139
1. Conclusions 139
2. Recommendations for Future Work 140
2.1. Carbon Mineralization with PGM Tailings 140
2.2. Technoeconomic Analysis Tool 141
2.3. Carbon Mineralization Product Utilization 141
2.4. Government Policy 141
2.5. Youth Engagement 141
Appendix 143
Chapter 2 143
Sample Homogenization 143
Sample Micronization 144
Photos of Instruments and Equipment 145
Chapter 3 148
Photos of Furnace and Samples 148
Chapter 4 149
Photos of Equipment, Residues, and Products 149
Chapter 5 153
Screenshots of Tool 153

Chapter 1

Introduction

1. Carbon Mineralization Problems Worth Solving

1.1 Introducing Carbon Mineralization

The increasing atmospheric concentration of CO_2 due to anthropogenic emissions brings about the need for new investments in combating global climate change. Recent studies emphasize the need to capture point-source carbon emissions from the energy and industrial sectors, and even directly from ambient air [1]–[3]. This method of climate mitigation, termed carbon capture and storage (CCS), has been developed and implemented globally [4]. However, a common problem among most CCS projects is access to safe and reliable storage. One technology that combines capture and storage is carbon mineralization, where CO_2 is reacted with alkalinity and is permanently stored in the form of carbonate minerals. The general carbon mineralization reaction is shown in Equation 1, where M is a divalent metal cation, Mg or Ca.

$$MO + CO_2 \rightarrow MCO_3 \quad (1)$$

The basic requirements for carbon mineralization are CO_2 and alkalinity. Sources of CO_2 could be ambient air, industrial flue gas, or concentrated streams from CCS or direct air capture technology. A portfolio of alkaline feedstock exists, broadly described by materials rich in Mg or Ca. Mineralization can be performed *ex-situ* with mined silicate minerals (e.g., olivine, serpentine, anorthite) or wastes from industrial and mining processes (e.g., steelmaking slags, mine tailings), or it can be performed *in-situ* in geologic formations (e.g., basalt, peridotite). Alternatively, surficial mineralization can be performed (i.e., on the surface of wastes at the waste storage facility) [5]. Alkalinity sources are expanded upon in a literature review in Chapter 6 of this Dissertation.

Seifritz first proposed the concept of carbon mineralization in 1990 [6], and this was further explored by Lackner in the following decade [7], [8]. At the time, the technology was more often referred to as mineral carbonation, but carbon mineralization has become the more universal term [9]. As research slowly developed, two primary *ex-situ* process routes emerged. One process, termed direct mineralization, involves reacting CO_2 *directly* with the alkalinity source. This simple one-step process works for highly alkaline feedstock, but the presence of undesired species limits overall conversion and product purity. An alternate process involves converting the alkalinity to a more reactive form before carbonation, thus *indirectly* reacting the alkalinity source with CO_2. Through indirect mineralization, undesired material initially present in the feedstock is removed to produce a higher-purity product.

There is a variety of methods to extract alkalinity among indirect carbon mineralization processes, including mechanical, chemical, and thermal extraction. Mechanical extraction increases the reactive surface area by decreasing particle size to the optimal size of about 75-150 μm [10]. Chemical extraction most often involves the use of acidic solutions to dissolve the mineral structure. While the use of strong acids has proven most effective [11], they pose economic and

health risks due to corrosivity [12]. Thermal extraction involves the use of high temperatures to break bonds within the alkaline feedstock, typically applied through the dehydroxylation of serpentine [10], [13]–[15]. The choice of extraction method(s) depends on the mineralogy of the alkaline feedstock.

1.2 Sibanye-Stillwater Mine Tailings: A Model for Broad Impact

Sibanye-Stillwater, located in the Beartooth Mountains of Nye, Montana, produces large volumes of copper and nickel, along with its most valuable products, palladium and platinum (i.e., platinum group metals, PGM). In addition to these valuable products, Sibanye-Stillwater produces about one million tonnes of mine tailings each year. Preliminary characterization of these tailings (further described in Chapter 2) indicate that the tailings contain alkalinity that could store CO_2, and the small particle size provides high reactive surface area. However, the tailings mineralogy is heterogeneous, presenting a variety of silicate structures that must be dissolved to maximize the CO_2 storage potential.

Tailings from mines like Sibanye-Stillwater will become increasingly prevalent in the coming decades. The global production of nickel and platinum group metals is currently less than 3 Mt and 0.5 kt per year, respectively [18]. However, several forecasts project these values to increase by an order of magnitude to 25 Mt and 5 kt per year by 2100. This corresponds with an annual production of up to 3.5 Gt of ultrabasic mine tailings [19]. Hence, developing an efficient method of storing CO_2 in the Sibanye-Stillwater tailings could help develop mineralization processes for billions of tonnes of tailings by the end of this century.

1.3 Related Problems on Multiple Scales

Intensification of the carbon mineralization process is often coupled with increases in economic costs. These added costs may be offset by utilizing the produced carbonates as products within the construction industry [12], [20], [21], or through government tax incentives like 45Q [22]. Opportunity also exists in the private sector, where there is growing interest in climate mitigation technologies to meet voluntary climate targets [23]. Still, harnessing these opportunities for economic improvement is met with challenges.

Investment decisions on new carbon mineralization projects are clouded by difficulties in economic evaluation. A variety of alkalinity sources are available for carbon mineralization, where different mineral structures bring drastic differences in reactivity. Process configuration is also a variable, including one-step and multi-step *ex-situ* processes, surficial processes, and *in-situ* processes [5]. These variances are further exacerbated by differences in mineral products – as several carbonate minerals can form depending on conditions, affecting whether they may be sold as building products [12], or if they are intended to be left on the ground. A method to help evaluate the economics of mineralization processes could solve this issue.

Despite the availability of tax incentives like 45Q that can aid in financing the utilization of mineralization products, market penetration into the construction industry is still hindered. In most cities and localities, producing green construction materials is inhibited by restrictive regulations on concrete mixtures. Further, manufacturers are reluctant to use new construction materials due

to high costs and uncertainties in long-term performance properties. Government action could help to overcome these barriers.

Despite the potential positive climate impacts of CCS, public awareness of the technology is lacking around the world [24], [25]. Public opinion has an important impact on government policy [26], which impacts the development of government incentives and tax credits critical to improving the economics of CCS technologies like carbon mineralization. In addition to the desire to increase public acceptance of CCS technology, the improvement of public communication and education is motivated by a need to increase human capital. Investment in human capital development (i.e., a more well-educated populous) leads to wider economic growth [27]. An approach to the improvement of public education and communication on CCS is to disseminate information to our youth.

2. Research Objectives

The research detailed in this Dissertation was undertaken with the aim to tackle the problems outlined in Section 1, taking a multi-faceted approach to advancing carbon mineralization. The research objectives of this work are:

1. Characterize the Sibanye-Stillwater tailings based on their chemical and mineralogical composition, particle size, and reactive surface area.
2. Develop an *ex-situ* carbon mineralization process suitable for the Sibanye-Stillwater mine tailings.
3. Develop a tool that can evaluate a variety of *ex-situ* carbon mineralization processes.
4. Evaluate the process economics of the carbon mineralization process(es) developed for the Sibanye-Stillwater mine tailings.
5. Review the current state and potential of utilizing carbon mineralization products in the construction industry.
6. Develop policy recommendations that can help advance the utilization of carbon mineralization products in the construction industry.
7. Develop materials that can educate youth and the general public on carbon mineralization.

3. Organization of Dissertation

This Dissertation is separated into nine chapters. The current chapter has broadly introduced the scope of challenges to carbon mineralization that will be addressed in the proceeding chapters. In Chapter 2, the Sibanye-Stillwater tailings are characterized, and an early assessment of their reactivity at ambient conditions is performed. In Chapters 3 and 4, two *ex-situ* processes are employed in an attempt to maximize alkalinity extraction from the Sibanye-Stillwater tailings. Chapter 5 introduces an Excel-based technoeconomic analysis tool, which is subsequently used to evaluate the *ex-situ* processes used in the two preceding chapters. Chapter 6 contains a review of carbon mineralization in general, along with a review and analysis of the current state and potential of utilizing carbon mineralization products in the construction industry. This is followed by Chapter 7, where policy recommendations are developed that can more broadly advance decarbonization methods in the concrete and pavement industries. In Chapter 8, carbon mineralization is summarized and described at a higher level for young readers and non-scientists. Finally, conclusions and recommendations for future work are detailed in Chapter 9.

References

[1] IPCC, "IPCC special report on the impacts of global warming of 1.5 °C - Summary for policy makers," William Solecki, 2018.

[2] National Academies Press, *Negative Emissions Technologies and Reliable Sequestration*. 2019.

[3] The Royal Society, *Greenhouse gas removal*. 2018.

[4] J. Yan and Z. Zhang, "Carbon Capture, Utilization and Storage (CCUS)," *Appl. Energy*, vol. 235, pp. 1289–1299, 2019.

[5] P. B. Kelemen, N. McQueen, J. Wilcox, P. Renforth, G. Dipple, and A. P. Vankeuren, "Engineered carbon mineralization in ultramafic rocks for CO2 removal from air: Review and new insights," *Chem. Geol.*, vol. 550, no. 119628, May 2020.

[6] W. Seifritz, "CO_2 disposal by means of silicates," *Nature*, vol. 345, no. 6275, p. 486, 1990.

[7] K. S. Lackner, C. H. Wendt, D. P. Butt, E. L. Joyce, and D. H. Sharp, "Carbon dioxide disposal in carbonate minerals," *Energy*, vol. 20, no. 11, pp. 1153–1170, 1995.

[8] K. S. Lackner, "Carbonate Chemistry for Sequestering Fossil Carbon," *Annu. Rev. Energy Env.*, vol. 27, pp. 193–232, 2002.

[9] I. M. Power *et al.*, "Carbon Mineralization: From Natural Analogues to Engineered Systems," *Rev. Mineral. Geochemistry*, vol. 77, no. 1, pp. 305–360, 2013.

[10] A. Sanna, X. Wang, A. Lacinska, M. Styles, T. Paulson, and M. M. Maroto-Valer, "Enhancing Mg extraction from lizardite-rich serpentine for CO_2 mineral sequestration," *Miner. Eng.*, vol. 49, pp. 135–144, Aug. 2013.

[11] S. Teir, H. Revitzer, S. Eloneva, C.-J. Fogelholm, and R. Zevenhoven, "Dissolution of natural serpentinite in mineral and organic acids," *Int. J. Miner. Process.*, vol. 83, no. 1–2, pp. 36–46, Jul. 2007.

[12] C. M. Woodall, N. McQueen, H. Pilorgé, and J. Wilcox, "Utilization of Mineral Carbonation Products: Current State and Potential," *Greenh. Gases Sci. Technol.*, 2019.

[13] M. J. McKelvy, A. V. G. Chizmeshya, J. Diefenbacher, H. Béarat, and G. Wolf, "Exploration of the role of heat activation in enhancing serpentine carbon sequestration reactions," *Environ. Sci. Technol.*, vol. 38, no. 24, pp. 6897–6903, 2004.

[14] M. Werner, S. B. Hariharan, A. V. Bortolan, D. Zingaretti, R. Baciocchi, and M. Mazzotti, "Carbonation of activated serpentine for direct flue gas mineralization," in *Energy Procedia*, 2013, vol. 37, pp. 5929–5937.

[15] S. J. Gerdemann, W. K. O'Connor, D. C. Dahlin, L. R. Penner, and H. Rush, "Ex Situ Aqueous Mineral Carbonation," *Environ. Sci. Technol.*, vol. 41, no. 7, pp. 2587–2593, Apr. 2007.

[16] S. Lavikko and O. Eklund, "The role of the Silicate Groups in the Extraction of Mg with the ÅA route method," *J. CO2 Util.*, vol. 16, pp. 466–473, Dec. 2016.

[17] F. K. Crundwell, "The mechanism of dissolution of minerals in acidic and alkaline solutions: Part II Application of a new theory to silicates, aluminosilicates and quartz," *Hydrometallurgy*, vol. 149, pp. 265–275, 2014.

[18] U.S. Geological Survey, *Mineral commodity summaries 2020*, no. 703. 2020.

[19] P. Renforth, "The negative emission potential of alkaline materials," *Nat. Commun.*, vol. 10, no. 1401, 2019.

[20] C. Hepburn *et al.*, "The technological and economic prospects for CO_2 utilization and removal," *Nature*, vol. 575, no. 7781, pp. 87–97, 2019.

[21] National Academies Press, *Gaseous Carbon Waste Streams Utilization: Status and Research Needs*. 2019.

[22] Energy Futures Initiative, "Advancing Large Scale Carbon Management: Expansion of the 45Q Tax Credit," no. May, 2018.

[23] N. C. Partners, "Deeds Not Words: The Growth of Climate Action in the Corporate World," no. September, 2019.

[24] A. Saito, K. Itaoka, and M. Akai, "Those who care about CCS-Results from a Japanese survey on public understanding of CCS-," in *14th Greenhouse Gas Control Technologies Conference Melbourne 21-26 October 2018 (GHGT-14)*, 2018.

[25] S. Perdan, C. R. Jones, and A. Azapagic, "Public awareness and acceptance of carbon capture and utilisation in the UK," *Sustain. Prod. Consum.*, vol. 10, pp. 74–84, Apr. 2017.

[26] B. I. Page and R. Y. Shapiro, "Effects of Public Opinion on Policy," *Am. Polit. Sci. Rev.*, vol. 77, no. 1, pp. 175–190, 1983.

[27] S.-L. Hsu, "Human Capital in a Climate-Changed World," in *Forthcoming in Climate Change and Its Impacts: Risks and Inequalities (C. Murphy, P. Gardoni & R. McKim, eds.), FSU College of Law, Public Law Research Paper No. 871*, 2018.

[28] N. Onishi, N. Tatsumi, S. Nakamura, and Y. Aoki, "Development of Educational Materials and Programs for Public Outreach of CCS," in *14th Greenhouse Gas Control Technologies Conference Melbourne 21-26 October 2018 (GHGT-14)*, 2018.

This page intentionally left blank.

Chapter 2

Characterization and Reactivity Analysis of PGM Tailings

Abstract

The urgency for climate action calls for serious management of past, current, and future CO_2 emissions, including development and deployment of methods to capture and securely store CO_2. Through carbon mineralization, CO_2 can be permanently stored in calcium- and magnesium-bearing mine tailings, simultaneously managing two wastes: CO_2 and mine tailings. Tailings samples from the Sibanye-Stillwater mine in Nye, Montana have been characterized, revealing that they primarily contain Ca-bearing plagioclase feldspar. Evidence of total inorganic carbon in the tailings and ion concentration in the tailings ponds suggests carbonation has taken place at ambient conditions. Two mineralization experiments (flow-through leaching and disk carbonation) were performed, revealing that less than 1% of the calcium within the tailings is labile, or easily released from silicate structures at ambient conditions. The Sibanye-Stillwater tailings could be useful for developing strategies of waste management as production of nickel and PGM minerals increase, but further work is needed to realize their full carbon storage potential. The majority of this chapter has been submitted for publication to the journal *Minerals* under the title "Carbon Mineralization with PGM Mine Tailings – Characterization and Reactivity Analysis."

List of Abbreviations

- BET - Brunauer-Emmett-Teller (reactive surface area)
- ICP-OES – Inductively coupled plasma optical emission spectroscopy
- PGM – platinum group metals
- QXRD – Quantitative X-ray diffraction
- PEEK – polyetheretherketone
- PTFE – polytetrafluoroethylene
- TCA – total carbon analysis
- TIC – Total inorganic carbon
- Wt. % – weight %
- XRD – X-ray diffraction
- XRF – X-ray fluorescence (spectroscopy)

1. Introduction

Climate mitigation efforts are accelerating to avoid a 2 ^{o}C increase in the average global temperature by 2100. Considerable progress has been made in decarbonizing the power sector, where US renewable electricity generation has doubled from 2008 to 2018 [1]. However, the potential climate impact of a global energy transition is currently limited for multiple reasons. Carbon-free power does not address "hard-to-avoid" emissions, like those in the industrial sector which result from chemical reactions involved in the production of commodities like cement and steel. Further, the global energy transition will require increases in mineral production by up to 900% in the electric sector, coupled with sharp increases in production of mine wastes [2].

To address the problem of "hard-to-avoid" emissions, technologies are being developed and deployed that can capture CO_2 from industrial flue gases [3] or remove CO_2 directly from the air [4]. Both of these technologies require a method of safe and reliable storage to prevent the CO_2 from being re-emitted. Carbon mineralization describes a set of technologies that react CO_2 with alkaline material to produce solid carbonate minerals, satisfying the need for safe and permanent CO_2 storage.

Sources of alkalinity for carbon mineralization feedstock are comprised of magnesium or calcium silicates, of which the availability in Earth's crust is estimated to be on the order of 10^8 to 10^{11} tonnes of rock [5]. Among the most reactive minerals are wollastonite, olivine, and brucite, along with fibrous serpentines like asbestiform chrysotile [5]. Another potential source is alkaline wastes produced by industrial processes (e.g., coal fly ash, iron and steel slag) and mining operations (e.g., diamond and nickel mine tailings) [6]. These wastes are produced on an annual basis on the order of hundreds of millions of tonnes per year. Further, their particle sizes are typically on the order of 10-100 microns, which presents sufficient reactive surface area to avoid energy-intensive size reduction.

Sibanye-Stillwater, located in the Beartooth Mountains of Nye, Montana, produces high volumes of copper and nickel, while its most valuable products are platinum and palladium. In addition to its products, the mine generates about 1 Mt of tailings per year. Based on previous work with tailings at nickel mines [7], [8], and platinum-group metal (PGM) mines [9], [10], the Sibanye-Stillwater tailings could present another viable source of feedstock for carbon mineralization. As stated in Chapter 1, wastes from mines like Sibanye-Stillwater will be very relevant in the years to come, as up to 3.5 Gt/year of ultrabasic mine tailings [11] could be generated by 2100 as a result of nickel and PGM mining. Hence, studying the mineralization behavior of the Sibanye-Stillwater tailings could help develop mineralization processes for billions of tonnes of tailings by the end of this century.

In this study, the suitability of PGM tailings for carbon mineralization is assessed by studying those of Sibanye-Stillwater. This was done through observation of the behavior of the Sibanye-Stillwater tailings in the tailings pond at ambient conditions. Several characterization tests were performed to determine physical and chemical traits of the tailings. These tests include laser diffraction particle size analysis, reactive surface area analysis, quantitative powder x-ray diffraction (QXRD), total carbon analysis (TCA), whole rock analysis, inductive coupled plasma

optical emission spectroscopy (ICP-OES), and ion chromatography (IC). Additionally, two experiments were conducted to directly assess the tailings' reactivity for carbon mineralization: flow-through dissolution and disk carbonation.

2. Materials & Methods

2.1 Samples

The Sibanye-Stillwater mine produces two types of non-hazardous solid wastes: tailings and waste rock. About 1 Mt of tailings are generated per year and have been stored at two different tailings storage facilities (Figure 1). The Nye Tailings Storage Facility (referred to here as "Pond 1") was idled circa 2002, and contains about 4 Mt of tailings. Now, tailings are actively being placed in the Hertzler Tailings Storage Facility (referred to here as "Pond 2"), which is 5-6 times larger than Pond 1. It currently contains approximately 15 Mt of tailings, with the capacity for 24 Mt. Additionally, the mine produces about 1 Mt per year of waste rock that has highly variable composition and is stored in piles above ground.

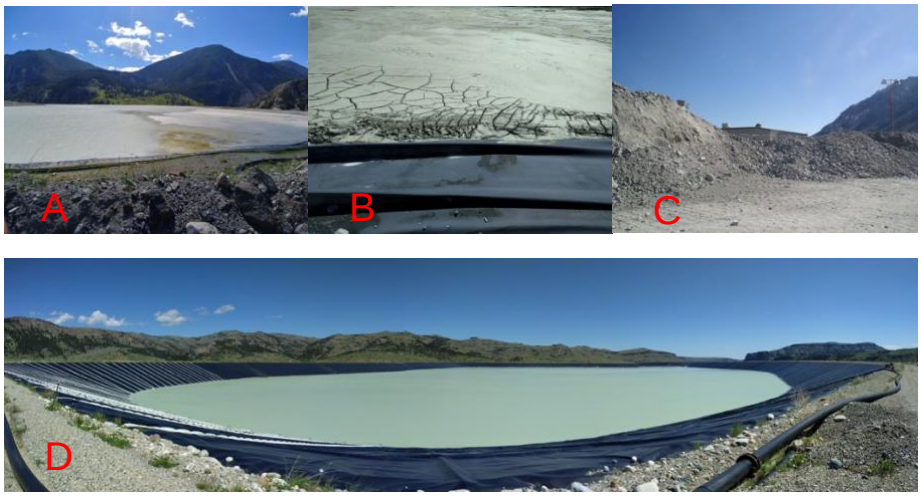

Figure 1: Photos of waste sampling Sites at Sibanye-Stillwater, photographed by Noah McQueen 2019. A: Pond 1, decommissioned; B: Closer photo of Pond 1, showing signs of crust at the pond surface; C: Waste Rock pile; D: Pond 2, which has a large remaining capacity for additional tailings.

Four tailings samples were used for characterization tests, displayed in Table 1 with brief descriptions of each. Information on sample homogenization and micronization is detailed in the Appendix.

Table 1: Mine tailings sample descriptions

Sample	Description
Tail 1	Tailings extracted from Pond 1, received June 2019, suspended in water.
Tail 2a	Tailings extracted from Pond 2, received August 2018, suspended in water.
Tail 2b	Dehydrated fraction of Pond 2 tailings (i.e., "slimes"), received June 2017, dry.
Tail 2c	Top fraction of Tail 2a sample after filtration.

2.2 Characterization Experiments

A Malvern® Mastersizer 2000 laser-diffraction particle-size analyzer was used to determine the particle-size distribution of each of the tailings samples. To minimize particle agglomeration, each sample was suspended in deionized water, stirred prior to analysis, and sonicated during analysis. Multiple measurements were taken for each sample to ensure repeatable results.

The reactive surface area was measured for all samples via multipoint Brunauer-Emmett-Teller (BET) Analysis with N_2 gas adsorption using a Quantachrome® Autosorb-1 Automated Gas Sorption System. Representative aliquots were taken and put into a cell for each tailings sample.

Quantitative powder x-ray diffraction (QXRD) was performed with a Bruker D8 Focus. To achieve quantitative results, corundum (Al_2O_3) was added as exactly 20 wt. % to each solid tailings sample. Following, samples were micronized and then placed in back-mount sample holders. Qualitative phase identification was performed with DIFFRACplus Eva 14 software [12] informed by the International Centre for Diffraction Data PDF-4+ 2010 database. The identified phases were quantified via Rietveld refinement using Topaz Version 5 software.

Total carbon analysis (TCA) was performed to measure the total inorganic carbon (TIC) content of the mine tailings samples. This provided an indication of the amount of CO_2 preexisting in the samples as carbonate. A CM5130 acidification module was used, with a Model CM5014 Carbon Dioxide Coulometer from UIC Inc. The CO_2 Coulometer detection range is <1-10000 µg carbon.

Whole rock analysis by fusion was performed on each sample using X-ray fluorescence spectroscopy (XRF) to determine major element oxide compositions of the Sibanye-Stillwater tailings. This analysis was completed externally at ALS Global Laboratories, North Vancouver, British Columbia.

As Tail 1 and Tail 2a were received wet, the liquid from each tailings sample was analyzed to determine chemical and ionic composition. Chemical composition was measured using a Varian 725-ES inductively coupled plasma optical emission spectrometer (ICP-OES). The instrument's detection limit for each of the elements measured is 0.1 ppm. The ionic compositions of liquids from Pond 1 and Pond 2 were also measured via ion chromatography using a Dionex ICS 2000 ion chromatograph.

2.3 Flow-Through Dissolution

To determine the labile calcium and magnesium cations present in the Sibanye-Stillwater tailings, a flow-through dissolution experiment was performed on Tail 2a using an apparatus shown in Figure 2 and described previously [13], [14]. Prior to the experiment, 10 % CO_2 (Praxair) was equilibrated with deionized water overnight to reach a pH of 4.41. Over a 60-hour period, a Dionex ICS-3000 dual-gradient pump constantly pumped carbonated water at 1 mL/min through a 1.2 mL reaction chamber containing 500 mg of Tail 2a atop a 0.2 µm polycarbonate membrane filter. The experiment was performed at room temperature and pressure (22 ^{o}C, 1.013 bar). A polypropylene Swinnex filter holder was used as the reaction chamber. The weighed sample was loaded into the chamber and shaken to ensure even distribution. The threading of the reaction chamber was wrapped with polytetrafluoroethylene (PTFE) sealant tape to prevent leakage due to increased

pressure. The chamber was mounted vertically between two solenoid valves and above a 0.2 µm syringe filter, which provided secondary filtration to prevent fine particulates from entering entirely metal-free polyetheretherketone (PEEK) flow tubes.

Upon exiting the reaction chamber, the effluent flowed through a pH sensor and subsequently into a Foxy®R1 fraction collector connected with entirely metal-free PEEK flow tubes. The pH sensor measured the effluent pH every second. The fraction collector intermittently collected 13 mL samples over 13-minute periods at 30-minute to 2-hour intervals, and stored the samples in 15 mL polypropylene tubes. When the effluent was not collected for sampling, it was pumped into a waste basin. For quality assurance and quality control, backup pH measurements were taken manually for using a Thermal Orion 4 Star Plus Portable pH meter, which has a measurable pH range of -2 to 19 and precision of ±0.002. After samples were collected, they were acidified with 15 M ultra-pure HNO_3 and stored at ~4 ºC prior to analysis. Samples were analyzed for concentrations of Al, Ca, Fe, K, Mg, Na, and Si with ICP-OES.

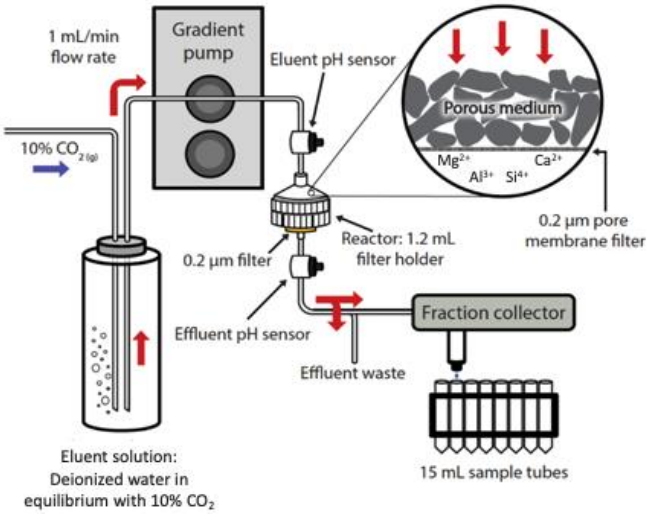

Figure 2: Process flow diagram of lab-scale flow-through leaching apparatus

The dissolution rate of Tail 2a was calculated using 1:

$$R_M(mol\ M\ m^{-2}s^{-1}) = \frac{r_f \Delta_{[M]}}{\eta_M A_{BET} m_0} \quad 1$$

where "M" represents the metal cation being leached, r_f is the carbonated water flow rate (L s^{-1}), $\Delta_{[M]}$ is difference in the effluent and eluent concentration of M (mol L^{-1}), η_M is mineral stoichiometric coefficient of M, A_{BET} is the BET reactive surface area of Tail 2a (m^2 g^{-1}), and m_0 is the initial mass of Tail 2a (g). Results are used to quantify the number of labile cations present in the Sibanye-Stillwater tailings. That is, the number of cations that are loosely bound and can be quickly released at ambient conditions [13]. The dissolution rates and accumulation of dissolved cation in solution is monitored and compared to the dissolution of various minerals, including anorthite, lizardite, diopside, and calcite, shown in Equations 2-5.

$$CaAl_2Si_2O_8 + 8H^+ \rightarrow Ca^{2+} + 2Al^{3+} + 2SiO_2 + 4H_2O \quad (2)$$

$$2Mg_3Si_2O_5(OH)_4 + 5H^+ \rightarrow 6Mg^{2+} + 4SiO_2 + 10H_2O \quad (3)$$

$$CaMgSi_2O_6 + 4H^+ \rightarrow Ca^{2+} + Mg^{2+} + SiO_2 + 2H_2O \quad (4)$$

$$CaCO_3 + 2H^+ \rightarrow Ca^{2+} + CO_2 + H_2O \quad (5)$$

2.4 Disk Carbonation

To assess the tailings' reactivity with ambient CO_2, a disk carbonation experiment was performed within a chamber. This experiment has been described previously [13]. Several small disks (hereafter referred to as "dimes," approximately the size of an American dime) were fabricated of each sample.

Dimes of each tailings sample were composed of dry mine tailings mixed with water in the amount of 15-16 wt. % of the sample mass, targeting the ideal range of 30 % - 60 % pore water saturation as proposed previously [15]. The viscous slurry was mixed in a beaker and subsequently placed in a premade Perspex glass mount with 17.9 mm radius and 1.8 mm thickness. When the mount was filled with the sample slurry, a premade Perspex glass piston press was used to push the sample out of the mount and into a weigh boat, creating a dime. Five to ten dimes were made for each tailings sample, depending on the total amount of sample available. All dime masses were measured within the weight boat before the 16-day testing period.

Once fabricated, dimes were placed in a 60 L polycarbonate reaction chamber. A cylinder of compressed CO_2 (10%) was attached to the chamber using Tygon R 3606 tubing, which directed the gas at ~200 mL min^{-1} a small water bath within the chamber, allowing humidified CO_2 to bubble out into the chamber atmosphere. Sponges were placed within in the chamber to help maintain a relative humidity above 90%, minimizing evaporative water loss from dimes in the reaction chamber. The chamber temperature was maintained at atmospheric conditions (~ 22 ^oC). The chamber temperature and humidity were monitored using a portable HUMICAP® humidity and temperature probe HMP110 from VAISALA. For this probe, humidity and temperature measurements have ranges of 0-100% and -40-80 ^oC, and relative errors of ±1.5% and 0.1 ^oC, respectively. Over a 16-day period, dimes were intermittently removed from the chamber, where the frequency was dependent on the number of dimes fabricated for each sample. The mass of each dime was measured upon its removal from the chamber. After completion of the 16-day period, every dime was homogenized with a corundum mortar and pestle, and subsequently analyzed for total inorganic carbon content. The experimental conditions for each of the Sibanye-Stillwater tailings are given in Table 2.

Table 2: Experimental conditions for disk carbonation

Sample Name	Dime Quantity	Water:Solid Mass Ratio	Initial TIC (%)
Tail 1	7	0.156	0.213
Tail 2a	10	0.156	0.060
Tail 2b	10	0.156	0.051
Tail 2c	10	0.155	0.111

3. Results

3.1 Characterization Experiments

3.1.1 Characteristics of mine tailings

Results from QXRD, TIC, Particle Size Analysis, and BET Reactive Surface Area are detailed in Table 3. Total inorganic carbon is presented as %C (g carbon / g sample).

Table 3: Characteristics of Sibanye-Stillwater tailings: mineral phase abundance (wt. %), total inorganic carbon (TIC), particle size and BET reactive surface area. d(0.9) indicates 90% of the sample tested is below the given particle size

Silicate Group	Mineral Type	Mineral	Tail 1	Tail 2a	Tail 2b	Tail 2c
Tecto- (3-D framework)	Plagioclase Feldspar	**Anorthite** – $CaAl_2Si_2O_8$	36.73%	54.26%	54.27%	35.93%
		Albite – $NaAlSi_3O_8$	3.19%	3.94%	3.69%	5.65%
Ino- (chain)	Pyroxene	**Enstatite** – $(Mg,Fe)Si_2O_6$	10.12%	11.90%	14.74%	4.47%
		Diopside – $CaMgSi_2O_6$	11.49%	9.74%	9.26%	6.54%
	Amphibole	**Tremolite** – $Ca_2Mg_5(Si_8O_{22})(OH)_2$	3.04%	2.24%	2.56%	2.36%
		Cummingtonite – $Mg_7(Si_8O_{22})(OH)_2$	0.44%	1.27%	1.27%	1.16%
Phyllo- (sheet)	Serpentine	**Lizardite** – $Mg_3Si_2O_5(OH)_4$	2.23%	8.41%	6.48%	12.26%
	Clay	**Talc** – $Mg_3Si_4O_{10}(OH)_2$	8.11%	2.27%	2.77%	8.95%
	Mica	**Clinochlore** – $(Mg,Fe)_5Al_2Si_3O_{10}(OH)$	21.74%	5.99%	4.95%	20.57%
N/A	Carbonate	**Calcite** – $CaCO_3$	2.91%	-	-	-
		Hydromagnesite – $Mg_5(CO_3)_4(OH)_2$-$4H_2O$	-	-	-	2.09%
TIC (%C)			0.25%	0.07%	0.06%	0.13%
d(0.9) (μm)			20.79	51.17	60.71	9.75
BET Reactive Surface Area (m^2/g)			3.8	1.29	0.69	11.15

As shown in Table 3, all samples have d(0.9) less than 100 μm, which is generally considered to be optimal for carbon mineralization processes [16], presenting sufficient reactive surface area so that further energy-intensive size reduction is not necessary.

As typical of mine tailings, the composition is heterogeneous, with a variety of mineral structures. The most abundant mineral in all samples is anorthite, an aluminosilicate in the plagioclase feldspar mineral group. While this mineral group is not typically viewed as ideal for carbon

mineralization due to its low reactivity [17], [18], its high abundance (comprising 39 wt. % of Earth's crust [19]) might still present volumes large enough for climate relevance.

The relative abundance of each mineral phase varies across the different tailings samples. Inosilicates (amphiboles and pyroxenes) remain relatively unchanged across all samples. The minerals that have significant differences in abundance among the samples are tectosilicates and phyllosilicates.

Comparison of the mineralogy in Tail 1 and Tail 2a can give insight into what might naturally occur when the Sibanye-Stillwater tailings have been undisturbed in the tailings pond and have interacted with atmospheric CO_2. The talc and lizardite compositions are practically reversed among Tail 1 and Tail 2a; this could be evidence of incongruent lizardite dissolution in alkaline pond water, where some of the leached Mg^{2+} was able to form carbonates, while the remaining lizardite structure was modified to talc, as in Equation 6 [20]:

$$2Mg_3Si_2O_5(OH)_4 + 6H^+ \rightarrow Mg_3Si_4O_{10}(OH)_2 + 3Mg^{2+} + 6H_2O \qquad 6$$

Further evidence of ambient dissolution of tailings in Pond 1 is given by a notable decrease in the anorthite concentration of Tail 1 relative to Tail 2a. This decreased anorthite concentration is coupled with an increased TIC content and presence of calcite in Tail 1. This could be evidence of ambient dissolution of anorthite in Pond 1, where the dissolved Ca^{2+} reacts with dissolved CO_2 to produce calcite.

In Tail 2c, there is also a decrease in anorthite concentration relative to Tail 2a. This could be explained by the fact that Tail 2c is the finer fraction of Tail 2a, and tectosilicate minerals are bulkier 3-dimensional structures that may be present in larger particles. Similarly, there is less CaO in Tail 2c relative to Tail 2a (Table 4). This indicates that the true anorthite concentration in the Sibanye-Stillwater tailings is somewhere between that of Tail 2a and Tail 2c.

The composition of Tail 2b can give more insight into Sibanye-Stillwater tailings representative composition. As noted in Table 1, Tail 2b is a dehydrated fraction of Tail 2a, which is corroborated by the practically identical mineralogy (Table 3) and chemistry (Table 4) of these two samples. The primary difference among these two samples is the decreased LOI in Tail 2b, as expected due to it being dehydrated. Thus, the Tail 2a anorthite concentration is likely close to the true Sibanye-Stillwater tailings composition.

Table 4: Whole rock analysis results, measured via XRF, shown in wt.%

Sample	SiO_2	Al_2O_3	Fe_2O_3	CaO	MgO	Na_2O	K_2O	LOI
Tail 1	45.07	18.34	5.93	11.50	11.40	1.07	0.14	5.95
Tail 2a	45.58	22.98	5.14	13.30	8.55	1.30	0.08	2.29
Tail 2b	46.44	22.91	5.12	13.55	8.43	1.29	0.06	1.90
Tail 2c	43.52	19.00	6.78	9.27	13.90	1.12	0.11	5.76

Sample	BaO	Cr_2O_3	MnO	P_2O_5	SO_3	SrO	TiO_2	Total
Tail 1	0.02	0.16	0.10	0.01	0.14	0.01	0.12	99.96
Tail 2a	0.01	0.09	0.08	<0.01	0.09	0.01	0.09	99.59
Tail 2b	0.01	0.12	0.08	<0.01	0.07	0.01	0.09	100.08
Tail 2c	0.01	0.09	0.10	0.02	0.14	0.01	0.08	99.91

3.1.2 Composition of tailings ponds

As previously mentioned, tailings from Pond 1 and Pond 2 were received in a liquid suspension. After the tailings were filtered and centrifuged, the resultant liquids were analyzed for their chemical compositions, and results are shown in Table 5. Analysis yielded very different concentrations of Al, Ca, Fe, and Mg within the two liquids, as indicated by the ratio of Pond 1 to Pond 2. Comparison of Pond 1 and Pond 2 can give further insight into how the Sibanye-Stillwater tailings have interacted with the pond water over the nearly two decades that Pond 1 has been idled.

Table 5: Chemical composition of tailings liquids, measured via ICP-OES

Tailings Sample	Tailings Pond	Composition (ppm)						
		Al	Ca	Fe	K	Mg	Na	Si
Tail 1	1	0.65	156.47	0.44	7.04	53.58	189.20	11.20
Tail 2a	2	0.02	33.58	0.00	7.41	10.05	151.50	5.90
~Ratio Pond 1:2		31	5	113	1	5	1	2

One plausible explanation for the vast increase in cation concentration of Pond 1 relative to Pond 2 is evapoconcentration. This phenomenon describes water evaporating from Pond 1 over time, leaving behind the leached cations and effectively increasing their concentration by decreasing the liquid volume. Evapoconcentration would be evidenced by a similar ratio of Pond 1 to Pond 2 in concentrations of all elements. However, the degree of increase among different cations is inconsistent. For Ca and Mg, there is about a five-fold increase, but for Fe and Al the increase is much larger. Therefore, while evapoconcentration might partially explain the difference in concentration, it cannot be the only explanation.

Another possible explanation of the different pond water concentrations is that mineral dissolution has occurred in Pond 1, followed by carbonation of Ca and Mg. This theory is evidenced by the

smaller Pond 1:2 ratio of Ca and Mg relative to Al and Fe, as Ca and Mg are more likely to form carbonates.

The presence of dissolved CO_2 in the tailings ponds would further indicate that ambient mineral dissolution and carbonation is taking place. Ion Chromatography (IC) results (Table 6) were used to perform a charge balance on the two tailings liquids, shown in Table 7. The charge balance performed in Table 7 indicates that there is a significant increase of undetected ion concentration in Pond 1 relative to Pond 2. To identify the phases undetected by IC, a PHREEQC geochemical model was generated with the IC results. As illustrated in Table 8, the PHREEQC model revealed that both ponds contain alkalinity. The presence of alkalinity and multiple dissolved CO_2 phases suggest that dissolved CO_2 has provided a favorable environment for dissolution and carbonation of the Sibanye-Stillwater tailings.

Table 6: Results of ion chromatography analysis of tailings liquids

Tailings Sample	Tailings Pond	Anions (meq/L)			Cations (meq/L)						
		Cl^-	SO_4^{2-}	NO_3^-	Al^{3+}	Ca^{2+}	Fe^{3+}	K^+	Mg^{2+}	Na^+	Si^{4+}
Tail 1	1	10.61	16.44	1.55	6.18	9.59	1.27	90.46	7.53	16.45	6.67
Tail 2a	2	3.56	7.55	3.46	0.04	1.74	0.00	15.86	0.81	12.10	0.75
~Ratio Pond 1:2		3	2	0	167	6	365	6	9	1	9

Table 7: Charge balance for Sibanye-Stillwater tailings ponds

Tailings Liquid	Tailings Pond	Charge Balance (meq/L)		
		Anion	Cation	Difference
Tail 1	Pond 1	28.60	138.27	109.67
Tail 2a	Pond 2	14.57	31.33	16.76
~Ratio Pond 1:2		2	4	7

Table 8: Remaining charge balance vis PHREEQC analysis

Tailings Sample	Tailings Pond	pH	Alkalinity (meq/L)			
			Total	OH^-	HCO_3^-	CO_3^{2-}
Tail 1	1	9.68	96.91	0.06	37.02	35.59
Tail 2a	2	8.70	4.06	0.01	3.54	0.26

3.2 Flow-Through Dissolution

The use of the flow-through dissolution experiment allows quantification of labile cations present in the Sibanye-Stillwater tailings (i.e., the number of cations that can be readily dissolved at ambient conditions). Tail 2a is most representative of the tailings being currently produced at the Sibanye-Stillwater mine. Additionally, Tail 2a has a lower TIC content than Tail 1, indicating that it has a higher capacity for carbonation. For these reasons, Tail 2a was chosen for the flow-through dissolution experiments.

Dissolution rates for both Al^{3+} and Ca^{2+} in Tail 2a were calculated using Equation 1. The mineral stoichiometric coefficients were estimated using a weighted average of the respective stoichiometric coefficients of each mineral phase detected in Tail 2a.

The evolution of the measured dissolution rates of Ca^{2+} and Al^{3+} in Tail 2a over time is displayed with the accumulation of Ca^{2+} and Al^{2+} in solution in Figure 3. The measured Tail 2a dissolution rates are directly compared to published dissolution rates of anorthite and diopside [21], representing the most likely Ca-bearing mineral phases of Tail 2a to react. The majority of measurements for all cations except Ca^{2+} and Al^{3+} were below the ICP-OES detection limit of 0.1 ppm, indicating limited dissolution of Tail 2a in the 60-hour experiment. All measurements are plotted for Ca^{2+} and Al^{3+}, where a solid accumulation curve indicates measurements above the ICP detection limit, while a dashed accumulation curve indicates measurements below the ICP detection limit.

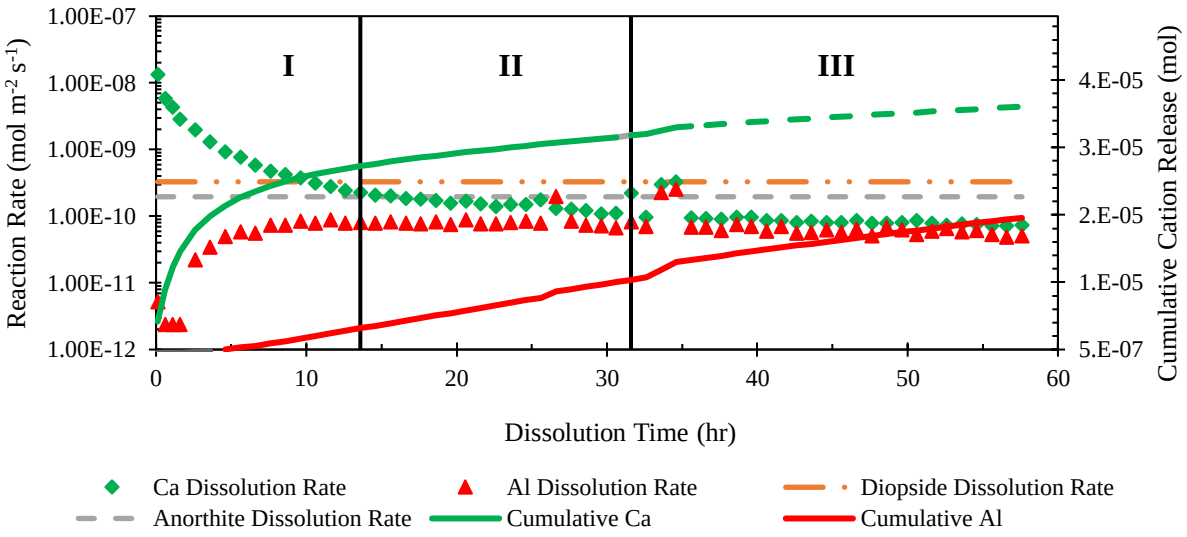

Figure 3: Evolution of Ca^{2+} and Al^{3+} dissolution rate in Tail 2a (left axis) paired with Ca^{2+} and Al^{3+} accumulation in solution (right axis). Published dissolution rates of diopside and anorthite are displayed for comparison [21]. The solid accumulation curve indicates values above the ICP detection limit, while the dashed curve indicates values below the ICP detection limit. Vertical lines separate distinct regions in the 60-hour dissolution process, discussed in the text.

There are three distinct regions on the plots (separated by vertical lines) that may represent the dissolution of different minerals over the duration of the experiment. Region I involves rapid accumulation of Ca^{2+}, which could be explained by calcite dissolution. Detection of low-abundance carbonate-bearing minerals through XRD has been reported to suffer large relative error values [22]. Consequently, the small amount of TIC in Tail 2a (Table 3) indicates that some carbonate is likely present despite no detection of calcite in through XRD. Assuming all of the 0.07% TIC measured in Tail 2a is in the form of calcite, there would be 2.77 mg of calcite in the reaction chamber. Dissolution of all the calcite would produce 1.11 mg of Ca^{2+}. This value of dissolved Ca^{2+} is accumulated after 13 hours, marked by Region I. Seeing as though the Ca^{2+} dissolution rate in Figure 3 has steadied before this point, it is possible that not all of the TIC is present as calcite, and could in fact also be present as a hydrated magnesium carbonate like hydromagnesite. In this case, the 0.029 mg of Mg^{2+} released in the first hour of the experiment would equate to 0.112 mg of hydromagnesite, or 0.012 mg of carbon.

In Region II, the Ca^{2+} dissolution rate is nearly the same as the published dissolution rate for anorthite. Here, the steady accumulation of Ca^{2+} is coupled with a steady accumulation of Al^{3+}, as would be expected for the dissolution of anorthite in Equation (2). Further, a linear regression of Ca^{2+} and Al^{3+} accumulation in Region II reveals the slope for Al^{3+} is double that of Ca^{2+}, also indicative of anorthite dissolution. While the accumulation of Ca^{2+} and Al^{3+} in Region II is stoichiometric with respect to each other, the lack of measurable Si^{4+} indicates incongruent dissolution of anorthite.

At the beginning of Region III, a sudden "jump" occurs in the accumulation of Ca^{2+}, Al^{3+}, and most notably, a few measurable points of Si^{4+} release, which are not shown. As illustrated in Table 9, the silicon ratios decrease and approach their stoichiometric values. After this "jump", the cation ratios return to their original values before the "jump". This too is indicative of incongruent anorthite dissolution. Incongruent dissolution has been reported to occur in feldspars on a varying degree, directly proportional to anorthite content [23]–[25]. Incongruent dissolution would leave behind a siliceous layer, but in the case of high-anorthite content feldspars, there is not enough silicon to form a stable structure, resulting in increased Si^{4+} dissolution [25]. This could perhaps explain this momentary "jump" in Si^{4+} accumulation, where a weak siliceous layer, formed from Ca- and Al-depletion, breaks down and releases the left-behind Si^{4+}.

Table 9: Ratios of cation accumulation during flow-through dissolution data generated through linear regression of slopes in **Error! Reference source not found.**

Cation Ratio	Stoichiometric	Region II (14-32 hr)	Region III, jump (33-36 hr)	Region III, post jump (37-58 hr)
Ca^{2+} / Al^{3+}	0.5	0.6	1.1	0.5
Ca^{2+} / Si^{4+}	0.5	1.4	0.7	1.3
Al^{3+} / Si^{4+}	1	2.3	0.7	2.9

Limited dissolution of Mg^{2+} occurred, where the dissolution did not correspond with published lizardite values on the order of 10^{-10} [21]. Phyllosilicates like lizardite are reported to react more slowly compared to anhydrous silicates such as olivine due to the abundance of tetrahedra containing Si-O bonds, which are stronger than the Mg-O bond [26], [27]. In [13], less than 5 % of serpentine-bound Mg^{2+} was found to be labile in similar reaction conditions. In the Sibanye-Stillwater tailings sample used here, 4% of lizardite-bound Mg^{2+} equates to only about 0.4 mg, which is still more than the accumulation of Mg^{2+} measured here. The apparent lack of dissolution for the low-abundant lizardite in Tail 2a might also be due to transport limitations through the remaining bulk sample, and might be improved with use of stirring and reaction times longer than 60 hours.

Over the 60-hour dissolution period, effluent concentration measurements above the ICP detection limit accumulated to about 1.35 mg of Ca^{2+} and 0.03 mg of Mg^{2+}. After correcting for the Ca^{2+} and Mg^{2+} likely released from calcite and hydromagnesite, results indicate that about 0.59% of the total Ca^{2+} and none of the Mg^{2+} available in the 501.6 mg sample are labile from silicate structures. This is illustrated in Table 10.

Table 10: Final cation leaching results from flow-through dissolution experiment of Tail 2a

Cation	Tail 2a Composition (wt%)	Mass in Sample (mg)	Leached from Sample (mg)	Leached from Carbonate* (mg)	Leached from Silicate (mg)	Labile (Total)$^{+}$ (wt%)	Labile (Silicate)$^{++}$ (wt%)
Calcium	9.50%	47.65	1.35	1.07	0.28	2.83%	0.59%
Magnesium	5.16%	25.86	0.03	0.03	0.00	0.11%	0.00%

*estimated conversion of Tail 2a TIC to calcite and hydromagnesite

$^{+}$referring to cations easily released from Tail 2a

$^{++}$referring to cation seasily released from silicate structures

3.3 Disk Carbonation

While flow-through dissolution is an effective method to measure the mineral dissolution rate and determine the number of labile cations that can be quickly released from the Sibanye-Stillwater tailings at ambient conditions, it does not directly measure the tailings' change in carbon uptake over time. Alternatively, disk carbonation is a simpler method that can be used to evaluate whether the tailings can be carbonated under ambient conditions. The analysis of carbon uptake through disk carbonation is based on change in TIC measured in each dime. While the mass of each dime was recorded as an estimate of carbonation, evaporative mass loss caused the analysis to be too difficult, as is common in this sort of experiment [15], so mass measurements are not reported. The carbon uptake among all of the dimes is displayed in Table 11.

Table 11: Summary of Change in TIC in Dimes of Sibanye-Stillwater Tailings

Sample	Initial TIC (%)	Final TIC (%)	Carbon Uptake (ΔTIC, wt%)	Carbon Uptake (% Change)
Tail 1	0.211	0.334	0.123	58%
Tail 2a	0.059	0.086	0.027	46%
Tail 2b	0.051	0.047	-0.004	-7%
Tail 2c	0.110	0.163	0.053	48%

The results in Table 11 indicate that three of the four samples exhibited an overall net increase in carbon content over the 16-day period. The only sample that did not exhibit an increase in carbon content is Tail 2b. This might be explained by more closely examining the carbonation of Tail 2a dimes, as Tail 2a and Tail 2b have similar mineralogy. Using the labile magnesium and calcium of Tail 2a measured in the flow-through dissolution experiment (Table 10), a maximum carbon uptake value was estimated for the disk carbonation experiment by assuming magnesium and calcium will carbonate to form hydromagnesite and calcite, respectively. This value is plotted with the carbon content of Tail 2a in Figure 4, showing that slightly more than 100% of the labile calcium and magnesium was carbonated.

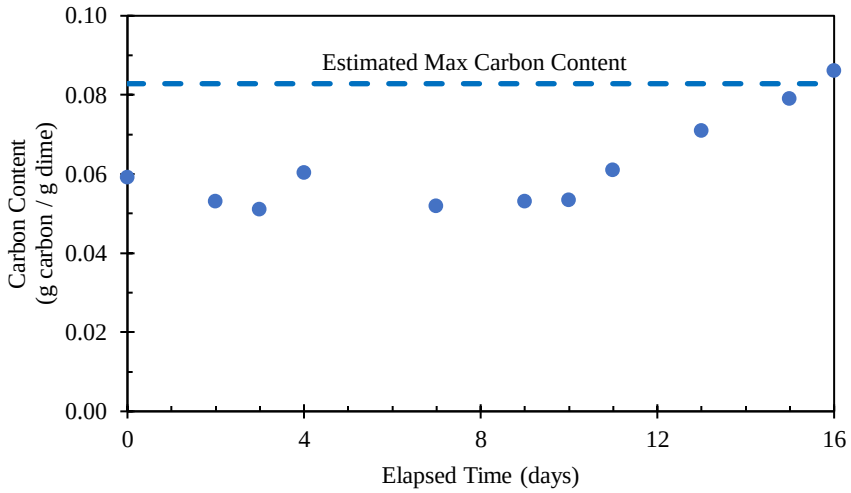

Figure 4: Change in carbon content in Tail 2a dimes. Maximum carbon content is estimated based on labile Ca and Mg observed in flow-through dissolution experiment

Before the estimated maximum carbon content is reached, Tail 2a dimes actually had a net-decrease in carbon content, similar to the behavior of Tail 2b during the full 16-day period. This initial decrease in Tail 2a corresponds with the initial CO_2 release from carbonate dissolution examined in Region I of the flow-through dissolution experiment. The carbonate already present in the tailings would first dissolve before being reformed via carbonation. Because Tail 2b has half the reactive surface area of Tail 2a (Table 3), the carbonation reaction may be delayed. Therefore, longer reaction times might be necessary for carbon uptake to occur in Tail 2b.

4. Discussion

4.1 Significance of results

The reactivity for carbon mineralization of Sibanye-Stillwater Mine tailings was indirectly assessed through characterization experiments, and was directly assessed through dissolution and disk carbonation. Results present varying degrees of potential for use as a feedstock for carbon mineralization.

Based on observation of liquids from the two tailings ponds, it is clear that the Sibanye-Stillwater tailings are capable of dissolving and releasing alkaline cations that can react with dissolved CO_2 at ambient conditions. However, even after interacting with the atmosphere for nearly two decades, there remains a considerable amount of alkalinity in the tailings (Tail 1) which could be used to store more CO_2. Additionally, the smaller particle size and large surface area presented by the Sibanye-Stillwater tailings provides favorable conditions for reaction.

The mineralogy across all tailings samples was heterogeneous, composed of several mineral constituents with varying silicate structures and reactivity. Similarly, the chemistries of the tailings samples are diverse, with nearly equimolar concentrations of calcium and magnesium. This heterogeneity presents some difficulty for targeting conditions of dissolution and carbonation. For example, while the flow-through dissolution experiment was able to release some Ca^{2+} (likely from anorthite), it was unable to release Mg^{2+} from lizardite.

Low reactivity of serpentine in mine tailings through flow-through dissolution has been previously reported [13]. In Lu's study, two tailings samples composed of 43 % and 77 % serpentine were measured to have labile Mg^{2+} contents of 5 % and 21 %. These values of labile Mg^{2+} are far higher than the 0.3 % measured here. However, the tailings also benefited from brucite content, which is far more reactive than serpentine [27]. Because Tail 2a is composed of only about 8 % lizardite, with no brucite, leaching of lizardite-related Mg might have suffered from transport limitations through the remainder of the tailings sample. This could be improved with stirring and longer reaction times.

The most prominent mineral phase in the Sibanye-Stillwater tailings, anorthite, can achieve dissolution rates of $>10^{-8}$ mol m^{-2} s^{-1} at 25 ^{o}C and $>10^{-7}$ mol m^{-2} s^{-1} at 180 ^{o}C, on par with dissolution rates of wollastonite and brucite at low temperatures and faster than records of olivine added to soil [18]. However, in the flow-through dissolution experiment presented here, the dissolution rate was on the order of 10^{-10} mol m^{-2} s^{-1}. This may be a consequence of the tailings' heterogeneity, and could represent a more realistic rate for PGM tailings.

Despite the fact that the dissolution rates measured here are rather slow, Figure 4 confirms that the flow-through dissolution experiment accurately depicted the number of labile cations in the Sibanye-Stillwater tailings. While there is a notable amount of Ca and Mg available in the tailings, the majority of the alkaline cations are not labile at ambient conditions. Elevated conditions may be necessary to realize the full mineralization potential – meaning longer reaction times, higher temperature, higher pressure, or the use of reagents to manipulate pH. Of course, implementation of such conditions would have to be weighed with the environmental impact they impose.

As an example of elevated reaction conditions, the Sibanye-Stillwater tailings characterized here are similar in mineralogy and composition to anorthosite and basalt rocks described elsewhere [28]. In this study, carbonation was tested with conditions mimicking geologic storage sites (185 ºC, 139 atm, 1 M NaCl + 0.64 M $NaHCO_3$) with particle size d(0.9) = 11.94 and 7.81 µm, respectively. Here, carbonation extents of 19 % and 9 % were achieved for anorthosite and basalt, respectively, where the extent is the amount of CO_2 stored as solid carbonate relative to the theoretical storage capacity. These values are considerably higher than the approximately 1 % of calcium carbonated in this study.

4.2 Opportunity for Climate Impact

As the 21st century unfolds, efforts will continue to accelerate to minimize the impacts of climate change due to excess carbon emissions. This will be realized in part through transformations in the electric sector, which is projected to see a 900 % increase in mineral production [2]. In parallel, up to 3.5 Gt/year of mine wastes will be generated at nickel and PGM mines like Sibanye-Stillwater [11]. As the motivation of this electric sector transformation is for increased sustainability, it is imperative that sustainable practices of tailings handling and storage be developed and maintained.

In this study, it was found that while about 15 % of Tail 2a mass is made up of Ca and Mg cations, only less than 1 % of the Ca and 0 % of the Mg are readily released from silicate structures to easily produce carbonates. If this labile Ca and Mg were to be carbonated as calcite and hydromagnesite, respectively, about 1.79 kg CO_2 could be stored in a tonne of Sibanye-Stillwater tailings. If this same carbonation process was applied to the 1 Mt of tailings produced per year at Sibanye-Stillwater, it would result in about 1.8 kt CO_2 stored per year. Further, if this process was applied to the 3.5 Gt of tailings projected to be produced across the world, it would result in 6 Mt CO_2 stored per year. The potential to store additional CO_2 increases further if employing an improved process like [28]. Additional estimations are displayed in Table 12. These global estimates assume that all tailings possess the same mineralogy as the Sibanye-Stillwater tailings characterized in this study, and further increases in storage could be achieved with tailings containing more reactive mineral phases such as brucite.

Table 12: CO_2 Storage Potential for Mineralization of PGM Tailings

Efficiency Achieved	**Carbonation Extent**	**kg-CO_2 per t-tailings**	**Total t CO_2 / year**	
			Sibanye-Stillwater (1 Mt tailings / yr)	**World*** (3.5 Gt tailings / yr)
This work	1.0%	1.79	1,792	6,273,599
[28]	9.0%	16.13	16,132	56,462,389
[28]	19.0%	34.06	34,057	119,198,377
Potential target	50.0%	89.62	89,623	313,679,938

*assumes all tailings have the same composition as the Sibanye-Stillwater tailings analyzed in this study

The potential increases in CO_2 storage from improved mineralization processes should serve as motivation to expand on this work. Future work should involve investigating new ways to extract and carbonate the calcium and magnesium from heterogeneous PGM tailings like those of Sibanye-Stillwater, as well as assessment and characterization of other tailings sources in locations where mining practices are expected to increase the most.

References:

[1] C. Marcy, "U.S. renewable electricity generation has doubled since 2008," *March*, 2019. [Online]. Available: https://www.eia.gov/todayinenergy/detail.php?id=38752.

[2] T. Watari, B. C. McLellan, D. Giurco, E. Dominish, E. Yamasue, and K. Nansai, "Total material requirement for the global energy transition to 2050: A focus on transport and electricity," *Resour. Conserv. Recycl.*, vol. 148, no. March, pp. 91–103, 2019.

[3] H. Pilorgé *et al.*, "Cost Analysis of Carbon Capture and Sequestration of Process Emissions from the U.S. Industrial Sector," *Envion. Sci, Technol*, vol. 54, no. 12, pp. 7524–7532, 2020.

[4] N. Mcqueen *et al.*, "Cost Analysis of Direct Air Capture and Sequestration Coupled to Low-Carbon Thermal Energy in the United States," *Environ. Sci. Technol*, 2020.

[5] National Academies Press, *Negative Emissions Technologies and Reliable Sequestration*. 2019.

[6] C. M. Woodall, N. McQueen, H. Pilorgé, and J. Wilcox, "Utilization of Mineral Carbonation Products: Current State and Potential," *Greenh. Gases Sci. Technol.*, 2019.

[7] I. M. Power, G. M. Dipple, P. M. D. Bradshaw, and A. L. Harrison, "Prospects for CO2 mineralization and enhanced weathering of ultramafic mine tailings from the Baptiste nickel deposit in British Columbia, Canada," *Int. J. Greenh. Gas Control*, vol. 94, no. October 2019, p. 102895, 2020.

[8] A. Gras *et al.*, "Isotopic evidence of passive mineral carbonation in mine wastes from the Dumont Nickel Project (Abitibi, Quebec)," *Int. J. Greenh. Gas Control*, vol. 60, pp. 10–23, May 2017.

[9] J. Vogeli, D. L. Reid, M. Becker, J. Broadhurst, and J. P. Franzidis, "Investigation of the potential for mineral carbonation of PGM tailings in South Africa," *Miner. Eng.*, vol. 24, no. 12, pp. 1348–1356, 2011.

[10] N. A. Meyer, J. U. Vögeli, M. Becker, J. L. Broadhurst, D. L. Reid, and J.-P. Franzidis, "Mineral carbonation of PGM mine tailings for CO2 storage in South Africa: A case study," *Miner. Eng.*, vol. 59, pp. 45–51, 2014.

[11] P. Renforth, "The negative emission potential of alkaline materials," *Nat. Commun.*, vol. 10, no. 1401, 2019.

[12] Bruker AXS, "DIFFRACplus EVA 14." Germany, 2008.

[13] X. Lu, "Characterization of Ultramafic Mine Tailings Reactivity for Carbon Capture and Storage," The University of British Columbia, 2020.

[14] B. De Baere, R. François, and K. U. Mayer, "Measuring mineral dissolution kinetics using on-line flow-through time resolved analysis (FT-TRA): An exploratory study with forsterite," *Chem. Geol.*, vol. 413, no. 2015, pp. 107–118, 2015.

[15] A. L. Harrison, G. M. Dipple, I. M. Power, and K. U. Mayer, "Influence of surface passivation and water content on mineral reactions in unsaturated porous media: Implications for brucite carbonation and CO_2 sequestration," *Geochim. Cosmochim. Acta*, vol. 148, pp. 477–495, 2015.

[16] A. Sanna, L. Steel, and M. M. Maroto-Valer, "Carbon dioxide sequestration using NaHSO4 and NaOH: A dissolution and carbonation optimisation study," *J. Environ. Manage.*, vol. 189, pp. 84–97, 2017.

[17] S. Lavikko and O. Eklund, "The role of the Silicate Groups in the Extraction of Mg with the ÅA route method," *J. CO2 Util.*, vol. 16, pp. 466–473, Dec. 2016.

[18] P. B. Kelemen, N. McQueen, J. Wilcox, P. Renforth, G. Dipple, and A. P. Vankeuren, "Engineered carbon mineralization in ultramafic rocks for CO2 removal from air: Review and new insights," *Chem. Geol.*, vol. 550, no. 119628, May 2020.

[19] S. Sepp, "Composition of the Earth's Crust," *Sandatlas*, 2012. [Online]. Available: https://www.sandatlas.org/composition-of-the-earths-crust/. [Accessed: 07-Jan-2021].

[20] H. Yalçin and Ö. Bozkaya, "Mineralogy and geochemistry of Paleocene ultramafic- and sedimentary-hosted talc deposits in the southern part of the Sivas Basin, Turkey," *Clays Clay Miner.*, vol. 54, no. 3, pp. 333–350, 2006.

[21] J. L. Palandri and Y. K. Kharaka, "A Compilation of Rate Parameters of Water-Mineral Interaction Kinetics for Application to Geochemical Modeling," 2004.

[22] C. C. Turvey, J. L. Hamilton, and S. A. Wilson, "Comparison of Rietveld-compatible structureless fitting analysis methods for accurate quantification of carbon dioxide fixation in ultramafic mine tailings," *Am. Mineral.*, vol. 103, no. 10, pp. 1649–1662, 2018.

[23] T. Murakami, T. Kogure, H. Kadohara, and T. Ohnuki, "Formation of secondary minerals and its effect on anorthite dissolution," *Am. Mineral.*, vol. 83, no. 11-12 PART 1, pp. 1209–1219, 1998.

[24] L. L. Stillings and S. L. Brantley, "Feldspar dissolution at 25°C and pH 3: Reaction stoichiometry and the effect of cations," *Geochim. Cosmochim. Acta*, vol. 59, no. 8, pp. 1483–1496, 1995.

[25] W. Shotyk and H. W. Nesbitt, "Incongruent and congruent dissolution of plagioclase feldspar: effect of feldspar composition and ligand complexation," *Geoderma*, vol. 55, no. 1–2, pp. 55–78, 1992.

[26] F. K. Crundwell, "The mechanism of dissolution of minerals in acidic and alkaline solutions: Part II Application of a new theory to silicates, aluminosilicates and quartz," *Hydrometallurgy*, vol. 149, pp. 265–275, 2014.

[27] D. Daval, R. Hellmann, I. Martinez, S. Gangloff, and F. Guyot, "Lizardite serpentine dissolution kinetics as a function of pH and temperature, including effects of elevated pCO2," *Chem. Geol.*, vol. 351, pp. 245–256, 2013.

[28] G. Gadikota, J. Matter, P. Kelemen, P. V. Brady, and A. H. A. Park, “Elucidating the differences in the carbon mineralization behaviors of calcium and magnesium bearing alumino-silicates and magnesium silicates for CO2 storage,” *Fuel*, vol. 277, no. 117900, Oct. 2020.

This page intentionally left blank.

Chapter 3

Optimizing Carbon Mineralization with PGM Tailings via Thermal Cation Extraction

Abstract

The possibility of capturing and storing CO_2 in mine tailings has gained significant traction as a viable climate mitigation technique. Tailings from Sibanye-Stillwater, a mine in Nye, Montana, USA that produces nickel, copper, and platinum group metals (PGM), possess sufficient calcium and magnesium to store CO_2. This study involved using the Alternative ÅA Route to efficiently extract calcium and magnesium from the Sibanye-Stillwater tailings. At optimized conditions (450 ^oC, 30 min), about 39% of the Mg and 15% of the Ca in the tailings were extracted. While the Alternative ÅA Route proved successful in extracting phyllosilicate-bound magnesium, it was ineffective in extracting calcium from the tailings, which is mostly present in the form of plagioclase feldspar. Further studies will be necessary to realize the full potential of CO_2 storage in the Sibanye-Stillwater tailings. The majority of this chapter was published in the Proceedings of the 15th Greenhouse Gas Control Technologies Conference.

List of Abbreviations

ÅA – Åbo Akademi

CM – Carbon mineralization

LOI – loss on ignition

m_{feed} – initial mass of feedstock.

η_{ex} – extraction efficiency

PGM – platinum group metal

V_{fil} – total liquid filtrate volume

wt.% – weight %

x_M – weight fraction of the cation M in the initial alkaline feedstock

y_M – volumetric concentration of the cation M in the filtrate solution

1. Introduction

To avoid potentially devastating effects of climate change due to anthropogenic emissions of CO_2, technologies are being developed and deployed that can capture CO_2 from industrial flue gases [1] or remove CO_2 directly from the air [2]. As discussed in previous chapters, mine tailings have become relevant to carbon capture and carbon removal, as they can be used to capture and store CO_2 via carbon mineralization. The Sibanye-Stillwater US platinum group metal (PGM) operations, located in the Beartooth Mountains of Nye, Montana, produces high volumes of copper, nickel, along with its most valuable products, platinum and palladium. Additionally, it produces about one Mt of mine tailings each year.

Samples of Sibanye-Stillwater tailings were characterized in Chapter 2. Tailings from both of the mine's two tailings storage facilities were evaluated, one of which is still active ("Pond 1") and the other has been idled for nearly two decades, where the tailings have been allowed to interact with the atmosphere ("Pond 2"). Laser diffraction particle size analysis revealed that the tailings are of sufficient size (< 100 μm) to avoid the mass transfer limitations associated with larger particles. Quantitative x-ray diffraction revealed that the tailings are heterogeneous, notably consisting of anorthite, lizardite, pyroxenes, and amphiboles. Comparison of samples from Pond 1 relative to those from Pond 2 revealed a decrease in alkaline silicate composition among the tailings, coupled with an increase in inorganic carbon content. Additionally, alkaline ion concentration in the liquid of Pond 1 was much higher than Pond 2. These results give indication that carbon mineralization has occurred in Pond 1 at ambient conditions, presenting opportunity to use the Sibanye- Stillwater tailings as a mineralization feedstock.

Chapter 2 of this Dissertation also describes experiments that were performed to assess the reactivity of the tailings at low-cost ambient conditions. These experiments revealed that only about 1% and 0% of the calcium and magnesium can be easily released from the silicate structures within the tailings at low-cost ambient conditions. This indicates that elevated reaction conditions may be necessary to utilize a larger share of the alkalinity available in the tailings.

One method to increase the dissolution rate of alkaline silicates is through conversion to a more reactive intermediate product, like hydroxides, followed by carbonation. This method is called indirect carbon mineralization (CM). An indirect CM process that has published success is the "Alternative ÅA Route," shown in Figure 1. It involves 3 steps: thermal extraction, aqueous dissolution, and aqueous carbonation, where the carbonation and dissolution occur in the same low-temperature aqueous solution [3].

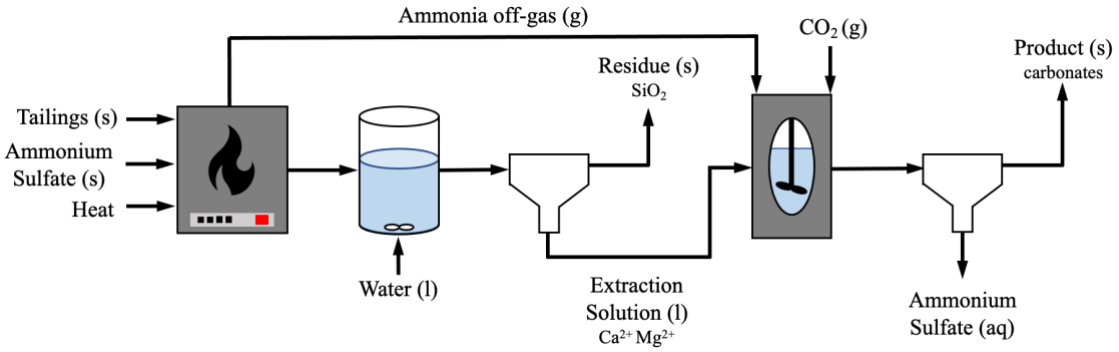

Figure 1: Process flow diagram of Alternative ÅA Route

The first step of the Alternative ÅA Route involves extracting metals from the alkaline feedstock through a solid/solid cation exchange reaction ammonium sulfate [4]. This reaction creates water vapor and ammonia gas as byproducts. For example, with serpentine:

$$Mg_3Si_2O_5(OH)_4\,(s) + 3(NH_4)_2SO_4\,(s) + \text{heat} \rightarrow 3MgSO_4\,(s) + 2SiO_2\,(s) + 5H_2O\,(g) + 6NH_3\,(g) \quad (1)$$

and with olivine:

$$Mg_2SiO_4\,(s) + 2(NH_4)_2SO_4\,(s) + \text{heat} \rightarrow 2MgSO_4\,(s) + SiO_2(s) + 2H_2O(g) + 4NH_3(g) \quad (2)$$

This thermal extraction step of the Alternative ÅA Route is followed by an aqueous dissolution and carbonation step. To increase solution pH and promote CO_2 conversion to carbonate anions, ammonia gas is recycled from the thermal extraction step (Equations 1 and 2) hydroxide is used to produce magnesium hydroxide [5]:

$$5MgSO_4\,(s) + 10H_2O\,(l) + 10\,NH_3\,(g) + 4\,CO_2\,(g) \rightarrow Mg_5(OH)_2(CO_3)_4{\bullet}4H_2O\,(s) + 5(NH_4)_2SO_4\,(aq) \quad (3)$$

Results from Chapter 2 indicate that cation extraction is a clear limiting factor for mineralization with the Sibanye-Stillwater tailings – where only about 1% of the Ca and 0% of the Mg in Tail 2a was “labile” (i.e., could be easily released at atmospheric conditions). In an effort to increase the extraction of Mg in the Sibanye-Stillwater tailings, the study in this chapter focused on optimizing cation extraction via the thermal extraction step of the Alternative ÅA Route (Equation 1 and 2). This study measured cation extraction by foregoing the subsequent carbonation step of Equation 3 and instead analyzing the extraction solution produced after aqueous dissolution and filtration of the reacted alkaline feedstock and ammonium sulfate (Figure 1). In this study, several parameters that influence thermal extraction were varied, including temperature, length of time, furnace type, heating rate, humidity, solid to liquid ratio [6]–[9].

Additionally, a separate alkaline sample which primarily consists of olivine was tested for comparison. It is hypothesized that under the right conditions, the rock samples studied here can be used for efficient and economical carbon mineralization under the Alternative ÅA route.

2. **Materials & Methods**

2.1 Materials

Two alkalinity sources were used as feedstock in this study. The first feedstock, "Tail 2b," is the dehydrated fraction of mine tailings produced at the Sibanye-Stillwater. Tail 2b was characterized in Chapter 2 of this Dissertation, where it was revealed that it is heterogeneous, primarily made up of anorthite, enstatite, diopside, and lizardite, among other mineral constituents (Table 1). The second feedstock, "Oliv 1," originated in North Carolina, USA, and was purchased as bulk rock. Oliv 1 was used as a secondary feedstock in this early study for the purpose of providing data comparison, and was not used in other chapters of this Dissertation. Qualitative x-ray diffraction results showed that the mineralogy of Oliv 1 consists primarily of olivine, lizardite, and pyroaurite (Table 1). A bulk chemical analysis was performed on both alkalinity sources, although at different labs. For Tail 2b, the analysis was completed at ALS Global Laboratories, North Vancouver, British Columbia. For Oliv 1, the analysis was completed at Hazen Research, Inc, Golden, Colorado. The results for both alkalinity sources are shown in Table 2.

Table 1: Mineralogical data of alkaline feedstock
Tail 2b – quantitative XRD, wt.%; Oliv 1 – qualitative XRD

Silicate Group	**Mineral Type**	**Mineral**	**Tail 2b** (Quantitative)	**Oliv 1** (Qualitative)
Tecto- (3-D framework)	Plagioclase Feldspar	**Anorthite** – $CaAl_2Si_2O_8$	54.27%	-
		Albite – $NaAlSi_3O_8$	3.69%	-
Ino- (chain)	Pyroxene	**Enstatite** – $(Mg,Fe)Si_2O_6$	14.74%	-
		Diopside – $CaMgSi_2O_6$	9.26%	-
	Amphibole	**Tremolite** – $Ca_2Mg_5(Si_8O_{22})(OH)_2$	2.56%	-
		Cummingtonite – $Mg_7(Si_8O_{22})(OH)_2$	1.27%	-
Phyllo- (sheet)	Serpentine	**Lizardite** – $Mg_3Si_2O_5(OH)_4$	6.48%	X
	Clay	**Talc** – $Mg_3Si_4O_{10}(OH)_2$	2.77%	-
	Mica	**Clinochlore** – $(Mg,Fe)_5Al_2Si_3O_{10}(OH)$	4.95%	-
Neso- (island)	Olivine	**Forsterite** – Mg_2SiO_4	-	X
N/A	Carbonate	**Pyroaurite** – $Mg_6Fe_2(OH)_{16}[CO_3]$-$4H_2O$	-	X

Table 2: Bulk chemical analysis of alkaline feedstock, wt.%
LOI – loss on ignition (mass of moisture in a sample)

Sample	**SiO_2**	**Al_2O_3**	**Fe_2O_3**	**CaO**	**MgO**	**Na_2O**	**K_2O**	**LOI**
Tail 2b	46.44	22.91	5.12	13.55	8.43	1.29	0.06	1.90
Oliv 1	40.60	0.18	7.17	0.04	42.20	<0.04	0.01	8.48

Oliv 1 contains significantly more MgO than Tail 2b, and also has more crystallized water (LOI), both as would be expected from its olivine and lizardite contents. Meanwhile, Tail 2b has high amounts of aluminum and calcium relative to Oliv 1, as expected from its plagioclase feldspar content. Lavikko *et al.* published a flow chart that defines suitability of an alkalinity source for the ÅA route, deeming that an ideal source would contain > 17 % MgO, > 12.5 % crystalline water, and primarily phyllosilicates [10]. Crystalline water, or water directly incorporated into the mineral structure, is important for this mineralization route because it relates to softer minerals with higher

surface areas [11]. In the case that the feedstock contains more nesosilicates than phyllosilicates (e.g., more olivine than serpentine), the feedstock would have "reduced suitability" for the ÅA Route [10]. The mineralogy of Oliv 1 fits the description for "reduced suitability," but its low crystalline water content is still lower than recommended. While Tail 2b as a whole is rich in tectosilicates and does not contain sufficient amounts of MgO and crystalline water, the Mg-bearing minerals within the tailings are phyllosilicates. Thus, use of the Alternative ÅA Route for Tail 2b and Oliv 1 has the potential to produce interesting results.

2.2 Methods

Because Oliv 1 was received as a 1 kg rock, its size was reduced via manual crushing with a mallet followed by milling in a ball mill. The resulting particles were sieved and particles with size 75-150 μm were used for experiments. Tail 2b was received in processed form of particle size <75 μm, so no further size reduction was performed prior to experimentation.

All experiments run for this study followed the extraction step of the "Alternative ÅA Route". The standard procedure, unless otherwise stated, involved placing 4 g of feedstock, either Tail 2b or Oliv 1, with 6 g of ammonium sulfate in a 250 mL beaker. Ammonium sulfate was purchased from Fisher Chemical (Catalog No. A702-500). The two solid reagents (each having a different color) were manually stirred in the beaker until they were visibly blended throughout. After mixing, the beaker was placed in a Thermolyne Barnstead 48000 chamber furnace preheated to the trial's specified temperature. The furnace was situated under a fume hood so that any gas produced during the thermal reaction was released through the furnace chimney and into the fume hood ventilation system.

Each experimental trial involved placing two beakers in the furnace at once: one with Tail 2b and one with Oliv 1; furnace placement was consistent in all trials. The beakers were left in the furnace for the trial's specified reaction time (most frequently 60 minutes). At the end of reaction time, beakers were promptly removed and allowed to cool under a hood for 15 minutes.

After cooling, 100 mL of water was added to each beaker, and the beakers were stirred with a magnetic stir bar for 40 minutes at ~450 rpm. Once dissolution was complete, the liquid filtrate was separated from the remaining solid residue using a Whatman 1001 filter with 110 cm diameter and 9 μm pore size. Aliquots of the liquid were placed in 20 mL glass scintillation vials and analyzed for cation content via inductively coupled plasma optical emission spectroscopy (ICP-OES) using a PerkinElmer Optima 8300.

Experimental results were analyzed according to the percentage of cations released from the alkaline feedstock and dissolved into the extraction solution. Aqueous cation concentration results from ICP-OES were compared to the initial cation concentration in the alkaline feedstock to yield an extraction efficiency, as in Equation 5:

$$\eta_{ex} = \frac{y_M V_{fil}}{x_M m_{feed}} \quad 4$$

where η_{ex} is the extraction efficiency, y_M is the volumetric concentration of the cation M in the filtrate solution, V_{fil} is the total liquid filtrate volume, x_M is the weight fraction of the cation M in the initial alkaline feedstock, and m_{feed} is the initial mass of feedstock.

3. Results

3.1 Standard Deviation of Initial Temperature Trials

Temperature measurements were performed in triplicate for the initially tested temperatures of 375 ºC, 400 ºC, 450 ºC, and 500 ºC. Test results yielded repeatable data, especially for Tail 2b (Table 3). Following these initial triplicate temperature experiments, all other experiments were performed without repetition.

Table 3: Standard deviation in triplicate temperature trials for extraction of relevant cations

Standard Deviation in Triplicate Temperature Trials				
	375 ºC	**400 ºC**	**450 ºC**	**500 ºC**
Tail 2b - Ca	0.11%	0.11%	0.83%	0.15%
Tail 2b - Mg	0.50%	0.71%	0.57%	0.13%
Oliv 1 - Mg	0.40%	1.35%	3.49%	0.52%

3.2 Effect of Reaction Temperature

To begin extraction experiments, the reaction temperature was investigated for both of the samples, and results are displayed in Figure 2.

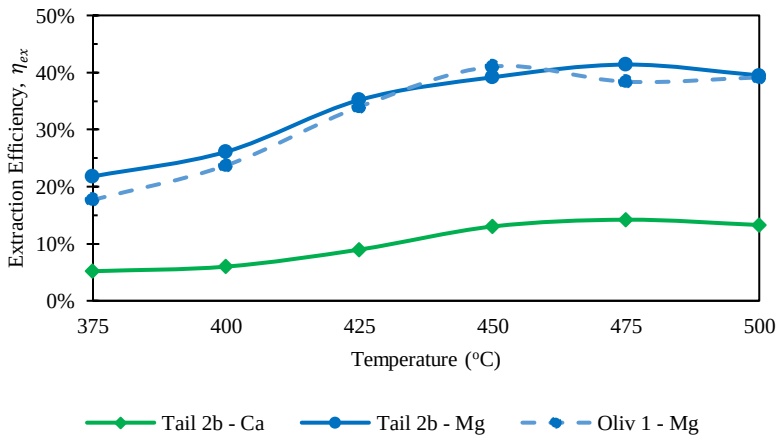

Figure 2: Effect of temperature on cation extraction

Extraction efficiency increases with temperature for both samples, but only to an extent. For Oliv 1, extraction efficiency peaks at 450 ºC, indicating this temperature to be the optimal conditions of those tested. While extraction efficiency for Tail 2b was highest at 475 ºC, results at 450 ºC were only 2% and 1% less for Mg and Ca, respectively. Therefore, 450 ºC was determined to be the optimal temperature for both Tail 2b and Oliv 1 in the temperature range tested, and was the temperature used for the remaining experiments.

3.3 Effect of Heat Ramp

The use of different heat ramps in the extraction step is known to have an effect on extraction. Nduagu *et al.*[6] found that at a heat rate of 40 K/min, the weight loss measured by thermogravimetric analysis was significantly lower than at a heat rate of 10 K/min (i.e., 46% vs 54%), indicating higher ammonium sulfate flux retention and a more efficient magnesium extraction.

Extraction experiments were performed with heating rates of 10 and 20 °C/min. These heating rates were applied the same way in each experiment: beakers containing the reagents were placed in the furnace at room temperature, the specified rate would be used to reach 450 °C, and the reagents would proceed to react at 450 °C for 60 minutes. In Figure 3, extraction results from the four heat rates are compared to the optimal 450 °C results from Figure 2 where no heat ramp was used, and the samples were placed directly in the furnace at the specified temperature.

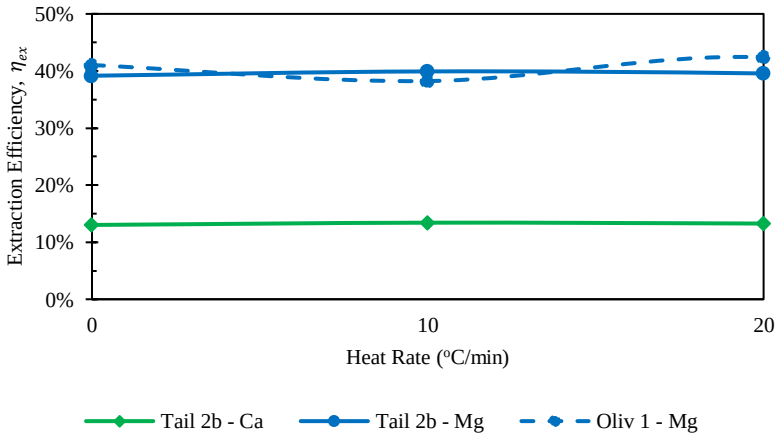

Figure 3: Effect of heat rate on cation extraction
(Heat rate of 0 °C/min indicates results from Figure 2 at 450 °C, where furnace was preheated)

As seen in Figure 3, no clear trend can be observed from varying the heating rate for either sample. It is possible that because the reagents were kept in the furnace for an hour at 450 °C, the full extent of reaction was reached for each heating rate. This complication likely stems from the furnace being old, causing one of its coils to be incapable of heating at high rates.

Based on results in Figure 3, preheating is more efficient than using a heat ramp. The preheat case would be more industrially practical, as a furnace already at a set temperature could be on standby for the reagents, as opposed to requiring the furnace to repeatedly cool down and heat up.

3.4 Effect of Reaction Time

Multiple sources have reported that longer reaction times benefit extraction efficiency, but only up to one hour.[7], [12] However, this is typically with serpentine materials, and since the materials being tested here are different, it was decided to test different reaction times other than 60 minutes. The results can be seen in Figure 4.

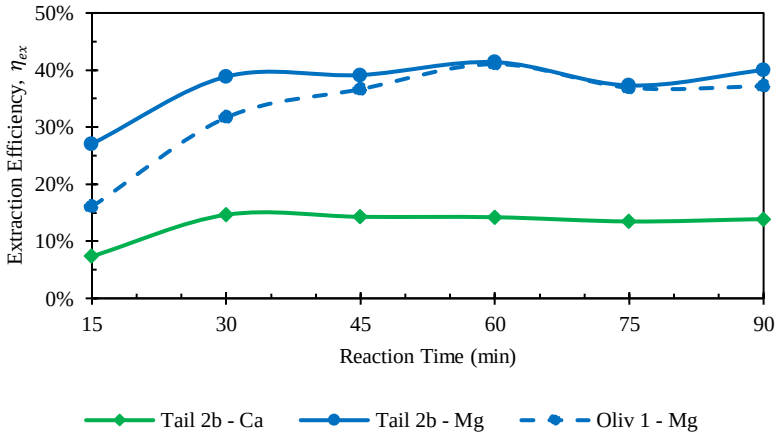

Figure 4: Effect of reaction time on cation extraction

It is clear that 60 minutes is the optimal reaction time for Oliv 1 within the tested range. Interestingly, extraction performance shows minimal improvement past 30 minutes for Tail 2b. This could be due to the low amount of Mg already in the sample, which limits the overall potential for extraction without mixing during the reaction. Hence, 30 minutes is the optimal reaction time for Tail 2b within the time range tested.

3.5 Effect of Water Presence

It has been reported that water improves extraction efficiency [7], [8]. During the thermal reaction, water can contribute to capillary forces (enhancing inter-particle contact), and can decrease the evaporation of intermediate products. Extraction tests were performed where 1, 2, and 3 mL of water were mixed with the alkaline feedstock and ammonium sulfate within the reaction beaker. Results are shown in Figure 5 and are compared to the 450 ^{o}C results from Figure 2 where no water was added.

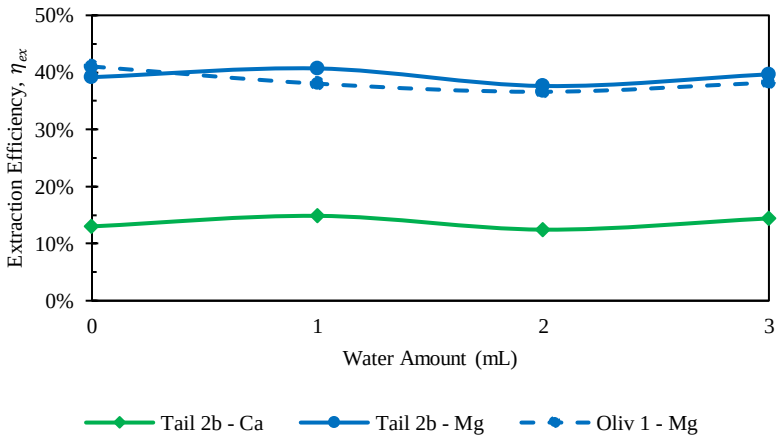

Figure 5: Effect of water amount on cation extraction

Contrary to what was expected from the literature, addition of water to the reagent mixture was found to be not increase the extraction efficiency. Slight variations in the conditions used here compared to past reports could be the cause of this difference. The success of water is typically reported with serpentine as the primary source mineral rather than olivine. Further, ammonium bisulfate in combination with ammonium sulfate is more typically used as the reagent.

3.6 Effect of Reagent Ratio

As described earlier, the reagent ratio used in the experiments of this chapter is 4 grams of alkaline feedstock with 6 grams of ammonium sulfate, as this is the standard ratio used for the ÅA Route [13]. To investigate the change in extraction due to excess ammonium sulfate, tests were performed reacting 7 and 8 grams of ammonium sulfate with a constant alkaline feedstock mass of 4 grams for one hour. The results are shown in Figure 6.

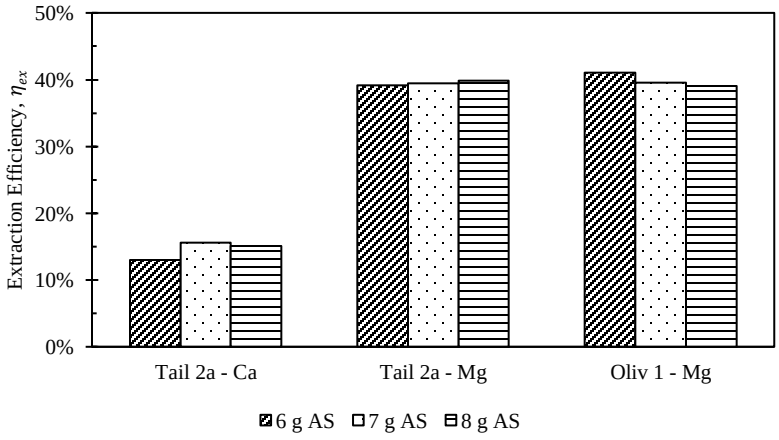

Figure 6: Effect of ammonium sulfate (AS) mass on cation extraction

Results indicate that excess ammonium sulfate is not beneficial to extraction efficiency for either feedstock. Considering instrumental error limits, there is no significant difference in extraction efficiency among the three different amounts of ammonium sulfate. This may be because the reaction has reached its full extent before one hour, so any additions to ammonium sulfate mass is

not beneficial. To test this theory, additional experiments were performed with 8 grams of ammonium sulfate, but for 30 minutes. The additional results are shown in Figure 7.

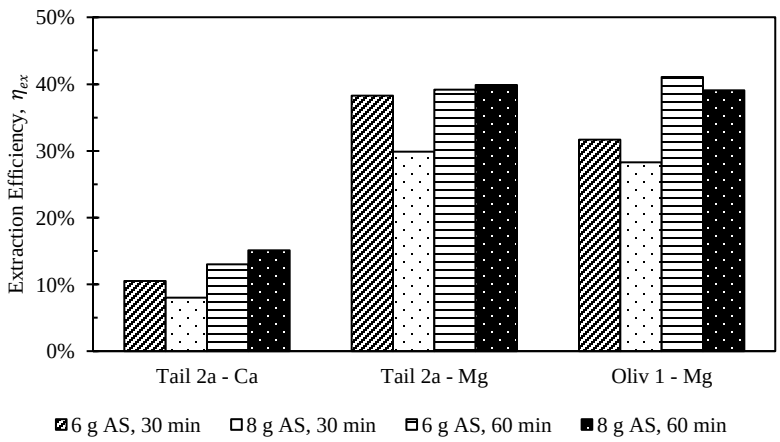

Figure 7: Effect of ammonium sulfate (AS) mass on cation extraction, at different reaction times

When reactions were run for 30 minutes with 8 grams of ammonium sulfate, both Tail 2b and Oliv 1 extracted Mg and Ca less efficiently than with 6 grams. This might indicate that the additional ammonium sulfate causes transport limitations within the reaction mixture. Additionally, there might be opportunity to use less that 6 grams of ammonium sulfate, which could further decrease material usage and operating expenses.

4. Discussion

4.1 Review of Results

This study helped to determine the extent of metal extraction for two North American alkalinity sources via the Alternative ÅA Route. The optimal experimental conditions within the tested ranges are detailed in Table 4 for Tail 2b and Oliv 1.

Table 4: Optimal conditions for each source rock tested in Alternative ÅA Route

Condition	Tail 2b	Oliv 1
Temperature (°C)	450	450
Heating Rate	Preheat	Preheat
Water Amount (mL)	0	0
Feed / Amm. Sulfate Ratio	2/3	2/3
Reaction Time (min)	30	60
Mg Extraction Efficiency	38.85%	41.04%
Ca Extraction Efficiency	14.64%	n/a

It is challenging to extract all of the alkaline cations from Tail 2b due to the heterogeneous mineralogy of the tailings. The contribution of each mineral phase to the Mg and Ca composition in Tail 2b can be estimated based on the average elemental compositions of the mineral phases of Tail 2b given in Table 1. These estimations are given in Table 5.

Table 5: Approximate contribution of mineral phases in Tail 2b to Mg and Ca composition

Silicate Group	Mineral Type	Mineral	Contribution to Tail 2b	
			Mg	Ca
Tecto- (3-D framework)	Plagioclase Feldspar	Anorthite	0%	79%
		Albite	0%	0%
Ino- (chain)	Pyroxene	Enstatite	43%	0%
		Diopside	13%	18%
	Amphibole	Tremolite	5%	3%
		Cummingtonite	3%	0%
Phyllo- (sheet)	Serpentine	Lizardite	21%	0%
	Clay	Talc	6%	0%
	Mica	Clinochlore	9%	0%

The phyllosilicates are known to be the most favored for the Alternative ÅA Route [10], and their combined contribution to Mg in Tail 2b is about 36% (Table 5). The 38% Mg extraction efficiency achieved in this study closely corresponds to the amount of phyllosilicate-bound Mg in Tail 2b. This might indicate that the Alternative ÅA Route is effective in extracting the phyllosilicate-based Mg from Tail 2b, but ineffective at extracting Mg from inosilicates.

While the Alternative ÅA Route can efficiently extract Mg from phyllosilicates, it does not work well for Ca-silicates due to the low solubility of $CaSO_4$. Most of the Ca that was extracted in the thermal reaction would have remained a solid during the aqueous dissolution step.

Because Oliv 1 is a more homogenous sample than Tail 2b, the Alternative ÅA Route was expected to be more effective in extracting Mg. However, it was noted that Oliv 1 had less crystalline water than is suggested to be "suitable" for the ÅA Route [10]. This study confirms that Oliv 1 does indeed have "reduced suitability" for the Alternative ÅA Route.

The samples tested in these experiments did not reach other extraction efficiency levels previously shown in the literature, as shown in Table 6. However, when examined more closely it can be seen that Oliv 1 in this report out-performed another olivine sample in the literature. Furthermore, while Tail 2b did not perform as well as other mine waste samples, it also had the least Mg content to begin with.

Table 6: Comparison of extraction efficiency in Alternative ÅA Route to results in literature

Source	Feedstock	Mg Weight%	Mg Extraction%	Temperature (ºC)	Reagent Ratio	Reaction Time (min)	Furnace Type
[8]	Peridotite	23%	62%	500	1.5	25	C
[8]	Peridotite	23%	59%	450	1.5*	25	C
[14]	Serpentine	21%	54%	520	1.5	20	C
[10]	Vermiculite	13%	53%	480	1.5	30	R
[15]	Waste - Talc Mine	27%	49%	480	1.5	30	R
[15]	Waste - Ni Mine	26%	48%	480	1.5	30	R
This work	Olivine	25%	41%	450	1.5	60	C
This work	Waste - PGE Mine	5%	41%	475	1.5	60	C
[10]	Olivine	28%	14%	480	1.5	30	R
[15]	Waste - multi-metal	11%	9%	480	1.5	30	R

*also 3.5 mL water added; R: rotary, C: chamber

4.2 Recommendations for Future Work

This work explored optimizing the Alternative ÅA Route, a process typically used for serpentine-like minerals, for two North American feedstocks less suitable for the process. While the large amount of olivine and substantial Mg composition of Oliv 1 presents great potential for carbon mineralization, its lack of crystallized water hinders its suitability for the Alternative ÅA Route.

The Sibanye-Stillwater tailings require a mineralization process that mineralizes CO_2 with both Mg^{2+} and Ca^{2+} to fully utilize the material's alkalinity, increase the carbonation efficiency, and subsequently decrease the process cost. Another potential process could use alternate ammonium salts. Researchers have used ammonium nitrate and ammonium chloride to extract alkalinity from Mg- and Ca-rich industrial wastes [16]–[21]. Use of these ammonium salts produces associated Ca-salts with dramatically higher solubility than $CaSO_4$ (Table 7) resulting in increased Ca^{2+} extraction. The application of ammonium nitrate and ammonium acetate within a process like the ÅA Route for carbonation of mine tailings has not yet been attempted.

Table 7: Solubility of Relevant Alkaline Salts at 25 ºC, g/100 g H_2O [22]

	Mg-	Ca-
-Chloride	56.0	81.3
-Nitrate	71.2	144.0
-Sulfate	35.7	0.2

Another potential process would use weak acids. It has been shown that weak organic acids such as acetic acid, propionic acid, oxalic acid, and citric acid can effectively dissolve plagioclase structures [23]. Further, the polyfunctional acids (oxalic and citric) have displayed selective leaching of Ca, K, Na, and Al from plagioclase [23], [24]. This is advantageous for the purposes of carbon mineralization with Sibanye-Stillwater tailings containing high amounts of anorthite, the Ca-rich end member of the plagioclase feldspar mineral series.

If continuing with a thermal process, alkalinity extraction is expected to improve with the use of a rotary furnace, as opposed to the stationary furnace available for this study. The constant mixing during reaction offered by a rotary furnace should allow for better inter-particle contact [7].

References

[1] H. Pilorgé *et al.*, "Cost Analysis of Carbon Capture and Sequestration of Process Emissions from the U.S. Industrial Sector," *Envion. Sci, Technol*, vol. 54, no. 12, pp. 7524–7532, 2020.

[2] N. Mcqueen *et al.*, "Cost Analysis of Direct Air Capture and Sequestration Coupled to Low-Carbon Thermal Energy in the United States," *Environ. Sci. Technol*, 2020.

[3] R. Zevenhoven, M. Slotte, E. Koivisto, and R. Erlund, "Serpentinite Carbonation Process Routes using Ammonium Sulfate and Integration in Industry," *Energy Technol.*, vol. 5, no. 6, pp. 945–954, 2017.

[4] E. Nduagu, T. Björklöf, J. Fagerlund, J. Wärn, H. Geerlings, and R. Zevenhoven, "Production of magnesium hydroxide from magnesium silicate for the purpose of CO_2 mineralisation - Part 1: Application to Finnish serpentinite," *Miner. Eng.*, vol. 30, pp. 75–86, Apr. 2012.

[5] R. Zevenhoven, M. Slotte, J. Åbacka, and J. Highfield, "A comparison of CO_2 mineral sequestration processes involving a dry or wet carbonation step," *Energy*, vol. 117, pp. 604–611, Dec. 2016.

[6] E. I. Nduagu, J. Highfield, J. Chen, and R. Zevenhoven, "Mechanisms of serpentine–ammonium sulfate reactions: towards higher efficiencies in flux recovery and Mg extraction for CO_2 mineral sequestration," *RSC Adv.*, vol. 4, no. 110, pp. 64494–64505, 2014.

[7] E. Koivisto, R. Erlund, M. Fagerholm, and R. Zevenhoven, "Extraction of magnesium from four Finnish magnesium silicate rocks for CO2 mineralisation - Part 1: Thermal solid/solid extraction," *Hydrometallurgy*, vol. 166, pp. 222–228, Dec. 2016.

[8] I. S. Romão, L. M. Gando-Ferreira, M. M. V. G. Da Silva, and R. Zevenhoven, "CO2 sequestration with serpentinite and metaperidotite from Northeast Portugal," *Miner. Eng.*, vol. 94, pp. 104–114, Aug. 2016.

[9] E. Nduagu, I. Romão, and R. Zevenhoven, "Production of $Mg(OH)_2$ for CO_2 emissions removal applications: parametric and process evaluation," in *Proceedings of the 25th International Conference on Efficiency, Cost, Optimization, Simulation and Environmental Impact of Energy Systems (ECOS 2012), Perugia, Italy, June 26-29, 2012*, 2012, pp. 233–250.

[10] S. Lavikko and O. Eklund, "The role of the Silicate Groups in the Extraction of Mg with the ÅA route method," *J. CO2 Util.*, vol. 16, pp. 466–473, Dec. 2016.

[11] E. Nduagu *et al.*, "Production of magnesium hydroxide from magnesium silicate for the purpose of CO_2 mineralization - Part 2: Mg extraction modeling and application to different Mg silicate rocks," *Miner. Eng.*, vol. 30, pp. 87–94, Apr. 2012.

[12] E. Nduagu, I. Romão, J. Fagerlund, and R. Zevenhoven, "Performance assessment of producing $Mg(OH)_2$ for CO2 mineral sequestration," *Appl. Energy*, vol. 106, pp. 116–126, Jun. 2013.

[13] E. Nduagu, “Production of Mg(OH)2 from Mg-silicate rock for CO2 mineral sequestration,” 2012.

[14] I. Stasiulaitiene *et al.*, “Parameters affecting Mg(OH)2 extraction from serpentinites in lithuania for the purpose of CO2 reduction by mineral carbonation,” *Am. Inst. Chem. Eng. Environ. Progr.*, vol. 33, no. 2, pp. 512–518, 2014.

[15] S. Sjöblom and O. Eklund, “Suitability of Finnish mine waste (rocks and tailings) for Mineral Carbonation,” in *Proceedings of ECOS 2014 - THE 27TH International Conference on Efficiency, Cost, Optimization, Simulation and Environmental Impact of Energy Systems June 15-19, 2014, Turku, Finland*, 2014, pp. 1–24.

[16] S. Eloneva, “Reduction of CO_2 emissions by mineral carbonation: steelmaking slags and raw material with a pure calcium carbonate end product,” 2010.

[17] W. Gao, J. Wen, and Z. Li, “Dissolution Kinetics of Magnesium from Calcined Serpentine in NH_4Cl Solution,” *Ind. Eng. Chem. Res.*, vol. 53, pp. 7947–7955, May 2014.

[18] M. Mun, H. Cho, and J. Kwon, “Study on characteristics of various extractants for mineral carbonation of industrial wastes,” *J. Environ. Chem. Eng.*, vol. 5, no. 4, pp. 3803–3821, 2017.

[19] S. Kodama, T. Nishimoto, N. Yamamoto, K. Yogo, and K. Yamada, “Development of a new pH-swing CO_2 mineralization process with a recyclable reaction solution,” *Energy*, vol. 33, no. 5, pp. 776–784, May 2008.

[20] T. Hosseini, C. Selomulya, N. Haque, and L. Zhang, “Indirect carbonation of victorian brown coal fly ash for CO_2 sequestration: Multiple-cycle leaching-carbonation and magnesium leaching kinetic modeling,” *Energy and Fuels*, vol. 28, no. 10, pp. 6481–6493, 2014.

[21] H. Jo, S. H. Park, Y. N. Jang, S. C. Chae, P. K. Lee, and H. Y. Jo, “Metal extraction and indirect mineral carbonation of waste cement material using ammonium salt solutions,” *Chem. Eng. J.*, vol. 254, pp. 313–323, Oct. 2014.

[22] W. M. Haynes, *CRC Handbook of Chemistry and Physics*, 100th ed. Boca Raton, FL: CRC Press/Taylor & Francis.

[23] S. A. Welch and W. J. Ullman, “The effect of organic acids on plagioclase dissolution rates and stoichiometry,” *Geochim. Cosmochim. Acta*, vol. 57, pp. 2725–2736, 1993.

[24] W. Shotyk and H. W. Nesbitt, “Ligand-Promoted Dissolution of Plagioclase Feldspar: A Comparison of the Surface Chemistry of Dissolving Labradorite and Bytownite Using SIMS,” in *Geochemistry of the Earth’s Surface and of Mienral Formation*, 1990, pp. 320–321.

Chapter 4

Optimizing Carbon Mineralization with PGM Tailings via Acidic Cation Extraction

Abstract

Platinum group metal (PGM) mine tailings from Sibanye-Stillwater have been used in previous chapters for lab-scale carbon mineralization experiments at ambient conditions and at elevated conditions using a thermal reaction with ammonium sulfate. Previous results indicated that an alternate process is necessary to maximize the use of alkalinity available in the tailings, especially in the case of anorthite-bound calcium. The present chapter used a pH swing process to optimize the extraction of calcium and magnesium from the tailings. Both organic (citric, acetic, oxalic) and mineral (hydrochloric, sulfuric) acids were used at various concentrations, solid/liquid ratios, and dissolution times. The time of dissolution was shown to greatly enhance alkalinity extraction for organic acids. Sulfuric acid was the most effective at extracting both magnesium and calcium, but the additional costs associated with corrosion-resistant equipment might make its use impractical. Citric and oxalic acids were selective towards Mg and Ca, respectively, where 0.5 M citric solution extracted 44 % of available Mg in 72 hours. While oxalic acid was effective in extracting Ca from plagioclase structures, it precipitated most Ca as whewellite (Ca-oxalate) rather than releasing to solution. Recycling the solid residue from citric acid dissolution into oxalic acid solution improved overall extraction efficiency, but further studies will be necessary to optimize this process configuration. Increases in the ratio of solid tailings to liquid acid solution up to 40 g/L were shown to cause minimal decreases in extraction efficiency when the dissolution time is prolonged (72 hours), but this will also require more studies to optimize.

List of Abbreviations

A_{BET} – BET reactive surface area of Tail 2a ($m^2\ g^{-1}$)

g/L – grams/liter (for solid/liquid ratio)

I – ionic strength

IC – ion chromatography

M – metal cation being dissolved

$n_{M,t}$ – number of moles of M released at a given time, t (seconds)

PGM – platinum group metal

XRD – X-ray diffraction

1. Introduction

In Chapter 2, four tailings samples from Sibanye-Stillwater were characterized and their reactivity with CO_2 at ambient conditions was assessed. Characterization results showed that the tailings are heterogeneous, where the primary component is anorthite – the Ca-endmember of the plagioclase feldspar group of aluminosilicates. Observation of the tailings storage facilities indicates that older tailings have been slowly carbonating over nearly two decades. However, low reactivity in experiments simulating ambient conditions shows that a process with elevated conditions (temperature, pressure, time, pH) might be necessary to maximize the CO_2 stored in the tailings.

In Chapter 3, the Alternative ÅA Route [3] was used to increase alkalinity extraction in the Sibanye-Stillwater tailings. The Alternative ÅA Route is an indirect carbon mineralization process that uses a thermal solid/solid reaction with ammonium sulfate to extract alkalinity. While this process was optimized to extract up to 41% of the Mg in the Sibanye-Stillwater tailings, the Ca extraction was limited to 13%. This issue stems from the aqueous dissolution step: because $CaSO_4$ is practically insoluble, the extracted calcium is kept with the "waste residue" and does not progress to the carbonation step with the extracted magnesium. This study indicated that to maximize the CO_2 storage potential of the Sibanye-Stillwater tailings, a different process is necessary that can extract both calcium and magnesium.

One process that has been identified is the pH swing [4] using organic acids. Weak organic acids such as acetic acid, oxalic acid, and citric acid have been demonstrated to effectively dissolve plagioclase structures [5]. Oxalic and citric acids also have displayed selective leaching of Ca, K, Na, and Al from plagioclase [5], [6]. Because plagioclase feldspar makes up more than half of the Sibanye-Stillwater tailings, use of organic acids could prove effective in alkalinity extraction.

There are two different mechanisms at play when studying acidic mineral dissolution. Organic acids aid in dissolution of mineral structures primarily via organic ligands that attack cations at the mineral surface (i.e., ligand-promoted dissolution). Ligands like acetate, citrate, and oxalate adsorb on the mineral surface, forming complexes with metal ions that typically have high solubility [7]. Alternatively, mineral acids, such as hydrochloric and sulfuric acids, dissolve minerals via proton-promoted dissolution, where the cations at the mineral surface are protonated. The ability of either of these mechanisms to promote mineral dissolution depends on the nature of the mineral surface and the ligand, and the concentration of surface active sites, ligands, and protons [8].

Both mineral and organic acids have been used to extract alkalinity from silicate structures for the purpose of carbon mineralization, with varying degrees of success. The structures of tecto-, ino-, and phyllosilicates possess different susceptibility to proton and ligand attack. The majority of previous studies used mined material that is relatively homogenous in mineralogy (e.g., serpentine, olivine, pyroxene, plagioclase) and chemistry (i.e., primarily rich in calcium or magnesium). The heterogeneity of the Sibanye-Stillwater tailings complicates the use of acids, because while organic acids might be effective in dissolving plagioclase structures, they might not be the best option for the other mineral phases within the tailings (Table 1).

This study aimed to optimize alkalinity extraction and carbonation via a pH swing process for PGM tailings from Sibanye-Stillwater.

2. Materials & Methods

2.1 Materials

All experiments in this study were performed using the Sibanye-Stillwater tailings sample Tail 2a. This tailings sample was characterized in Chapter 2 of this Dissertation, and a summary of the results are shown in Table 1 and Table 2.

Table 1: Characteristics of Sibanye-Stillwater Tailings Sample – Tail 2a
%Ca from TIC assumes C is present as calcite ($CaCO_3$)

Silicate Group	Mineral Type	Mineral	Tail 2a	Contribution to Tail 2a	
				Mg	Ca
Tecto- (3-D framework)	Plagioclase Feldspar	**Anorthite** – $CaAl_2Si_2O_8$	54.26%	0.00%	76.60%
		Albite – $NaAlSi_3O_8$	3.94%	0.00%	0.31%
Ino- (chain)	Pyroxene	**Enstatite** – $(Mg,Fe)Si_2O_6$	11.90%	35.34%	0.00%
		Diopside – $CaMgSi_2O_6$	9.74%	13.41%	18.55%
	Amphibole	**Tremolite** – $Ca_2Mg_5(Si_8O_{22})(OH)_2$	2.24%	4.10%	2.27%
		Cummingtonite – $Mg_7(Si_8O_{22})(OH)_2$	1.27%	3.39%	0.00%
Phyllo- (sheet)	Serpentine	**Lizardite** – $Mg_3Si_2O_5(OH)_4$	8.41%	27.14%	0.00%
	Clay	**Talc** – $Mg_3Si_4O_{10}(OH)_2$	2.27%	5.37%	0.00%
	Mica	**Clinochlore** – $(Mg,Fe)_5Al_2Si_3O_{10}(OH)$	5.99%	11.25%	0.00%
TIC (%C)			0.07%	0.00%	2.27%
d(0.9) (µm)				51.17	
BET Reactive Surface Area (m^2/g)				1.29	

Table 2: Bulk Chemical Analysis of Sibanye-Stillwater Tailings Sample – Tail 2a

SiO_2	Al_2O_3	Fe_2O_3	CaO	MgO	Na_2O	K_2O	LOI
%	%	%	%	%	%	%	%
45.58	22.98	5.14	13.30	8.55	1.30	0.08	2.29

Five acids were used to facilitate the tailings dissolution in these experiments: acetic, citric, oxalic, sulfuric, and hydrochloric. Additionally, sodium hydroxide and ammonium hydroxide were used to facilitate the carbonation. Chemical suppliers are as follows: acetic acid: Sigma Aldrich, 33209; citric acid: Roth 7642.1; oxalic acid: Alfa Aesar 44410; sulfuric acid: VWR 1.00714.100; hydrochloric acid: Roth HN53.3; 20% ammonium hydroxide solution: Roth 6753.1; sodium hydroxide: Merck 1.09137.1000.

2.2 Methods

The experiments were run using the pH swing process shown in Figure 1. Unless otherwise noted, experiments involved dissolving 20 grams of Tail 2a in one liter of acid solution (0.1 M – 1.0 M) for a set time (6 – 72 hours). Each dissolution experiment was facilitated in a Schott Duran 1-liter glass volumetric flask, stirred at 500 rpm at room temperature (~22 ºC). After dissolution, solutions were filtered using a round paper filter with pore size ~15µm. Following filtration, the liquid extraction solution was stored in a 1-liter glass bottle until later use, and the mass of the solid residue was measured after drying overnight.

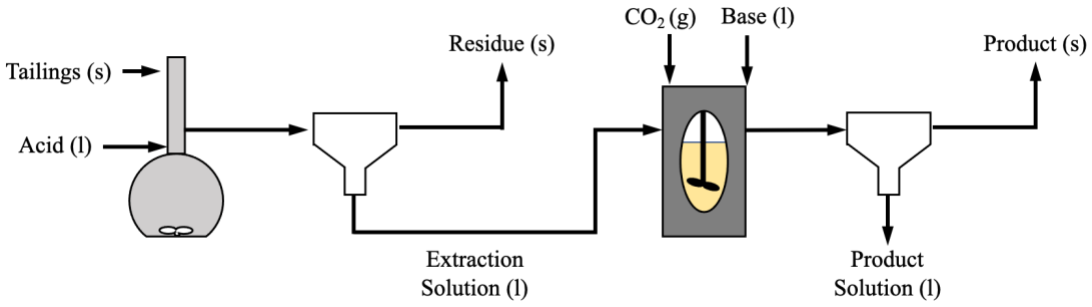

Figure 1: Process Flow Diagram for pH Swing Process

It is difficult to compare all five acids on a consistent basis due to their different dissolution mechanisms, where ligand- and proton-promoted dissolution are primarily affected by the concentration of ligands and protons (pH) in solution, respectively. For this study, it was decided to use constant solution concentration. The approximate associated pH of each acid at each concentration tested is shown in Table 3. The effects of ligand- and proton-promoted dissolution can be directly compared among oxalic, hydrochloric, and sulfuric acids, as these all provide the same solution pH at each concentration.

Table 3: Approximate pH of all acid solutions used in experiments

	Solution Concentration		
Acid	**0.1M**	**0.5M**	**1.0M**
Citric	2.1	1.7	1.6
Acetic	2.9	2.5	2.4
Oxalic	1.0	0.3	0.0
Hydrochloric	1.0	0.3	0.0
Sulfuric	1.0	0.3	0.0

In cases where carbonation was carried out, a measured volume of liquid extraction solution was added to a reactor with a base, ammonium hydroxide. Volumetric proportions of extraction solution and base were measured to achieve a pH of about 10, in order to favor carbonate anion formation in solution (pKa = 10.33). The reactor was 1.5-liter stainless steel from Juchheim with a pressure rating of 10 bar. Reaction conditions (temperature, pressure, flow rate) were monitored in real-time using Siemens WinCC for Appelhaus Reactor System. The liquid extraction solution

and base were added to the reactor as batch additions at the beginning of a carbonation experiment, prior to the introduction of CO_2. In some cases, additional base was pumped into the reactor with a ProMinent Beta® BT4a, set at a constant flow rate of 33 mL/min. After the extraction solution and base were added, the reactor was sealed and stirred at 500 rpm for about 5 minutes before adding CO_2 at a rate of 1 L min^{-1}. The CO_2 cylinder (Linde AG) was connected to the reactor via stainless steel tubing. CO_2 was steadily added to the reaction until the reactor pressure reached 9 bar, after which the CO_2 valve was shut and the reactor stirring was increased to 900 rpm. The reaction would be deemed complete when the reactor pressure was steady for at least 5 minutes. At this point, the reaction solution would be filtered using a round paper filter with pore size ~15µm. Following filtration, the liquid product solution was stored in a 1-liter glass bottle until later IC analysis, and the mass of the solid product was measured after drying overnight. The solid product would be analyzed via x-ray diffraction using a Malvern PANalytical Empyrean XRD.

Most experimental trials involved optimizing the cation extraction step of the pH swing process, where the liquid extraction solution was analyzed via Ion Chromatography (IC). The IC instrument was a Metrohm 930 Compact IC Flex, with a cation column capable of measuring Ca^{2+}, Mg^{2+}, Na^{+}, K^{+}, NH_4^{+}.

In some cases, the solid residue was analyzed for mineralogical changes relative to Tail 2a. This was done via powder X-ray diffraction (XRD) using back-mounting technique.

Experimental results were analyzed according to the percentage of cations released from Tail 2a and dissolved into the extraction solution. Aqueous cation concentration results from IC were compared to the initial cation concentration in the alkaline feedstock to yield an extraction efficiency, as in Equation 1:

$$\eta_{ex} = \frac{y_{M,ex} V_{ex}}{x_M m_{feed}} \quad (1)$$

where η_{ex} is the extraction efficiency, $y_{M,ex}$ is the volumetric concentration of the cation M in the extraction solution, V_{ex} is the total liquid extraction solution volume, x_M is the weight fraction of the cation M in the initial alkaline feedstock, and m_{feed} is the initial mass of feedstock.

3. Results

3.1 Comparison of Organic and Mineral Acids

Tail 2a was dissolved overnight (~18 hours) with separate solutions of five acids at three concentrations (0.1 M, 0.5 M, 1.0 M), with 20 grams of Tail 2a per liter of acid solution. The Ca and Mg extraction efficiencies for each acid solution are displayed in Figure 2.

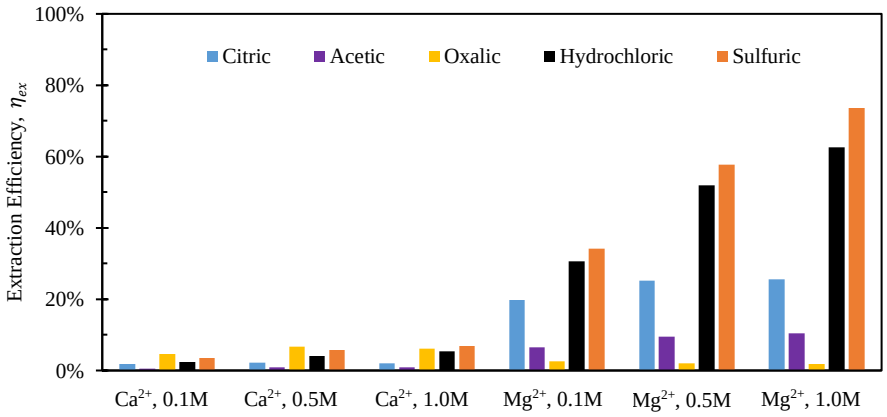

Figure 2: Extraction Efficiencies of All Acids at 01 M, 0.5 M, 1.0 M, overnight dissolution

The mineral acids (i.e., hydrochloric, sulfuric) were much more effective at extracting magnesium than the organic acids (i.e., citric, acetic, oxalic), especially at higher concentrations, indicating that proton-promoted dissolution is more prevalent for the Mg-containing mineral phases in Tail 2a (i.e., phyllosilicates, inosilicates). Meanwhile, the increase in concentration from 0.5 M to 1.0 M had minimal effect on the extraction efficiency for organic acid solutions.

Based on the relative stability of the ligand-metal complexes (Table 4), the expected performance of each organic acid would be citric > oxalic > sulfuric > acetic for calcium extraction, and oxalic > citric > sulfuric > acetic for magnesium extraction. However, the results in Figure 2 do not correlate with this predicted order (aside from the low extraction for acetic acid). While sulfuric acid creates relatively weak complexes, it also contributes strongly to dissolution via proton-promoted dissolution, with two protons per sulfate ligand. This likely explains why sulfuric acid extracted the most magnesium (and nearly the most calcium) at all concentrations. Further, the ability of sulfuric acid to contribute to ligand-promoted dissolution could explain the slightly higher extraction relative to hydrochloric acid, which only contributes to proton-promoted dissolution [9], [10].

Table 4: Stability Constants (logK) of Relevant Ligand-Metal Complexes at 25 °C, I = 0 M, unless noted

Ligand	Mg^{2+}	Ca^{2+}	Source
Cit^{3-}	3.37*	3.50*	[11]
$HCit^{2-}$	1.92*	3.09	[11]
H_2Cit^{-}	1.00	1.10	[12]
Ox_2^{2-}	4.24*	2.69**	[11]
Ox^{2-}	3.43	3.00	[11]
HOx^{-}	-	1.38*	[11]
HOx_2^{2-}	-	1.80*	[11]
HSO_4^{-}	2.23	2.31	[13]
Ace^{-}	1.27	1.18	[11]

*I = 0.1 M; **I = 1.0M

Based on stability constants, oxalic and citric acids would be expected to be more effective in extracting Mg and Ca, respectively, which contradicts the results in Figure 2. This contradiction is likely due to the difference in the way Ca and Mg are bound to the various silicate structures within Tail 2a, and is investigated further in the following sections.

3.2 Effect of Time in Organic Acid Dissolution

To further investigate the difference in alkalinity extraction among citric and oxalic acids, experiments were carried out varying the dissolution time in 0.5 M solutions. Tail 2a was dissolved in the amount of 30 grams in 1 liter of solution for dissolution times of 6 hours to 18 days, and results are shown in Figure 3.

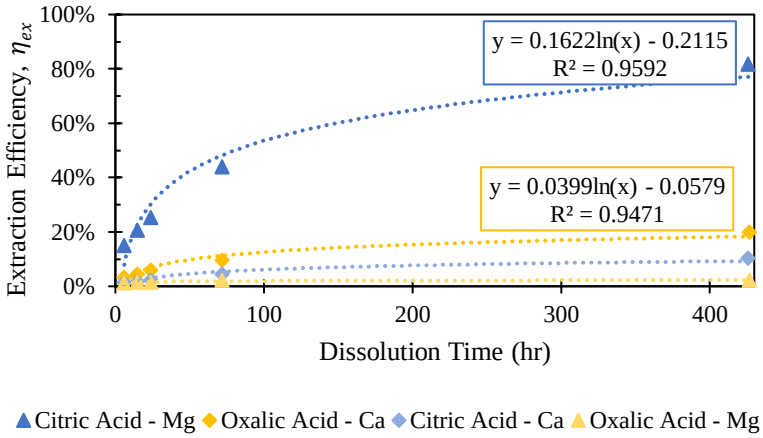

Figure 3: Effect of dissolution time in 0.5 M citric and oxalic acid solutions on Mg and Ca extraction

Indeed, dissolution at extended periods substantially increases the extraction efficiency of Mg and Ca. The Mg extraction efficiency of citric acid reaches about 44 % after dissolving for 72 hours, and even exceeds 80% after 18 days. However, oxalic acid extracts minimal amounts of Mg, only

reaching 2% after 18 days. In the case of Ca extraction, oxalic acid nearly extracts 10 % in 72 hours, and doubles that in 18 days, while citric acid extracts about half that of oxalic acid at all times.

The difference in cation extraction behavior among the two organic acids is surprising given the relatively similar complex stability constants and equal cation concentration. The effect of pH does not seem to explain this, as oxalic acid presents a lower pH, providing more protons for dissolution.

Other answers might be found in the solid residues left behind after dissolution. In Figure 4, XRD diffractograms of the solid residues show the time-dependent mineralogical changes of Tail 2a during organic acid dissolution. The largest peak at 28^{o}, associated with anorthite, steadily decreases in both acids. This decrease is more prevalent in oxalic acid, especially after 72 hours, and is coupled with the disappearance of another small anorthite peak at 22^{o}. Another major difference among the two acids is the appearance of a new phase in oxalic acid residues, around 15^{o}. This phase has been identified as whewellite – a highly insoluble calcium oxalate mineral ($CaC_2O_4 \bullet H_2O$), and is not uncommon when Ca-bearing minerals dissolve in in oxalic acid [14]–[16]. Precipitation of new phases correlates with the far longer filtration times observed for the oxalic acid solutions following dissolution, which could be caused by increased solid mass in solution. These results indicate that while oxalic acid is effectively dissolving the anorthite structure, it is forming undesired Ca-precipitates which are not staying in solution for later carbonation.

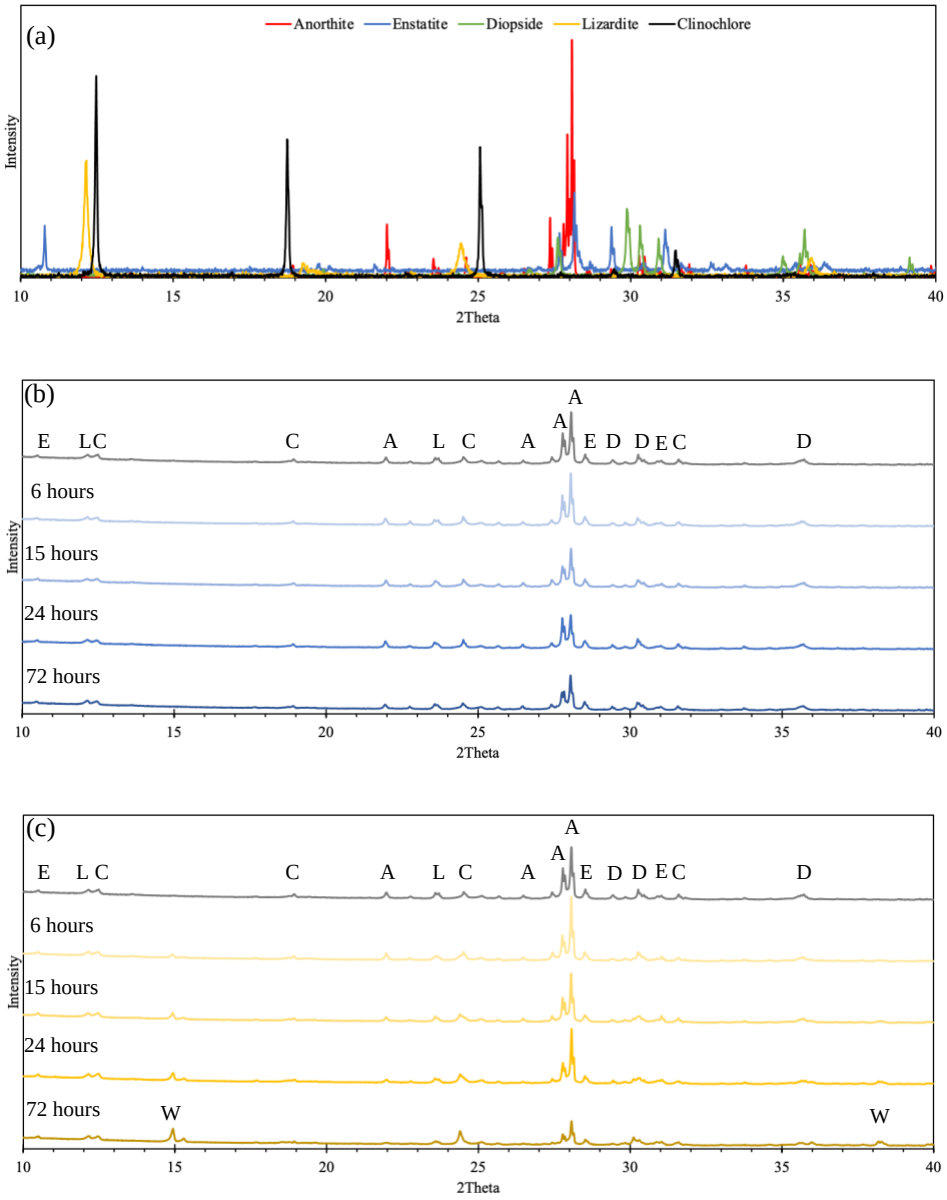

Figure 4: Comparison of XRD diffractograms for: (a) raw minerals constituting > 5% of mineral phases in Tail 2a, data from RRUFF database; solid residues from dissolution in 0.5 M solutions of (b) citric acid and (c) oxalic acid. In (b) and (c), top diffractogram is unreacted Tail 2a. Letters represent mineral phases: A – anorthite, C – clinochlore, D – diopside, E – enstatite, L – lizardite, W - whewellite

The precipitation of whewellite during dissolution in oxalic acid could provide some explanation of the extraction efficiency results observed in Figure 2. First, the precipitation of whewellite from solution removes available oxalate ligands to extract Mg [17], potentially causing the minimal Mg extraction of oxalic acid. Further, if extracted calcium is precipitating as well, then it is not in solution during IC analysis, meaning that the Ca extraction efficiency for oxalic acid is in fact higher than shown in Figure 2. This finding can be interpreted as good news and bad news – while it is good that oxalic acid actually has extracted Ca and dissolved anorthite better than initially suggested, the precipitation of highly insoluble whewellite may in fact render the extracted Ca unusable for the purpose of carbon mineralization.

Perhaps more impactful is the interaction of oxalate and aluminum, which form strong multiligand complexes with each other [18]. Because plagioclase is dissolved at the Al-O sites [10], every dissolved Ca cation would require formation of a strong complex (e.g., $AlOx_2^-$), essentially removing oxalate anions from solution to react with Mg-bearing phases.

The explanations for extraction in oxalic acid solution do not hold for that in citric acid solution. In Figure 4, the anorthite peak is steadily dissolved over time in citric acid (albeit at a slower rate than in oxalic acid), but there is no evidence of citrate precipitation to explain a decreased Ca extraction, potentially nullifying the hypothesis that Ca extraction in oxalic acid is actually higher than indicated in IC results. This finding remains an open question that should be further investigated.

3.3 Effect of Solid/Liquid Ratio

In an attempt to minimize the volume of acid consumed by the mineralization process, the ratio of solid Tail 2a mass to acid solution volume was increased from the 20 g/L ratio used in the initial studies. First, the ratio was increased to 30 g/L in an overnight (~18 hour) dissolution period. The results (Figure 5a) show that during overnight dissolution, the extraction efficiency of Mg^{2+} and Ca^{2+} in both acids decreased due to an increase in the solid/liquid ratio. This would be expected, as less ligands are available to extract each cation. However, this same effect was not observed using elevated solid/liquid ratios during 72-hour dissolution (Figure 5b). In this case, the decreases in efficiency due to increased solid/liquid ratios were minimized, and even some marginal increases in efficiency were observed for oxalic acid. These observations have practical implications for later scale-up, indicating that if dissolution time is long enough, less acid is necessary for similar extraction efficiency results.

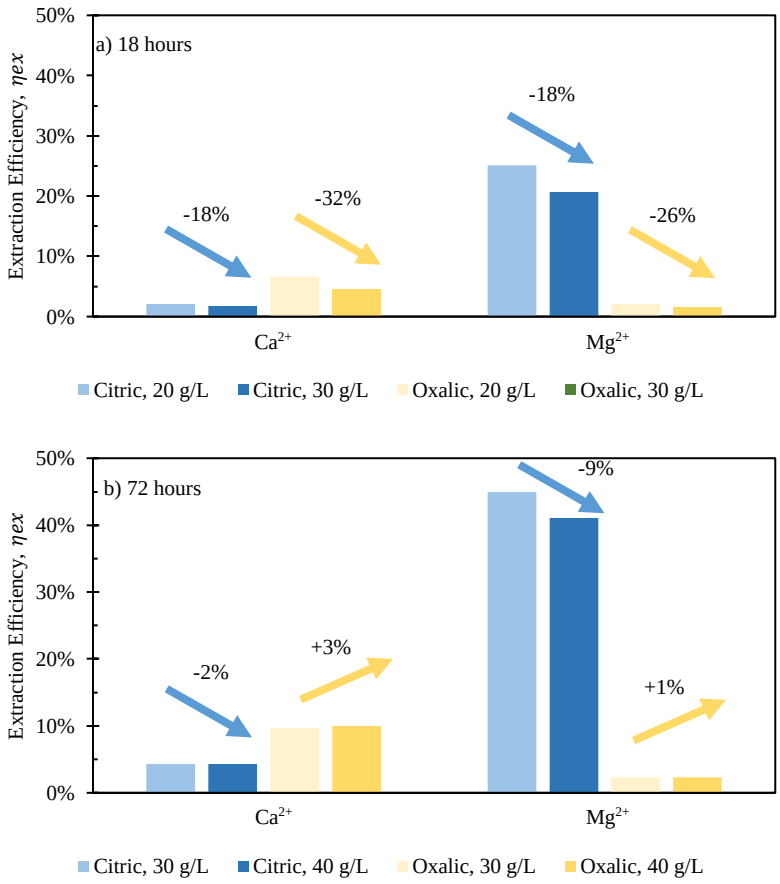

Figure 5: Effect of solid/liquid ratio on alkalinity extraction in 0.5 M citric and oxalic acid solutions dissolving for (a) 18 hours and (b) 72 hours. Percentage differences are displayed above each set of bars

The effect of solid/liquid ratio was also investigated on extraction in sulfuric acid solutions. Two experiments were performed with 1-liter 0.5 M and 1.0 M sulfuric acid solutions, each dissolving 30 g Tail 2a for 72 hours. In Figure 6, these results are compared to results of sulfuric acid solutions from Figure 2. When comparing solutions of the same concentration, the Ca^{2+} and Mg^{2+} extraction efficiency results differ drastically.

In both solution concentrations, the extraction efficiency for Ca^{2+} increased, while it decreased for Mg^{2+}. There might be a mechanism occurring at longer dissolution times that is preventing Mg^{2+} from being released with sulfuric acid. Oxoanions, like sulfates, can inhibit dissolution by forming multinuclear dissolution-inert surface complexes, occupying otherwise reactive sites [8], [19]. However, it is difficult to elucidate what exactly caused these observations because two parameters were changed between the two sulfuric acid trials. More studies should be done to further investigate dissolution with sulfuric acid at various solid/liquid ratios and dissolution times.

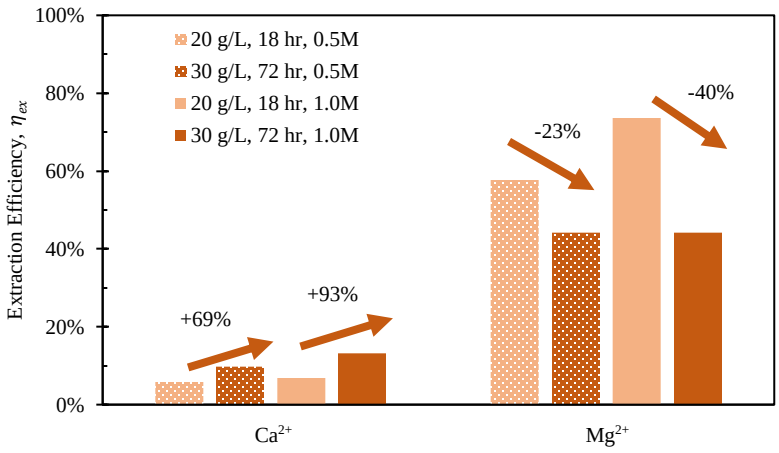

Figure 6: Effect of solid/liquid ratio on alkalinity extraction in 0.5 M and 1.0 M sulfuric acid solutions dissolving for 18 hours and 72 hours. Percentage differences are displayed above each set of bars

3.4 Series and Parallel Dissolution for Increased Efficiency

To further elucidate the effect of different acids on dissolution of the varying mineral phases in Tail 2a, and potentially further increase cation extraction, multiple acids were combined in one process. As illustrated in Figure 7, this was be performed in two different ways: (1) "parallel," where both citric and oxalic acids are combined in one reaction solution, and (2) "series," where one acid is used to produce a liquid extraction solution and solid residue, and a different acid is used to dissolve the solid residue.

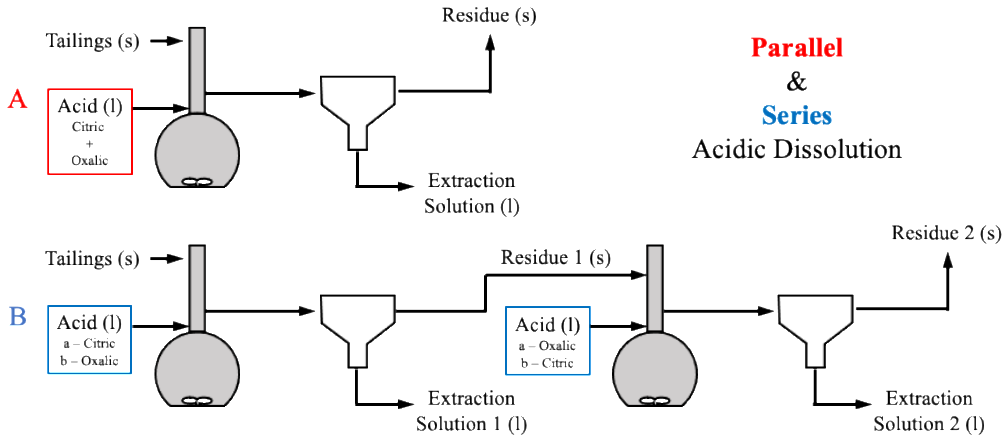

Figure 7: Process flow diagrams of (a) parallel and (b) series acidic alkalinity extraction process configurations

3.4.1 Parallel dissolution with organic acids

Parallel acid dissolution was performed for 15 hours and 72 hours, where citric and oxalic acid were added to one 1-liter solution, each with concentration of 0.5 M and 30 g Tail 2a. In Figure 8, extraction results from parallel dissolution are compared with results from single acid dissolution, which were shown in Figure 3.

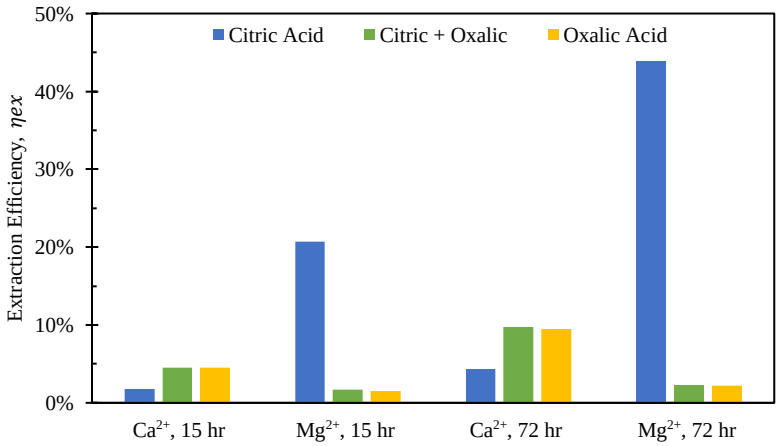

Figure 8: Comparison of extraction efficiency through parallel dissolution (green) with single acid dissolution (blue/yellow) at 15 and 72 hours. In all cases, each acid was 0.5 M in solution

Rather than increasing the extraction of both cations, the parallel acid dissolution showed results that are practically identical to those of oxalic acid. Evidently, when citric and oxalic acids are combined at the same concentration with Tail 2a, oxalic acid exhibits a dominance over citric acid. As noted in Table 4, oxalate forms stronger Mg complexes than citrate. This could be evidence that oxalate is irreversibly adhering to the surface of Mg-containing mineral phases in Tail 2a, essentially rendering them inert. If this is true, it could also explain the limited Mg extraction in oxalic acid observed in Figure 3.

3.4.2 Series dissolution with organic acids

The series dissolution experiments involved using the solid residues generated by the time-trial experiments displayed in Figure 3. In this case, 20 grams of solid residue were placed in a 1-liter, 0.5 M solution of citric or oxalic acid, where the acid used in this second step is the opposite of the acid used in the first step (Figure 7). In this second step, the solid residues were dissolved in the 1-liter acid solutions for 16 hours. Extraction efficiency results are displayed in Figure 9, where data are organized by the time of dissolution for the first step of the series, and the naming convention refers to the order of acid used (e.g., citric/oxalic means citric acid in the first step, followed by oxalic acid in the second step).

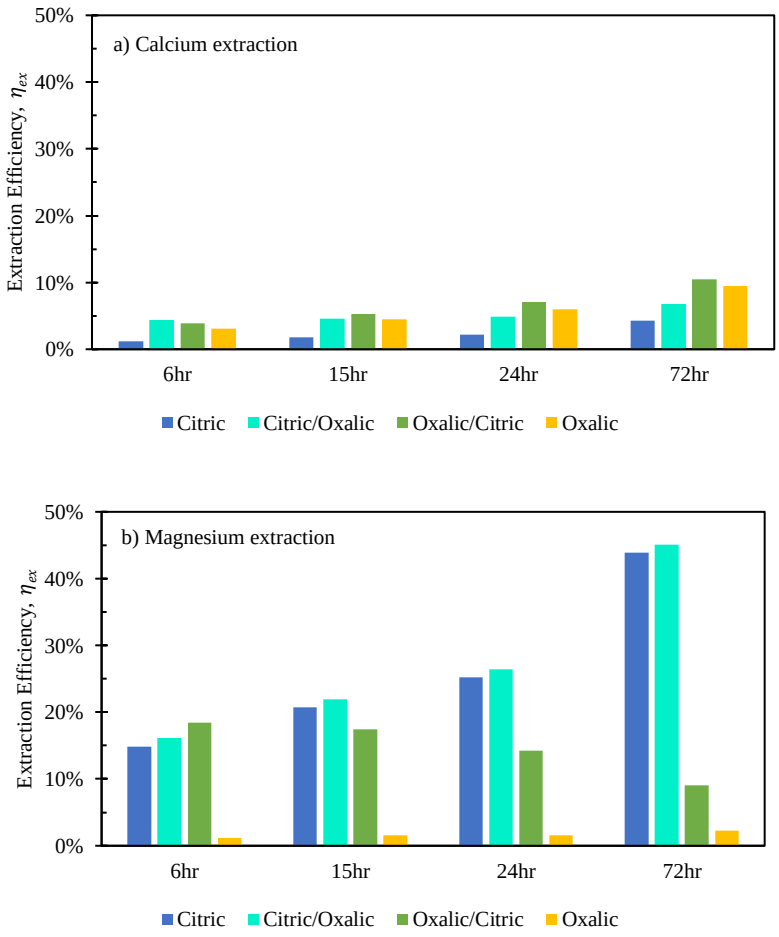

Figure 9: Extraction efficiency of (a) Ca and (b) Mg in organic acid series dissolution, compared to single acid dissolution. Data organized by the time of dissolution for the first step of the series. Naming convention refers to the order of the acid(s) used.

Extraction of Mg for oxalic/citric improves upon that of oxalic alone, but this improvement decreases as with increasing time of initial oxalic acid dissolution. This might be further evidence of irreversible oxalate adsorption onto mineral surfaces, where longer dissolution times allow more oxalate adsorption.

Although citric/oxalic series dissolution improves upon the Ca extraction of citric acid alone, it remains relatively constant at all four times. As proposed earlier, the Ca extraction from anorthite could in fact be enhanced with citric/oxalic dissolution, but the Ca could have precipitated as whewellite. Some evidence shows that Mg can inhibit Ca-oxalate aggregation [20]. In citric/oxalic, Mg has already been removed from Tail 2a via citric acid dissolution, providing less Mg to inhibit whewellite precipitation during oxalic acid dissolution.

Viewing the total alkalinity extracted on a molar basis gives a sense of how much CO_2 can be stored with each dissolution method. As illustrated in Figure 10, while Mg extraction is already higher than Ca extraction on a mass basis, the disparity is exacerbated in overall alkalinity extraction on a molar basis due to the lower molecular weight of magnesium.

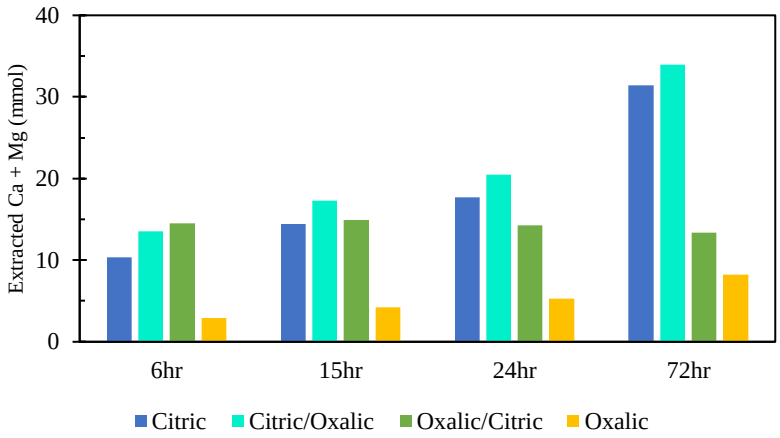

Figure 10: Combined alkalinity extraction from acid series dissolution, compared to single acid dissolution

Although oxalic acid was effective in releasing Ca, its poor Mg extraction causes it to have the lowest overall alkalinity extraction. Meanwhile, the reduced Ca extraction of citric acid is compensated by its high Mg extraction. While citric/oxalic has the highest overall extraction at all times tested, the marginal increase in extraction over that of citric is likely not worth double the acid consumption. Hence, citric acid is the optimal organic acid for dissolving Tail 2a among those tested.

3.4.3 Series dissolution with mineral acids

Series dissolution experiments were also performed with the residues produced from the mineral acid experiments displayed in Figure 2. As noted by Table 3, the three acids tested here provide the same pH at 0.5 M concentrations, so ligand- and proton-promoted dissolution can be directly compared in these experiments. Here, 10 grams of solid residue were placed in a 0.5-liter, 0.5 M solution of oxalic acid for 72 hours. Results are displayed in Figure 11, where data are organized by the solution concentration for the first step of the series, and the naming convention refers to the order of acid used (e.g., hydrochloric/oxalic means hydrochloric acid in the first step, followed by oxalic acid in the second step).

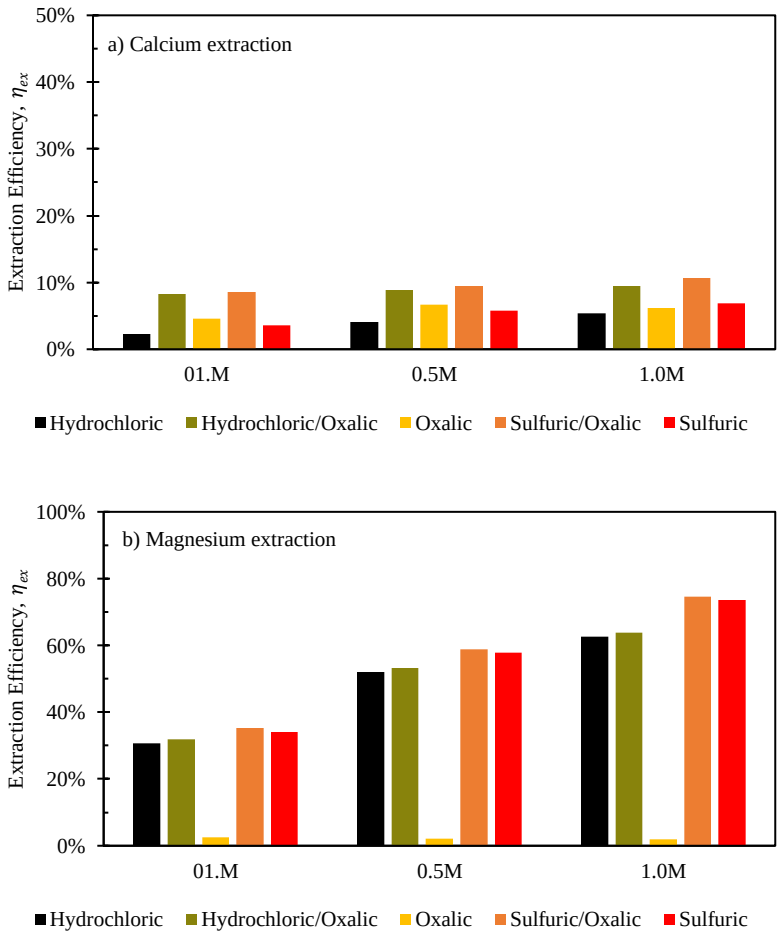

Figure 11: Extraction efficiency of (a) Ca^{2+} and (b) Mg^{2+} in mineral acid series dissolution, compared to single acid dissolution. Data organized by the solution concentration step of the series. Naming convention refers to the order of the acid(s) used

As expected from the poor Mg extraction of oxalic acid alone, the mineral/oxalic acid series dissolution had minimal effect on Mg^{2+} extraction. However, in all cases, the mineral/oxalic acid series dissolution extracted more Ca than any acid alone. In fact, the Ca extraction of mineral/oxalic series dissolution is nearly equal to the sum of the extraction from the two individual acids. The increase in Ca extraction might have been caused, in part, by the longer dissolution time of the oxalic acid step – which was 72 hours, compared to the 18-hour duration of the single acids. But another explanation could be that different mineral phases within Tail 2a are targeted by proton- and ligand-promoted dissolution. Perhaps oxalic acid effectively extracts Ca from anorthite (plagioclase), while the mineral acids extract Ca from diopside (pyroxene). Organic acids like oxalic acid have been shown to be more effective than mineral acids for dissolving plagioclase structures [5], while having a negligible effect on Mg extraction from pyroxenes [21]. Further, proton-promoted dissolution has been suggested to preferentially occur with pyroxenes over plagioclase [22].

Again, the total alkalinity extraction from the mineral acid series is displayed on a molar basis in Figure 12. Both series dissolutions out-performed any acid alone, and the sulfuric/oxalic series

consistently had the highest overall dissolution. As is the case with citric/oxalic dissolution, the increase of sulfuric/oxalic over sulfuric alone may not be worth the cost of additional acid consumption.

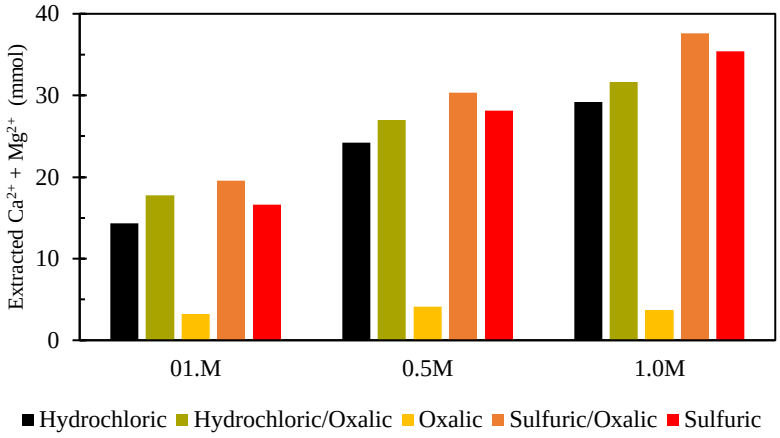

Figure 12: Combined alkalinity extraction from mineral acid series dissolution, compared to single acid dissolution

4. Discussion

Results in Section 3 can be further unfolded to reveal broader implications for storing CO_2 in PGM tailings such as those of Sibanye-Stillwater.

4.1 Estimating Tail 2a Dissolution Rates

In this study, the parameter that was most influential on extraction efficiency was the time of dissolution. From a standpoint of additional emissions, elevation of time might be less impactful than parameters like energy and material usage, which can cause additional emissions and might defeat the purpose of carbon mineralization [23]. Discussion of the dissolution rates observed in this study can give further insight into the extent the extraction efficiency can be improved by dissolution time. Using the data in Figure 3 and the BET reactive surface area of Tail 2a, dissolution rates can be calculated in mol m^{-2} s^{-1}.

$$R_M(mol\ M\ m^{-2}s^{-1}) = \frac{n_{M,t}}{A_{BET}t} \quad (2)$$

where M represents the metal cation being dissolved, $n_{M,t}$ is the number of moles of M released at a given time, t (seconds), and A_{BET} is the BET reactive surface area of Tail 2a (m^2 g^{-1}). Measured dissolution rates are plotted in Figure 13 with the dissolution rates of other minerals published by Palandri and Kharaka [24]. Additionally, the release of Ca at ambient conditions measured in Chapter 2 is plotted for comparison. (Measured ambient release of Mg is omitted because of data below instrument detection limit; see Chapter 2.)

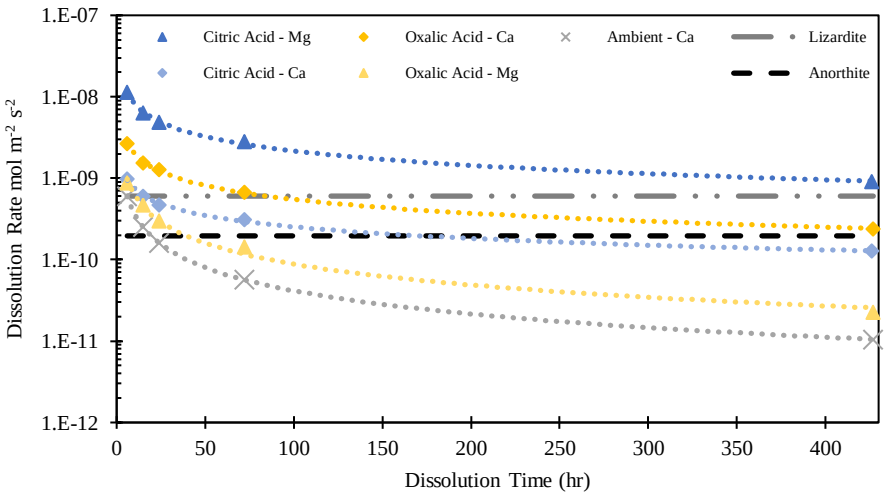

Figure 13: Measured Dissolution Rates based on release of Mg and Ca in 0.5M citric and oxalic acid solutions. Compared to measured Ca release rate (Chapter 2) and steady state anorthite dissolution [24], both at ambient temperature/pressure and pH=4.49

In both acid solutions, Ca release rates exceed the rate measured at ambient conditions. Based on the findings in Chapter 2, it is expected that Ca^{2+} is being leached from anorthite. As shown in Figure 13, the steady state release rates of Ca^{2+} in both acid solutions converge upon the steady state rate of anorthite dissolution at ambient conditions. The release rate of Mg in citric acid solution converges upon the steady state dissolution rate of lizardite, suggesting that citric acid is leaching Mg from the phyllosilicate content in Tail 2a.

4.2 Relating Dissolution Mechanisms and Mineral Phases

In this chapter, the ability of various mineral and organic acids to extract alkalinity from the Sibanye-Stillwater tailings was tested. The comparison of dissolution in single acid solutions with "parallel" and "series" dissolution configurations gives insight into how the acids attack the varying mineral surfaces within heterogeneous PGM tailings.

In 0.5 M citric acid, about 44% of Mg was extracted in 72 hours. In Figure 3, this extraction was achieved during the linear portion of the curve, indicating that this leaching occurs before steady state dissolution. As dissolution extends from 3-18 days, the Mg extraction in citric acid nearly doubles. This evidence suggests that citric acid extracts Mg from phyllosilicates in Tail 2a (about 44% of the Mg in Tail 2a) at a relatively fast rate, and continues to extract Mg from inosilicates when dissolution time is extended.

Ligand-promoted dissolution of Mg-bearing minerals in Tail 2a might also be expected to occur in oxalic acid solution, especially because oxalate makes strong complexes with Mg (Table 4). However, Mg extraction efficiency in oxalic acid was extremely limited, only reaching about 2% after 72 hours without improving over 18 days. Oxalate might have irreversibly adhered to the mineral surface of the phyllo- and inosilicates within Tail 2a, as suggested by multiple experiments in this study. When oxalic and citric acids were combined in solution, Mg extraction matched that of oxalic acid alone, rather than the much higher Mg extraction of citric acid (Figure 8). Further,

Mg extraction efficiency in the oxalic/citric series dissolution decreased with increasing oxalic acid dissolution time (Figure 9b). These results indicate that oxalate strongly interacts with Mg atoms at the phyllo- and inosilicate surface, irreversibly binding to the surface and rendering it inert. This finding is different than what has been previously reported with oxalate and serpentine [25], potentially due to such high oxalate concentrations and low pH used in these experiments.

The mineral acids (sulfuric, hydrochloric) readily released Mg with much higher extraction efficiencies in 18 hours than citric acid did in 72 hours, extracting up to about 74% with 1.0 M sulfuric acid solution. This amount exceeds the Mg present in any one mineral phase, suggesting that both ino- and phyllosilicates containing Mg in Tail 2a can quickly undergo proton-promoted dissolution.

In addition to Mg release, inosilicate dissolution would result in Ca release (diopside, tremolite). This might explain the limited Ca extraction exhibited by the mineral acids, which are known to be less effective in dissolving tectosilicates such as plagioclase [5], [9], [10], [19], [21]. This hypothesis is reinforced by the mineral/oxalic acid series dissolution, where the mineral acids appeared to have extracted Ca from different mineral sources than oxalic acid (Figure 11a).

The Ca extraction of citric and oxalic acid are controlled by ligand-promoted dissolution of anorthite, where the ligands primarily attack the Al-O sites to liberate Ca by forming Ca-ligand complexes. Based on the comparative XRD diffractograms of the solid residue left behind after dissolution, both organic acids effectively dissolved anorthite over the 72-hour period, especially oxalic acid. However, despite anorthite holding about 77% of the Ca in Tail 2a, dissolution in 0.5M oxalic and citric acid solutions resulted in Ca extraction efficiencies of only about 20% and 10%, respectively.

For oxalic acid, the low Ca extraction efficiency can be explained by precipitation of a Ca-oxalate salt, whewellite. When solid whewellite precipitates, calcium is removed from solution and is not measured in the extraction solution. However, this does not explain the low Ca extraction efficiency of citric acid. Another possibility is that some stable Ca complexes with citrate and oxalate are undetected by ion chromatography, but evidence of this in the literature is lacking.

The behavior of mineral phases within Tail 2a undergoing dissolution with the acids tested in this study is summarized in Table 5, corroborated with other published literature results. This table can be used to develop strategies on how to approach acid-promoted carbon mineralization with heterogenous tailings like those of Sibanye-Stillwater. Tailings rich in a particular silicate group may have higher alkalinity extraction in a corresponding acid with darker shading in Table 5.

Table 5: Predictions of dissolution behaviour of mineral phases within heterogenous tailings with various organic and mineral acids

Tail 2a		Citric	Oxalic	Sulfuric	Hydrochloric
Tectosilicates	Mg (0%) Ca (77%)	Attacks Al-O bonds to dissolve structure [5], [9], slower than oxalic	Attacks Al-O bonds to dissolve structure [5], [9], [10], [17], [21]; precipitates whewellite [14], [15]	Sulfate sticks to surface [8], [19]; protons less effective than ligands [5]	Protons less effective than ligands [5], [9], [26]
Inosilicates	Mg (56%) Ca (21%)	Leaches only at extended periods [27]	Adheres to surface, makes inert [21], [27]	Leaches faster than tectosilicates [22]	Leaches clinopyroxene [21]; faster than tectosilicates [22]
Phyllosilicates	Mg (44%) Ca (0%)	Selectively leaches Mg, [25]; slower than mineral acids	Less effective than citric [25] Adheres to surface, makes inert	Leaches completely at high rate [28], [29]	Leaches completely at high rate [29], [30]

4.3 Problems with Carbonation

The ultimate motivation of carbon mineralization is to store CO_2 in the form of carbonate minerals. For the pH swing process, this involves a carbonation step after the alkalinity extraction via acidic dissolution. Unfortunately, the carbonation step of the pH swing process presented multiple complications during this study.

The most recent carbonation trial used an extraction solution from a 72-hour dissolution in a 0.5 M citric acid solution with 30 g/L. The change in carbonation reactor temperature, pressure, and flows of base (NaOH) and CO_2 are plotted in Figure 14. At the beginning of the carbonation trial, 750 mL of the extraction solution was added to the reactor with about 250 mL NaOH. Once the reactor was sealed, additional NaOH was pumped into the reactor until reaching a pH of 11.8. Samples of about 10 mL were taken at each red X point on Figure 14 to manually measure the pH. After the pH of 11.8 was measured, the NaOH was stopped and CO_2 was added to the reactor at a rate of 1 L/min until the reactor pressure reached 9 bar, at which point the CO_2 flow would be stopped. When the pressure decreased to about 6.5 bar, the CO_2 flow was restarted, and this process was repeated. After the CO_2 flow was halted again, the pH was measured and found to have returned to neutral, so more NaOH was added to the reactor along with CO_2 until the pressure was 9 bar again. After one final input of CO_2, the reactor was allowed to sit for about one hour while stirring at 500 rpm.

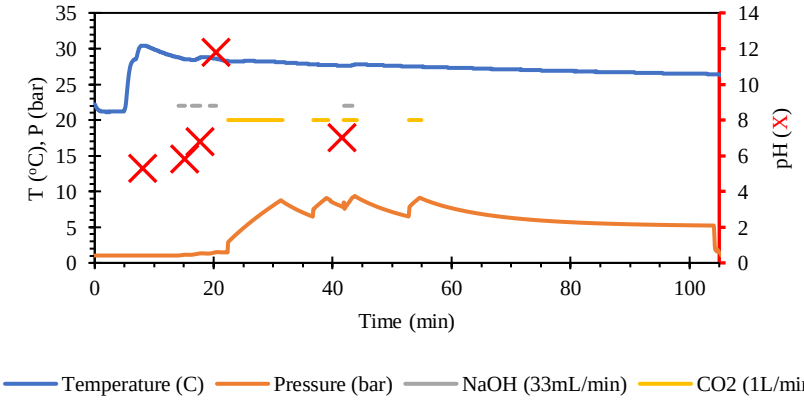

Figure 14: Reaction progress for carbonation of extraction solution (citric acid, 72 hr, 30 g L^{-1}). Red X indicates pH measurements. Flow of NaOH and CO_2 was constant at 33 mL/min and 1 L/min, respectively, and associated lines on plot indicate when flow as turned on.

About 3.3 grams of precipitates were produced from the reaction, and are currently unidentified by XRD, but appear to be amorphous materials. These precipitates were likely amorphous carbonates, but this cannot be confirmed without performing a total carbon analysis which was not available at the time of experimentation. Investigation on controlling the transition of amorphous to crystalline carbonates will be carried out in later trials [31].

This carbonation trial highlights the drawbacks of the carbonation system used in this study. As implied in the process name, carbonation in the pH swing process requires addition of a base to "swing" the pH up to high levels (pH > 9) to facilitate carbonate anion formation. In initial experiments, ammonium hydroxide was used as the base. When ammonium hydroxide was added to oxalic acid extraction solutions, large volumes of a white "snowy" substance was precipitated, and was later identified as ammonium oxalate (photos in Appendix). Sodium hydroxide was used as the base after this realization.

Although enough base was added to the acidic extraction solution to reach a pH > 9, the reactor solution pH would decrease upon introduction of CO_2. In the carbonation reactor setup, there was no convenient way to monitor pH in real time. Rather, small samples were intermittently taken from the reactor, and their pH was measured with a portable pH meter. The volume of these small samples would accumulate over the entire experiment, making it difficult to maintain a consistent mass balance. Future trials should have an *in-situ* pH measurement built into the reactor system.

Further, pumping sufficient volumes of base to increase the pH would sometimes result in filling the 1.5-liter reactor volume. Hence, preparation of the reactor required careful planning of how much extraction solution and base volume to start with in order to leave sufficient room for additional base.

5. Conclusions and Recommendations

5.1 Results Summary and Climate Context

The highest carbonation efficiencies measured in this study are tabulated in Table 6, coupled with estimations of the CO_2 that could potentially be stored in all of the tailings at Sibanye-Stillwater (~1 Mt-tailings per year) and in all of the tailings projected to be produced at nickel and PGM mining operations (3.5 Gt yr^{-1}) [2].

Table 6: Highest extraction efficiencies measured in this study
Max CO_2 Capacity assumes all extracted Ca/Mg is converted to carbonate with 1:1 ratio of cation to CO_2

Acid	Acid Conc. (mol L^{-1})	Time. (hr)	s/L ratio (g L^{-1})	Extraction Efficiency		Max CO_2 Capacity (kgCO_2 t-tailings^{-1})	Potential CO_2 Storage (tCO_2 yr^{-1})	
				Ca^{2+}	Mg^{2+}		Stillwater (1 Mt yr^{-1})	World (3.5 Gt yr^{-1})
Citric	0.5	72	40	4.28%	41.09%	4.3	4,283	14,990,199
Oxalic	0.5	72	40	10.03%	2.36%	1.3	1,268	4,438,356
Citric	0.5	426	30	10.29%	81.73%	8.7	8,704	30,464,223
Oxalic	0.5	427	30	19.82%	2.10%	2.3	2,267	7,936,142
Hydrochloric	1.0	18	20	5.34%	62.63%	6.4	6,404	22,414,071
Sulfuric	1.0	18	20	6.88%	73.55%	7.6	7,585	26,546,379
Citric / Oxalic	0.5 / 0.5	72 + 16	30 / 20	6.79%	45.08%	4.9	4,918	17,213,236
Sulfuric / Oxalic	1.0 / 0.5	18 + 72	20 / 20	10.65%	74.53%	8.1	8,071	28,247,181

Overall, the highest Mg extraction efficiencies were found with elevated conditions of time (citric acid, 18 days) and pH (1.0 M sulfuric acid solutions). These Mg extraction efficiencies far exceed those achieved at ambient conditions in Chapter 2 (< 1% Mg was labile) and by the Alternative ÅA Route used in Chapter 3 (~ 38 % Mg extracted at 450 ^{o}C using ammonium sulfate).

While the Ca extraction in this study also exceeded that of ambient conditions in Chapter 2 (< 3% Ca was labile), it only exceeded the level achieved by the Alternative ÅA Route (13%) when the tailings dissolved in 0.5 M oxalic acid solution for 18 days. The structure of anorthite which binds more than 75 % of the Ca in Tail 2a has been proven too restrictive for proton-promoted dissolution at the conditions tested in this study.

5.2 Recommendations for Future Work

In this study, for the first time, the effect of different acid solutions, solution concentration, dissolution time, and solid/liquid ratio on the alkalinity extraction of heterogeneous PGM mine tailings was examined for the purpose of carbon mineralization. While results give insight into how to best approach pH swing carbon mineralization for PGM mine tailings, further work is necessary to develop an efficient and economic process that can store CO_2 in the billions of tonnes of ultramafic mine tailings that will be generated in the coming century [2].

To store CO_2 in mine tailings with the alkalinity extraction methods used in this study, the problems with the carbonation step must be addressed and overcome (Section 4.3). These experiments will be ongoing. Specifically, in the near term, the use of an *in-situ* pH meter and a

more effective base is necessary to promote carbonate anion formation in solution. In the longer term, a control loop might aid in maintaining a proper pH level in solution.

An alternative acid to use that was not tested in this study is carbonic acid (CO_3^{2-}). Using carbonic acid has the potential to allow the dissolution and carbonation to occur in one step. Further, acid consumption would not be a problem like it is with the acids tested in this study, because carbonic acid consumption would mean the tailings are being carbonated. Hence, process economics could be improved by requiring less process equipment and consuming less raw material throughout the process. This was tested in Chapter 2 with pH of 4.4 with very limited cation release. However, by using a more concentrated acid solution (with lower pH), stirring, and perhaps pressure, Ca and Mg extraction might increase.

The solid/liquid ratio used in these experiments should be further optimized to minimize acid consumption. This is especially useful in the case of using citric dissolution or citric/oxalic series dissolution at prolonged dissolution times, where the solid/liquid ratio was shown in Figure 5 to be less of a detriment to extraction efficiency.

Molecular studies could be undertaken in order to better understand the effect of surface chemistry on cation extraction in heterogeneous mixtures. Additionally, undertaking a geochemical modelling study for this system could be beneficial. The relatively high concentrations of protons and ligands used in this study may likely had an impact on ligand adhesion to the surface and on whewellite precipitation. Geochemical modeling software like PHREEQC might help determine optimal acid concentrations that maximize calcium and magnesium extraction into solution.

Previous studies of the effect of ligands and protons on mineral dissolution typically use higher pH and lower acid concentrations than used in this study. Such high ligand and proton concentrations may have oversaturated the system, causing results to differ from literature (e.g., increased whewellite precipitation, surface inhibition of oxalate). Additionally, the low pH from the extraction step used here results in needing high amounts of base to increase pH for the carbonation step. Additional trials should be run with acids at lower concentrations ($\leq$ 0.1 M) at extended dissolution times.

This study compared acids based on concentration, which would directly relate to material consumption for economic purposes. However, a future study should compare acid solutions based on pH. While oxalic, hydrochloric, and sulfuric acids had approximately equivalent pH values at the concentrations tested, citric and acetic acids had higher pH values. Considering this pH discrepancy, citric acid extracted Mg rather effectively. More studies with citric acid at lower pH, or with other acids at higher pH, would provide a better comparison of the effect of proton- and ligand-promoted dissolution.

If the use of acids to leach alkalinity from the tailings is to be continued, another consideration to be made is the emissions associated with the acids used. For instance, sulfuric acid production has associated SO_2 emissions of 2-48 kg/t-H_2SO_4 (depending on process efficiency) and CO_2 emissions of 4.05 kg/t-H_2SO_4 [32]. These potential impacts might warrant a study on new potential sources of acids to use in a mineralization process like the one used in this study. Acid might be able to be sourced from acid mine drainage, but this would vary at each mine [33], as it is unlikely

to be available at Sibanye-Stillwater [34]. Alternatively, there are some studies of using CO_2 to produce organic acids like acetic acid [35] and oxalic acid [36], [37]. The potential to use a carbon-negative reagent would further increase the environmental beneficiation of the process.

In this study, the method of liquid solution composition analysis that was available (IC) could only measure Na, K, Ca, Mg. Concentrations of Al and Si are also very important to elucidate which mineral phase is dissolving. Future studies should ensure a method can also measure Al and Si concentrations.

Further TEA might also be necessary to determine whether it is economically advantageous to pursue the pH swing process tested in this chapter rather than the processes used in previous chapters. This will be studied in Chapter 5.

References

[1] C. M. Woodall, I. Piccione, M. Benazzi, and J. Wilcox, "Capturing and Reusing CO_2 by Converting it to Rocks," *Front. Young Minds*, vol. 8, no. 592018, 2021.

[2] P. Renforth, "The negative emission potential of alkaline materials," *Nat. Commun.*, vol. 10, no. 1401, 2019.

[3] R. Zevenhoven, M. Slotte, E. Koivisto, and R. Erlund, "Serpentinite Carbonation Process Routes using Ammonium Sulfate and Integration in Industry," *Energy Technol.*, vol. 5, no. 6, pp. 945–954, 2017.

[4] A. Azdarpour, M. Asadullah, E. Mohammadian, H. Hamidi, R. Junin, and M. A. Karaei, "A review on carbon dioxide mineral carbonation through pH-swing process," *Chem. Eng. J.*, vol. 279, pp. 615–630, 2015.

[5] S. A. Welch and W. J. Ullman, "The effect of organic acids on plagioclase dissolution rates and stoichiometry," *Geochim. Cosmochim. Acta*, vol. 57, pp. 2725–2736, 1993.

[6] W. Shotyk and H. W. Nesbitt, "Ligand-Promoted Dissolution of Plagioclase Feldspar: A Comparison of the Surface Chemistry of Dissolving Labradorite and Bytownite Using SIMS," in *Geochemistry of the Earth's Surface and of Mienral Formation*, 1990, pp. 320–321.

[7] E. R. Bobicki, Q. Liu, and Z. Xu, "Ligand-promoted dissolution of serpentine in ultramafic nickel ores," *Miner. Eng.*, vol. 64, pp. 109–119, 2014.

[8] W. Stumm, "Reactivity at the mineral-water interface: Dissolution and inhibition," *Colloids Surfaces A Physicochem. Eng. Asp.*, vol. 120, no. 1–3, pp. 143–166, 1997.

[9] W. Shotyk and H. W. Nesbitt, "Ligand-Promoted Dissolution of Plagioclase Feldspar: A Comparison of the Surface Chemistry of Dissolving Labradorite and Bytownite Using SIMS," in *Geochemistry of the Earth's Surface and of Mineral Formation*, 1990, pp. 320–321.

[10] W. Shotyk and H. W. Nesbitt, "Incongruent and congruent dissolution of plagioclase feldspar: effect of feldspar composition and ligand complexation," *Geoderma*, vol. 55, no. 1–2, pp. 55–78, 1992.

[11] A. E. Martell and R. M. Smith, *Critical Stability Constants Volume 3: Other Organic Ligands*. Springer, 1977.

[12] P. G. Daniele, C. Foti, A. Gianguzza, E. Prenesti, and S. Sammartano, "Weak alkali and alkaline earth metal complexes of low molecular weight ligands in aqueous solution," *Coord. Chem. Rev.*, vol. 252, no. 10–11, pp. 1093–1107, 2008.

[13] R. M. Smith and A. E. Martell, *Critical Stability Constants Volume 4: Inorganic Complexes*. Springer, 1976.

[14] G. Gadikota, C. Natali, C. Boschi, and A. H. A. Park, "Morphological changes during enhanced carbonation of asbestos containing material and its comparison to magnesium silicate minerals," *J. Hazard. Mater.*, vol. 264, pp. 42–52, 2014.

[15] L. L. Stillings, J. I. Drever, and S. R. Poulson, “Oxalate adsorption at a plagioclase (An_{47}) surface and models for ligand-promoted dissolution,” *Environ. Sci. Technol.*, vol. 32, no. 19, pp. 2856–2864, 1998.

[16] M. J. Eick, P. R. Grossl, D. C. Golden, D. L. Sparks, and D. W. Ming, “Dissolution of a lunar basalt simulant as affected by pH and organic anions,” *Geoderma*, vol. 74, no. 1–2, pp. 139–160, 1996.

[17] S. A. Welch and W. J. Ullman, “Feldspar dissolution in acidic and organic solutions: Compositional and pH dependence of dissolution rate,” *Geochim. Cosmochim. Acta*, vol. 60, no. 16, pp. 2939–2948, 1996.

[18] W. C. Graustein, K. Cromack, and P. Sollins, “Calcium oxalate: Occurrence in soils and effect on nutrient and geochemical cycles,” *Science (80-.).*, vol. 198, no. 4323, pp. 1252–1254, 1977.

[19] J. Ma, Y. Zhang, Y. Qin, Z. Wu, T. Wang, and C. Wang, “The leaching kinetics of K-feldspar in sulfuric acid with the aid of ultrasound,” *Ultrason. Sonochem.*, vol. 35, pp. 304–312, 2017.

[20] J. M. Riley, H. Kim, T. D. Averch, and H. J. Kim, “Effect of magnesium on calcium and oxalate ion binding,” *J. Endourol.*, vol. 27, no. 12, pp. 1487–1492, 2013.

[21] N. A. Meyer, J. U. Vögeli, M. Becker, J. L. Broadhurst, D. L. Reid, and J.-P. Franzidis, “Mineral carbonation of PGM mine tailings for CO2 storage in South Africa: A case study,” *Miner. Eng.*, vol. 59, pp. 45–51, 2014.

[22] A. C. McAdam, M. Y. Zolotov, T. G. Sharp, and L. A. Leshin, “Preferential low-pH dissolution of pyroxene in plagioclase-pyroxene mixtures: Implications for martian surface materials,” *Icarus*, vol. 196, no. 1, pp. 90–96, 2008.

[23] M. S. Ncongwane, J. L. Broadhurst, and J. Petersen, “Assessment of the potential carbon footprint of engineered processes for the mineral carbonation of PGM tailings,” *Int. J. Greenh. Gas Control*, vol. 77, pp. 70–81, Oct. 2018.

[24] J. L. Palandri and Y. K. Kharaka, “A Compilation of Rate Parameters of Water-Mineral Interaction Kinetics for Application to Geochemical Modeling,” 2004.

[25] S. C. M. Krevor and K. S. Lackner, “Enhancing serpentine dissolution kinetics for mineral carbon dioxide sequestration,” *Int. J. Greenh. Gas Control*, vol. 5, no. 4, pp. 1073–1080, Jul. 2011.

[26] L. Wei, H. Hu, Q. Chen, and J. Tan, “Effects of mechanical activation on the HCl leaching behavior of plagioclase, ilmenite and their mixtures,” *Hydrometallurgy*, vol. 99, no. 1–2, pp. 39–44, 2009.

[27] S. V. Golubev and O. S. Pokrovsky, “Experimental study of the effect of organic ligands on diopside dissolution kinetics,” *Chem. Geol.*, vol. 235, no. 3–4, pp. 377–389, Dec. 2006.

[28] K. Yoo, B. S. Kim, M. S. Kim, J. C. Lee, and J. Jeong, “Dissolution of magnesium from serpentine mineral in sulfuric acid solution,” *Mater. Trans.*, vol. 50, no. 5, pp. 1225–1230, 2009.

[29] S. Teir, H. Revitzer, S. Eloneva, C.-J. Fogelholm, and R. Zevenhoven, "Dissolution of natural serpentinite in mineral and organic acids," *Int. J. Miner. Process.*, vol. 83, no. 1–2, pp. 36–46, Jul. 2007.

[30] S. Teir, R. Kuusik, C.-J. Fogelholm, and R. Zevenhoven, "Production of magnesium carbonates from serpentinite for long-term storage of CO2," *85*, pp. 1–15, 2007.

[31] C. R. Blue, A. Giuffre, S. Mergelsberg, N. Han, J. J. De Yoreo, and P. M. Dove, "Chemical and physical controls on the transformation of amorphous calcium carbonate into crystalline CaCO3 polymorphs," *Geochim. Cosmochim. Acta*, vol. 196, pp. 179–196, 2017.

[32] EPA, "Sulfuric Acid Emission Final Report (AP 42, Fifth Edition, Volume I Chapter 8: Inorganic Chemical Industry)," *Corrosion*, vol. 8.10, pp. 1–9, 1993.

[33] A. D. Paktunc, "Characterization of Mine Wastes for Prediction of Acid Mine Drainage," *Environ. Impacts Min. Act.*, pp. 19–40, 1999.

[34] Montana Department of Environmental Quality and US Department of Agriculture, "Final Environmental Impact Statement Appendices - Stillwater Mining Company's Revised Water Management Plans and Boe Ranch LAD," 2012.

[35] A. Wilk, L. Wieclaw-Solny, T. Spietz, and A. Tatarczuk, "CO2-to-methanol conversion - an alternative energy storage solution," *Chemik*, vol. 70, no. 10, pp. 630–633, 2016.

[36] Michigan Technological University, "Captured carbon dioxide converts into oxalic acid to process rare earth elements," *ScienceDaily*, 2019.

[37] M. A. Murcia Valderrama, R. J. van Putten, and G. J. M. Gruter, "The potential of oxalic – and glycolic acid based polyesters (review). Towards CO_2 as a feedstock (Carbon Capture and Utilization – CCU)," *Eur. Polym. J.*, vol. 119, no. August, pp. 445–468, 2019.

This page intentionally left blank.

Chapter 5

Technoeconomic Analysis of Alkalinity Extraction Methods

Abstract

Advancements have been made in carbon mineralization research, development, and commercial deployment through the last two decades. Now with peak interest in carbon capture and removal technologies from companies and government agencies, there exists a need to easily and consistently compare potential mineralization processes. A techno-economic analysis tool has been developed that is applicable to a wide variety of mineralization processes, providing a common methodology to compare potential projects. The tool's primary input is the desired CO_2 capture per year, among other key parameters of alkaline feedstock and target product. A project's overall economics are calculated in terms of net cost per tonne CO_2 captured, by balancing capital expense, operating expense, and income generated from products and tax incentives. This tool was used to evaluate 5 scenarios from the previous three chapters to further elucidate optimal conditions and paths forward for using Sibanye-Stillwater mine tailings for carbon mineralization. Future developments will be necessary to improve the tool's robustness and accuracy. The majority of this chapter was published in the Proceedings of the 15th Greenhouse Gas Control Technologies Conference under the title "An economic- and resource-based tool to evaluate carbon mineralization processes."

List of Abbreviations

CAPEX – capital expense

CCS – carbon capture and storage

NPV – net present value

OPEX – operating expense

PGM – platinum group metal

1. Introduction

Carbon mineralization is a carbon capture and storage (CCS) technology where CO_2 is both captured and stored in one integrated process [1]. Through carbon mineralization, CO_2 is reacted with alkalinity found in mined silicates or industrial wastes. While research has advanced well through the last two decades, yielding several commercial projects around the world [2], more research and funding is needed for wider development and deployment [3].

Growing interest in investment in this technology has come as a result of various climate targets being set by companies [4] and nations [5]. However, it is difficult for potential funders like venture capitalists, major companies, and government agencies to choose which process to invest in without a consistent basis for comparison. To startup a new process site, it is helpful to assess the economics and compare to other potential processes. Due to differences in process conditions and alkaline feed, there is high variability among proposed processes in the literature in terms of process economics and kinetics.

Comparison of mineralization processes is difficult for a number of reasons. A variety of alkalinity sources are available, where different mineral structures bring differences in reactivity. Process configuration is also a variable, including one-step and multi-step *ex-situ* processes, surficial processes, and *in-situ* processes [6]. These variances are further exacerbated by differences in mineral products – as several carbonate minerals can form depending on conditions, affecting whether they may be sold as building products [7], or if they are intended to be left on the ground.

A techno-economic analysis tool has been developed that is applicable to a wide variety of carbon mineralization processes, providing a common methodology to compare potential processes. The tool is available online through Prime Coalition, where the user manual explains all components of the tool in detail [8]. This chapter will give a description of the methodology used to create the tool, followed by two example scenarios of how the tool may be used, and concluding with a discussion of future improvements to the tool.

2. Methodology

The tool is hosted in Microsoft Excel, where data inputs/outputs and datasets are organized in several tabs. The two primary tabs involve a front-end Summary tab and a back-end Process tab. Both tabs work through mass and energy balances to calculate expenses associated with the process being evaluated. A generalized Base Process is used as the base process of the tool, shown in Figure 1.

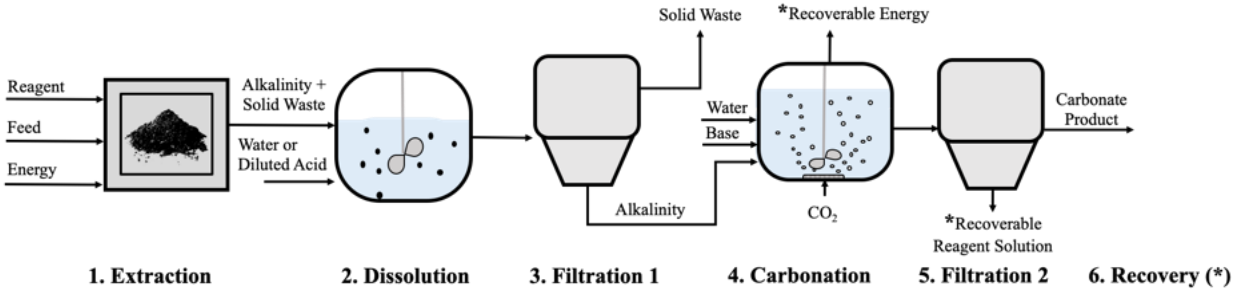

Figure 1: Base Process of Technoeconomic Analysis Tool

The tool's front Summary tab contains a control panel with the most essential parameters for the economic analysis (e.g., alkaline feedstock, particle size, target product). Next, there is a small control module for each step of the process in Figure 1, hosting cells for key input parameters. Here, the user is given the option to implement or remove any step of the Base Process to match the process being evaluated. Additional parameters for each process step can be altered in the back-end Process tab.

The tool's primary input is the targeted annual CO_2 sequestered, with the intent of corresponding with tax incentives like 45Q that specify annual CO_2 capture amounts for credit qualification. Calculations for material usage and CO_2 capture are made using a mass balance. Because the tool's primary input is the targeted annual CO_2 sequestered, the tool uses a bottom-up mass balance which begins at CO_2 stored in Step 4 of Figure 1, and works its way up to alkaline feed required in Step 1.

The most difficult aspect of creating a tool that can evaluate a wide variety of mineralization processes is that the kinetics of mineral dissolution and carbonation can vary widely depending on the mineral feed and process conditions. While it is possible to compile kinetic data available in the literature on the numerous process configurations and feedstocks, such a literature review is still limited by potential new processes to be used. Hence, for this version of the tool, it was chosen to use process efficiencies in lieu of kinetics, as shown in Figure 2.

Efficiency Assumptions		
Process	Alternative ÅA Route	pH Swing
Mg Extraction	41%	~~41%~~
Mg Dissolution	100%	74%
Mg Carbonation [Wet]	99%	99%
Ca Extraction	~~85%~~	~~85%~~
Ca Dissolution	~~70%~~	~~80%~~
Ca Carbonation [Wet]	~~99%~~	~~99%~~
Carbonation [Wet]	100%	100%
Carbonation [Dry]	~~50%~~	~~50%~~

Figure 2: Efficiency Assumption Control Panel, with parameters from Section 3.5 scenario analysis

By implementing efficiency parameters in the tool, it is assumed that the process has had adequate testing at the lab-scale and possible bench-scale, as the majority of published research reports the extent or efficiency of alkalinity extraction and carbonation. The efficiencies are defined as the

fraction of cations (Mg or Ca) extracted, dissolved, or carbonated during the respective process step, and are system dependent. The final efficiency (carbonation, wet/dry) is a measure to approximate the percent of CO_2 entering the system that is bound as carbonate, rather than leaving the system unbound. This can also be thought of as the capture efficiency.

To simplify the mass balance, the current version of the tool forces the user to pick Mg or Ca as the "target cation." Because most alkaline silicate minerals primarily contain only one of these two cations, this does not have a major impact on the majority of available feedstocks. Upon selection of the target cation, cells associated with the non-target cation become grey and are nullified, while those of the target cation remain green and require user inputs, as shown in Figure 2. This color scheme is also used when the user selects to not use a certain step from the Base Process in Figure 1, causing all applicable cells for the unused step to become grey, as exemplified in Figure 2.

The tool's outputs are final CO_2 sequestration and process economics. Any energy- or transport-related emissions are subtracted from the target annual CO_2 sequestered to get a "Net Sequestered" value. Process economics are evaluated based on Net Present Value (NPV), which evaluates all costs (i.e., capital, operating, transport) and revenues (i.e., marketable products, tax incentives) over the defined project lifespan (e.g., 30 years). The capital expense (CAPEX) is estimated using bare module costing, which is the sum of direct and indirect costs associated with installing plant equipment [9]. The bare module cost can be further converted to "total module cost" to account for installation and purchase costs, or "grassroots cost" to account for starting a brand-new facility on undeveloped land. The operating expense (OPEX) is based on reactant inputs, product outputs, and major energy requirements. This version of the tool only calculates energy from particle size reduction and thermal alkalinity extraction, while future versions should account for other energy requirements, such as mechanical stirring and CO_2 compression.

Finally, the Analysis tab provides analysis of various parameters throughout the tool. Cost distributions in capital and operating expense allow identification of areas with greatest need of cost reduction. Sensitivity analysis of the various assumptions made throughout the tool indicates the relative impact of certain assumptions on the final tool outputs.

3. Economic Analysis of Scenarios in Previous Dissertation Chapters

Several scenarios will be used to show the tool's capabilities and to determine optimal parameters and paths forward for developing the mineralization processes used. The scenarios pertain to optimizing alkalinity extraction from mine tailings generated at the Sibanye-Stillwater mine in Nye, Montana, as discussed in Chapters 2-4. The following scenarios all consider storing 1000 tCO_2 per year with a project life of 12 years and a 10 % discount rate.

3.1 Thermal Alkalinity Extraction – Effect of Reaction Temperature on Costs

This first scenario is mentioned in Chapter 3, where mine tailings from a platinum group metals mining facility are used in the Alternative ÅA Route [10]. Optimization experiments were run for temperature of thermal cation extraction using ammonium sulfate, and extraction at 450 ^oC and 475 ^oC yielded Mg extraction efficiencies of 39 % and 41 %, respectively. The cost tool was used to elucidate whether the additional 25 ^oC is worth the additional 2% in efficiency.

The tool revealed that although heating at 475 ^oC causes about a 1 % increase in energy costs, it also requires about 5% less ammonium sulfate, resulting in about a 4 % net-decrease of overall OPEX. As illustrated in the sensitivity plot of Figure 3, the overall cost of the project is more sensitive to extraction efficiency at low efficiency values, so it is critical that process conditions are used which produce the maximum extraction efficiency possible. This figure also helps illustrate the consequences of efficiency assumptions. In this scenario, the Mg carbonation efficiency was assumed to be 100%. Figure 3 shows that decreases in the Mg carbonation efficiency from 100 % to 80 % has minimal effect on the project's NPV.

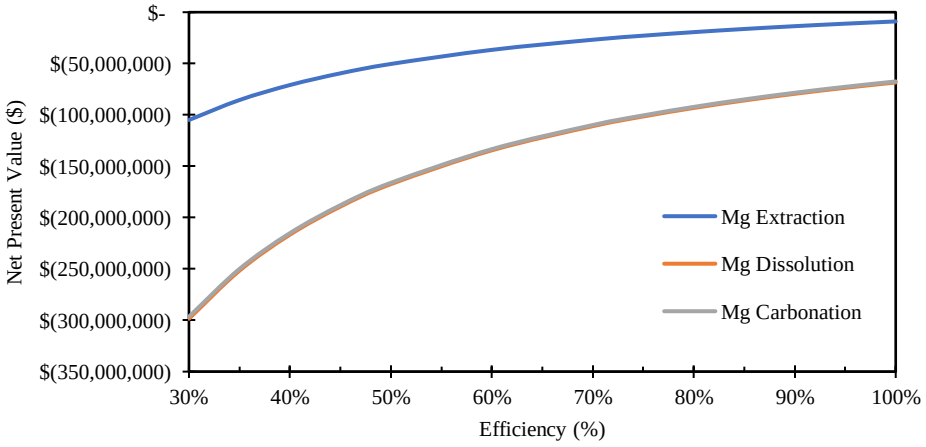

Figure 3: Sensitivity of Net Present Value to Efficiencies of the Alternative ÅA Route with Sibanye-Stillwater Tailings at 475 ^oC

The process simulated here initially had a target CO_2 sequestration of 1000 tCO_2 per year. This sequestration amount would require about 7000 tonnes of tailings per year, far less than the 1 Mt annually produced by Sibanye-Stillwater. The Excel Goal Seek function can be used within the tool to calculate the amount of CO_2 that can be sequestered through the modeled processes with the 1 Mt of tailings each year at Sibanye-Stillwater. Under these constraints, the tool shows that

about 142 and 149 $ktCO_2$ can be sequestered at 450 ^oC and 475 ^oC, respectively; this reduces to about 102 and 107 $ktCO_2$ net-sequestered, due to energy-related emissions. Because more than 100 $ktCO_2$ are sequestered through this process, it would qualify for a \$35/tCO_2 tax incentive through 45Q. Despite eligibility for this tax incentive, the process still has a negative NPV, and would not be profitable.

The process economics could be improved with additional income sources, as this evaluation also assumed no revenue would be generated from the hydromagnesite products. There is not currently a substantial market for hydromagnesite, but it could eventually be useful as a flame retardant filler [7]. A sensitivity analysis is shown in Figure 4, illustrating that to break even on the project, the tax credit would need to increase to about \$100 tCO_2^{-1}, or the hydromagnesite products would need to be sold at \$25 tCO_2^{-1}.

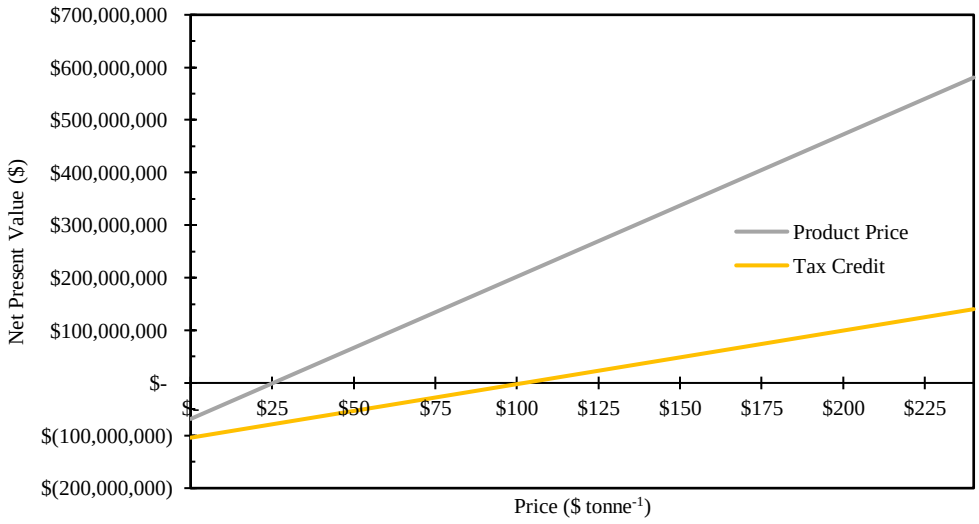

Figure 4: Sensitivity of Net Present Value to Potential Income Sources

3.2 Acidic Alkalinity Extraction – Effect of Solid/Liquid Ratio on Costs

In Chapter 4, several acids were used to extract calcium and magnesium from the Sibanye-Stillwater tailings through a pH swing process [11]. Tailings were dissolved in acid solutions of 0.1 – 1.0 M concentrations for 18 hours. To enhance alkalinity extraction and decrease acid consumption, the dissolution time was extended to 72 hours and the solid/liquid ratio of (i.e., solid tailings to liquid acid solution) was increased from 30 to 40 g/L. While increasing the solid/liquid ratio caused an 18 % decrease in Mg extraction efficiency at 18 hours, the decrease was minimized to 9 % when dissolution time was extended to 72 hours. This begs the question of whether the 9 % decrease in extraction efficiency is compensated by the decreased acid consumption.

In Figure 5, the capital expense, operating expense, and overall net present value are shown for dissolving Sibanye-Stillwater tailings in 0.5 M citric acid solution for 72 hours with solid/liquid ratios of 30 and 40 g/L. All equipment and materials used remained the same between the two processes, and all that changed was the equipment volume and material amounts. Clearly, the decrease in acid consumption by increasing the solid/liquid ratio is more impactful than the

minimized decrease in efficiency. Despite the economic improvement of the 40 g/L scenario, the project NPV is still negative, and would require efficiency improvements or sources of income to make the project profitable.

Process Summary		
Process	Citric Acid 30 g/L	Citric Acid 40 g/L
Process Economics		
Total Transport Expense ($/yr)	-	$ -
Total Capital Expense ($)	$ 7,626,558.08	$ 6,322,423.69
Total Operating Expense ($/yr)	$ 480,830.51	$ 387,187.92
Project Net Present Value	**$ (10,664,309.77)**	**$ (8,722,123.61)**

Figure 5: Summary of capital and operating expenses associated with different solid/liquid ratios in 0.5 M citric acid (72 hours)

3.3 Acidic Alkalinity Extraction – Effect of Sulfuric Acid Concentration on Costs

The 1.0 M sulfuric acid solution presented the highest extraction of Mg and Ca, extracting about 74 % and 7 %, respectively. Dissolution in mineral acids like sulfuric acid differed from dissolution in organic acids (e.g., citric, oxalic acids) in that the extraction efficiency significantly increased with increasing concentration – where 0.5 M sulfuric acid solution extracted about 58 % and 6 % of Mg and Ca, respectively, in 18 hours. However, with increased acid concentration comes increased raw material costs.

The cost tool was used to determine whether costs associated with higher sulfuric acid concentration are worth the additional acid consumption. The distribution of materials costs in the two systems are compared in Figure 6. While the 1.0 M sulfuric acid solution uses more acid, the concentration is so low (~0.6 %) that the consumption increase relative to 0.5 M is minimal. In fact, the more impactful material usage is the increase in water use in the more dilute sulfuric acid solution.

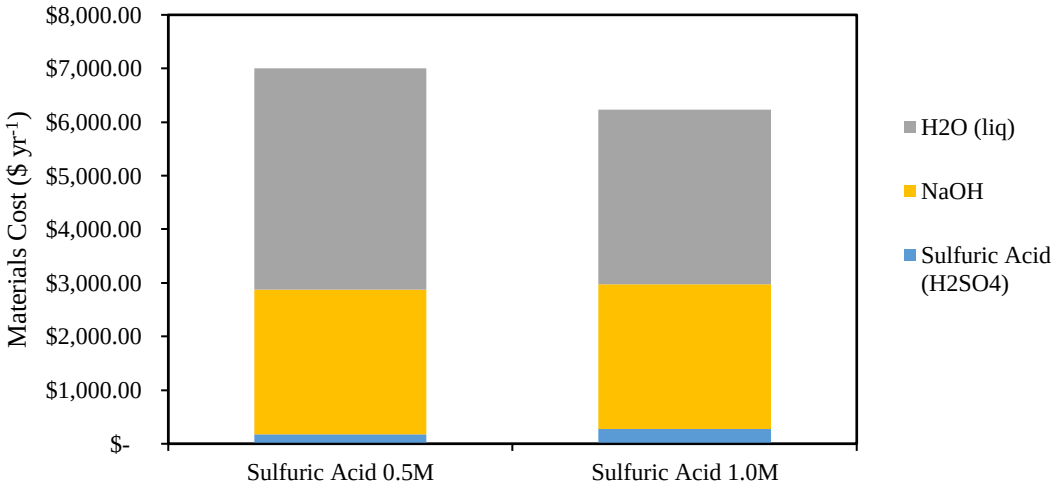

Figure 6: Material cost distribution in 0.5 M and 1.0 M sulfuric acid solutions

However, this is under an optimistic assumption of 90% acid recovery – meaning 90% of acid used in each reaction batch is recycled to the next batch. If lower acid recovery values are achieved, the associated cost of sulfuric acid would increase, potentially making the 0.5 M solution more

competitive. Figure 7, shows a sensitivity analysis of the sulfuric acid costs and the overall project NPV to acid recovery values. While sulfuric acid costs among the two concentrations do diverge with decreasing acid recovery, the effect on the overall project NPV is minimal. This is primarily because of the decreased Mg extraction efficiency of the 0.5 M system, where larger reactor volumes are required to achieve the same annual CO_2 storage of 1000 tCO_2. Hence, 1.0M is the optimal sulfuric acid concentration of those tested to extract alkalinity from Stillwater-Sibanye tailings.

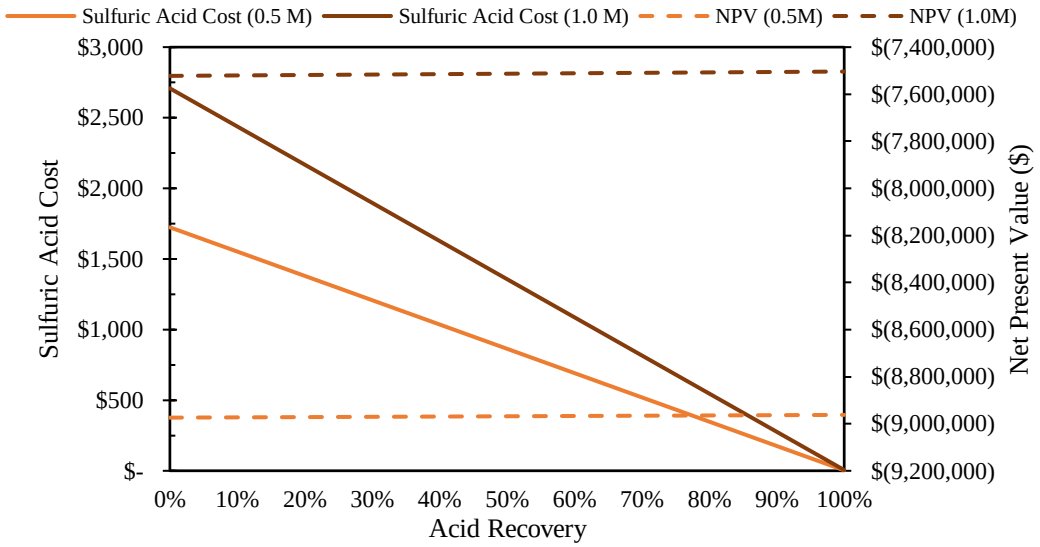

Figure 7: Sensitivity of sulfuric acid costs (left) and total project NPV (right) to acid recovery

The cost of NaOH here comes with a caveat – due to lack of quantifiable data for the carbonation step (see Chapter 4, section 4.3), it was assumed that both solutions would require the same amount of base for carbonation, where both systems also had a base recovery of 90 %. Future experiments will inform data on this step, and future models of the tool should involve carbonation kinetic and pH condition data to predict the amount of base needed for the system.

3.4 Acidic Alkalinity Extraction – Citric vs Sulfuric Acid Solutions

The analysis in Section 3.3 informed the optimal conditions for alkalinity extraction in citric and sulfuric acid solutions. Among these two acids, it is suspected that the use of sulfuric acid would result in a less economical process due to the need for corrosion-resistant equipment. While the Mg extraction efficiency of citric acid is far less than sulfuric acid, the ability to use less expensive equipment could cause the use of citric acid to be more favorable.

In Figure 8, the capital expense, operating expense, and overall net present value are summarized for the optimal conditions of citric and sulfuric acids. Ultimately, the 1.0 M sulfuric acid solution, which extracts about 74 % of Mg in 18 hours, presents a more economical process than the 0.5 M citric acid solution, which extracts about 41 % of Mg in 72 hours. While using sulfuric acid results in more expensive equipment (stainless steel, as opposed to carbon steel for citric acid), the dramatically improved efficiency requires lower volumes of raw materials and smaller equipment sizes. The impact of Mg extraction efficiency is shown in Figure 9. At any given Mg extraction

efficiency, citric acid would be more economical. However, because the efficiency achieved using sulfuric acid was so much higher than that of citric acid, sulfuric acid presents the more economical process at the conditions tested.

Process Summary		
Process	Citric Acid 0.5 M, 40 g/L	Sulfuric Acid 1.0M, 20 g/L
Process Economics		
Total Transport Expense ($/yr)	-	$ -
Total Capital Expense ($)	$ 6,322,423.69	$ 7,701,462.39
Total Operating Expense ($/yr)	$ 387,187.92	$ 6,238.05
Project Net Present Value	**$ (8,722,123.61)**	**$ (7,505,487.35)**

Figure 8: Summary of capital and operating expenses associated with different solid/liquid ratios in 0.5 M citric acid (72 hours)

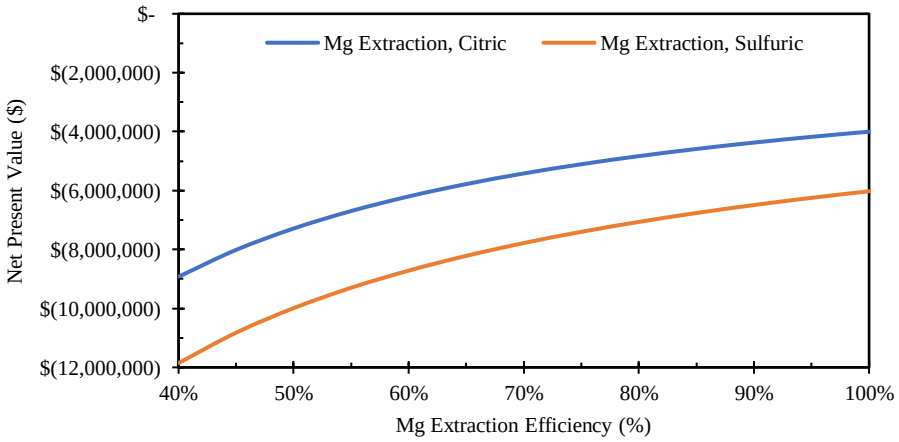

Figure 9: Sensitivity of project net present value to Mg extraction efficiency

Another parameter that proved influential in the comparison of citric and sulfuric acids is the acid price. The price used in this analysis for citric acid is more than 12 times the price of sulfuric acid (i.e., \$376 vs \$27 per m^{-3} [12], [13]). The sensitivity to acid price is illustrated in Figure 10, showing that the price of citric acid has a much larger effect on process economics. Based on this plot, using citric acid would become more economical if it can be acquired for less than about \$215 m^{-3}.

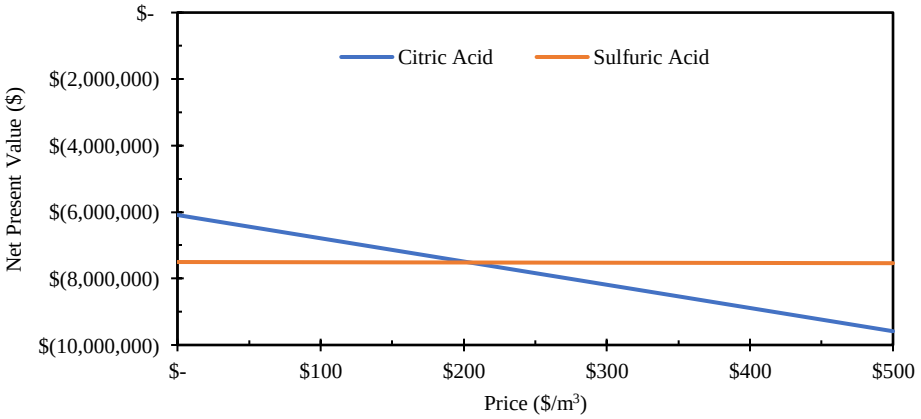

Figure 10: Sensitivity of project net present value to acid price

3.5 Comparison of Thermal and Acidic Alkalinity Extraction

The tool was used to evaluate which *ex-situ* process tested in this dissertation is more economical for extracting Mg. Results of comparing the two processes in a scenario that sequesters 1000 tCO_2 per year are shown in Figure 11, where the Excel Goal Seek function has been used to allow both processes to reach 1000 tCO_2 $year^{-1}$ NET sequestered (see Section 3.1).

MODEL OUTPUTS		
Process Summary		
Process	Alternative AA Route	pH Swing
Batch Time (min)	150.00	1,170.00
Batches Required (batch/yr)	3,504.00	449.23
Batch Sequestration Rate (tCO2/batch)	0.40	2.23
CO2 Sequestration		
Sequestered as Carbonate (tCO2/yr)	1,392.20	1,000.00
Emitted from Process (tCO2/yr)	392.20	-
Emitted from Transport (tCO2/yr)	-	-
Net Sequestered (tCO2/yr)	**1,000.00**	**1,000.00**
Process Economics		
Total Transport Expense ($/yr)	-	$ -
Total Capital Expense ($)	$ 676,396.92	$ 7,701,462.39
Total Operating Expense ($/yr)	$ 136,670.66	$ 4,459.20
Project Net Present Value	**$ (1,275,616.90)**	**$ (7,493,366.81)**

Figure 11: Tool outputs comparing the two *ex-situ* indirect carbon mineralization processes tested

As expected, the Alternative ÅA Route has higher OPEX due to the use of heat and ammonium sulfate [14]. Despite this decrease in OPEX, the pH swing results in dramatically increased CAPEX due to the use of corrosion-resistant stainless-steel vessels. The CAPEX distribution is displayed for both processes in Figure 12. The thermal reactor dominates CAPEX for the Alterative ÅA Process, while the two stainless steel reactors dominate CAPEX for the pH swing process. Based on this analysis, the Alternative ÅA Route is more economical for extracting Mg from the Sibanye-Stillwater tailings at the conditions tested.

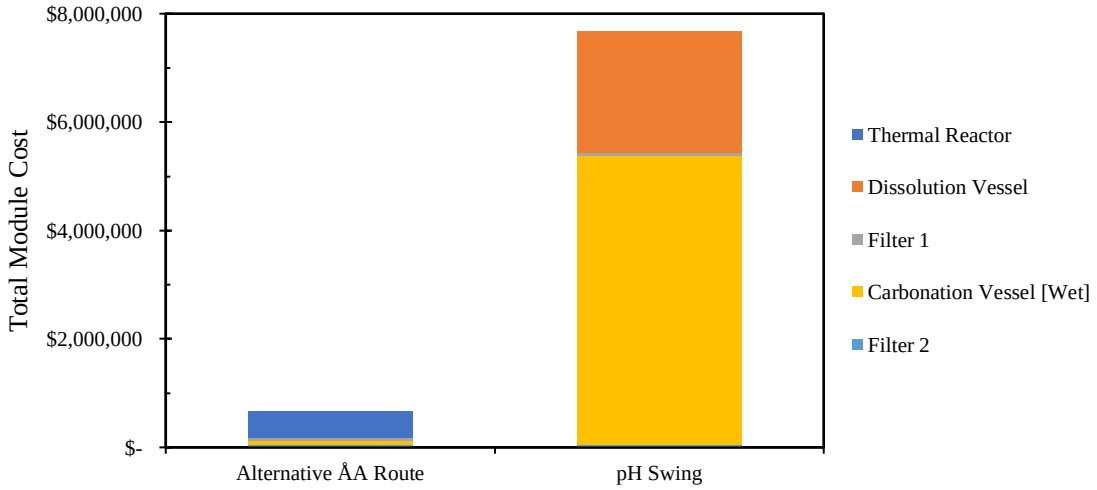

Figure 12: Capital expense distribution in Alternative ÅA Route and pH swing

4. Discussion of Carbon Mineralization Methods for Sibanye-Stillwater Tailings

4.1 Ex-situ Methods – Performance and Improvements

The two *ex-situ* mineralization processes tested in Chapters 3 and 4 have been economically evaluated, revealing that the most economical process tested is the Alternative ÅA Route, which extracted 41 % Mg and 14 % Ca at 475 ^{o}C in one hour. Based on the evaluation shown here, this economic best-case still presents a negative net present value, indicating the project is not profitable.

Several factors could change to improve the economics of the processes evaluated here. In the case of the Alternative ÅA Route, 450 ^{o}C was chosen as the optimal temperature within the range tested during experimentation, and was the temperature used for further optimization. Because this analysis revealed that 475 ^{o}C is in fact more economically favorable, additional optimization could be done at this temperature, particularly by decreasing the ratio of ammonium sulfate to tailings.

Similarly, additional optimization of the pH swing process could make it more competitive with the Alternative ÅA Route. The increased solid/liquid ratio was impactful on the economics of extraction with citric acid, and additional increases to this parameter should be explored. Sulfuric acid achieved Mg high extraction efficiency at 18 hours using 20 g/L, but additional optimization could be carried out by individually increasing the dissolution time and solid/liquid ratio. This was performed in Chapter 4 without avail, but both parameters were increased at once, making it difficult to elucidate the parameters' effects. The economics of using citric acid weighed heavily on the high citric acid price used in the evaluation, and it is worth investigating whether the acid can be acquired at a lower price. Finally, capital expense plays a large role in the poor economics of the pH swing process (Figure 12). Improvements to this aspect should be explored, such as the possibility of using one vessel for the dissolution and carbonation steps, decreasing capital expense by about one to two thirds depending on the vessel used.

The true 'game-changing' factor would be improvements in extraction of calcium, which accounts for half of the alkalinity in the Sibanye-Stillwater tailings. Of all the conditions tested, the maximum Ca extraction efficiency was 20 %, compared to Mg extraction efficiencies of 40-80 %. Clearly, more work has to be done to increase Ca extraction. In the economic evaluations shown here, only carbonation of extracted Mg was considered (a short-coming of the tool, explained later in Section 5). Hence, improvements in Ca extraction and implementation into economic evaluations could potentially double the amount of CO_2 stored, and has the potential to substantially improve the economics.

The use of *ex-situ* mineralization processes is well suited to produce carbonate products which can be sold for profit. Due to the lack of sufficient data for carbonation efficiency in the experiments in this Dissertation, product revenue was not considered in the evaluations shown here (aside from Section 3.1). This would present another opportunity for economic improvement.

4.2 Ex-situ vs Surficial Carbon Mineralization

The overall non-ideal economic performance of the *ex-situ* mineralization methods tested in this Dissertation poses a consideration of whether the low-cost ambient conditions tested in Chapter 2 are in fact the better solution to store CO_2 in PGM tailings like that of Sibanye-Stillwater. While this question is too broad to be answered in one small discussion section, some considerations can be put forward.

The extraction efficiencies of Mg and Ca achieved in the *ex-situ* processes tested Chapters 3 and 4 far exceed that of the labile Mg and Ca at low-cost ambient conditions determined in Chapter 2 (less than 3 % and 1 % for Ca and Mg, respectively). Increasing cation extraction and carbonation of Sibanye-Stillwater tailings at ambient conditions would require timespans of months-to-years, as opposed to the hours-to-days timespans demonstrated by the *ex-situ* processes. But even the Tail 1 sample which had been interacting with the atmosphere for nearly two decades still had significant amounts of non-carbonated alkalinity. Hence, changes to other parameters may be necessary increase carbon uptake at Sibanye-Stillwater, like increasing spreading out the tailings to expand the tailings' exposed surface area. The issue of time may not be as crucial in the grand scheme of net climate intervention, increased land use may have several unintended consequences of its own.

Considering the results presented in Chapters 2-5, it is the opinion of the author that further optimization of *ex-situ* mineralization should be pursued with the Sibanye-Stillwater tailings. In tandem, it would be beneficial to explore possibilities of enhanced ambient carbonation of the tailings.

5. Future Improvements to the Tool

This paper has presented a tool that can evaluate the economics of a variety of carbon mineralization processes. The tool has been effectively used to evaluate five scenarios for storing CO_2 in PGM tailings. The effect of simplifying assumptions on the project's NPV can be determined via sensitivity analysis. While the tool has many beneficial uses, it still has several aspects that will be improved in future versions.

For the tool to become more realistic, it should implement mineral dissolution and carbonation kinetics rather than using assumed efficiencies. Kinetic data are currently being curated from various sources [15]–[19], but some approximations and assumptions will still have to be made to simulate kinetic data for any new alkaline feedstock.

Another trade-off of using efficiencies rather than kinetics and chemical data is in the carbonation step. In the absence of carbonation efficiency data for these scenarios, both scenarios shown here assume an optimistic 99% Mg carbonation efficiency to form hydromagnesite, as the Mg extraction/dissolution step is the rate limiting step of the overall process. The tool should be able to calculate pH conditions and contain carbonation kinetic data to more accurately calculate carbonation behavior.

As stated in Section 2, the current version of the tool forces the user to pick Mg or Ca as the "target cation." While this doesn't affect the majority of available feedstocks, this simplification can

neglect a significant amount of available alkalinity for alkalinity sources like the Sibanye-Stillwater tailings that are equimolar in Mg and Ca. A future version of the tool would account for all alkalinity in the feedstock.

The current tool was made in Microsoft Excel, which has processing limitations related to the amount of data contained in the tool. This problem will be exacerbated as more data (like kinetics) are implemented. The tool could be replicated in Python, which is capable of hosting more data than Excel in an accessible manner. This could increase the calculator's functionality and be used to create a more straightforward and interactive user interface. Further, making the tool open-source will allow more researchers to implement their own data for kinetics and other parameters. This type of open-source tool has been recently released that estimates the cost of direct air capture [20], and plans are in place to release a similar tool to estimate the cost of carbon mineralization.

References

[1] C. M. Woodall, I. Piccione, M. Benazzi, and J. Wilcox, "Capturing and Reusing CO_2 by Converting it to Rocks," *Front. Young Minds*, vol. 8, no. 592018, 2021.

[2] D. Sandalow, R. Aines, J. Friedmann, C. McCormick, and S. McCoy, "Carbon Dioxide Utilization (CO2U) -- Icef Roadmap 2.0," 2017.

[3] C. D. Hills, N. Tripathi, and P. J. Carey, "Mineralization Technology for Carbon Capture, Utilization, and Storage," *Front. Energy Res.*, vol. 8, no. July, pp. 1–14, 2020.

[4] N. C. Partners, "Deeds Not Words: The Growth of Climate Action in the Corporate World," no. September, 2019.

[5] UNFCCC, "The Paris Agreement." [Online]. Available: https://unfccc.int/process-and-meetings/the-paris-agreement/the-paris-agreement. [Accessed: 04-Feb-2021].

[6] P. B. Kelemen, N. McQueen, J. Wilcox, P. Renforth, G. Dipple, and A. P. Vankeuren, "Engineered carbon mineralization in ultramafic rocks for CO2 removal from air: Review and new insights," *Chem. Geol.*, vol. 550, no. 119628, May 2020.

[7] C. M. Woodall, N. McQueen, H. Pilorgé, and J. Wilcox, "Utilization of Mineral Carbonation Products: Current State and Potential," *Greenh. Gases Sci. Technol.*, 2019.

[8] Prime Coalition, "Climate Impact." [Online]. Available: https://primecoalition.org/climate-impact/. [Accessed: 04-Feb-2021].

[9] R. Turton, R. C. Bailie, W. B. Whiting, J. A. Shaeiwitz, and D. Bhattacharyya, *Analysis, Synthesis, and Design of Chemical Processes*, 4th ed. Prentice Hall, 2012.

[10] R. Zevenhoven, M. Slotte, E. Koivisto, and R. Erlund, "Serpentinite Carbonation Process Routes using Ammonium Sulfate and Integration in Industry," *Energy Technol.*, vol. 5, no. 6, pp. 945–954, 2017.

[11] A. Azdarpour, M. Asadullah, E. Mohammadian, H. Hamidi, R. Junin, and M. A. Karaei, "A review on carbon dioxide mineral carbonation through pH-swing process," *Chem. Eng. J.*, vol. 279, pp. 615–630, 2015.

[12] ECHEMI, "Sulfuric Acid Price Analysis." [Online]. Available: https://www.echemi.com/productsInformation/pid_Rock19440-sulfuric-acid.html. [Accessed: 18-Feb-2021].

[13] ECHEMI, "Citric Acid Anhydrous Price Analysis." [Online]. Available: https://www.echemi.com/productsInformation/pd20150901044-citric-acid-anhydrous.html. [Accessed: 18-Feb-2021].

[14] G. Chu *et al.*, "Facile and cost-efficient indirect carbonation of blast furnace slag with multiple high value-added products through a completely wet process," *Energy*, vol. 166, pp. 1314–1322, Jan. 2019.

[15] J. L. Palandri and Y. K. Kharaka, “A Compilation of Rate Parameters of Water-Mineral Interaction Kinetics for Application to Geochemical Modeling,” 2004.

[16] M. Hänchen, V. Prigiobbe, R. Baciocchi, and M. Mazzotti, “Precipitation in the Mg-carbonate system-effects of temperature and CO2 pressure,” *Chem. Eng. Sci.*, vol. 63, no. 4, pp. 1012–1028, Feb. 2008.

[17] W. M. Haynes, *CRC Handbook of Chemistry and Physics*, 100th ed. Boca Raton, FL: CRC Press/Taylor & Francis.

[18] P. Renforth, “The negative emission potential of alkaline materials,” *Nat. Commun.*, vol. 10, no. 1401, 2019.

[19] A. Sanna, M. Uibu, G. Caramanna, R. Kuusik, and M. M. Maroto-Valer, “A review of mineral carbonation technologies to sequester CO_2,” *Chem. Soc. Rev.*, vol. 43, no. 43, pp. 8049–8080, 2014.

[20] N. Mcqueen, J. Wilcox, J. Hamman, and J. Freeman, “The cost of direct air capture,” *CarbonPlan*. [Online]. Available: https://carbonplan.org/research/dac-calculator-explainer. [Accessed: 04-Feb-2021].

This page intentionally left blank.

Chapter 6

Utilization of Carbon Mineralization Products: Current State and Potential

Abstract

Carbon mineralization (CM) is a form of carbon capture and storage that reacts CO_2 with alkaline feedstock to securely store CO_2 as solid carbonate minerals. To improve process economics and accelerate commercial deployment, research has increased around product utilization, where markets exist primarily in the construction industry. This review assesses the potential for advancing CM product utilization to decrease CO_2 emissions toward neutral, or even negative, values. First, the literature surrounding the current state and challenges for indirect CM processes is reviewed, indicating that process intensification and scale-up are important areas for further research. Alkalinity sources available for CM are examined, differentiating between those sourced from industrial processes and mining operations. Investigation of possible end-uses of carbonate products reveals that further CO_2 avoidance can be achieved by replacing conventional carbon-intensive products. Companies which are currently commercializing CM processes are categorized based on the feed used and materials produced. An analysis of company process types indicates that up to 3 $GtCO_2$/year could be avoided globally. It is suggested that upcoming commercial efforts should focus on the carbonation of industrial wastes located near CO_2 sources to produce precast concrete blocks. Carbonation of conventional concrete shows the highest potential for CO_2 avoidance, but may face some market resistance. Carbonation of Mg-silicates lacks sufficient market demand and requires the development of new high-value products to overcome the expense of mining and feed preparation. It is suggested that research focus on enhanced understanding of magnesia cement chemistry and the development of flame-retardant mineral fillers. This chapter was published in Greenhouse Gases: Science and Technology.

List of Abbreviations:

ACC – amorphous calcium carbonate

APCr – air pollution control residue

$C_{CO_2(aq)}$ – concentration of CO_2 in solution

CCUS – carbon capture, utilization and storage

CM – carbon mineralization

ΔH^o – standard enthalpy change

EUR – Euro

FA – fly ash

K_{H,CO_2} – Henry's constant

MSW – municipal solid waste

MSWI – municipal solid waste incineration

NET – negative emissions technology

$P_{CO_2(g)}$ – partial pressure of CO_2

PC – portland cement

PCC – precipitated calcium carbonate

SCM – supplementary cementitious material

SS – steelmaking slag

USD – US Dollar

1. The Role of Carbon Mineralization in Mitigating Climate Change

High levels of anthropogenic CO_2 emissions over the past century have given rise to changes in Earth's climate. More than 36 billion tonnes of CO_2 ($GtCO_2$) are emitted annually, and roughly 60 % are sourced from exhaust streams of industrial facilities and power plants (i.e., point-source emissions) [1]. Mitigation approaches such as increased energy efficiencies and implementation of carbon-free energy resources work well to decrease combustion-related emissions. However, the difficult-to-avoid emissions still remain. This includes emissions associated with the transportation and industrial sectors, in addition to the distributed emissions of industrial, commercial, and residential heating.

It is clear that combating climate change and avoiding 2 ^oC warming by 2100 will require a portfolio of climate mitigation strategies that includes both avoiding emissions and directly removing them from the atmosphere [2]–[4]. A recent report by the National Academy of Sciences states that to meet climate goals, it is necessary (and technically feasible) to remove 10 $GtCO_2$ per year up to 2050, with an increase to 20 $GtCO_2$ each year from 2050 to 2100 [5]. Emissions may be avoided through the capture of point-source CO_2 emissions and subsequent storage in a permanent form (i.e., carbon capture and storage, CCS). Additionally, CO_2 may be removed directly from the atmosphere and coupled with the permanent storage of CO_2 via negative emissions technologies (NETs). These NETs can help mitigate the impact of emissions from difficult-to-avoid sources.

Carbon mineralization (CM) involves reacting CO_2 with an alkalinity source to produce solid carbonate minerals. This approach may be coupled with point-source emissions to avoid emissions or coupled to direct air capture to achieve negative emissions. Hence, it has the potential to have significant impact on climate change mitigation. The general CM reaction is shown in Eq. (1, where M is a divalent metal cation, typically Mg^{2+} or Ca^{2+}.

$$MO + CO_2 \rightarrow MCO_3 \quad (1)$$

First introduced as a concept by Seifritz in 1990 [6] and further explored conceptually by Lackner in 1995 [7], research of CM as a means of CCS has accelerated considerably with related publications more than tripling each decade since 1990, rising from 154 in 1990-1999 to 1512 in 2010-2019 [8]. Recently, a few pilot projects have exploited favorable conditions to perform CM. In Iceland, the colocation of geothermal energy, CO_2 waste streams, water, and large basaltic formations has allowed Carbfix to perform CM *in-situ* [9]. The project has captured 12 $ktCO_2$ to date, and the technology has the potential capture more than 100,000 $GtCO_2$ [10]. Additionally, carbonation of diamond mine tailings by contact with atmospheric CO_2 has been demonstrated by the De Beers Group of Companies, who aims to make some of its mines carbon neutral within next few years [11], [12].

While other alkaline materials are present in vast quantities, some challenges have prevented CM from being widely implemented on a commercial scale. While CM is thermodynamically favorable, the natural kinetic rates occur on the geologic timescales (millennia). Accelerating the process requires the elevation of process conditions, such as the partial pressure of CO_2 and/or the use of caustic additives. Both of these acceleration methods can contribute considerably to increases in process economics and energy usage, potentially resulting in additional CO_2 emissions. To offset costs of CM, the carbonate minerals may be utilized in various industries

(e.g., construction industry), an approach often termed carbon capture, utilization and storage (CCUS).

Recently, several CO_2 utilization methods have been summarized and evaluated, primarily including the chemical or biological conversion of CO_2 to chemicals and fuels, the use of supercritical CO_2 as a solvent, and CM to produce construction materials [5], [13], [14]. Among these methods, the National Academy of Sciences reported that CM is among the largest and most energy-efficient, and is the method closest to commercial scale due to its thermodynamic favorability and market size [5]. Through life cycle analysis, CM was found to be most effectively reduce net CO_2 emissions [13].

There are already eighteen operational CCUS facilities around the world [15], and CO_2 utilization will become increasingly viable as carbon pricing and tax credits evolve. A relatively new US federal tax credit called 45Q gives a credit for operations that store at least 25 $ktCO_2$ per year for beneficial reuse, or at least 100 $ktCO_2$ for permanent storage. These credits amount to 22 and 34 USD/tCO_2 with incremental increases each year, respectively [16]. Both of these qualifiers could apply to CCUS with CM, potentially allowing for a combination of tax credits, but this is a slight ambiguity with 45Q that should be clarified.

1.1. *Carbon Mineralization and Market Potential*

Carbonate minerals are currently used in a wide array of industries, including construction, paper and pulp, pharmaceutical, agricultural, and refractory metals. However, as illustrated in Figure 1, some of these applications result in the release of CO_2, and thus are not well-suited for long-term CO_2 storage. Of the suitable applications, the construction industry presents the largest opportunity in terms of consumption volume, overall emission avoidance, and readiness for commercial scale [5].

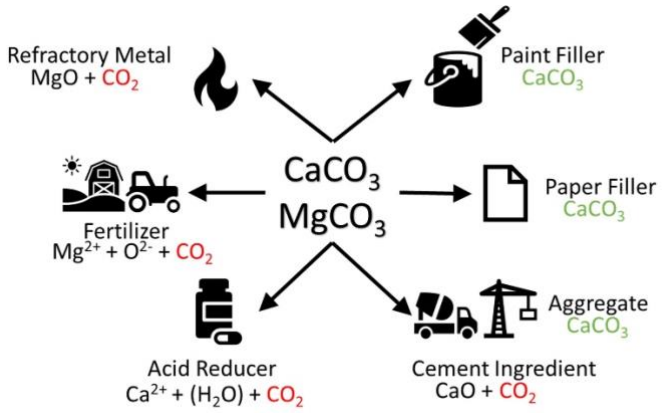

Figure 1: Current industrial uses of carbonate minerals and their final chemical form

The largest commodity of the construction industry is undoubtedly concrete. Conventional concrete consists of cement, water, and aggregates of varying size (gravel, sand, crushed stone). Portland cement (PC), making up 15 % by weight of concrete, is globally consumed at a rate of 4.1 Gt per year and emits about 840 $kgCO_2$ per tonne [17], [18]. The high emissions are a result of clinker production, PC's main ingredient. Clinker production requires considerable thermal energy for reactor temperatures above 1500 ^oC (i.e., combustion emissions) and also releases CO_2

as a byproduct of calcining limestone (i.e., process emissions). The use of a hydrogen-fired kiln or an electric kiln, such that the electricity is sourced from a low-carbon energy resource, could offset the combustion emissions of the process. However, these technologies remain in their infancy today and do not avoid the CO_2 that is released from the thermal reduction of $CaCO_3$ to CaO (lime) and CO_2. Although minimizing the use of PC in new construction projects would have a large impact on the industry's emissions, finding an alternative with equitable reliability and cost has proven difficult (see Sections 3 and 4).

Crushed stone construction aggregates have a global demand of 22.5 Gt [19], where the majority of material used is limestone and dolomite (carbonates). While this presents the largest conventional carbonate market today, crushed stone is inexpensive and readily available at just under 12 USD/t [18]. Although other applications like fillers for paints and paper have a value up to 550 USD/t [20], the higher-purity requirements (> 99 %) can add cost to CM processes, as discussed in greater detail in Section 4. Therefore, CM products should possess physical or economic characteristics superior to naturally mined carbonate minerals or present new end uses not yet established by their natural counterparts.

This review will begin with a brief overview of CM research to date in Section 2, with emphasis on the challenges that exist in the field today. Section 3 will cover the available sources of alkalinity to be used for CM, with implications of suitability for CCUS. Finally, Section 4 will discuss marketable products that may be possible through CM processes.

2. Overview of Carbon Mineralization Processes

Alkalinity sources can be carbonated by exposing them *directly* to CO_2 or by converting them to a more reactive form before CO_2 exposure, thus reacting them *indirectly*. Each pathway has its advantages and disadvantages. While direct CM provides a simpler and cheaper one-step process, it often does not completely carbonate the available alkalinity, and yields products of lower purity. Indirect CM employs extraction of available alkalinity from the initial source and removes undesired species (e.g., silica) before carbonation [21]. Therefore, indirect CM is more well-suited for utilization of the carbonate products, despite the more complicated process. Storing CO_2 in mineral form with the potential for utilization may assist in offsetting process costs; hence, indirect CM will be the focus of this review.

2.1 Challenges with Alkalinity Extraction

Extraction of alkalinity is naturally limited by the diffusional limitations of Mg^{2+} or Ca^{2+} out of the mineral's lattice structure. While the exact kinetics vary based on the alkalinity source, extraction is widely modelled by the shrinking core model for reacting particles [22], [23]. Due to the diffusive limitations, many mineral activation processes have been explored to expedite the reaction rate.

2.1.1. Mechanical Activation

A key parameter in CM systems is the reactant particle size. For larger particle sizes, the extraction of Mg^{2+} and Ca^{2+} out of the particle severely limits the reaction rate. Particle size reduction is often used to increase the reactive surface area, subsequently increasing the rate of reaction. Since larger particle sizes severely limit the reaction kinetics, particle size reduction via grinding is shown to have a large effect on the extraction rate [24]. Many researchers have evaluated the effects of grinding on the extraction processes [24]–[26]. Improvements in Mg^{2+} extraction are great when

the particle size is reduced from 500 µm to 300 µm, however, the magnitude of improvement decreases from 300 µm to <75 µm [24]. Based on these analyses, the optimum particle size is ~75 µm, where further particle size reductions do not exhibit the same increase in reaction rate. In addition to increased surface area, particle size reduction by grinding also changes the surface shape and can induce microcracks in the existing lattice structure [26]. This can lead to increased specific surface area and allow for increased diffusion rates. While grinding is advantageous, there are high energy requirements for grinding particles to the desired size [27]. Both the cost associated with grinding and the emissions from electricity consumption are challenges to this method.

2.1.2. Chemical Activation - Acid Extraction

Acid extraction involves submerging alkaline minerals in acidic solutions to expedite the process, effectively releasing the desired cation(s) into solution. Strong acids are shown to be more effective for extraction than weaker acids and bases [28]. While strong acids work well for extraction, they also pose many problems to the overall CM process. These challenges can be broken into two major categories: process cost and associated emissions. First, many acids that work well for the extraction process (such as HCl and H_2SO_4) are corrosive to metals. This increases the overall capital and operating costs of the system. In addition to corrosivity, Table 1 outlines other hazard considerations for many acids tested for CM purposes.

Table 1: Common Acids for CM Extraction Processes and Related Hazards
[a]Associated hazards information obtained from Fischer Science Education Safety Data Sheets

Acid	Associated Hazards[a]	Extraction Experiments
Hydrochloric Acid (HCl)	Corrosive to metals, skin burns and eye damage, respiratory irritation	[29]–[33]
Nitric Acid (HNO_3)	Corrosive to metals, eye and skin burns, permanent digestive tract damage if ingested	[28], [30], [33], [34]
Acetic Acid (CH_3COOH)	Flammable liquid and vapor, acute oral and inhalation toxicity, skin corrosion, eye damage	[28], [30], [35]–[37]
Sulfuric Acid (H_2SO_4)	Corrosive to metals, skin burns, eye damage, respiratory irritation	[30], [38]–[40]
Citric Acid ($C_6H_8O_7$)	Eye, skin, intestinal, and respiratory tract irritation	[37], [41], [42]
Ascorbic Acid ($C_6H_8O_6$)	Eye, skin, intestinal, and respiratory tract irritation	[36], [41], [43]
Formic Acid (HCOOH)	Flammable liquid, acute oral and inhalation toxicity, skin corrosion/irritation, eye damage, respiratory irritation	[28], [34], [44]
EDTA ($C_{10}H_{16}N_2O_8$)	Eye and skin irritation, intestinal irritation, respiratory irritation, organ damage upon prolonged or repeated exposure	[45]–[47]

Additionally, there is a high cost associated with obtaining the volumes necessary to perform alkalinity extraction on a large scale. While some acid may be recoverable, this cost will be periodically incurred due to losses within the system. Following extraction, the low pH of the solution inhibits the dissolution of CO_2 into carbonic acid (H_2CO_3) for subsequent carbonation

reactions. Therefore, additional costs are associated with bases required to raise the pH. Other considerations include the energy requirements and emissions associated with producing the acid.

2.1.3. Chemical Activation – Salt Extraction

Based on a 1967 patent by Frederick Pundsack [48], this process involves heating alkaline material with ammonium sulfate ($(NH_4)_2SO_4$). At elevated temperatures (> 400 ºC), the magnesium in the mineral reacts with $(NH_4)_2SO_4$ and is converted to magnesium sulfate ($MgSO_4$) and ammonia gas [49], [50]. The $MgSO_4$ is then dissolved in water, producing Mg^{2+} and SO_4^{2-} ions in a solution that can be used for subsequent carbonation steps. Additionally, the ammonia gas and the sulfate ions in solution can be used to regenerate the ammonium sulfate reactant [49]. A schematic is shown in Figure 2. It is important to note that this process specifically targets magnesium, and other pretreatment methods may be more advantageous for Ca-rich feedstocks.

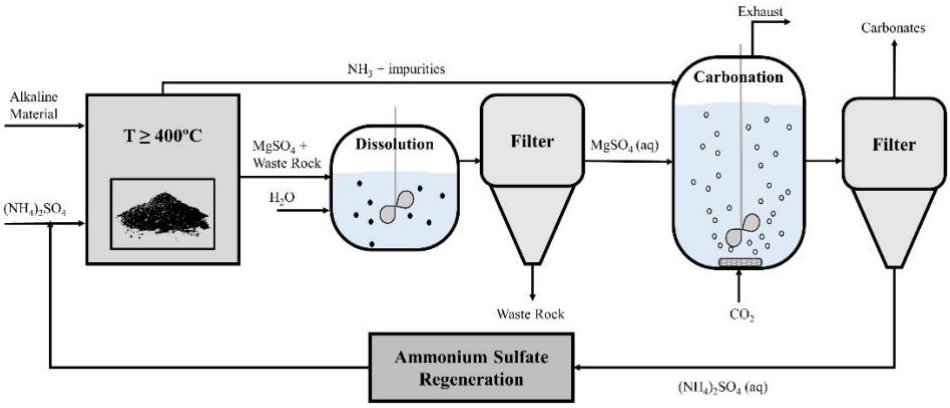

Figure 2: Schematic of the chemical activation visa a solid-solid reaction with ammonium sulfate

The solid-solid reaction with ammonium sulfate is highly energy intensive, requiring thermal energy to reach and sustain high temperatures. Additional energy penalties also result from adding the regeneration reaction for the ammonium sulfate. Thus, high operating cost and emissions from thermal energy are key challenges for this process.

2.1.4. Thermal Activation

Another pretreatment method is thermal activation, i.e., heating the alkaline material to maximize reactivity. The most rigorously studied thermal activation is the dehydroxylation of serpentine [51]–[53]. Similar to the solid-solid reaction above, the thermal pretreatment process requires energy to achieve and maintain high temperatures, leading to increased operating cost and greater process emissions, decreasing the net CO_2 captured and stored.

2.2 Challenges with the Carbonation Step

During indirect CM, the carbonation step is generally performed in aqueous solution. This creates various diffusion-related limitations and complications with formation of specific products, summarized in Figure 3.

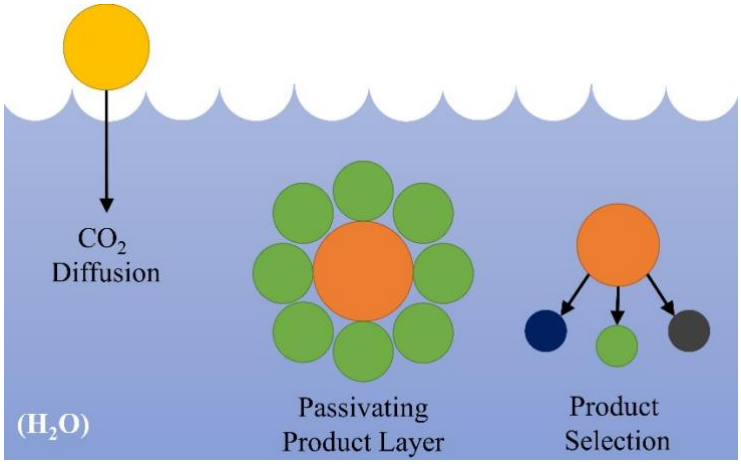

Figure 3: Illustration of main complications for carbonation step of indirect CM

2.2.1. Considerations with CO_2

The dissolution of carbon dioxide into water is controlled by Henry's law (Eq. 2), where the concentration of CO_2 in solution ($C_{CO_2(aq)}$) is directly proportional to the partial pressure of CO_2 ($P_{CO_2(g)}$) with Henry's constant (K_{H,CO_2}) [54]. An increase in temperature causes a decrease in solubility due to the governance of Henry's constant by the van't Hoff equation (3) [55], where $K_{H,CO_2}(298K)$ is $10^{-1.47}$ mol L^{-1} atm^{-1}. Here, the standard enthalpy change (ΔH^o) is assumed to be independent of temperature, and R is the ideal gas constant [56].

$$C_{CO_2(aq)} = K_{H,CO_2} * P_{CO_2} \quad (2)$$

$$K_{H,CO_2}(T) = K_{H,CO_2}(298K) * \exp\left(\frac{\Delta H^o}{R}\left(\frac{1}{T} - \frac{1}{298K}\right)\right) \quad (3)$$

Thus, carbonate precipitation rates decrease at higher temperatures despite hydroxide dissolution kinetics being positively proportional to temperature [57], [58]. Increases in reaction rate can be realized through the use of mixing and a high CO_2 flow rate. Further, CO_2 introduction through a smaller inlet to the reaction vessel or as small bubbles increases the reactive surface area, thus increasing the reaction rate [59].

2.2.2. Passivating Product Layer

Often during carbonate precipitation, a passivating layer forms around the reacting alkaline particles, inhibiting further carbonation [60]–[62]. Reports in the literature on the nature of this layer vary. Its composition typically consists of carbonate products [60], [61], but has also been deemed to be a decalcified Si-rich layer [62], indicating that the layer's composition depends on the composition of reactive species in the system. The effect of the passivating layer depends on its porosity [61], where a less porous layer has a higher passivating effect. Passivating layer formation is likely a result of the difference in the rates of carbonation and product diffusion. It has been found that milder conditions (pure H_2O vs dilute HCl) result in almost complete carbonation [63]. Here, the faster carbonation rate of dilute HCl likely causes a product layer to form and inhibit further reaction. Limitations due to product layer diffusion can be overcome by enhancing mass transfer within the multi-phase reaction system using a well-designed reactor [54], [64].

2.2.3. Product Selection

Different process conditions must be considered depending on the cation(s) present in the alkalinity source, as Mg^{2+} and Ca^{2+} behave differently in aqueous carbonation systems. The carbonation of Ca^{2+} occurs at a lower temperature because it has a smaller enthalpy of reaction (ΔH) than that of Mg^{2+} [65]. The difference in ionic radii among Mg^{2+} and Ca^{2+} (72 and 100 pm, respectively) gives rise to a difference in charge to radius ratios, affecting the interactions with other ions. Due to the higher ratio for Mg^{2+}, it has a high hydration activity and hosts strongly bonded hydration layers [66].

A low ratio of Mg^{2+} to CO_3^{2-} could overcome the increased hydration activity of Mg^{2+} ions, as carbonate anions have a larger radius and are not completely surrounded by water. This allows for easier adsorption on the crystal surface [67]. Practically, this could call for higher volumes of CO_2 fed into the system and the adoption of a recycling method of unreacted CO_2.

Precipitating Mg-based carbonates often involves dealing with both hydrated and anhydrous minerals, as shown in Table 2. Magnesite, the anhydrous form, has the most efficient use of Mg with a 1:1 ratio to CO_2, requires less process water due to its lack of crystalline water molecules, and is the most thermodynamically stable [68]. Magnesite is also lighter than hydrated carbonates, translating to cheaper transportation costs. Despite its favorability, production of magnesite requires extensive amounts of energy. An investigation of Mg-carbonate systems found that the first species formed is metastable nesquehonite (25 ^oC, 1 bar P_{CO_2}), followed by metastable hydromagnesite (120 ^oC, 3 bar). Hydromagnesite then very slowly transitions to magnesite until reaching 100 bar, the most favorable pressure for magnesite production [69]. In general, forming magnesite at rates adequate for large-scale processes requires temperatures above 100 ^oC, P_{CO_2}around 100 bar, and/or long reaction times [68].

Table 2: Common species in aqueous Mg-carbonate system, adapted[67], [70]

Mineral	Formula	ΔG_f^o (kJ/mol)	MW (g/mol)
Brucite	$Mg(OH)_2$	-835.32	58.32
Magnesite	$MgCO_3$	-1027.83	84.31
Nesquehonite	$MgCO_3 \cdot 3H_2O$	-1723.95	138.36
Hydromagnesite	$(MgCO_3)_4 \cdot Mg(OH)_2 \cdot 4H_2O$	-5864.66	467.64

To overcome the kinetic barrier for anhydrous magnesite precipitation, seeds can be incorporated into the reaction system. Use of magnesite seeds can completely bypass the formation of hydrated carbonate phases, and could be practically implemented through the addition of a product slip stream into the reactor [68]. Hydrophobic activated carbon seeds have been shown to increase magnesite concentration by up to 200 % by repelling water molecules during the transition from hydromagnesite to magnesite [71].

The rate constant for calcite precipitation at ambient conditions is six orders of magnitude larger than that of magnesite, as there is far less hydration activity involved [72]. However, there exist several polymorphs of calcium carbonate. Amorphous calcium carbonate (ACC) is the least stable, often transforming into one of three crystalline phases: calcite, aragonite, or vaterite. For indirect CM, calcite and aragonite are by far the most stable and commonly formed [73], and are the preferred forms in industry [74], [75].

2.3 Areas for Further Research

To overcome the challenges that exist in mineral activation processes, energy integration within the system may be helpful, as well as utilizing the exothermic nature of the carbonation reaction for dissolution. Further, additional research on brines and other alkaline-liquids that do not require a dissolution step but contain carbonation-ready alkalinity may also help in advancing CM technologies. This includes materials such as brines from desalination processes, natural gas or oil extraction, or some industrial mining processes [76], [77].

The field would also benefit from research on detailed scale-up of CM processes. Information from these experiments would provide insight into CM with flue gas conditions and processing larger volumes. Finally, materials characterization work should be performed on the various carbonates to determine which product is optimal for CCUS. This would involve determination of both the target market and the carbonate product that optimizes property superiority and production cost.

3. Alkalinity Available for Carbon Mineralization

To achieve CCUS with CM, one must start with a reactant source containing sufficient alkalinity (i.e., Mg^{2+} and Ca^{2+} cations). Alkalinity is abundant within both natural silicate minerals and wastes of industrial operations. Each alkalinity source comes with its own advantages and disadvantages in terms of ease of access, alkaline concentration, and cost, and should be assessed before subjecting to an CM process.

3.1 Industrial Alkalinity Sources

Industrial wastes are considered "low-hanging fruit" for CM due to their size and availability. The solid particles typically satisfy size requirements without additional grinding [21], [54]. Further, these wastes are produced annually as a byproduct of their respective industrial processes, presenting opportunity for a continual feedstock for CM. Oftentimes, wastes also exist in large stockpiled quantities that have accumulated over the years due to the lack of appropriate utilization or recycling methods. Carbonation of landfilled wastes also has the advantage of neutralizing potentially harmful waste and saving on high landfill costs (e.g., 150-500 EUR/tonne) [78].

Two industrial wastes most commonly investigated for CM are steel slags (SS) and coal fly ash (FA). Worldwide, SS and FA are produced at rates of about 400 and 660 Mt per year, respectively [79], [80]. Despite a lower production rate, SS is the more concentrated alkalinity source with the capacity to capture about 0.41 tCO_2/tSS, compared to about 0.22 tCO_2/tFA. These values are based on stoichiometric conversions from MgO and CaO content reported in the literature [81], [82].

Each year, it is estimated that 51.7 million m^3 of waste brine are produced from just under 16,000 operational desalination plants worldwide [83], containing an average concentration of 2360 and 730 g/m^3 in Mg^{2+} and Ca^{2+}, respectively [84]–[86]. Desalination is an energy-intensive process, requiring 4-23.5 kWh/m^3 of produced water, depending on the process used [87], and would benefit from carbon footprint reductions through CM.

Another form of alkaline waste is air pollution control residues (APCr) generated through municipal solid waste incineration (MSWI). When waste is incinerated, the acidic gaseous emissions are contacted with $Ca(OH)_2$ for neutralization, creating APCr that are often concentrated in both heavy metals and Ca-species [88]. Thus, carbonation of APCr presents opportunity for

carbon storage and hazardous waste neutralization. Globally, 11 % of the 2.01 Gt of municipal solid waste is incinerated [89], and a further 3.5 % is converted to APCr [90].

Concrete production/manufacturing is a carbon intensive process, but CCUS can be realized by taking advantage of chemistry in ordinary PC mixtures. There exists carbonation potential among the various Ca-silicate species and CaO that are hosted within cement and cement kiln dust. Cement kiln dust is a potentially hazardous waste generated during cement production. It is produced at a rate of about 500 Mt per year and consists of about 65 % CaO [91]. Additionally, concrete could be carbonated while it is being laid, resulting in enhanced properties. This process is discussed further in Section 4.1.

Table 3: Global Abundance and Carbonation Potential of Industrial Wastes
[a]million m^3/yr; [b]$kgCO_2/m^3$ feed; [c]capacity based on storing as magnesite/calcite

Feed	Production Rate	Carbonation Capacity[c]	Annual CCS Potential
	Mt/year	$kgCO_2$/tfeed	$MtCO_2$/year
Brines	[a]51700	[b]5.5	284
Cement Kiln Dust	500	570	284
Concrete	27333	10	273
Steel Slags	400	410	163
Fly Ash	660	220	144
APCr	7.7	330	3

Information for different alkaline wastes is summarized in Table 3. Carbonation capacity is calculated by converting all MgO and CaO contents to magnesite and calcite, respectively. This does not account for whether the alkaline oxide species are labile or strongly bound to other species (e.g., silicates) that would affect their ability to be carbonated. The annual CCS potential presented is based solely on feed abundance and carbonation capacity. This does not include any measure for efficiency and, as such, should be viewed as a maximum value. This equates to about 970 $MtCO_2$/year for the waste feeds listed.

3.1.1. Current markets and potential growth

For some industrial alkalinity sources, there already exists a market that would compete with new efforts for CM. Additionally, the production rate of some alkalinity sources is expected to change in the coming years. Most MSWI is performed by upper-middle- to high-income nations, while low-income nations openly dump most of their waste. Hence, MSWI installment should increase due to projected MSW generation growth to 2.6 Gt in the next decade [89] and the development of better waste handling practices in lower-income nations. Production of desalination brines is also expected to increase rapidly in the future due to increased water demands and water scarcity intensification [83].

Cement production in China is expected to decline in the long-term, where 60 % of the world's cement is produced. On the contrary, cement production increases are likely for developing Asian and African nations (e.g., India), resulting in an overall moderate growth in the next decade on the global scale [92]. It is estimated that concrete production during the period of 2016-2050 will be on the order of 650-800 Gt [93]. A common way to curb CO_2 emissions associated with concrete

is replacing portions of PC, concrete's most CO_2-intensive ingredient, with supplementary cementitious materials (SCMs). Two of the most typical SCMs used today are SS and FA, and while their use as SCMs results in decreased emissions in the concrete industry, it creates direct competition for utilization as CM feedstock. About 50 % of FA produced worldwide is already utilized [80]. The utilization rate of SS is at or near 100 % for many developed countries [94], but is quite low for most developing countries. China utilizes about 30 % of its SS, with nearly 300 Mt stockpiled in landfills as of 2016 [95]. While the global steel demand is expected to experience mild growth (about 0.8% per year until 2025) [96], pressure has been placed in several countries to decrease coal consumption. This could affect the long-term availability of these industrial wastes for the purpose of new CM operations.

3.2 Mined Alkalinity Sources

Another source of alkalinity for CM is found in natural silicate minerals, particularly within ultramafic rocks. Resources of ultramafic rock are in the range of 100s of millions to 100s of billions of tonnes [4]. This greatly increases the overall CCUS potential of CM due to its high carbonation potential compared to that of the wastes listed in Table 3. In contrast to industrial wastes, natural silicate minerals must be extracted from the ground and processed, and their availability would depend on the mining capabilities of CM operations. This is with the exception of mine tailings, which are the waste generated as a result of mining for commodity minerals. Like solid industrial wastes, tailings are typically of fine particle size, produced regularly, exist in stockpiles at various mine sites, and are also considered a "low-hanging fruit" for CM. Annual production of ultramafic (and mafic) tailings is estimated to be about 200-400 Mt/year [4], [91]. The carbonation capacity of both mined rock and mine tailings depends highly on the minerals present. Table 4 lists common silicate minerals containing alkalinity and the amount of CO_2 that can be stored with one tonne of each mineral. This amount varies with the ratio of CO_2 to metal oxide in the carbonate mineral and the distribution of divalent cations within the alkaline mineral feed [91]. The amount of water within hydromagnesite and nesquehonite should be noted, as this impacts the amount of material required for the CM process.

Table 4: Carbonation Capacity of Alkaline Minerals as Various Carbonate Products (Adapted)[91]

Carbonate Product	CO_2:MgO ratio	$kgCO_2$ per tonne alkaline mineral		
		Brucite $Mg(OH)_2$	Forsterite Mg_2SiO_4	Serpentine $Mg_3Si_2O_5(OH)_4$
Magnesite $MgCO_3$	1:1	752	625	476
Hydromagnesite $Mg_5(CO_3)_4(OH)_2•4H_2O$	4:5	602	500	382
Nesquehonite $MgCO_3•3H_2O$	1:1	752	625	476
Carbonate Product	CO_2:CaO ratio	$kgCO_2$ per tonne alkaline mineral		
		Portlandite $Ca(OH)_2$	Wollastonite $CaSiO_3$	Anorthite $CaAl_2Si_2O_8$
Calcite $CaCO_3$	1:1	590	380	160

In comparing the amounts of CO_2 stored as magnesite or calcite in Table 4 to those listed in Table 3, it is apparent that alkaline minerals are generally able to store far more CO_2 than industrial

wastes. However, while carbonation capacity for these natural silicate minerals is based on the individual mineral, most rocks also contain other minerals that are deficient in Mg^{2+} and Ca^{2+} or could compete for the cations and precipitate undesired products, like clays. This indicates that a significantly larger rock mass may be required to capture the same amount of CO_2 depicted in Table 4 [97]. Performing CM with mined minerals also carries the cost of mining. The added cost of mining depends primarily on the size of the operation and rock hardness, and is estimated to be about 7-15 USD/tCO_2 [98].

4. Marketable Products of Carbon Mineralization

4.1 Analysis of Current Commercial Efforts

It is important to consider the market size and value of the different products synthesized through CM. As discussed previously in Section 1 and illustrated in Figure 1, not all of the current end-uses of carbonate minerals result in stable storage of CO_2. While other plausible products present options for utilization (to be discussed later in this section), the construction industry presents the most viable opportunity for utilization. Presently, there are several commercial efforts involving CM in which products are sold in the construction industry [99], [100]. Such efforts may be grouped by those that are making changes to PC-based concrete mixtures (Type 1) and those that are producing materials without PC (Type 2). Within the two main types, processes differ by product and/or alkalinity source, making the five generalized categories shown in Figure 4.

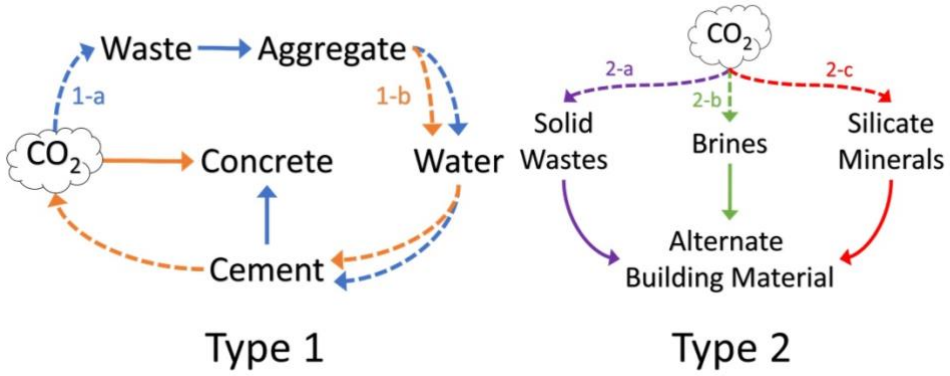

Figure 4: Generalized Commercial Carbon Mineralization Processes
(dashed lines indicate additions; solid lines indicate conversions)

Process Type 1-a involves the production of synthetic aggregates, which are an essential ingredient of concrete as they provide volume and stability. The global aggregate market, including sand, gravel, crushed stone, and others, amounts to about 53 Gt/year [101]. Because conventional aggregates are low-value commodities with relatively low associated emissions (7.85 kgCO_2-e per tonne of aggregate) [102], synthetic aggregates produced through CM should present superior qualities and/or contain large amounts of CO_2 in order to be competitive. It should be noted that while aggregates are necessary for PC-based concrete, they may also be used in the non-PC based mixtures of some Type 2 processes.

Processes in Type 1-b refer to the CCUS method alluded to in Section 3.1, where concrete is cured with CO_2. Immediately after concrete has been placed, its properties begin to develop through hydration reactions, the rate and extent of which are affected by moisture presence and

temperature. The process of curing involves regulating moisture content and temperature to allow the specified properties to be achieved [103]. While curing generally occurs due to water presence, it is also possible to cure with CO_2, enhancing durability and strength properties and storing CO_2 [104], [105]. Based on stoichiometry, up to 10 kgCO_2 may be stored per tonne of concrete [5]. This results in a concrete product with superior properties to conventional concrete, and has already been successful in current markets [106]–[108]. Concrete products such as this face less issues with acceptance within the industry compared to alternative cementitious materials due to the similarities in chemistry with the more established conventional concrete.

Solid industrial wastes, namely SS and FA, have been widely used in concrete mixtures since the 1950s as SCMs alongside PC as a means to enhance performance and decrease carbon footprint [109], [110]. Companies within process Type 2-a aim to expand upon this method by carbonating these solid wastes to manufacture cementitious materials without using PC. Performing CM with waste brines (process Type 2-b) generally results in the synthesis of nesquehonite, which can exhibit strength properties similar to gypsum-based products [111]. Gypsum fiberboards are used for their properties of fire resistance and thermal and acoustic insulation [112], and are consumed at a rate of nearly 800 million boards per year in the US [18].

A common theme amongst Type 2 processes (and sometimes Type 1-b) is the synthesis of precast concrete materials such as concrete blocks and cement boards. Precast concrete has been used in US construction projects predating 1920 [113], and now constitutes up to 30 % of the country's concrete market [104]. The use of precast concrete brings the advantages of an accelerated construction process, enhanced quality, decreased project costs, and increased sustainability [114]. This manner of concrete production is advantageous for utilization of CM products as it provides more opportunity for quality control in a factory setting as opposed to manufacturing in the field (e.g., for curing with CO_2). The consumption of concrete blocks and cement boards in North America in 2018 was about 6025 and 2950 million units, respectively [104], [115]. The value of a standard 8"×8"×16" concrete block is on the order of 1 USD [116], while that of a 4'×8'×0.5" cement board is about 30 USD. Although the value is seemingly low, the consumption volume is enough to present a viable utilization opportunity, especially as sentiment of construction industry professionals towards precast materials continues to increase [114].

Table 5 summarizes the market size and related emissions of commodities that could be produced through CM processes. The CO_2 intensity of products conventionally used presents opportunity for further avoided emissions. Cement and concrete comprise the largest amount of market use and emissions, where bulk concrete estimations are based on being composed of 15 % cement. Despite having a relatively low market use, production of gypsum boards has a high emissions intensity. The problem of CCUS with Mg-based carbonates is further illustrated here, as the two main products, magnesite and gypsum boards, have the smallest markets shown in the table. Although the cost of magnesite is relatively high, it reflects the market price of magnesite for the production of magnesia [117], where additional energy is used to calcine magnesite and release the stored CO_2. Work should continue to find new uses for Mg-carbonates for the purpose of CCUS.

Table 5: Emission and Market Information of Conventional Products to be Replaced by CM Products
[18], [19], [77], [90], [102], [116]–[121]
[a]North America data

End-Use	Product Unit	CO_2 Intensity	Market Use	CO_2 Emitted	Value
	[PU]	tCO_2/[PU]	M[PU]/yr	$MtCO_2$/yr	USD/[PU]
Aggregate	t	0.0079	53000	416	10
Bulk Cement	t	0.9270	4100	3800	125
Bulk Concrete	t	0.1391	27333	3800	95
Precast Concrete Block[a]	block	0.0024	6000	15	1
Precast Cement Board[a]	board	0.0551	3000	165	30
Magnesite	t	0.0147	13	0.2	80
Gypsum Board[a]	board	0.0004	800	0.34	30

By combining data from Tables 3-5 with information from company publications and websites, the potential for CO_2 avoidance by each process type has been evaluated on a global scale, shown in Table 6. The "CO_2 Capacity" is the amount of CO_2 embodied by each product and is based on information from company publications and websites. The "CO_2 Avoided per Product" is the sum of the product CO_2 capacity and the emissions avoided by replacing the conventional product. The "limiting factor" indicates whether the amount of feed available is much smaller than the product market size, or vice versa. The "global CO_2 avoidance" is a function of the limiting factor and is the maximum value of CO_2 avoided each year if all available feed is carbonated or the entire current product market is filled with the respective process type.

Table 6: CO_2 Avoidance Capability by CM Process Type
([a]F = feed availability, P = product market)
Values are calculated based on feed availability and CO_2 capacity given in Tables 3-5. Information for products from specific companies are interpreted from released publications or company websites.[5], [77], [84], [122]–[131]

Type	Feed	Product Replaced	CO_2 Capacity	CO_2 Avoided per Product	Limiting Factor[a]	Global CO_2 Avoidance
			(tCO_2/t-product)	(tCO_2/t-product)		($MtCO_2$/year)
1-a	Solid Wastes	Aggregate	0.087 - 0.440	0.098 - 0.448	F	93
1-b	Concrete	Conventional Concrete	0.001 - 0.050	0.001 - 0.057	P	1561
2-a	Solid Wastes	PC	0.001 - 0.137	0.003 - 1.064	F	307
2-b	Brines	PC &Fiber Boards	0.008 - 0.300	0.085 - 0.300	P	1092
2-c	Silicate Minerals	Magnesite	0.522 - 0.522	0.537 - 0.537	P	14

Despite its relatively low CO_2 capacity and CO_2 avoidance per product, process Type 1-b presents the largest annual emissions avoidance. Type 1-b and 2-b both benefit from the vast feed availability of concrete and brines, respectively. The market size of conventional concrete further amplifies the potential global CO_2 avoidance of Type 1-b.

Process Type 1-a and Type 2-a both use solid wastes for CM to produce aggregate and alternate cement, respectively. To avoid overlap of feed usage, it was assumed that APCr and ultramafic tailings are used for 1-a, and SS and FA are used for 2-a. In both cases here, the product markets of aggregate and cement are much larger than the available feedstock. Hence, the global CO_2 avoidance is based on carbonating all the available feed to its maximum extent.

Process Type 2-c shows low potential for global CO_2 avoidance due to the low demand of magnesite-based products. The potential could be increased for Type 2-c through the development of new products, to be discussed in Section 4.2.

Overall, Table 6 indicates that global deployment current commercial efforts could result in the avoidance of more than 3 $GtCO_2$/year. The major limitation of the analysis shown here is a lack of knowledge on the process efficiency for commercial processes. Energy requirements for the process could result in additional carbon emissions, decreasing the process's emission avoidance. However, this could be ignored if the process is powered by carbon-free energy. Additionally, due to lack of specific company process specifications, it was assumed that 100 % Mg and Ca contained in the feed was converted to carbonate products. This is an optimistic value and is likely unachievable. Still, technological advancements as the processes mature can be expected to bring further increases in conversion. These factors further necessitate the distinction of global CO_2 avoidance values as a "maximum."

4.2 Proposing New Products

Most of the current commercial efforts involve creating Ca-based products due to many factors, as prefaced previously in this review. Generally, industrial wastes are richer in Ca, while natural minerals and brines are often richer in Mg. Further, it has been found that CO_2 binds more strongly to CaO than MgO [132]. Although creating Ca-based products is currently easier and cheaper, developing viable Mg-based products is necessary to exploit the vast quantity of Mg-silicate minerals available for CCUS. The following sections outline additional options that could be explored for CCUS through CM. While the use of carbonates in the pharmaceutical, agricultural, and refractory metals industries could be suggested (Figure 1), the end uses ultimately result in the release of CO_2 and will not be discussed further.

4.2.1. Precipitated Calcium Carbonate

Precipitated calcium carbonate (PCC) is a form of calcium carbonate that is a well-established filler material and coating pigment in premium paper products, particularly due to its brightness, and is often produced in slurry form near paper mills. As PCC is chemically synthesized, its manufacture can be controlled to achieve specific particle sizes and crystal shapes, giving it unique polymer applications [133]. PCC differs from limestone, i.e., ground calcium carbonate, in that it is brighter, smaller in particle size, less abrasive, and purer [20]. As of 2014, the market for mineral fillers and pigments is about 14 Mt/year with a high value of 375-550 USD/t, while the world's ground calcium carbonate market is 75 Mt with a lower value of 26-185 USD/t depending on fineness [20]. A challenge in producing PCC is product purity, as specifications often require > 99 % [134]. However, the selling value of PCC could be high enough to absorb additional costs incurred through achieving such high purity.

4.2.2. Magnesia Cements

The addition of MgO to ordinary PC mixtures brings complications due to added expansion. Hydration of MgO to brucite results in a molar solid volume expansion of 117 %, compared to that of CaO to portlandite of about 90 % [135]. However, MgO-based cements have been proposed as an alternative to PC, bringing the advantage of lower calcination temperature and ability to carbonate MgO within the cement. Despite this, overall research is not sufficiently developed to overcome the barriers to large-scale implementation. When considering the (MgO/CaO)-Al_2O_3-SiO_2 phase diagrams, there is no Mg-analog for the basic Ca-based cement species, indicating that using MgO-based cements is not nearly as simple as replacing CaO with MgO. While MgO-based cements may find markets in niche applications like precast concrete, the lack of understanding and higher cost will prevent them from large-scale implementation [136].

4.2.3. Flame-retardant Fillers

Hydrous Mg-carbonates are used in some cases as flame-retardant fillers in products like textiles, polymers, rubbers, and paints. As the more conventionally used flame-retardants involve release of halogen radicals, mineral fillers have gained attention as a more environmentally friendly option. In fact, a flame-retardant product using a mixture of hydromagnesite and huntite exists on the market today with increasing demand [137]. Mineral fillers are ideal as they absorb heat through endothermic decomposition, form a protective inert layer on the material surface, and release inert diluent gases, i.e., H_2O and CO_2 [138]. The decomposition of hydromagnesite and nesquehonite occurs in separate stages, where the loss of water molecules occurs around the initial decomposition temperature in Table 7, and the CO_2 molecule(s) are removed later around 456-650 and 450 ^oC, respectively [138], [139]. Although this end-use could result in release of captured CO_2, the combustion reaction would need to proceed to a higher temperature. Moreover, this end-use is still an upgrade from conventional flame-retardants in terms of performance and emissions of halogenic fumes. Additionally, it incorporates hydrous Mg-carbonates that are otherwise difficult to utilize.

Table 7: Physical properties of potential fire retarding mineral fillers [138]

Filler	Formula	T_{decomp} (^oC)	ΔH_{decomp} (kJ/g)
Nesquehonite	$MgCO_3 \cdot 3H_2O$	70-100	1750
Hydromagnesite	$Mg_5(CO_3)_4(OH)_2 \cdot 4H_2O$	220-240	1300
Huntite	$Mg_3Ca(CO_3)_4$	400	980

A troubling aspect of this end use is the market size, as only about 2.21 Mt of flame retardants are used per year within plastics, electronics, construction material, and textiles [140]. Despite this, new market potential exists for fire resistant paints. Most traditional paints lack fire retarding properties, and construction methods are evolving to adopt fire resistant materials [141]. The incorporation of hydromagnesite at 5.5 wt% in a paint causes the paint to form a dense foam due to the crystalline water present in hydromagnesite. This foam acts as a protective surface barrier that prevents diffusion of combustible gases [139]. This application gives first responders invaluable time to arrive at the scene, minimizing property damage and injuries. We estimate that coating an average new US home's [142] interior walls with this paint would account for just over 1 kgCO_2 utilized. Considering the 1.4 billion gallon demand of paints and coatings in 2020 [143], up to 162 MtCO_2 could be utilized.

Work still needs to be done on determining the effects of different mineral fillers on the properties of the material in which they are being implemented. The high filler volume sometimes necessary for adequate fire protection can exacerbate any other detrimental effects. Further, their use can also be limited by particle size, which should be smaller than the host material [144].

4.2.4. Utilization of Silica Byproduct

Additionally, there may be a new market for replacing sand as a fine aggregate. Sand is a key ingredient for concrete, asphalt, glass, electronics, land reclamation projects, shale gas extraction, and beach nourishment programs [145]. About 16.5 Gt of sand is used each year as a construction aggregate alone [101]. Among others, sand mining has an impact on biodiversity, water supply by lowering the water table, and loss of land through erosion [146]. The banning of sand mining in some countries has even led to rise of organized crime groups involved in illegal trade of soil and sand [145]. While it has become a scarce resource in some parts of the world, it is unclear whether global demand exceeds supply [147]. Most sands used are mainly quartz, SiO_2, and are defined by a particle size 0.0625-2 mm [148]. This could be replaced by the SiO_2 that is produced as a byproduct in CM processes.

5. Outlook for CCUS with Carbon Mineralization

Carbon mineralization presents the opportunity to mitigate a significant portion of anthropogenic CO_2 emissions. While the process is still gaining maturity on the industrial level in terms of efficiency and cost, some of the cost can be compensated through the utilization of carbonate products. This study reviewed the state-of-the-art in indirect CM processing, alkaline feedstock availability, and market potential of carbonate products. Several commercial efforts currently exist which use CM to create and sell products, all of which are concentrated within the construction industry. General company process types were identified based on their alkaline feed and carbonate products (Figure 4) and their potential for global CO_2 avoidance was evaluated (Table 6). While each process type presents varying degrees of potential to avoid CO_2 emissions, further investigation reveals that other factors play a role in overall market readiness. The essential findings of the review are given below, with emphasis on relevance to the field's outlook:

1. Immediate commercial efforts should look towards carbonation of industrial or mining wastes to produce precast concrete blocks. Here, the alkalinity source requires minimal preparation or transportation, and the products face less resistance to market acceptance. Locations like iron/steel plants without pre-existing waste utilization should evaluate CM processes for immediate deployment.

2. Processes which alter traditional PC-based concrete present the highest potential for CO_2 avoidance and have exhibited commercial readiness but are likely to face some resistance. Contractors and manufacturers are hesitant to switch from familiar products to new and unproven ones. Additionally, most industry standards prescribe specific amounts of materials rather than specifications based on product performance. Efforts are being made around the world to convert to such performance-based standards to ease the integration of new building materials from CM products [110], [149]. Upcoming CM CCUS endeavors should adopt business models that cater to the industry professionals, e.g., producing alternative cement at the site of the cement producer, where they are able to have more control over process conditions to ensure the reliability of the product [123].

3. Utilization of Mg-based carbonates still faces multiple limitations. While Mg-rich silicate minerals are highly abundant, they require costly mining and transportation to CO_2 sources for CM processing. Further, product selectivity is difficult to control, where several hydrated and anhydrous carbonates can be synthesized possessing different properties. Moreover, there is not currently a sufficient market demand for Mg-based carbonates. Research should focus on an increased understanding of long-term properties of MgO cements and the development of new products, like the flame-retardant mineral fillers proposed here.

4. Areas of research were also proposed to advance indirect CM processes. This primarily involves energy integration using the exothermic carbonation reaction, process scale-up through carbonation with flue-gas conditions, and product materials characterization.

References

[1] H. Ritchie and M. Roser, "CO_2 and Other Greenhouse Gas Emissions," *Our World in Data*, 2019. [Online]. Available: https://ourworldindata.org/co2-and-other-greenhouse-gas-emissions#co2-emissions-global-and-regional-trends.

[2] IPCC, "IPCC special report on the impacts of global warming of 1.5 °C - Summary for policy makers," William Solecki, 2018.

[3] The Royal Society, *Greenhouse gas removal*. 2018.

[4] National Academies Press, *Negative Emissions Technologies and Reliable Sequestration*. 2019.

[5] National Academies of Science Engineering and Medicine, *Gaseous Carbon Waste Streams Utilization: Status and Research Needs*. Washington, DC: The National Academies Press, 2019.

[6] W. Seifritz, "CO_2 disposal by means of silicates," *Nature*, vol. 345, no. 6275, p. 486, 1990.

[7] K. S. Lackner, C. H. Wendt, D. P. Butt, E. L. Joyce, and D. H. Sharp, "Carbon dioxide disposal in carbonate minerals," *Energy*, vol. 20, no. 11, pp. 1153–1170, 1995.

[8] "Web of Science." [Online]. Available: http://apps.webofknowledge.com/. [Accessed: 01-May-2019].

[9] E. S. P. Aradóttir, H. Sigurdardóttir, B. Sigfússon, and E. Gunnlaugsson, "CarbFix: A CCS pilot project imitating and accelerating natural CO_2 sequestration," *Greenh. Gases Sci. Technol.*, vol. 1, no. 2, pp. 105–118, Jun. 2011.

[10] B. Sigfússon, "CarbFix: Permanent and efficient carbon capture and mineral storage in basalts," 2018.

[11] E. M. Mervine *et al.*, "Potential for Offsetting Diamond Mine Carbon Emissions through Mineral Carbonation of Processed Kimberlite," in *11th International Kimberlite Conference*, 2017, pp. 2011–2013.

[12] De Beers Group of Companies, "Fact Sheet De Beers Group carbon storage research project."

[13] F. M. Baena-Moreno, M. Rodríguez-Galán, F. Vega, B. Alonso-Fariñas, L. F. V. Arenas, and B. Navarrete, "Carbon capture and utilization technologies: a literature review and recent advances," *Energy Sources, Part A Recover. Util. Environ. Eff.*, vol. 41, no. 12, pp. 1403–1433, 2019.

[14] S. Y. Pan, P. C. Chiang, W. Pan, and H. Kim, "Advances in state-of-art valorization technologies for captured CO2 toward sustainable carbon cycle," *Crit. Rev. Environ. Sci. Technol.*, vol. 48, no. 5, pp. 471–534, 2018.

[15] J. Yan and Z. Zhang, "Carbon Capture, Utilization and Storage (CCUS)," *Appl. Energy*, vol. 235, pp. 1289–1299, 2019.

[16] Energy Futures Initiative, “Advancing Large Scale Carbon Management: Expansion of the 45Q Tax Credit,” no. May, 2018.

[17] Cembureau, “Activity Report 2018,” Brussels, 2018.

[18] U.S. Geological Survey, “Mineral commodity summaries 2019: U.S. Geological Survey,” 2019.

[19] M. S. Kuhar, “World Aggregates Market,” *Rock Products*, 2014. [Online]. Available: http://www.rockproducts.com/features/13045-world-aggregates-market.html#.XK_hcOhKjD4. [Accessed: 15-Apr-2019].

[20] P. Stratton, “An Overview of the North American Calcium Carbonate Market,” no. October, p. 43, 2012.

[21] E. R. Bobicki, Q. Liu, Z. Xu, and H. Zeng, “Carbon capture and storage using alkaline industrial wastes,” *Prog. Energy Combust. Sci.*, vol. 38, no. 2, pp. 302–320, 2012.

[22] P. Renforth, P. A. E. Pogge von Strandmann, and G. M. Henderson, “The dissolution of olivine added to soil: Implications for enhanced weathering,” *Appl. Geochemistry*, vol. 61, pp. 109–118, 2015.

[23] M. F. Irfan, M. R. Usman, and A. Rashid, “A detailed statistical study of heterogeneous, homogeneous and nucleation models for dissolution of waste concrete sample for mineral carbonation,” *Energy*, vol. 158, pp. 580–591, Sep. 2018.

[24] A. Sanna, X. Wang, A. Lacinska, M. Styles, T. Paulson, and M. M. Maroto-Valer, “Enhancing Mg extraction from lizardite-rich serpentine for CO_2 mineral sequestration,” *Miner. Eng.*, vol. 49, pp. 135–144, Aug. 2013.

[25] W. K. O’Connor, D. C. Dahlin, G. E. Rush, S. J. Gerdemann, L. R. Penner, and D. N. Nilsen, “Aqueous Mineral Carbonation: Mineral Availability, Pretreatment, Reaction Parametrics, and Process Studies,” 2005.

[26] T. A. Haug, R. A. Kleiv, and I. A. Munz, “Investigating dissolution of mechanically activated olivine for carbonation purposes,” *Appl. Geochemistry*, vol. 25, no. 10, pp. 1547–1563, 2010.

[27] S. Martins, “Size-energy relationship in comminution, incorporating scaling laws and heat,” *Int. J. Miner. Process.*, vol. 153, pp. 29–43, 2016.

[28] S. Teir, H. Revitzer, S. Eloneva, C.-J. Fogelholm, and R. Zevenhoven, “Dissolution of natural serpentinite in mineral and organic acids,” *Int. J. Miner. Process.*, vol. 83, no. 1–2, pp. 36–46, Jul. 2007.

[29] S. Vanderzee and F. Zeman, “Recovery and carbonation of 100% of calcium in waste concrete fines: Experimental results,” *J. Clean. Prod.*, vol. 174, pp. 718–727, Feb. 2018.

[30] M. M. Maroto-Valer, D. J. Fauth, M. E. Kuchta, Y. Zhang, and J. M. Andrésen, “Activation of magnesium rich minerals as carbonation feedstock materials for CO2 sequestration,” in *Fuel Processing Technology*, 2005, vol. 86, no. 14–15, pp. 1627–1645.

[31] T. A. Haug, I. A. Munz, and R. A. Kleiv, “Importance of dissolution and precipitation

kinetics for mineral carbonation," *Energy Procedia*, vol. 4, pp. 5029–5036, Jan. 2011.

[32] G. L. A. F. Arce, T. G. Soares Neto, I. Ávila, C. M. R. Luna, and J. A. Carvalho, "Leaching optimization of mining wastes with lizardite and brucite contents for use in indirect mineral carbonation through the pH swing method," *J. Clean. Prod.*, vol. 141, pp. 1324–1336, 2017.

[33] A. Azdarpour *et al.*, "Extraction of calcium from red gypsum for calcium carbonate production," *Fuel Process. Technol.*, vol. 130, no. C, pp. 12–19, Feb. 2015.

[34] M. Ghoorah, B. Z. Dlugogorski, R. D. Balucan, and E. M. Kennedy, "Selection of acid for weak acid processing of wollastonite for mineralisation of CO2," *Fuel*, vol. 122, pp. 277–286, 2014.

[35] M. Kakizawa, A. Yamasaki, and Y. Yanagisawa, "A new CO2 disposal process via artificial weathering of calcium silicate accelerated by acetic acid," *Energy*, vol. 26, no. 4, pp. 341–354, Apr. 2001.

[36] D. N. Huntzinger, J. S. Gierke, L. L. Sutter, S. K. Kawatra, and T. C. Eisele, "Mineral carbonation for carbon sequestration in cement kiln dust from waste piles," *J. Hazard. Mater.*, vol. 168, no. 1, pp. 31–37, 2009.

[37] S. K. Seo, C. M. Kwon, F. S. Kim, and C. J. Lee, "Experiment and kinetic modeling for leaching of blast furnace slag using ligand," *J. CO2 Util.*, vol. 27, no. February, pp. 188–195, Oct. 2018.

[38] K. Kosuge, K. Shimada, and A. Tsunashima, "Micropore Formation by Acid Treatment of Antigorite," *Chem. Mater.*, vol. 7, no. 12, pp. 2241–2246, 1995.

[39] A. Azdarpour, M. Asadullah, E. Mohammadian, H. Hamidi, R. Junin, and M. A. Karaei, "A review on carbon dioxide mineral carbonation through pH-swing process," *Chemical Engineering Journal*, vol. 279. Elsevier, pp. 615–630, 01-Nov-2015.

[40] O. Rahmani, "CO_2 sequestration by indirect mineral carbonation of industrial waste red gypsum," *J. CO2 Util.*, vol. 27, pp. 374–380, Oct. 2018.

[41] M. Hänchen, V. Prigiobbe, G. Storti, T. M. Seward, and M. Mazzotti, "Dissolution kinetics of fosteritic olivine at 90–150°C including effects of the presence of CO2," *Geochim. Cosmochim. Acta*, vol. 70, no. 17, pp. 4403–4416, Sep. 2006.

[42] S. Teir, S. Eloneva, C.-J. Fogelholm, and R. Zevenhoven, "Fixation of carbon dioxide by producing hydromagnesite from serpentinite," *Appl. Energy*, vol. 86, no. 2, pp. 214–218, Feb. 2009.

[43] A.-H. A. Park, R. Jadhav, and L.-S. Fan, "CO2 Mineral Sequestration: Chemically Enhanced Aqueous Carbonation of Serpentine," *Can. J. Chem. Eng.*, vol. 81, no. 3–4, pp. 885–890, May 2003.

[44] J. Fagerlund, S. Teir, E. Nduagu, and R. Zevenhoven, "Carbonation of magnesium silicate mineral using a pressurised gas/solid process," *Energy Procedia*, vol. 1, no. 1, pp. 4907–4914, Feb. 2009.

[45] B. Bonfils, C. Julcour-Lebigue, F. Guyot, F. Bodénan, P. Chiquet, and F. Bourgeois, "Comprehensive analysis of direct aqueous mineral carbonation using dissolution enhancing organic additives," *Int. J. Greenh. Gas Control*, vol. 9, pp. 334–346, 2012.

[46] E. R. Bobicki, Q. Liu, and Z. Xu, "Mineral carbon storage in pre-treated ultramafic ores," *Miner. Eng.*, vol. 70, pp. 43–54, 2015.

[47] N. A. Meyer, J. U. Vögeli, M. Becker, J. L. Broadhurst, D. L. Reid, and J.-P. Franzidis, "Mineral carbonation of PGM mine tailings for CO2 storage in South Africa: A case study," *Miner. Eng.*, vol. 59, pp. 45–51, 2014.

[48] F. L. Pundsack, "Recovery of Silica, Iron Oxide and Magnesium Carbonate from the Treatment of Serpentine with Ammonium Bisulfate," 1967.

[49] R. Zevenhoven and J. Fagerlund, "Mineral sequestration for CCS in Finland and abroad," *World Renew. Energy Congr. 2011-Sweden, Clim. Chang. Issues*, pp. 660–667, 2011.

[50] R. Zevenhoven, M. Slotte, E. Koivisto, and R. Erlund, "Serpentinite Carbonation Process Routes using Ammonium Sulfate and Integration in Industry," *Energy Technol.*, vol. 5, no. 6, pp. 945–954, 2017.

[51] M. Werner, S. B. Hariharan, A. V. Bortolan, D. Zingaretti, R. Baciocchi, and M. Mazzotti, "Carbonation of activated serpentine for direct flue gas mineralization," in *Energy Procedia*, 2013, vol. 37, pp. 5929–5937.

[52] S. J. Gerdemann, W. K. O'Connor, D. C. Dahlin, L. R. Penner, and H. Rush, "Ex situ aqueous mineral carbonation," *Environ. Sci. Technol.*, vol. 41, no. 7, pp. 2587–2593, 2007.

[53] M. J. McKelvy, A. V. G. Chizmeshya, J. Diefenbacher, H. Béarat, and G. Wolf, "Exploration of the role of heat activation in enhancing serpentine carbon sequestration reactions," *Environ. Sci. Technol.*, vol. 38, no. 24, pp. 6897–6903, 2004.

[54] S. Y. Pan, E. E. Chang, and P. C. Chiang, "CO_2 Capture by Accelerated Carbonation of Alkaline Wastes: A Review on its Principles and Applications," *Aerosol Air Qual. Res.*, vol. 12, no. 5, pp. 770–791, 2012.

[55] NIST, "Carbon dioxide." [Online]. Available: https://webbook.nist.gov/cgi/inchi?ID=C124389&Mask=10#Solubility. [Accessed: 10-Jul-2019].

[56] V. L. Snoeyink and D. Jenkins, *Water Chemistry*. 1980.

[57] C. H. Rhee, J. Y. Kim, K. Han, C. K. Ahn, and H. D. Chun, "Process analysis for ammonia-based CO_2 capture in ironmaking industry," in *Energy Procedia*, 2011, vol. 4, pp. 1486–1493.

[58] J. Hövelmann, C. V. Putnis, E. Ruiz-Agudo, and H. Austrheim, "Direct nanoscale observations of CO2 sequestration during brucite [Mg(OH)2] dissolution," *Environ. Sci. Technol.*, vol. 46, no. 9, pp. 5253–5260, 2012.

[59] H. P. Mattila, I. Grigaliu-naite, and R. Zevenhoven, "Chemical kinetics modeling and

process parameter sensitivity for precipitated calcium carbonate production from steelmaking slags," *Chem. Eng. J.*, vol. 192, pp. 77–89, Jun. 2012.

[60] Ö. Cizer, K. Van Balen, J. Elsen, and D. Van Gemert, "Real-time investigation of reaction rate and mineral phase modifications of lime carbonation," *Constr. Build. Mater.*, vol. 35, pp. 741–751, 2012.

[61] A. L. Harrison, G. M. Dipple, I. M. Power, and K. U. Mayer, "Influence of surface passivation and water content on mineral reactions in unsaturated porous media: Implications for brucite carbonation and CO_2 sequestration," *Geochim. Cosmochim. Acta*, vol. 148, pp. 477–495, 2015.

[62] D. Medas, G. Cappai, G. De Giudici, M. Piredda, and S. Podda, "Accelerated carbonation by cement kiln dust in aqueous slurries: chemical and mineralogical investigation," *Greenh. Gases Sci. Technol.*, vol. 7, pp. 692–705, 2017.

[63] L. Zhao, L. Sang, J. Chen, J. Ji, and H. Henry Teng, "Aqueous Carbonation of Natural Brucite: Relevance to CO_2 Sequestration," *Envion. Sci, Technol*, vol. 44, pp. 406–411, 2010.

[64] J. Hövelmann, C. V. Putnis, E. Ruiz-Agudo, and H. Austrheim, "Direct nanoscale observations of CO_2 sequestration during brucite [$Mg(OH)_2$] dissolution," *Environ. Sci. Technol.*, vol. 46, no. 9, pp. 5253–5260, 2012.

[65] S. Teir, R. Kuusik, C.-J. Fogelholm, and R. Zevenhoven, "Production of magnesium carbonates from serpentinite for long-term storage of CO2," *85*, pp. 1–15, 2007.

[66] J. Bo, Y. Zhang, and Y. Zhang, "Mechanism, kinetic model and hydrogen ion apparent diffusion coefficient in magnesium hydroxide dissolution by pressurized carbonated water," *React. Kinet. Mech. Catal.*, vol. 122, no. 2, pp. 819–838, 2017.

[67] M. Hänchen, V. Prigiobbe, R. Baciocchi, and M. Mazzotti, "Precipitation in the Mg-carbonate system-effects of temperature and CO_2 pressure," *Chem. Eng. Sci.*, vol. 63, no. 4, pp. 1012–1028, Feb. 2008.

[68] E. J. Swanson, K. J. Fricker, M. Sun, and A.-H. Alissa Park, "Directed precipitation of hydrated and anhydrous magnesium carbonates for carbon storage," *Phys. Chem. Chem. Phys*, vol. 16, p. 23440, 2014.

[69] M. Hänchen, V. Prigiobbe, R. Baciocchi, and M. Mazzotti, "Precipitation in the Mg-carbonate system-effects of temperature and CO2 pressure," *Chem. Eng. Sci.*, vol. 63, no. 4, pp. 1012–1028, Feb. 2008.

[70] E. M. Walling, P. A. Rock, and W. H. Casey, "The Gibbs energy of formation of huntite, $CaMg_3(CO_3)_4$, at 295 K and 1 bar from electrochemical cell measurements," *Am. Mineral.*, vol. 80, no. 3–4, pp. 355–360, 1995.

[71] S. Atashin, R. A. Varin, and J. Z. Wen, "Directed precipitation of anhydrous magnesite for improved performance of mineral carbonation of CO2," *J. Environ. Chem. Eng.*, vol. 5, pp. 3362–3372, Aug. 2017.

[72] G. D. Saldi, G. Jordan, J. Schott, and E. H. Oelkers, "Magnesite growth rates as a function

of temperature and saturation state," *Geochim. Cosmochim. Acta*, vol. 73, no. 19, pp. 5646–5657, 2009.

[73] X. Y. Liu, *Bioinspiration - From Nano to Micro Scales*. Springer, 2012.

[74] S. Y. Pan, R. Adhikari, Y. H. Chen, P. Li, and P. C. Chiang, "Integrated and innovative steel slag utilization for iron reclamation, green material production and CO_2 fixation via accelerated carbonation," *Journal of Cleaner Production*, vol. 137. Elsevier, pp. 617–631, 20-Nov-2016.

[75] S. Teir, S. Eloneva, and R. Zevenhoven, "Production of precipitated calcium carbonate from calcium silicates and carbon dioxide," *Energy Convers. Manag.*, vol. 46, pp. 2954–2979, Nov. 2005.

[76] J. H. Bang, Y. Yoo, S. W. Lee, K. Song, and S. Chae, "CO_2 Mineralization Using Brine Discharged from a Seawater Desalination Plant," *Minerals*, vol. 7, no. 11, 2017.

[77] J. L. Galvez-Martos *et al.*, "Environmental assessment of aqueous alkaline absorption of carbon dioxide and its use to produce a construction material," *Resour. Conserv. Recycl.*, vol. 107, pp. 129–141, Feb. 2016.

[78] M. J. Quina *et al.*, "Technologies for the management of MSW incineration ashes from gas cleaning: New perspectives on recovery of secondary raw materials and circular economy," *Science of the Total Environment*, vol. 635. Elsevier, pp. 526–542, 01-Sep-2018.

[79] World Steel Association, "Steel Statistical Yearbook 2018," 2018.

[80] C. Heidrich, H.-J. Feuerborn, and A. Weir, "Coal Combustion Products: a Global Perspective," in *World of Coal Ash Conference*, 2013, p. 17.

[81] Z. Wei *et al.*, "Clinkering-free cementation by fly ash carbonation," *J. CO_2 Util.*, vol. 23, pp. 117–127, Jan. 2018.

[82] W. Liu *et al.*, "Optimising the recovery of high-value-added ammonium alum during mineral carbonation of blast furnace slag," *J. Alloys Compd.*, vol. 774, pp. 1151–1159, Feb. 2019.

[83] E. Jones, M. Qadir, M. T. H. van Vliet, V. Smakhtin, and S. Kang, "The state of desalination and brine production: A global outlook," *Sci. Total Environ.*, vol. 657, pp. 1343–1356, 2019.

[84] F. P. Glasser, G. Jauffret, J. Morrison, J.-L. Galvez-Martos, N. Patterson, and M. S.-E. Imbabi, "Sequestering CO2 by Mineralization into Useful Nesquehonite-Based Products," *Front. Energy Res.*, vol. 4, no. February, pp. 1–7, 2016.

[85] J. Zhou, V. W.-C. Chang, and A. G. Fane, "An improved life cycle impact assessment (LCIA) approach for assessing aquatic eco-toxic impact of brine disposal from seawater desalination plants," *Desalination*, vol. 308, pp. 233–241, 2013.

[86] H. Dong, C. Unluer, E.-H. Yang, and A. Al-Tabbaa, "Recovery of reactive MgO from reject brine via the addition of NaOH," *Desalination*, vol. 429, pp. 88–95, 2018.

[87] P. K. Cornejo, M. V. E. Santana, D. R. Hokanson, J. R. Mihelcic, and Q. Zhang, “Carbon footprint of water reuse and desalination: a review of greenhouse gas emissions and estimation tools,” 2014.

[88] A. Bogush, J. A. Stegemann, I. Wood, and A. Roy, “Element composition and mineralogical characterisation of air pollution control residue from UK energy-from-waste facilities,” *Waste Manag.*, vol. 36, pp. 119–129, 2015.

[89] S. Kaza, L. Yao, P. Bhada-Tata, and F. Van Woerden, *What a Waste 2.0*. 2018.

[90] D. Amutha Rani, A. R. Boccaccini, D. Deegan, and C. R. Cheeseman, “Air pollution control residues from waste incineration: Current UK situation and assessment of alternative technologies,” *Waste Manag.*, vol. 28, no. 11, pp. 2279–2292, 2008.

[91] I. M. Power *et al.*, “Carbon Mineralization: From Natural Analogues to Engineered Systems,” *Rev. Mineral. Geochemistry*, vol. 77, no. 1, pp. 305–360, 2013.

[92] T. Vass, A. Fernandez-Pales, and P. Levi, “Tracking Clean Energy Progress - Cement,” *International Energy Agency*, 2019. [Online]. Available: https://www.iea.org/tcep/industry/cement/. [Accessed: 08-Jul-2019].

[93] S. A. Miller, A. Horvath, and P. J. M. Monteiro, “Impacts of booming concrete production on water resources worldwide - Supplementary Information,” *Nat. Sustain.*, vol. 1, no. 1, pp. 69–76, 2018.

[94] J. T. Gao, S. Q. Li, Y. T. Zhang, Y. L. Zhang, P. Y. Chen, and P. Shen, “Process of re-resourcing of converter slag,” *J. Iron Steel Res. Int.*, vol. 18, no. 12, pp. 32–39, Dec. 2011.

[95] J. Guo, Y. Bao, and M. Wang, “Steel slag in China: Treatment, recycling, and management,” *Waste Manag.*, vol. 78, pp. 318–330, Aug. 2018.

[96] A. Chalabyan, L. Mori, and S. Vercammen, “The current capacity shake-up in steel and how the industry is adapting,” 2018.

[97] E. H. Oelkers, S. R. Gislason, and J. Matter, “Mineral carbonation of CO2,” *Elements*, vol. 4, no. 5, pp. 333–337, 2008.

[98] K. S. Lackner, “Carbonate Chemistry for Sequestering Fossil Carbon,” *Annu. Rev. Energy Env.*, vol. 27, pp. 193–232, 2002.

[99] D. Sandalow, R. Aines, J. Friedmann, C. McCormick, and S. McCoy, “Carbon Dioxide Utilization (CO2U) -- ICEF Roadmap 2.0,” 2017.

[100] CO2 Sciences The Global CO2 Initiative, “Global Roadmap for Implementing CO2 Utilization,” 2016.

[101] M. S. Kuhar, “World Aggregates Market,” *Rock Products*, 2014. [Online]. Available: http://www.rockproducts.com/features/13045-world-aggregates-market.html#.XK_hcOhKjD4.

[102] A. Bascetin, D. Adiguzel, and S. Tuylu, “The investigation of CO_2 emissions for different rock units in the production of aggregate,” *Environ. Earth Sci.*, vol. 76, no. 7, 2017.

[103] NRMCA, “CIP 11 - Curing In-Place Concrete,” 2000.

[104] Y. Shao, “Beneficial Use of Carbon Dioxide in Precast Concrete Production,” 2014.

[105] S. Monkman, P. A. Kenward, G. Dipple, M. MacDonald, and M. Raudsepp, “Activation of cement hydration with carbon dioxide,” *J. Sustain. Cem. Mater.*, vol. 7, no. 3, pp. 160–181, 2018.

[106] D. Sandalow, R. Aines, J. Friedmann, C. McCormick, and S. McCoy, “Carbon Dioxide Utilization (CO2U) -- Icef Roadmap 2.0,” 2017.

[107] V. Atakan, S. Sahu, and N. DeCristofaro, “A case for low-lime cement,” *International Cement Review*, no. February, pp. 1–2, 2017.

[108] CarbonCure, “Linde enters strategic alliance with clean technology innovator CarbonCure,” 2019. [Online]. Available: https://www.carboncure.com/news-press/linde. [Accessed: 08-Aug-2019].

[109] M. Thomas, *Supplementary Cementing Materials in Concrete*. Boca Raton, FL: CRC Press, 2013.

[110] P. Duxson and J. Provis, “Low CO_2 Concrete: Are We Making Any Progress?,” *BEDP Environ. Des. Guid.*, vol. PRO 24, no. November, pp. 1–7, 2008.

[111] J. Morrison, G. Jauffret, J. L. Galvez-Martos, and F. P. Glasser, “Magnesium-based cements for CO_2 capture and utilisation,” *Cem. Concr. Res.*, vol. 85, pp. 183–191, Jul. 2016.

[112] J. Karni and E. Karni, “Gypsum in construction: origin and properties,” *Mater. Struct.*, vol. 28, pp. 92–100, 1995.

[113] J. L. Peterson, “History and Development of Precast Concrete in the United States,” *Proc. Am. Inst. Concr.*, vol. 50, no. 2, pp. 477–496, 1953.

[114] G. Polat, “Factors Affecting the Use of Precast Concrete Systems in the United States,” *J. Constr. Eng. Manag.*, vol. 134, no. 3, pp. 169–178, 2008.

[115] The Freedonia Group, “Industry Study: Bricks, Blocks, & Pavers,” 2014. [Online]. Available: https://www.freedoniagroup.com/industry-study/bricks-blocks-pavers-3236.htm.

[116] “Construction Economics,” *Eng. News-Record*, vol. 280, no. 3, pp. 36–38, 2018.

[117] European Commission, *Study on the review of the list of critical raw materials: Non-critical raw materials factsheets.*, no. June. 2017.

[118] Government of Iowa, “Analyzed Unit Cost schedule.”

[119] NRMCA, “Concrete CO_2 Fact Sheet,” 2012.

[120] M. C. Johnson and J. L. Sullivan, “Lightweight Materials for Automotive Application,” *ANL/ESD-14/7*, 2014.

[121] Mt Grace Resources, “An Assessment of the Greenhouse Gas Consequences the Proposed

Batchelor Magnesium Project," 2002.

[122] "Cement-Free, Carbon-Negative Concrete | Carbicrete." [Online]. Available: http://carbicrete.com/. [Accessed: 16-Apr-2019].

[123] G. Ounoughene, "Orbix. Personal Communication." 2019.

[124] M. Quaghebeur, P. Nielsen, B. Laenen, E. Nguyen, and D. van Mechelen, "Carbstone: sustainable valorisation technology for fine grained steel slags and CO2," *Refract. worldforum*, vol. 2, no. 2, pp. 75–79, 2010.

[125] Z. Wei *et al.*, "Clinkering-free cementation by fly ash carbonation," *J. CO2 Util.*, vol. 23, pp. 117–127, Jan. 2018.

[126] "Calera | Beneficial Reuse of CO_2." [Online]. Available: http://www.calera.com/beneficial-reuse-of-co2/index.html. [Accessed: 16-Apr-2019].

[127] S. Monkman and M. Macdonald, "On carbon dioxide utilization as a means to improve the sustainability of ready-mixed concrete," *J. Clean. Prod.*, vol. 167, pp. 365–375, 2017.

[128] "Solidia Technologies." [Online]. Available: solidiatech.com. [Accessed: 01-Apr-2019].

[129] "O.C.O Technology." [Online]. Available: oco.co.uk. [Accessed: 10-Sep-2019].

[130] Blue Planet Ltd, "Blue Planet | Economically Sustainable Carbon Capture." [Online]. Available: http://www.blueplanet-ltd.com/. [Accessed: 09-Apr-2019].

[131] V. Atakan, S. Sahu, S. Quinn, X. Hu, and N. DeCristofaro, "Why CO_2 matters - advances in a new class of cement," *ZKG Int.*, vol. 3, 2014.

[132] M. B. Jensen, L. G. M. Pettersson, O. Swang, and U. Olsbye, "CO2 sorption on MgO and CaO surfaces: A comparative quantum chemical cluster study," *J. Phys. Chem. B*, vol. 109, no. 35, pp. 16774–16781, 2005.

[133] National Lime Association, "Precipitated Calcium Carbonate," 2019. [Online]. Available: https://www.lime.org/lime-basics/uses-of-lime/other-uses-of-lime/precipitated-calcium-carbonate/.

[134] N. Erdogan and H. A. Eken, "Precipitated Calcium Carbonate Production, Synthesis and Properties," *Physicochem. Probl. Miner. Process*, vol. 53, no. 1, pp. 57–68, 2017.

[135] S. Chatterji, "Mechanism of expansion of concrete due to the presence of dead-burnt CaO and MgO," *Cem. Concr. Res.*, vol. 25, no. 1, pp. 51–56, Jan. 1995.

[136] S. A. Walling and J. L. Provis, "Magnesia-Based Cements: A Journey of 150 Years, and Cements for the Future?," *Chem. Rev.*, vol. 116, pp. 4170–4204, 2016.

[137] LKAB Minerals, "ATH shortages and price hikes further increase demand for UltraCarb," 2018. [Online]. Available: https://www.lkabminerals.com/en/ath-shortages-and-price-hikes-further-increase-demand-for-ultracarb/.

[138] T. R. Hull, A. Witkowski, and L. Hollingbery, "Fire retardant action of mineral fillers," *Polym. Degrad. Stab.*, vol. 96, no. 8, pp. 1462–1469, 2011.

[139] O. Kazmina, E. Lebedeva, N. Mitina, and A. Kuzmenko, “Fire-proof silicate coatings with magnesium-containing fire retardant,” *J. Coatings Technol. Res.*, vol. 15, no. 3, pp. 543–554, 2018.

[140] Ceresana, “Flame Retardants Market Report,” 2018. [Online]. Available: https://www.ceresana.com/en/market-studies/chemicals/flame-retardants/.

[141] Future Market Insights, “Fire Resistant Paints Market: Global Industry Analysis and Opportunity Assessment 2014-2020,” 2019. [Online]. Available: https://www.futuremarketinsights.com/reports/global-fire-resistant-paints-market.

[142] U.S. Department of Housing and Urban Development, “2017 Characteristics of New Housing,” 2013.

[143] The Freedonia Group, “US Paint & Coatings Sales to Reach 1.4 Billion Gallons in 2020,” *PR Newswire*, 2017. [Online]. Available: https://www.prnewswire.com/news-releases/us-paint--coatings-sales-to-reach-14-billion-gallons-in-2020-300417385.html. [Accessed: 01-May-2019].

[144] P. R. Hornsby, “The Application of Fire-Retardant Fillers for Use in Textile Barrier Materials,” in *Multifunctional Barriers for Flexible Structure*, Vol 97., Berlin, Heidelberg: Springer, 2007, pp. 3–22.

[145] A. Torres, J. Liu, J. Brandt, and K. Lear, “The World is Facing a Global Sand Crisis,” *The Conversation*, 2017. [Online]. Available: http://theconversation.com/the-world-is-facing-a-global-sand-crisis-83557. [Accessed: 25-Apr-2019].

[146] P. Peduzzi, “Sand, rarer than one thinks Article reproduced from United Nations Environment Programme (UNEP) Global Environmental Alert Service (GEAS),” *Environ. Dev.*, vol. 11, pp. 208–218, 2014.

[147] A. Torres, J. Brandt, K. Lear, and J. Liu, “A looming tragedy of the sand commons,” *Science (80-.).*, vol. 357, no. 6355, pp. 970–971, 2017.

[148] D. Owen, “The World is Running out of Sand,” *The New Yorker*, 2017. [Online]. Available: https://www.newyorker.com/magazine/2017/05/29/the-world-is-running-out-of-sand. [Accessed: 25-Apr-2019].

[149] R. Garbini, “A Concrete Connection to Highway Quality.”

Chapter 7

Policy Recommendations for Decarbonization in Concrete and Pavements

Abstract

In Chapter 6, several methods for utilization of carbon mineralization products in the concrete industry were identified. While these methods were revealed to have the potential to avoid up to 3 $GtCO_2$ per year globally, they face direct competition with conventional concrete products that are relatively cheap and have established long-term strength and durability properties. One way to increase the market penetration of these new carbon mineralization-based products is through government policy. This chapter was written as a report that makes policy recommendations for the decarbonization of concrete and pavements, and was published by ClearPath, Inc. The formatting of this chapter is slightly different than previous chapters, as it is meant to appeal to a broader audience. The figures were stylized by the graphic design team of ClearPath, Inc.

List of Abbreviations

CCS – carbon capture and storage

HMA – hot mix asphalt

LEILAC – Low Emissions Intensity Lime and Cement

SCM – supplementary cementitious materials

WMA – warm mix asphatl

Executive Summary

For centuries, concrete has helped advance society as the basic building block in our roads, buildings, and bridges. Today, cement (i.e., the "glue" in concrete mixtures) is produced at an annual rate of 86 million tons in the U.S., and 4.1 billion tons worldwide. Current production methods of cement generate significant carbon emissions, and globally, cement facilities account for 8% of anthropogenic carbon dioxide emissions, equivalent to roughly one-third of all power plant emissions. Since cement will also continue to be an essential commodity in the years to come, noted by a projected production increase of up to 23% by 2050, it is important to accelerate low-cost technology solutions that can reduce the environmental footprint of the cement and concrete industries.

Three primary opportunities have been identified for the decarbonization of the concrete industry: (1) carbon capture at cement plants, (2) alterations to concrete mixtures, and (3) new materials with stored CO_2. Their impact on the cement industry's emissions is shown below:

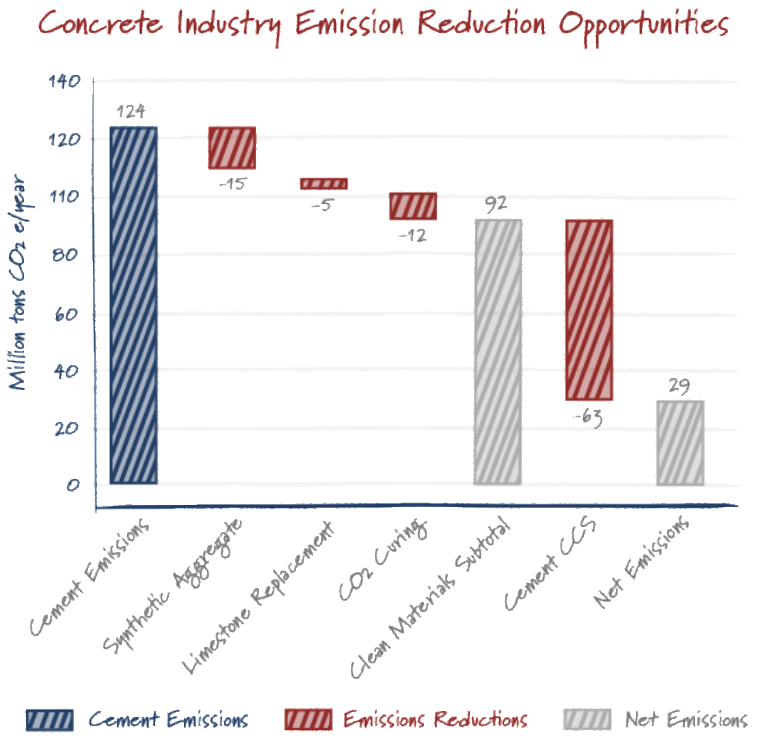

In sum, about 100 million tons of CO_2 can be avoided with the combined measures shown here. This is equivalent to about two-thirds of the cement emissions and about 1.2% of U.S. emissions. Based on magnitude and feasibility of near- and long-term impact, the following R&D policies are recommended:

1. **Demonstration and Deployment -** Fund pilot or demonstration carbon capture projects at cement plants.
2. **Research and Development -** Increase research for supplementary cementitious materials and materials produced with carbon mineralization.
3. **Regulatory Revisions -** Encourage regulating bodies to shift to performance-based specifications in asphalt and concrete.

1. Introduction

Since the Roman Empire, cement has been used to facilitate societal growth. Its unmatched strength and durability provided to concrete mixtures have helped to *cement* itself as an essential building material across the world. Today, at a use rate of 4.1 billion tons per year, cement is the most used man-made material on the planet [1]. Unfortunately, its current production method is very carbon-intensive, accounting for 8% of global anthropogenic CO_2 emissions [2]. With a projected growth in production of 12-23% [3], universities, companies, and governments around the world are supporting research and development to improve cement's environmental footprint. Recently in the U.S., new economic drivers have emerged, including federal incentives, corporate sustainability goals, and emerging domestic and international regulations. Therefore, cement — the key ingredient in concrete used in major public works projects like highways, bridges, and buildings — presents an opportunity to decrease a large portion of U.S. industrial emissions. Now more than ever, with advanced technologies and bipartisan support for new infrastructure investments, serious attention to decarbonization opportunities in the concrete industry could result in significant emissions reductions.

Traditionally, the power sector has been the focus of clean energy technology policy. Clean power technology and business model innovations, from cheap renewable power to abundant low-carbon natural gas, provide a template for reductions in the industrial sector, the source of 22% of U.S. carbon dioxide emissions [4].

1.1 Concrete and Pavement Terms Defined

Concrete is primarily composed of cement, aggregates, and water. Cement (also called "binder") acts as the glue in concrete mixtures, while aggregates provide volume and stability.

Cement + Aggregates + Water = Concrete

The mixture most commonly known as "concrete" uses portland cement, and is also called portland cement concrete. Alternatively, asphalt concrete uses asphalt cement, and does not use water in its production. This is further illustrated in Figure 1. While these two mixtures are products of two separate industries which compete with each other, they share the need to decrease embodied emissions and will both be discussed. For the purposes of this Chapter, the two mixtures will be referred to as "concrete" and "asphalt," respectively.

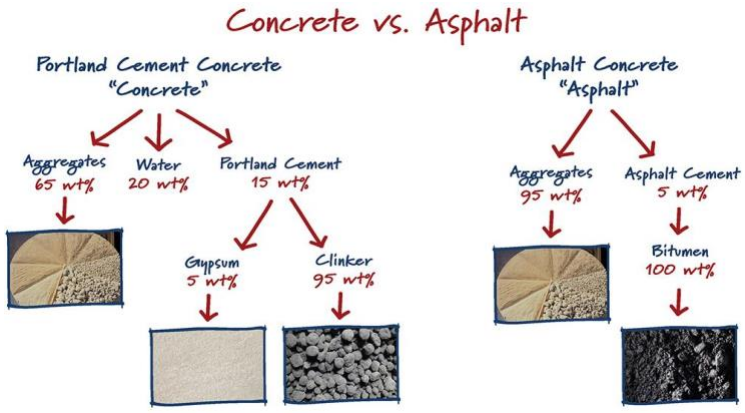

Figure 1: Comparison of the approximate amounts of ingredients in concrete [5] and asphalt [6].

One of the major uses of concrete and asphalt is pavement. Pavement refers to a smooth artificial surface on the ground typical of U.S. roadways, for which both concrete and asphalt are used to produce. In the U.S., about 94% of paved roads are surfaced with asphalt [7]. The two pavement types can often be distinguished by color – concrete is typically grey or white, while asphalt is typically black. While concrete roads are generally only used in highways and bigger cities, concrete is the more widely used material overall due to its applications in buildings, bridges, dams, and more (see Figure 2). Asphalt is produced at a rate of about 350 million metric tons per year [7], compared to about 570 million metric tons produced of concrete.[1,2]

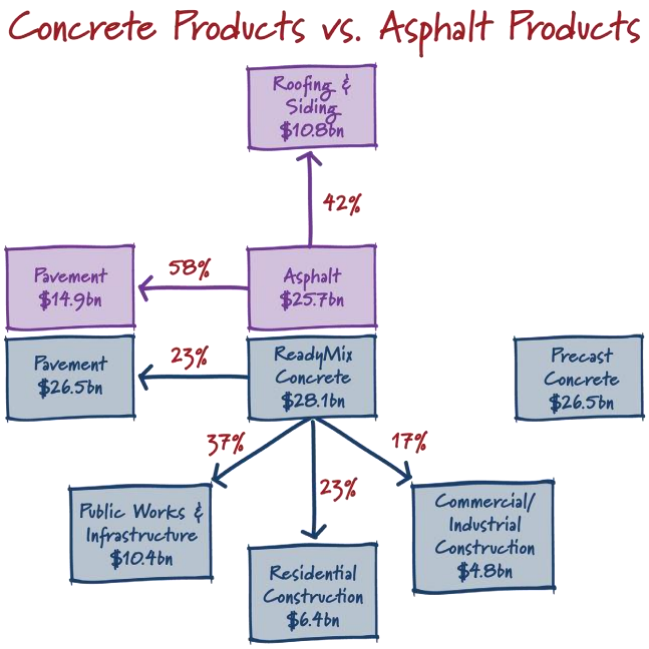

Figure 2: Comparison of Products from Concrete and Asphalt Industries [8]–[10].

A more contrasting characteristic of concrete and asphalt is their emissions: concrete emits an estimated 144 kg CO_2 per ton, compared to about 61 kg CO_2 per ton of asphalt.[3] To understand the source of these emissions, it is important to first examine the most carbon-intensive ingredients of concrete and asphalt, which are shown in Figure 3.

[1] A metric ton equals 1.1 English tons. In this report, "tons" refers to metric tons.

[2] More than 86 million metric tons of portland cement were produced in 2019 [1]. Assuming this accounts for 15% of concrete mixtures, this means 573 million tons of concrete were produced.

[3] Estimated based on emissions of concrete and asphalt ingredients and proportions given in Figure 1 and published emission factor data [29], [39], [40].

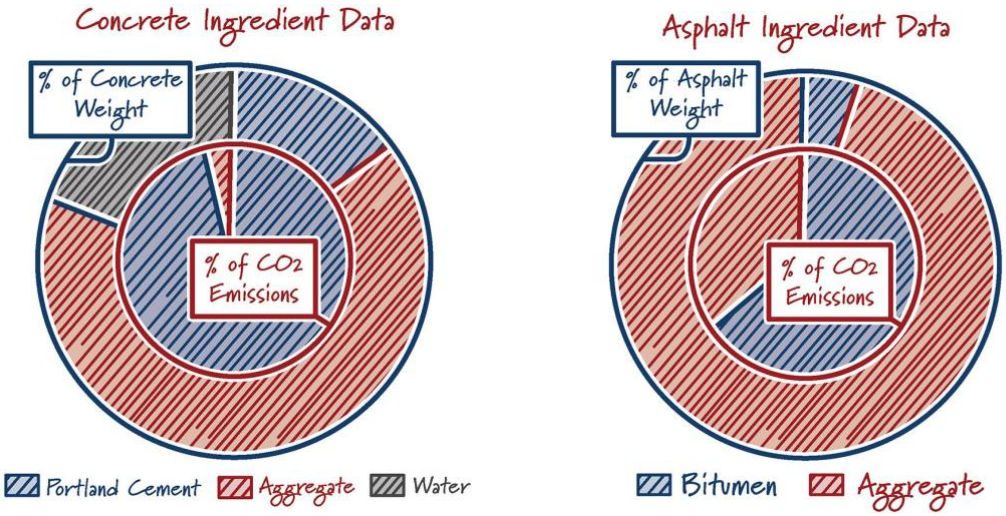

Figure 3: Relative contribution of portland cement- and asphalt-based concrete ingredients to the overall mixture weight and CO_2 emissions

Interestingly, the ingredients with the lowest contribution to weight (portland cement in concrete and bitumen in asphalt) have the largest contributions to CO_2 emissions. Therefore, small alterations in these mixture recipes could yield significant emissions reductions.

The major emissions source for concrete is the production of clinker, which is the main ingredient in portland cement. In this process, abundant naturally occurring rock called limestone (calcium carbonate) is mixed with other materials like clay and heated at very high temperatures (> 2700 ^{o}F), producing clinker and CO_2. The basic reaction is shown in Figure 4:

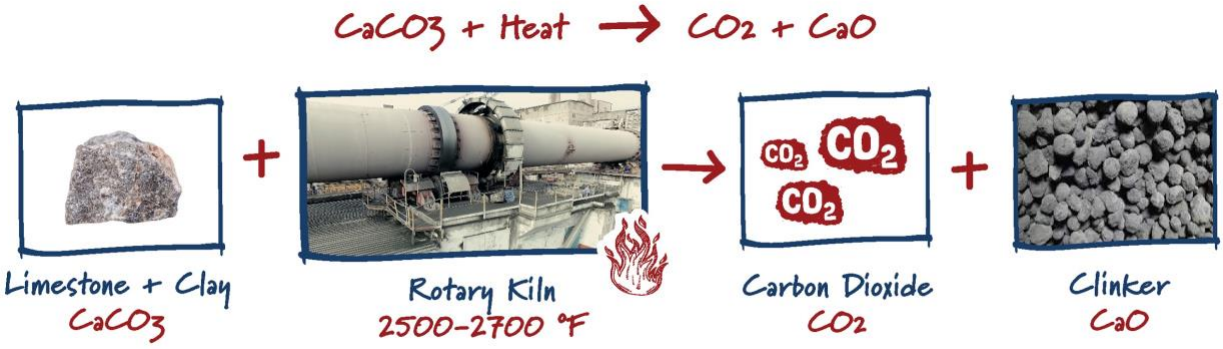

Figure 4: Clinker production process with basic chemical reaction

The CO_2 emitted in this reaction is referred to as "process emissions," as opposed to the "combustion emissions" that result from the combustion of fossil fuels to supply heat for the reaction. About 60% of a cement plant's emissions are process emissions, which cannot be mitigated by use of carbon-free energy. This underscores the need for carbon capture or production of alternate clean materials to decrease concrete's carbon footprint.

Upfront emissions and costs from production do not tell the full story of a pavement's environmental impact. Designing new roads requires the balance of initial costs of production with lifecycle costs of maintenance, material usage and carbon emissions. As such, pavements that

decrease emissions at production may still result in a net-increase of emissions over their lifetime. Further, use of new pavement technologies is limited by the abilities of local and state agencies, which may lack funding to support higher initial pavement costs, and are better equipped to finance the repeated maintenance costs of pavements with decreased longevity.

It is important to note a portfolio of solutions is needed to decarbonize the industry. The remainder of this Chapter outlines several opportunities for the decarbonization of concrete and pavements, and identifies the best options to optimize impact in both the near and long term. These opportunities pertain to the pavement production phase, while discussion of environmental impacts associated with the use phase are outlined elsewhere [11].

2. Decarbonization Opportunities

2.1 Carbon Capture at Cement Plants

Big takeaway: Cement plants are a low-hanging fruit for carbon capture, which can result in significant carbon reductions for the industry. A few early demonstration projects are helping its development, but more are needed to drive down the costs and bring the technology to scale. If applied to all U.S. cement plants, carbon capture could avoid up to 72 million tons of CO_2 emissions per year. This is equivalent to taking more than 15 million cars off the road.[4]

Description: Process emissions resulting from cement production can be avoided through post combustion carbon capture technology, which removes carbon dioxide from a facility's exhaust gas before it is released into the atmosphere. The captured CO_2 can be stored or converted to a useful product, in turn generating revenue through market sales and, potentially, the U.S. federal carbon capture tax incentive, 45Q. A number of capture processes can be applied to cement plants, including amine scrubbing, calcium looping, and oxycombustion. New processes are also being explored, such as the single-tube direct separation system by Project LEILAC.

Benefits:

- Invests in existing infrastructure. Because carbon capture leverages existing infrastructure and facilities, it can be deployed relatively quickly [12].
- Reduces emissions in line with global targets. A combined 72 million tons of CO_2 per year could be captured with carbon capture retrofit technology at all cement plants in the U.S.[5] This is distributed among 91 different plants, as shown in Figure 5. The majority of cement plants generate 100,000 to 1 million tons of CO_2 each year.
- Federal monetary support. The U.S. Department of Energy released a call for front-end engineering design studies for carbon capture at industrial sources [13]. If the CO_2 captured at cement plants is utilized or geologically stored, it is eligible for the U.S. federal carbon capture tax incentive, 45Q. Section 4002 of The Energy Act of 2020 established a carbon capture technology program to improve the efficiency, effectiveness, economics, and environmental performance of carbon capture in the industrial sector, among other sectors [14].

[4] Assuming 4.6 tons CO_2 per passenger vehicle per year.[41]

[5] About 25% of US industrial emissions are stationary process emissions that allow for installment carbon capture retrofit technology, totaling to about 320 $MtCO_2$-e per year. Cement accounts for 22.5% of this amount, or 72 $MtCO_2$-e.

- Low-hanging fruit for carbon capture. The flue gas concentration of CO_2 affects the cost of carbon capture, where it is more expensive to capture from a more dilute stream. The concentration of CO_2 in flue gas at cement plants is relatively high (14-33%), compared to about 12% and 4% for pulverized coal and natural gas combustion, respectively. Furthermore, because 96% of a cement facility's process emissions are emitted through a central exhaust stack, the installment of one retrofit carbon capture system could capture nearly all of the plant's process emissions [12].

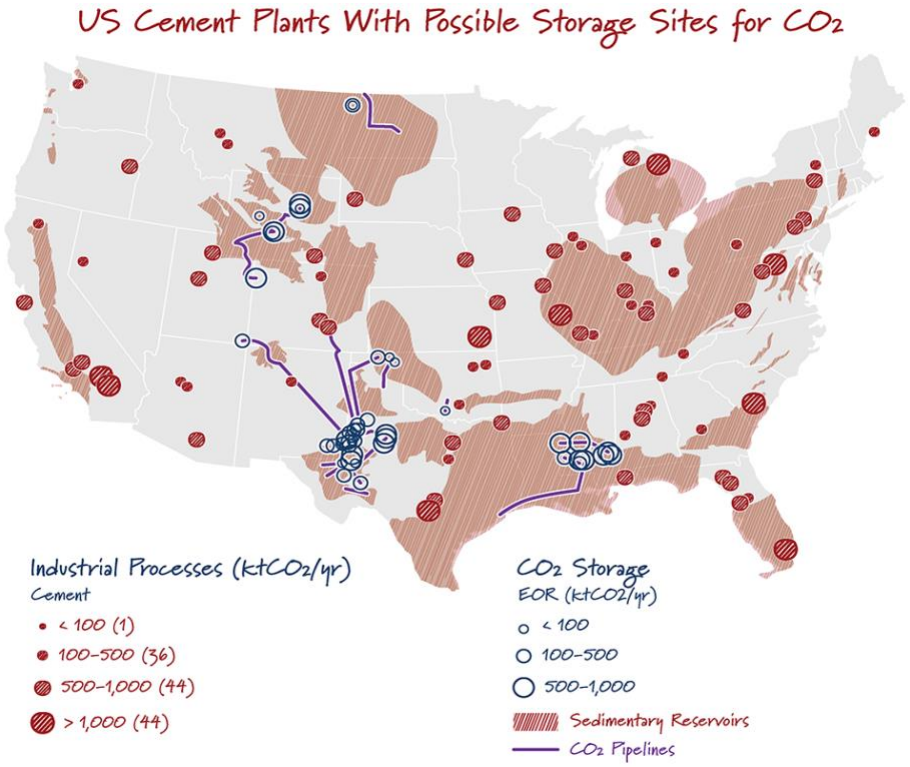

Figure 5: Map of US cement plants with possible storage sites for CO_2, edited with permission [12]

Challenges:

- Cost. Installing carbon capture equipment, especially in the industrial sector where carbon capture has not yet been widely implemented, requires significant investment. Estimated costs range from $17 to $164.6 per ton CO_2 avoided. Combining oxycombustion with calcium looping is likely to be the most economical option, with an average cost of $39.4 per ton CO_2 avoided [15].
- Permissions and spacing. Equipment installment at cement plants could also be problematic. Some plants do not have the space required for a carbon capture system, or would require some rearrangement of plant equipment. Increases in land area or plant height could bring objections from local government and/or residents [16]. The complications of spacing and permissions, along with the inherent risk of large investments in a relatively new technology, can cause some plant managers to be hesitant to make significant changes to the equipment in place.

Current Examples: Commercial and large-scale projects are underway across the world.

Holcim Portland Cement Plant [17]
In the beginning of 2020, Svante Inc, LafargeHolcim, Oxy Low Carbon Ventures, and Total initiated a study to evaluate commercial-scale carbon capture at the Holcim Portland Cement Plant in Colorado. The facility would capture up to 725,000 tons of CO_2 per year, to be permanently sequestered by Oxy Low Carbon Ventures. The initiative merges Svante's proprietary low-cost "sorbent" capture system with a federal carbon capture tax credit (45Q) to make a profitable project.

Norcem Brevik CO_2 Capture Project [18]
The Norcem project started as one of four post combustion capture pilot projects in Norway in 2014. In 2019, Norcem was one of two facilities chosen to scale up to capture 400,000 tons of CO_2 per year. The CO_2 will be transported to Norway's west coast for temporary storage. A primary objective of this demonstration phase is to increase the use of waste heat already present within the plant evaluations, decreasing the additional energy needed to power CCS at the cement plant.

Low Emissions Intensity Lime and Cement (LEILAC) [19]
This pilot was constructed in 2018 in Belgium, and introduced a new way to produce cement clinker that makes it easier to capture the process emissions. The technology is called single-tube direct separation, and is shown in Figure 6. While this technology has been commercialized by Calix Limited for more than two years to produce magnesia, applying it to cement production will require much higher temperatures. Accordingly, pilot-scale tests will be undergone to confirm more than 95% of emissions can be captured at high temperatures.

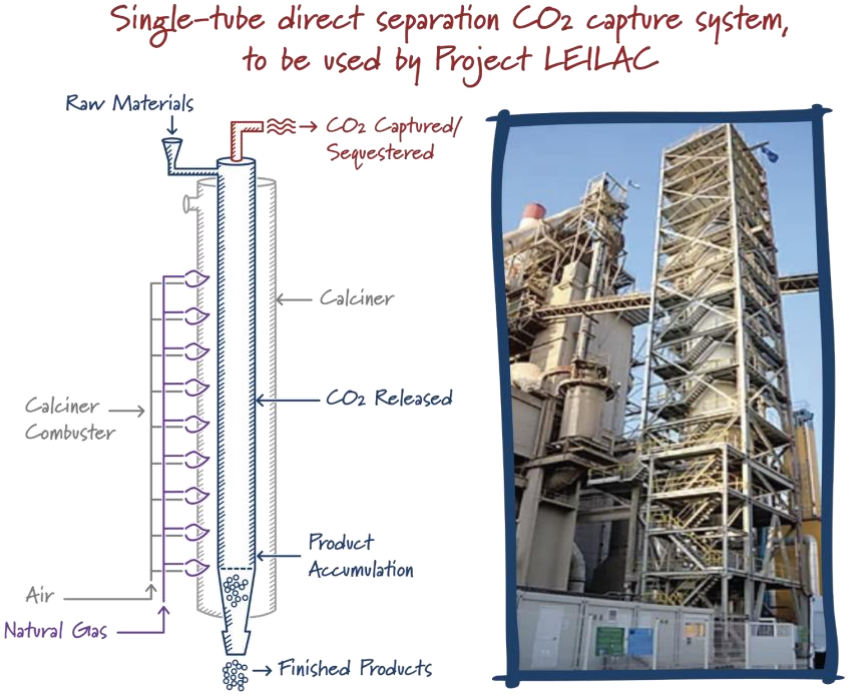

Figure 6: Single-tube direct separation CO_2 capture system, to be used by Project LEILAC [19]

2.2 Alterations to Concrete and Asphalt Mixtures

Big Takeaway: For decades, concrete mixtures have been altered to reduce raw materials costs by replacing portions of cement with cheaper materials like industrial wastes or limestone, simultaneously reducing concrete's carbon footprint. Similarly, emissions and costs from asphalt can be reduced by decreasing production temperatures and increasing recycled material usage. While many of these practices are not new, they suffer from outdated regulatory specifications and/or lack of communication on best uses. In some cases, R&D is also needed to evaluate new materials and their effect on long-term material properties.

Concrete Alterations - Description: Because cement is concrete's primary source of cost and emissions, replacing cement with alternative materials is a practice that has become relatively common in the industry, and has been examined previously by the U.S. EPA. [20] These alternative materials are called "supplementary cementitious materials" (SCMs).

Some concrete mixtures replace a portion of the portland cement with limestone, a mixture called portland-limestone cement. This can significantly reduce cost and emissions, but the reports of its effects on concrete properties are mixed. Based on average literature values, the decrease in strength for concrete is minimal at limestone replacement levels below 10%, with significant strength losses past 17.5% [21]. The relation of loss in strength and avoided CO_2 emissions is shown in Figure 7.

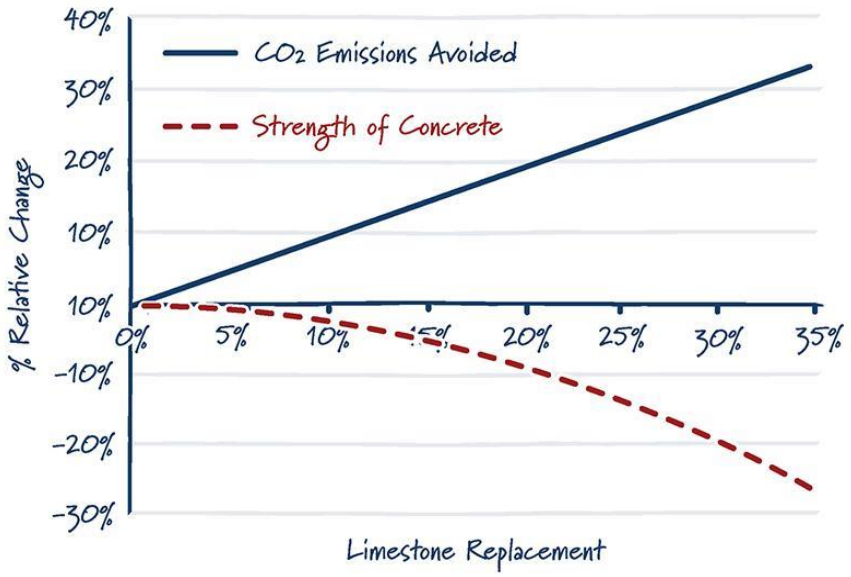

Figure 7: Comparison of the relative change in CO_2 emissions avoided and concrete strength due to limestone replacement in concrete

For a sense of scale, if a 15% limestone replacement is applied to a quarter of all concrete produced in the U.S., it would avoid nearly 3 million tons of CO_2 each year from portland cement production. Further, if this technique is applied to new concrete pavement, it would result in about 90 tons of CO_2 avoided per mile of pavement, a reduction of about 14%.

Concrete Alterations - Benefits:

- Reduce costs and emissions. For more than 50 years, SCMs have been used in concrete mixtures to enhance long-term strength and durability properties, decrease costs, and more recently, decrease emissions. These are often wastes from other industries, the two most common being from coal combustion (fly ash) and iron production (blast furnace slags).
- Waste reclamation. Several alternate materials are available with varying chemistry and availability, most of which are wastes from industrial processes [22].

Concrete Alterations - Challenges:

- Material availability. A 2008 EPA report listed the advantages of several SCMs, and emphasized fly ash and blast furnace slags. [20] Now, nearly half of the fly ash and all of the blast furnace slags produced in the U.S. are already used as SCMs [22], [23]. Due to the decreased use of coal in the power sector and the economic struggles of the steel industry, new materials need to be sought out to sustain, or increase, the economic and environmental impact of SCMs.
- Research and development. Many of the potential materials to use as SCMs are available on the scale of millions of tons per year, but more research is required to determine their ability to replace cement without sacrificing performance.
- Regulatory restrictions. Limestone is a promising alternative due to its wide availability and its established use in the U.S., but a shift to performance-based standards is required to increase the permitted replacement levels of limestone and other new SCMs.

Asphalt Alterations - Description: One method to reduce energy consumption in asphalt production is to decrease the production temperature. Hot mix asphalt (HMA) is the traditional asphalt mix and is produced at 300-350 ^{o}F. Alternatively, warm mix asphalt (WMA) is produced at much cooler temperatures, resulting in reduced costs and emissions due to a decreased fuel demand [24]. Other sustainable methods involve recycling (e.g., reclaimed asphalt pavement, cold in-place recycling).

Asphalt Alterations - Benefits:

- Can be implemented quickly. With Federal Highway Administration support, WMA was adopted very widely and rapidly in the last decade, with a 777% increase in WMA usage from 2009 to 2017 [25]. About 39% of asphalt in the U.S. was made using WMA in 2017, up from just 5% in 2009.
- Reduces carbon emissions. Using WMA is estimated to give a 10-15% carbon footprint reduction compared to HMA production, equating to emissions reductions of about 4.5 to 11 tons of CO_2 per mile of WMA pavement. In 2017, recycled asphalt accounted for 20% of asphalt mixtures. This avoided the production of additional asphalt cement and virgin aggregate, and resulted in a combined CO_2 avoidance of about 1.5 million tons [25].
- Broader impacts. Aside from decreasing fuel consumption and emissions, WMA enables the paving season to be extended into winter months, material to be hauled longer distances, and more recycled materials to be used [25]. Use of recycled asphalt also saved

nearly 50 million cubic yards of landfill space and more than $2 billion during the 2017 construction season.

Asphalt Alterations - Challenges:

- Material availability. Recycled asphalt is assumed to be able to constitute up to 40% of an asphalt mixture [6], but its current amount is about half of that, due to issues with quality control and processing. In 2017, asphalt producers cited material availability, along with specification limits, and plant capabilities, as limiting factors for increasing use of recycled asphalt [25].
- Research and development. The various types of available recycled materials require further research to determine optimal use cases [26].
- Regulatory restrictions. Despite the availability and potential advantages of recycling agents for asphalt mixtures, it was found that most state agencies and contractors do not use or allow the use of them. Acceptance of these practices could be improved through broader education on the available options and continued efforts to adjust regulatory specifications [27].

2.3 Synthesizing New Materials with Stored CO_2

Big takeaway: Building materials can be synthesized containing CO_2 in the form of mineral carbonates. This can take the form of synthetic aggregates, CO_2-cured concrete, or alternative cement, some of which have already seen some commercial success. Funding is needed for additional R&D and life cycle analysis. Technologies would also benefit from additional incentives to help compete with the cheap established materials. If applied to all U.S. concrete, we estimate synthetic aggregates and CO_2-cured concrete could avoid nearly 15 and 12 million tons of CO_2, respectively.

Description: Using a technology called carbon mineralization, building materials can be synthesized by reacting CO_2 gas with an alkaline feedstock. These materials permanently store CO_2 in the form of solid carbonate minerals, like those that make up seashells. Further, the materials often exhibit superior strength and durability properties compared to conventional building materials. Thus, this method presents an opportunity to replace materials that emit CO_2 with materials that store CO_2, all while improving the performance of the final product. Moreover, the use of CO_2 to produce these materials qualifies as a utilization method in the 45Q tax incentive, improving the economics of the technology.

Background: Alkaline feedstocks rich in calcium or magnesium are readily available in industrial wastes and mined materials. Industrial wastes are advantageous because their small particle size makes them more reactive, and they are produced annually at facilities that produce CO_2 streams. Examples include steelmaking slags, coal fly ash, and cement kiln dust. As previously mentioned, some of the wastes suitable for mineralization feedstock are already utilized as SCMs. Hence, the field would benefit from characterization and identification of additional feed sources. Alternatively, alkalinity can be obtained by mining ultramafic rocks. While these mined rocks might be more pure than industrial wastes, the mining operation can be cost- and energy-intensive.

Current Examples: There are several companies that are commercializing carbon mineralization to produce building materials. As illustrated in Figure 8, the companies can be categorized into two pathways: those that are making changes to portland cement-based concrete mixtures (Pathway 1), and those that are making alternative building materials without portland cement (Pathway 2).

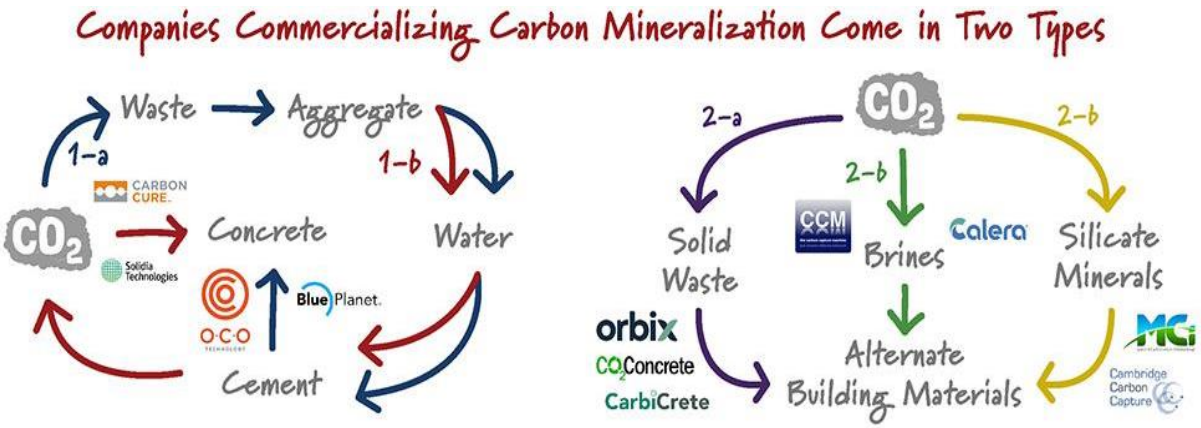

Figure 8: Companies commercializing carbon mineralization come in two types:
Pathway 1 - making changes to portland cement-based concrete mixtures, or
Pathway 2 - making alternative building materials without portland cement

Pathway 1-a: Synthetic aggregates

Aggregates are essential to concrete, bringing its volume and stability. The global aggregate market, including sand, gravel, crushed stone, and others, amounts to about 53 Gt/year [28]. Because conventional aggregates are low-value commodities with relatively low associated emissions (7.85 kg CO_2-e per metric ton) [29], synthetic aggregates produced by carbon mineralization should present superior qualities and/or contain large amounts of CO_2. O.C.O Technologies (U.K.) and BluePlanet (U.S.) are examples of this pathway.

Pathway 1-b: CO_2-cured Concrete

Immediately after concrete has been placed, its properties begin to develop through hydration reactions, the rate and extent of which are affected by moisture presence and temperature. The process of curing involves regulating moisture content and temperature to allow the specified properties to be achieved. While curing generally occurs due to water presence, it can also be achieved with CO_2. This technique securely stores CO_2 while enhancing the strength and durability properties of concrete. CarbonCure (Canada, U.S.) and Solidia (U.S.) are examples of this pathway.

Pathway 2: Alternative cement materials

These companies use different alkalinity sources to produce building materials free of portland cement. The primary alkalinity source varies among solid industrial wastes (e.g., steel slags, coal fly ash), water desalination brines, and naturally occurring minerals (e.g., lizardite), as shown in the figure above. Companies here are still in development phases, and have not yet reached the

same scale as some Pathway 1 companies. Orbix (Belgium), CO_2Concrete (U.S.), and CarbiCrete (Canada) are examples of Pathway 2-a. Carbon Capture Machine (U.K.) and Calera (U.S.) are examples of Pathway 2-b. Cambridge Carbon Capture (U.K.) and Mineral Carbonation International (Australia) are examples of Pathway 2-c.

Benefits:

- Improved Properties. O.C.O Technologies creates a versatile, lightweight aggregate that can replace or accompany other aggregates. Blue Planet's layered aggregate can be produced in sizes ranging from that of sand to gravel [30]. CarbonCure's process results in a stronger overall concrete that requires less cement to achieve the same strength [31]. Solidia's process sequesters CO_2 during curing and can produce strength and durability properties that exceed conventional concrete.
- Current Funding Opportunities. In addition to the 45Q tax incentive, other avenues to fund these projects currently exist. Three of the companies here – CO_2Concrete, Carbon Capture Machine, CarbonCure – are finalists in the NRG COSIA Carbon XPRIZE [32], which is scheduled to announce the winners of a $20 million prize in Fall 2020. CarbiCrete was also a Carbon XPRIZE finalist, but withdrew after receiving funding from Sustainable Development Technology Canada to build a limited production facility at a pre-existing concrete plant [33].
- Scalable. The NRG COSIA Carbon XPRIZE finalists benefit from pilot-scale testing required for the competition, and CO_2Concrete is planning to perform additional pilot tests at the National Carbon Capture Center in the near future [34]. CarbiCrete has received more than $5 million combined from the Canadian government and Harsco Corp to help fund an industrial-scale pilot project [35]. Additionally, Mineral Carbonation International plans to design a demonstration plant that can process 5,000-10,000 tons of CO_2 per year [36]. Orbix's Carbstone Technology is in development at Belgian steel and brick facilities. O.C.O Technologies has three facilities in the UK, the first of which was built in 2012 and is undergoing an expansion to double its capacity to produce more than 50,000 tons of aggregate per year. CarbonCure's technology has been installed at several concrete facilities in the U.S. and Canada.
- Flexible Business Models. A common theme among the more successful companies here is business models that ease adoption for existing manufacturers. CarbiCrete's business model is to license its technology to precast concrete manufacturers, providing the means and support for its partners to produce high-quality, carbon-negative concrete. Orbix has developed a mobile container that can be transported to concrete manufacturers as a way for them to replace cement while maintaining control over the process [37]. As their name suggests, Carbon Capture Machine constructs modular "Carbon Capture Machines" that can be installed at plants with access to waste CO_2 and alkaline brine streams. CarbonCure technology is easily retrofitted at a concrete plant and has already been installed in

locations across the U.S. [38]. Solidia's process can be carried out with the same equipment and raw materials already used in the cement industry.

Challenges:

- CO_2 Source. Technologies which require a pure CO_2 stream, like CO_2-curing, would have to obtain it from DAC or post-combustion capture. CO_2Concrete, Calera, and potentially other companies here, are testing their mineralization technologies using raw flue gas, removing the additional cost of capture and compression.
- Life Cycle Assessment. Although many of the companies list the amount of CO_2 contained in their products, it is difficult to know the net amount avoided on a lifecycle basis. This is because there is likely a considerable amount of energy required for process conditions of temperature and pressure, along with mining feedstock or synthesizing other reagents. More R&D could be put forth into these efforts.
- Performance-based Specifications. Most of the technologies listed here also suffer from restrictive regulations on concrete mixtures. A shift to performance-based specifications will help to allow the use of new carbonate-based concrete materials that satisfy the requirements of strength, durability, and longevity.

3. Summary of Options

A portfolio of solutions is necessary for the decarbonization of concrete and pavements. Summing up all the decarbonization opportunities, it is feasible to develop concrete with about two-thirds less carbon emissions than currently emitted today using known technologies and processes. These opportunities, however, are unlikely to be implemented without addressing systemic barriers, such as costs and restrictive regulations. Several decarbonization options were discussed in this Chapter, and they are aggregated in the two waterfall charts in Figure 9. Concrete mixture proportions used in this chart are based on the values given in Figure 1. On the left, the emissions for the U.S. concrete industry are reduced by two-thirds. A 25% limestone replacement is applied to 25% of U.S. concrete. Because this would reduce the amount of cement produced, CCS is applied to the remaining 75% of U.S. cement production, avoiding up to 54 million tons of CO_2 per year (as opposed to the 72 million tons mentioned earlier in the Chapter). On the right of Figure 9, the case of emission reductions for new concrete pavements is given per mile of road, where the cumulative emissions reductions show the possibility of pavement becoming CO_2-negative.[6]

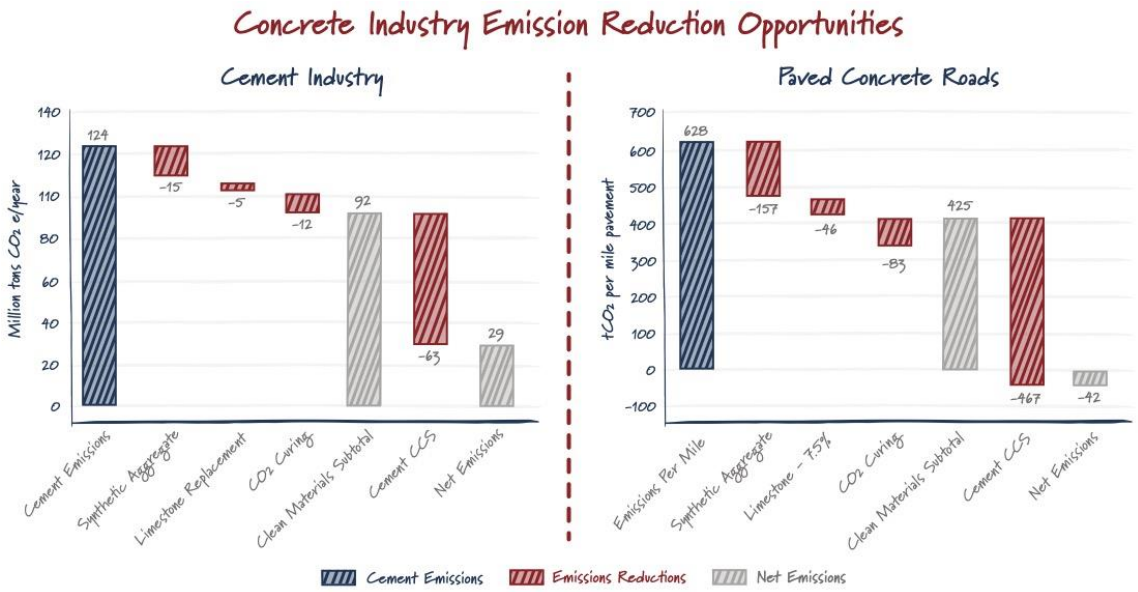

Figure 9: Cumulative reduction of cement emissions various decarbonization options.
Left: Impact on emissions of U.S. cement industry, per year
Right: Impact on emissions of concrete pavement, per mile

[6] For a process to be carbon negative, CO_2 must be sourced from the atmosphere. For example, the CO_2 for curing could be sourced from a DAC plant.

The decarbonization opportunities discussed are further summarized in the table below:

Option	Technology	Impact on Emissions	Scalability	Status	Area of Need
1	Carbon Capture	Could capture 96% of process emissions; 72 $MtCO_2$/year	Restricted by available plant space	European demonstration projects ongoing	Fund demonstration projects
2	Limestone Replacement	Directly replace cement; ~900 kg CO_2 avoided per ton cement replaced	Vast resources available	Established in many countries, but reports of effects on performance vary	Performance-based specifications, identify applications
	Other Supplementary Cementitious Materials	Likely slightly less reduction than limestone	Various materials produced at ~100s Mt/year	Some used in niche applications	Research effects of alternate materials on concrete properties
	Warm Mix Asphalt	About 15% reduction compared to hot mix asphalt	Limited by manufacturer adoption (install equipment)	Used in ~40% of US asphalt, but could be 100%	Increased education and communication
	Recycled Asphalt Materials	Replaces portion of asphalt cement, but difficult to quantify full reduction	Limited by amount of waste asphalt	Used in ~20% of US asphalt, but could be ~40%	Increased education and R&D; performance-based specifications
3	Synthetic Aggregate	Could contain 50-200 kg CO_2 per ton aggregate	Limited by availability of alkalinity sources	Commercialized on small scale	Incentives to compete with cheap natural aggregates
	CO_2-Curing	Could contain up to 50 kg CO_2 per ton concrete, but needs life cycle assessment	Could theoretically be applied to all concrete	Commercialized on small scale	Incentives; R&D for life cycle assessment
	Alternate Building Materials	Could contain significant CO_2, but process might also significantly emit CO_2	Limited by availability of alkalinity sources	Pilot-scale testing	Funding and incentives; performance-based specifications

4. Recommendations

Several impactful opportunities exist to decarbonize the concrete industry, all at varying readiness levels. When selecting among the options to make policy recommendations, the most important factors are short- and long-term impact and likelihood of adoption. The industry is very reluctant to change existing practices due to liabilities and costs associated with unfamiliar technologies. Further, preservation of strength and durability, along with costs, are prioritized over any economic concerns.

Based on the above considerations, the following recommendations are made:

1. Fund demonstration projects for carbon capture at cement plants. Of the decarbonization opportunities discussed here, this is the readiest technology, and has the most minimal impact on current production practices. Captured CO_2 streams could be allocated to help develop CO_2-curing projects.

2. Increase research for supplementary cementitious materials ("SCMs") and materials made with carbon mineralization. This includes the effect of increased limestone replacement, as well as new SCMs to supplement declining supply of coal fly ash and blast furnace slag. The program should identify safe levels of use for various applications. Research in mineralization materials would accelerate advancement of a technology that has not yet reached wide adoption, but has potential for large-scale carbon reductions. Characterization and identification studies of potential feedstock sources should be performed. Improvements to life cycle assessment of building material products should be made. Research in all of these areas should also consider long-term impacts on emissions during the material's use.

3. Encourage regulating bodies to move to performance-based specifications in asphalt and concrete. Change from specifying mixture proportions to requirements of strength, durability, etc. This would help to increase adoption of limestone replacement, SCMs, recycled asphalt materials, and (eventually) alternate building materials.

References

[1] U.S. Geological Survey, *Mineral commodity summaries 2020*, no. 703. 2020.

[2] R. M. Andrew, "Global CO_2 emissions from cement production," *Earth Syst. Sci. Data*, vol. 10, pp. 195–217, 2018.

[3] International Energy Agency, "Technology Roadmap - Low-Carbon Transition in the Cement Industry," Paris, 2018.

[4] U.S. Environmental Protection Agency, "Sources of Greenhouse Gas Emissions." [Online]. Available: www.epa.gov/ghgemissions/sources-greenhouse-gas-emissions. [Accessed: 14-Jan-2021].

[5] Portland Cement Association, "How Concrete is Made." [Online]. Available: https://www.cement.org/cement-concrete-applications/how-concrete-is-made. [Accessed: 14-Jan-2021].

[6] S. T. Muench, E. Martinez Caraballo, Y. Y. Lin, S. Gutub, K. Willoughby, and J. Uhlmeyer, "Impact on Emissions and Energy Consumption of Evolving Pavement Materials Practices from 1990 to 2010: A Washington State Department of Transportation Case Study," 2013.

[7] National Asphalt Pavement Association, "Fast Facts," 2011.

[8] G. Holcomb, "Asphalt manufacturing in the US," 2020.

[9] G. Holcomb, "Ready-Mix Concrete Manufacturing in the US," 2020.

[10] S. Egan, "Precast Concrete Manufacturing in the US," 2020.

[11] X. Xu, M. Akbarian, J. Gregory, and R. Kirchain, "Role of the use phase and pavement-vehicle interaction in comparative pavement life cycle assessment as a function of context," *J. Clean. Prod.*, vol. 230, pp. 1156–1164, 2019.

[12] H. Pilorgé *et al.*, "Cost Analysis of Carbon Capture and Sequestration of Process Emissions from the U.S. Industrial Sector," *Envion. Sci, Technol*, vol. 54, no. 12, pp. 7524–7532, 2020.

[13] U.S. Department of Energy, "U.S. Department of Energy Announces $131 Million for CCUS Technologies," 2020. .

[14] "Murkowski, Manchin, House Colleagues Reach Agreement on Energy Package for Year-End Appropriations Bill," *Senate Committee on Energy & Natural Resources*, 2020. [Online]. Available: https://www.energy.senate.gov/2020/12/murkowski-manchin-house-colleagues-reach-agreement-on-energy-package-for-year-end-appropriations-bill. [Accessed: 14-Jan-2021].

[15] D. Leeson, P. Fennell, N. Shah, C. Petit, and N. Mac Dowell, "A Techno-economic Analysis and Systematic Review of Carbon Capture and Storage (CCS) Applied to the Iron and Steel, Cement, Oil Refining and Pulp and Paper Industries," *Energy Procedia*,

vol. 114, pp. 6297–6302, 2017.

[16] T. P. Hills, M. G. Sceats, and P. S. Fennell, “Applications of CCS in the Cement Industry,” in *Carbon Capture and Storage*, Royal Society of Chemistry, 2020.

[17] “Svante, LafargeHolcim, Oxy Low Carbon Ventures and Total launch study for commercial-scale carbon capture and end-use at U.S. plant,” 2020. [Online]. Available: https://www.lafargeholcim.com/joint-carbon-capture-project-usa-plant. [Accessed: 14-Jan-2021].

[18] “CCS at Norcem Brevik: Background.” .

[19] “Low Emissions Intensity Lime & Cement.” .

[20] United States Environmental Protection Agency, “Study on Increasing the Usage of Recovered Mineral Components in Federally Funded Projects Involving Procurement of Cement or Concrete,” 2008.

[21] A. A. Elgalhud, R. K. Dhir, and G. Ghataora, “Limestone addition effects on concrete porosity,” *Cem. Concr. Compos.*, vol. 72, pp. 222–234, Sep. 2016.

[22] M. C. G. Juenger, R. Snellings, and S. A. Bernal, “Supplementary cementitious materials: New sources, characterization, and performance insights,” *Cem. Concr. Res.*, vol. 122, pp. 257–273, Aug. 2019.

[23] American Road & Transportation Builders Association, “Production and Use of Coal Combustion Products in the U.S.,” 2015.

[24] U.S. Department of Transportation Federal Highway Administration, “Warm Mix Asphalt FAQs,” 2016. [Online]. Available: https://www.fhwa.dot.gov/innovation/everydaycounts/edc-1/wma-faqs.cfm. [Accessed: 14-Jan-2021].

[25] B. A. Williams, A. Copeland, and T. C. Ross, “Asphalt Pavement Industry Survey on Recycled Materials and Warm-Mix Asphalt Usage,” 2018.

[26] F. Kaseer, A. E. Martin, and E. Arámbula-Mercado, “Use of recycling agents in asphalt mixtures with high recycled materials contents in the United States: A literature review,” *Constr. Build. Mater.*, vol. 211, no. April, pp. 974–987, 2019.

[27] B. F. Bowers, D. E. Allain, and B. K. Diefenderfer, “Review of Agency Pavement Recycling Construction Specifications,” *Transp. Res. Rec. J. Transp. Res. Board*, 2020.

[28] M. S. Kuhar, “World Aggregates Market,” *Rock Products*, 2014. [Online]. Available: http://www.rockproducts.com/features/13045-world-aggregates-market.html#.XK_hcOhKjD4.

[29] A. Bascetin, D. Adiguzel, and S. Tuylu, “The investigation of Co_2 emissions for different rock units in the production of aggregate,” *Environ. Earth Sci.*, vol. 76, no. 7, 2017.

[30] Blue Planet Ltd, “Blue Planet | Economically Sustainable Carbon Capture.” [Online].

Available: http://www.blueplanet-ltd.com/. [Accessed: 09-Apr-2019].

[31] S. Monkman and M. Macdonald, “On carbon dioxide utilization as a means to improve the sustainability of ready-mixed concrete,” *J. Clean. Prod.*, vol. 167, pp. 365–375, 2017.

[32] “Carbon XPRIZE.” [Online]. Available: https://www.xprize.org/prizes/carbon. [Accessed: 14-Jan-2021].

[33] “Cement-Free, Carbon-Negative Concrete | Carbicrete.” [Online]. Available: http://carbicrete.com/. [Accessed: 14-Jan-2021].

[34] M. Gallucci, “Capture Carbon in Concrete Made with CO2,” *IEEE Spectrum*, 2020. [Online]. Available: https://spectrum.ieee.org/energywise/energy/fossil-fuels/carbon-capture-power-plant-co2-concrete. [Accessed: 14-Jan-2021].

[35] C. Chipello, “Clean concrete technology ready for ramp-up,” *McGill Reporter*, 2020. .

[36] “Mineral Carbonation International.” [Online]. Available: https://www.mineralcarbonation.com/. [Accessed: 14-Jan-2021].

[37] G. Ounoughene, “Orbix. Personal Communication.” 2019.

[38] “CarbonCure Technologies.” [Online]. Available: https://www.carboncure.com/. [Accessed: 14-Jan-2021].

[39] NRMCA, “Concrete CO2 Fact Sheet,” 2012.

[40] M. Wildnauer, E. Mulholland, and J. Liddie, “Life Cycle Assessment of Asphalt Binder,” 2019.

[41] United States Environmental Protection Agency, “Greenhouse Gas Emissions from a Typical Passenger Vehicle,” 2018.

Chapter 8

Description of Carbon Mineralization for Young Minds and Non-Scientists

Advancing carbon mineralization requires more than just scientists and engineers. People like venture capitalists, policymakers, and journalists are crucial for providing funding, incentives, and broader communication. Perhaps even more important is the cultivation of future generations of scientists, policymakers, etc. by inspiring them to pursue careers that can make a difference to the field of carbon mineralization or other climate-related fields. This chapter was published in Frontiers for Young Minds under the title "Capturing and Reusing CO_2 by Converting it to Rocks" as a higher-level description of carbon mineralization for readers aged 12-15 [1]. In addition to young science enthusiasts, this chapter was intended to aid other non-scientists in learning about the field of carbon mineralization.

Abstract

Within Earth's surface, there are billions of tons of rocks containing minerals that are reactive with CO_2, which is a greenhouse gas that has harmful effects on our planet's climate. Over thousands of years, these minerals interact with the CO_2 in the air, converting the gas into new carbonate minerals and permanently storing the CO_2 in a solid form. Today, as society develops solutions to combat the harmful effects of excess CO_2 in our atmosphere, the processes carried out by these reactive minerals could present a valuable opportunity. There is a challenge of speeding up the reactions so they happen within days (or even weeks), rather than thousands of years. Climate solutions like this are still new and will require more young and enthusiastic minds to advance their development so our climate is livable for generations to come!

1. Why is CO_2 Harmful, and What Can Be Done?

Since the late 1880s, we have used fossil fuels as our main source of energy. Fossil fuels include coal, petroleum, and natural gas. While they give us a lot of energy, they are also in limited supply, and they emit carbon dioxide (CO_2) when we burn them. Release of CO_2 into the atmosphere contributes to unfavorable changes in our planet's climate.

There are several ways to reduce the amount of CO_2 being emitted into Earth's atmosphere. One approach is replacing fossil fuel energy with **renewable energy**, like solar and wind, which do not emit CO_2. Another approach is to use energy-efficient technologies that require less energy, such as electric cars and LED bulbs. However, some CO_2 emissions cannot be avoided, and we call these "hard-to-avoid" emissions. These are most often found in industrial processes, like those that produce cement, iron, and steel. Because these products are necessary for building our roads, bridges, and buildings, it is important to find ways to avoid the emissions caused by their production. That's where **carbon capture** comes in to save the day!

Carbon capture works exactly as it sounds: technologies that "capture" CO_2 from emission sources. There are a lot of ways to go about capturing CO_2. One approach is called carbon mineralization, in which the CO_2 gas reacts with certain minerals to form new minerals, called **carbonates**.

2. What are Carbonate Minerals?

You've likely already seen lots of carbonate minerals since they are the building blocks of things like seashells, chalk, and concrete. These three examples all contain calcium carbonate ($CaCO_3$), which is also called limestone. The idea of carbon mineralization is based on a natural process called **mineral weathering**, in which certain minerals interact with CO_2 in the air, forming white carbonate minerals like those in the White Cliffs of Dover below (Figure 1*)*. This process occurs over thousands of years, but if it could be sped up to take place over hours or days, we could use this approach to capture and store CO_2!

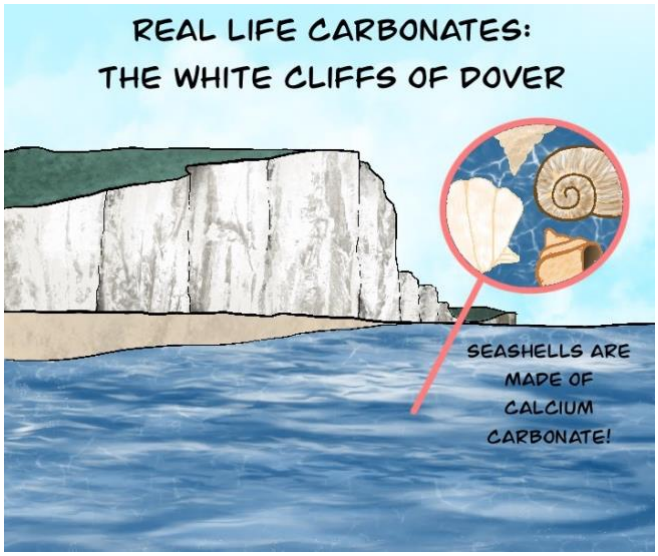

Figure 1 – You may have already seen carbonate minerals without realizing it. Calcium carbonate makes up seashells, chalk, and even the White Cliffs of Dover shown here. Carbonates can form from a variety of ways, all involving interactions with calcium and CO_2 that is dissolved in the water.

3. How Does Carbon Mineralization Work?

The idea of a gas changing to a solid may seem strange, but it happens in other ways that you see every day. The orange rust you see on old metal objects like cars and bikes forms when iron gets wet and reacts with oxygen in the air. The frost you might see on your window in the winter is due to the water vapor in warm humid air touching the cold glass surface. In the case of carbon mineralization, when certain reactive minerals become wet and come into contact with CO_2, they react to form carbonates, permanently storing CO_2 and keeping it out of the atmosphere for hundreds to potentially thousands of years.

The reactive minerals used for carbon mineralization need to contain high amounts of calcium or magnesium. These can be found naturally in **ultramafic rocks**, which are found in the earth on a scale of up to hundreds of billions of tons (>100,000,000,000 tons). Reactive minerals can also be found in wastes from industrial and mining processes. When important materials are made (like iron, steel, or cement) or mined (like diamonds, nickel, or copper), waste is generated and placed in piles near the facility. Much of this waste is rich in calcium or magnesium.

It is important to remember that CO_2 is also a waste gas in our atmosphere. Ever since human civilization started using fossil fuels, this heat-trapping gas has been released into the air as a waste product of combustion. Using carbon mineralization, ultramafic rocks and industrial/mining waste could react with the waste CO_2 present in the air to form carbonate minerals, helping to remove CO_2 from the air and prevent it from accumulating to excessive amounts.

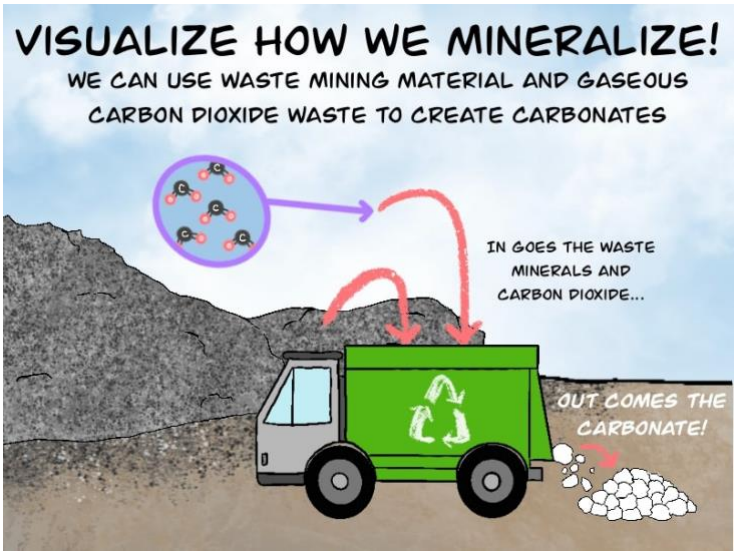

Figure 2 - Carbon mineralization involves combining two forms of waste to make new carbonate products. When valuable materials are made (like iron, steel, and cement) or mined (like diamonds, nickel, and copper), solid wastes are also produced, which are often rich calcium or magnesium. The same processes that produce or mine these valuable materials often also product CO_2 as a waste that is emitted into the atmosphere. As shown in this figure, the waste CO_2 can be combined with the solid wastes to produce new carbonate minerals.

4. What Can We Do with the Carbonate Products?

The process of using the products produced from carbon mineralization is known as **CO_2 utilization**. Carbon mineralization can be expensive, so by selling the carbonate products, money can be made so that the process is more affordable. Also, if the carbonate products can be made into building materials, like concrete, these new building materials could replace current building materials that emit CO_2 when produced, so CO_2 utilization could potentially avoid tons of CO_2 emissions!

Let's look at concrete as an example. Concrete is made from a mixture of cement, aggregates, and water (Figure 3). Cement acts as the glue that binds the ingredients together. Various sizes of **aggregates**, such as gravel or sand, are used to provide volume and stability to the concrete. The water allows the concrete to be mixed well before it hardens.

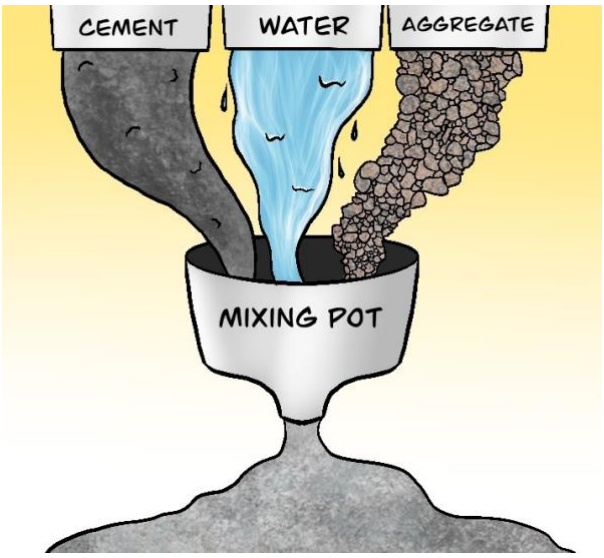

Figure 3 - Concrete is made up of cement, water, and aggregates. Aggregates are particles of various sizes, such as gravel or sand, and they provide volume and stability to the concrete. Cement acts as the glue that binds the aggregates together. Water is added to allow the concrete to mix well before it hardens.

Cement production creates a lot of CO_2 - it accounts for 8% of all of humanity's CO_2 emissions! Researchers are trying to find ways to reduce cement-related emissions by reducing the amount of cement used in concrete or by changing the way cement is produced. Successful changes in the cement industry could have a major impact on the amount of CO_2 being emitted into our atmosphere! Some companies are using carbonate minerals to create new aggregates for concrete that are more useful than normal aggregates. Some companies have figured out a way to inject CO_2 directly into wet concrete, where it reacts and causes the concrete to become even stronger once it dries. Other companies get creative by using different sources of calcium (like industrial wastes) as a new cement in their concrete.

There are already companies around the world that are using carbon mineralization to create new building products, but they are facing a difficult task. Most of the building materials we have today are cheap and relatively easy to use, so replacing them requires some creativity. It is not impossible to replace a cheap and useful product with a new one; take phones as an example. Before we had

iPhones, we had basic flip phones that were simple, functional, and cheap. The iPhone became popular not because it was more affordable than a flip phone, but because it was a better product. Hence, new carbonate building materials must offer better features than materials that are currently available and release less CO_2 during their manufacture than current products do.

5. How Developed is this Technology?

Building materials made from mineral carbonates have significant potential to decrease CO_2 emissions in the cement industry. However, for the technology to become popular, work still needs to be done in several areas:

- **Research:** The process to make carbonates with CO_2 is still expensive and complicated, and it needs to be improved. More research is also needed to prove that the new cement and concrete are better than the ones we have now.

- **Carbon incentives**: There are ways for the government to pay money to people who store CO_2 and prevent it from entering the air, "incentivizing" CO_2 storage and use. This would help carbon mineralization be more affordable.

- **Regulations**: There are strict regulations that dictate which materials can be used to make concrete for roads and buildings. Some of the regulations are old and could be updated to encourage the use of new carbonate materials. This would depend on whether the new materials are proven to perform well.

6. Carbon Mineralization in the Ocean

Just as CO_2 is floating in our air, it is also dissolved into our oceans. This is similar to how CO_2 is dissolved in your fizzy soft drinks. The CO_2 gas likes to be in **equilibrium** between the air and water. Because there is more CO_2 in a soda can than in the air around it, when you open a soda can, the CO_2 quickly leaves the can and enters the air so it can reach equilibrium.

Our oceans do not make bubbles like soda because the CO_2 is already in equilibrium between the ocean and the air. By adding calcium and magnesium to the ocean, the CO_2 dissolved in the ocean can mineralize and form carbonate minerals, reducing amount of CO_2 in the water and disturbing the equilibrium. This will cause more CO_2 to leave the air and enter the ocean. Scientists are researching safe ways to add calcium and magnesium to the oceans so that we can use the help of the oceans to remove CO_2 from the atmosphere [2]!

7. How Can You Get Involved?

Carbon mineralization is just one of the many solutions that are needed to stop Earth's climate from changing. All of the solutions will require help from all sorts of minds. For example, while scientists and engineers can help to develop carbon mineralization and other technologies, politicians and lawyers can help with government policies that encourage climate solutions, and journalists can communicate new technologies to the public. Additionally, we can all try to reduce our own carbon emissions by changing our everyday habits, such as by using less electricity or carpooling. Climate change will be a big problem for many years to come, but if everyone takes their own steps to help the fight, the problem could very well be solved!

Glossary

Renewable energy: Energy that comes from a source that is in such abundance that it cannot be used up, such as wind or solar energies.

Carbon capture: A technology that captures CO_2 from emission sources (or directly from the air) to prevent the CO_2 from causing changes to Earth's climate.

Carbonates: Solid minerals that are formed from interactions with CO_2 and water.

Mineral weathering: A natural process where rocks and minerals break down to form new rocks and minerals. Weathering can involve reactions with CO_2 from the atmosphere, leading to carbonate formation.

Ultramafic rock: Rocks with relatively large amounts of magnesium, making them ideal for carbon mineralization.

CO_2 utilization: The process of changing CO_2 into a new form and using it as a valuable product.

Equilibrium: A balance between opposite forces.

Aggregates: Non-reactive materials that provide volume and stability to concrete, ranging from small sand particles to larger gravel rocks.

References

[1] C. M. Woodall, I. Piccione, M. Benazzi, and J. Wilcox, "Capturing and Reusing CO_2 by Converting it to Rocks," *Front. Young Minds*, vol. 8, no. 592018, 2021.

[2] P. Renforth and G. Henderson, "Assessing ocean alkalinity for carbon sequestration," *Rev. Geophys.*, vol. 55, no. 3, pp. 636–674, 2017.

Chapter 9

Conclusions and Recommendations for Future Work

1. Conclusions

This Dissertation used a multi-faceted approach to advance carbon mineralization. In the first half of the Dissertation, platinum group metal (PGM) tailings from Sibanye-Stillwater were characterized and their reactivity was analyzed. Three methods were employed to extract alkalinity from the Sibanye-Stillwater tailings for the purpose of CO_2 storage, including ambient conditions (Chapter 2), the Alternative ÅA Route (Chapter 3), and the pH Swing process (Chapter 4). The economics of these methods were evaluated in Chapter 5, indicating key economic barriers to overcome. The results are summarized in Table 1.

Table 1: Summary of Results for Alkalinity Extraction from Sibanye-Stillwater Tailings

Chapter	Process	Reagent	Time. (hr)	Extraction Efficiency		Max CO_2 Capacity ($kgCO_2$ $t\text{-tailings}^{-1}$)	Economic Barrier
				Ca	Mg		
2	Ambient	10% CO_2	60	2.83%	0.11%	0.3	LU
3	Alternative ÅA	Ammonium Sulfate, 450 ºC	0.5	13.02%	39.17%	5.0	RC, EU
3	Alternative ÅA	Ammonium Sulfate, 475 ºC	1	14.21%	41.39%	5.3	RC, EU
4	pH Swing	0.5M Citric	72	4.28%	41.09%	4.3	RC, EV
4	pH Swing	0.5M Citric	426	10.29%	81.73%	8.7	RC, EV
4	pH Swing	0.5M Sulfuric	18	6.88%	73.55%	7.6	RC, EM
4	pH Swing Series	0.5M Sulfuric / 0.5M Oxalic	18 + 72	10.65%	74.53%	8.1	RC, EM, EV

EM – equipment material; EU – energy use; EV – equipment volume; LU – land area use; RC – reagent cost;

Based on the experimental results and economic evaluation, there is not a clear optimal process to store CO_2 in the Sibanye-Stillwater tailings via carbon mineralization. Chapter 5 identified the Alternative ÅA Route as the most economical process at the conditions tested in this Dissertation, but as indicated in Table 1, the overall CO_2 capacity of this process is limited relative to the pH swing. The major limiting factor in all processes is Ca extraction efficiency, which never eclipsed 15 %. Further optimization of the processes used is required to increase Ca extraction and improve process economics.

The technoeconomic analysis tool presented in Chapter 5 proved to be effective in comparing the economics of different *ex-situ* carbon mineralization processes. With sufficient data from lab-scale experimental trials and familiarity with the tool's navigation, the tool can be used to identify economic barriers via tallying of capital and operating expenses and sensitivity analyses. Future updates to the tool could increase its usability and robustness.

Utilizing carbon mineralization products in the construction industry shows the potential to avoid up to three $GtCO_2$ globally per year, where the best near-term opportunity lies in producing precast concrete products using low- to no-cost feedstock like industrial wastes (Chapter 6). As detailed in Chapter 7, decarbonization methods for concrete and pavement, like using carbon mineralization products, could cut the US concrete industry's emissions by more than two thirds, but this requires further research and change in government policies.

2. Recommendations for Future Work

A Dissertation would be remiss without leaving a legacy for future improvement in the work that has been covered. The following sections detail recommendations to continue the momentum that has been started in this Dissertation.

2.1 Carbon Mineralization with PGM Tailings

All carbon mineralization processes investigated in this Dissertation could be further optimized to improve the performance with PGM tailings like those of Sibanye-Stillwater.

The economics of the Alternative ÅA Route tested in Chapter 3 proved to be more sensitive to extraction efficiency at low values (below about 60%). Further optimization using the temperature with the highest extraction efficiency, 475 ^{o}C, could help to improve the process economics, as would further decreases in extraction time and ammonium sulfate consumption. Extraction of Ca was limited, likely due to low solubility of Ca-sulfate. Methods should be investigated that maintain the extracted Ca, like using salts which create more soluble Ca-salts, or processing of the solid residue to separate the solid Ca-sulfate. In the latter case, it would be important to first characterize the solid residue and determine if the plagioclase structure has been broken by the thermal reaction, and whether much of the extracted Ca does indeed remain in the residue.

The pH swing evaluated in Chapter 4 proved to be far too costly due to acid- and equipment-related expenses. Sulfuric acid solutions most efficiently extracted alkalinity in the shortest time, but might be further optimized by investigating longer times and/or higher solid/liquid ratios. However, extraction in sulfuric acid is hindered by the expensive corrosion-resistant equipment required. Alternatively, citric acid solutions extracted more than 80 % of available Mg, but required 18 days to do so. Considering the trajectory of dissolution in citric acid with time, investigation into dissolution times between 3 and 18 days could provide a more optimal time of dissolution, decreasing the vessel volume required. Further decreases in the acid concentration used, particularly for organic acids, might decrease any negative effects caused by ligands irreversibly adhering to the mineral surface, and would also decrease acid consumption.

Further investigation into the carbonation step and subsequent acid solution recovery is paramount for either of these processes to be viable. This should involve a reaction vessel with *in-situ* measurements of pH, temperature, pressure, and *in-situ* Raman spectroscopy. Products should be analyzed with CO_2 coulometry to analyze their total inorganic carbon content. Studies on the transformation of carbonate products from amorphous to crystalline might also be required.

Another acid that should be further investigated is carbonic acid. This was tested at low concentrations in Chapter 2, yielding limited results, but could be intensified by using higher concentrations, stirring, or pressure. Using carbonic acid would eliminate the problem of acid consumption, as consumption of dissolved CO_2 is the primary goal of carbon mineralization.

It is worth considering whether a surficial mineralization method should be used rather than the *ex-situ* methods tested in Chapters 3 and 4. Given the dramatically low reactivity at ambient conditions (Chapter 2), and the potential to use carbonated products in the construction industry (Chapters 6 and 7), further investigation into *ex-situ* mineralization methods appears worthwhile

in the near-term. However, economics of *ex-situ* methods should continually be compared to more robust economic evaluations of potential surficial mineralization methods. If further optimization of *ex-situ* methods proves to be unfruitful, surficial mineralization might in fact be the best method to store CO_2 in PGM tailings, albeit at a much slower rate.

Finally, the Sibanye-Stillwater mine is one mine that produces copper, nickel, and PGMs. Increased production of metals from other mines like Sibanye-Stillwater will provide additional sources of tailings, which may differ from the tailings evaluated here. Collection of alternate tailings samples could provide a more realistic estimation of the potential of the different mineralization methods in storing CO_2 in the billions of tonnes of tailings to be produced in the coming decades.

2.2 Technoeconomic Analysis Tool

Future versions of the tool presented in Chapter 5 should employ kinetic data for mineral dissolution and carbonation, rather than using efficiency assumptions for these to process steps. Additionally, calculation of pH conditions would help to predict which species will be present in solution, and which species (carbonates or other) would precipitate. The tool should also be able to evaluate the carbonation of both Mg and Ca in solution, as the current version forces the user to pick one target cation. Finally, the tool is currently based in Microsoft Excel, which has limitations for processing power and usability. Conversion to a software like Python would improve the calculation speed and volume, and provide more clarity for user inputs and controls.

2.3 Carbon Mineralization Product Utilization

Additional research is required to improve the quality of construction products produced from carbon mineralization, as outlined in Chapter 6, Section 5. In short, more demonstration of long-term strength and durability is required for deeper market penetration. Additionally, development of products which utilize Mg-carbonates is needed.

2.4 Government Policy

In Chapter 7, three policy recommendations were developed to advance the decarbonization of concrete and pavements. These include:

1. Demonstration and Deployment - Fund pilot or demonstration carbon capture projects at cement plants.
2. Research and Development - Increase research for supplementary cementitious materials and materials produced with carbon mineralization.
3. Regulatory Revisions - Encourage regulating bodies to shift to performance-based specifications in asphalt and concrete.

2.5 Youth Engagement

The high-level description of carbon mineralization given in Chapter 8 received positive feedback from primary school teachers, congressional staffers, young reviewers, and other peers in non-engineering fields. To extend the reach of this work's impact, projects and collaborations could be started with primary schools, particularly in science classrooms. The paper could be presented to

young minds, with an accompanying question and answer session. Additionally, climate-related experiments could be carried out to give hands-on experience to students. The initial intent for the "youth outreach" portion of this Dissertation was to run a modified version of the "Disk Carbonation" experiment detailed in Chapter 2. However, due to extenuated circumstances in the year 2020, this was not able to happen. When or if in-person collaboration becomes more feasible, an experiment like this could be performed.

Feedback on the material in Chapter 8 was particularly given from non-scientists in the policy realm, citing that the reading provided a high-level description but still rather informative. More work like this could be done to summarize other difficult topics for climate mitigation technologies, like direct air capture, bioenergy with CCS, or geologic CO_2 storage. Improvement in the way those who make policy decisions are informed on advanced scientific topics could help with development of more robust technology-advancing policies.

Appendix

Additional information on experimental techniques and photos for illustration are provided here from each experimental chapter.

Chapter 2

Sample Homogenization

Bulk samples were split into representative portions for each experiment to be undertaken. This was done by placing a wide sheet of aluminum foil under a fume hood, folding each edge upward to prevent any sample from leaving the surface of the aluminum sheet. The bulk sample was poured onto the aluminum sheet, and using a pestle, any large particle agglomerations were broken apart. The bulk sample was homogenized by scraping along four axes with a scoopula, as shown in Figure A- 1.

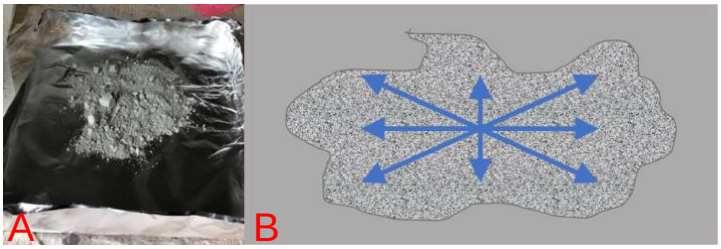

Figure A- 1: Homogenization of mine waste samples.
A: Photo of one sample on foil sheet; B: Mixing axes to homogenize sample

During the homogenization process, the bulk sample was shaped into an approximately even oval. After sufficient homogenization, the bulk sample was separated into portions according to amounts necessary for each characterization test. An example of the split is given in Table A- 1, and shown in Figure A- 2. Each portion was placed in a conical vial and labeled according to its designated characterization test.

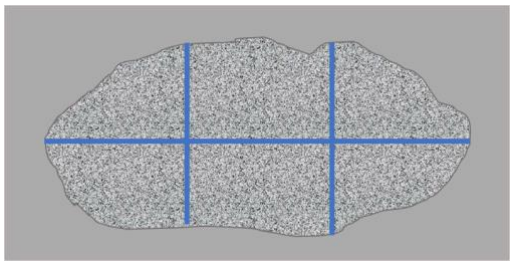

Figure A- 2: Approximate portioning of mine waste sample

Table A- 1: Allocations of Mine Tailings Samples for Each Characterization Test

Characterization Test	Required Sample Mass (g)	Approximated Bulk Portion
QXRD/TIC	2 + 5	1/6
BET	10	2/6
Grain Size	5	1/6
Leaching	8	2/6

Sample Micronization

Samples used for QXRD and TIC tests were combined, as they required micronization to generate powder samples. In preparation for this process, corundum (Al_2O_3) was added as exactly 20 % by weight to each solid mine sample in order to achieve quantitative results in later experiments. This was performed in a micronizing mill. The mill chamber was loaded with agate pellets (Figure A-3). All pellets were placed in the chamber except for the top middle pellet. The black frame was removed, the sample was poured into the chamber, and ethanol was poured to fill approximately one third of the chamber. Afterward, the final pellet was added to the chamber, and it was closed and placed in the mill, which ran for seven minutes.

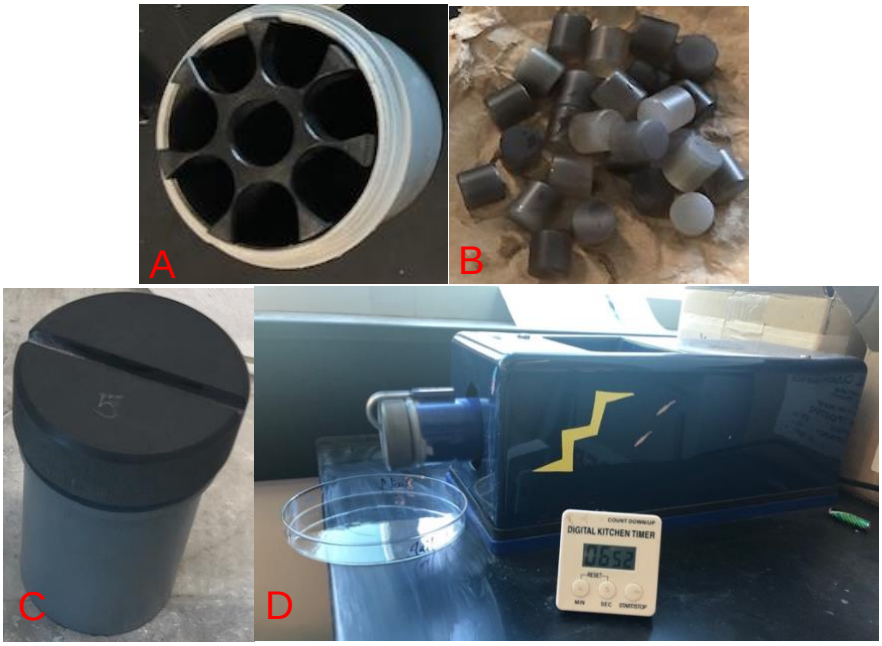

Figure A- 3: Components of the micronizing mill: A) Empty micronizing chamber; B) Agate pellets; C) Closed micronizing chamber; D) Micronizing mill

After micronization, the chamber was removed and the original lid was replaced with a pouring lid. The solution in the chamber was poured into a petri dish. To remove any remaining solid within the chamber, additional ethanol was added to the chamber, followed by stirring and pouring of solution. This process was repeated until the solution leaving the chamber appeared transparent.

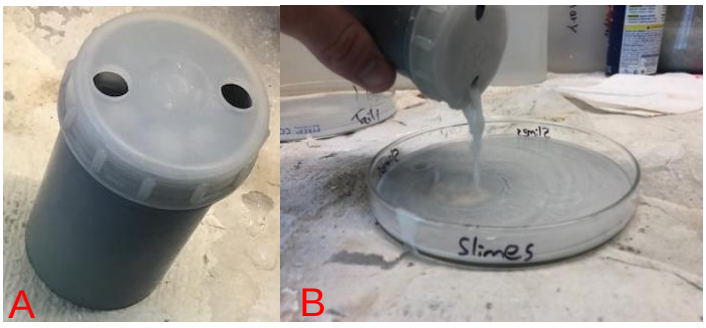

Figure A- 4: Removal of micronized sample solution from chamber.
A) Micronizing chamber with pouring lid; B) pouring sample solution into petri dish

The petri dishes sat under a hood overnight, allowing the ethanol to evaporate and leave the dry micronized sample, shown in Figure A- 5. Samples were removed from the petri dishes using a razor blade and placed in a conical vial.

Figure A- 5: Petri dishes with micronized samples after drying overnight. One sample has been scraped with a razorblade and partially removed from its petri dish.

Photos of Instruments and Equipment

The following figures are photographs of instruments and equipment used in the characterization experiments detailed in Chapter 2. These photos were taken at the University of British Columbia in June and July 2019.

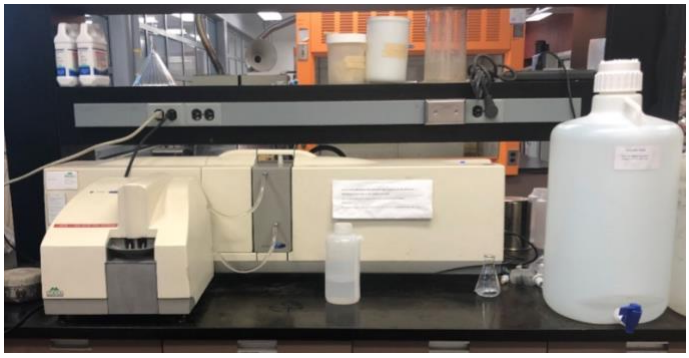

Figure A- 6: Malvern Instruments Mastersizer 2000 instrument for grain size analysis

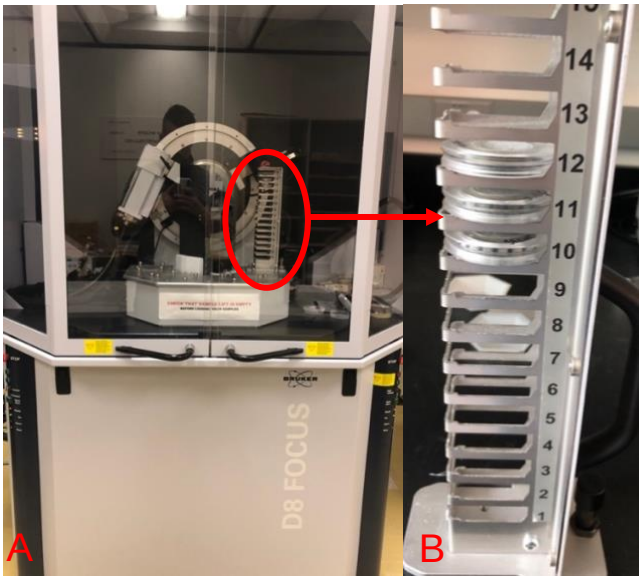

Figure A- 7: Materials for QXRD testing: A) Bruker D8 Focus XRD Instrument; B) 15-tier sample holder

Figure A- 8: Varian 725-ES ICP-OES Instrument

Figure A- 9: Materials for flow-through reaction chamber. Top left to right: two chambers, with lids sitting above bottoms; box of 0.2 µm filters; tweezers; beaker containing rubber gaskets. Bottom left: polytetrafluoroethylene (PTFE) tape to seal chamber threading. (The chamber bottom on the left is shown with tape wrapped around threading.)

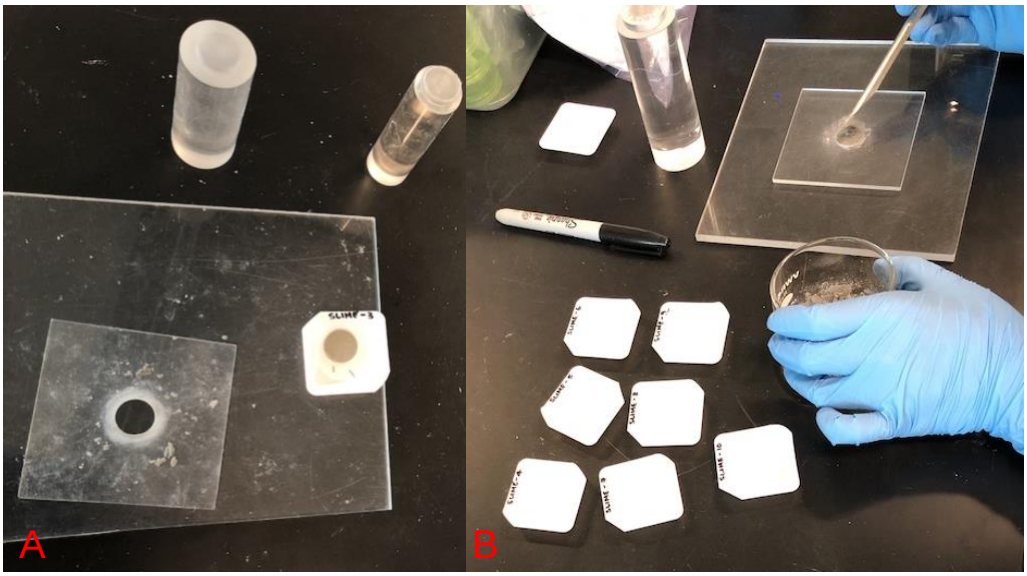

Figure A- 10: A) Dime fabrication materials, showing the premade Perspex glass mount, Perspex glass piston press, and a fabricated dime product; B) Dime fabrication process

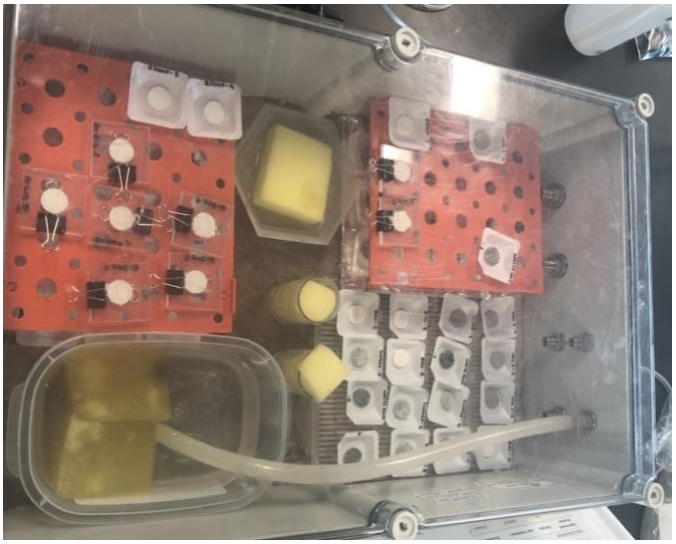

Figure A- 11: Chamber for passive carbonation of dimes

Chapter 3

The following figures are photographs of the furnace and alkalinity sources used in the Alternative ÅA Route optimization detailed in Chapter 2. These photos were taken at the Colorado School of Mines in June and July 2018.

Figure A- 12: Furnace used for Alternative ÅA Route optimization

Figure A- 13: Sample of Tail 2b

Figure A- 14: Sample of olivine

Chapter 4

Photos of Equipment, Residues, and Products

The following photos are from experiments described in Chapter 4, where tailings were dissolved with organic and mineral acids. These photos were taken at Otto von Guericke University in November and December 2020.

Figure A- 15: Experimental setup for (a) alkalinity extraction via acid dissolution and (b) vacuum filtration

Figure A- 16: MiniPlant Reactor for Carbonation step

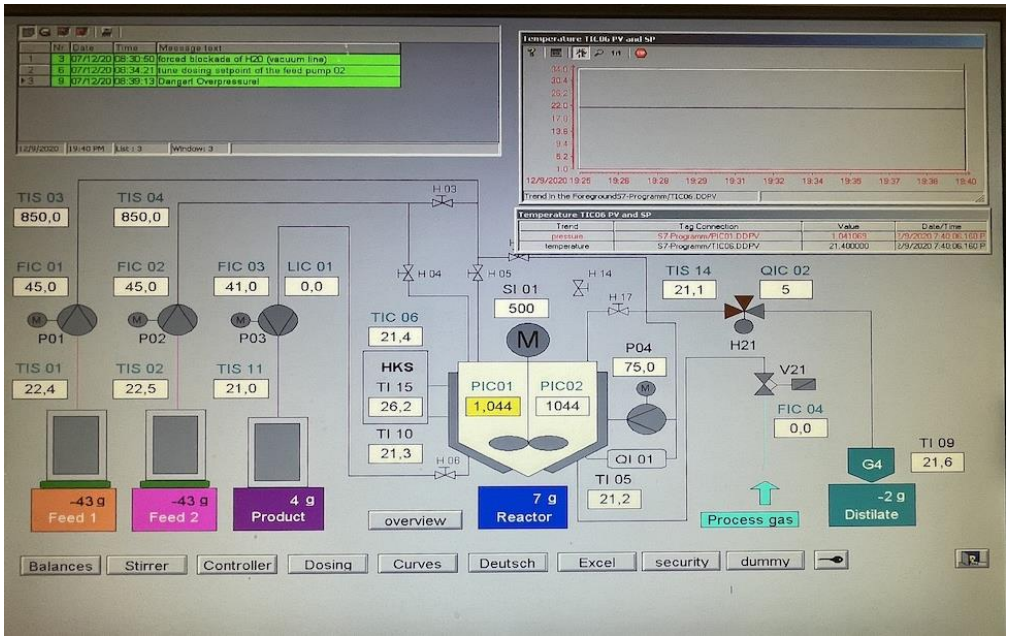

Figure A- 17: Control board for MiniPlant Reactor

Figure A- 18: Back-loaded mounts for quantitative XRD measurements

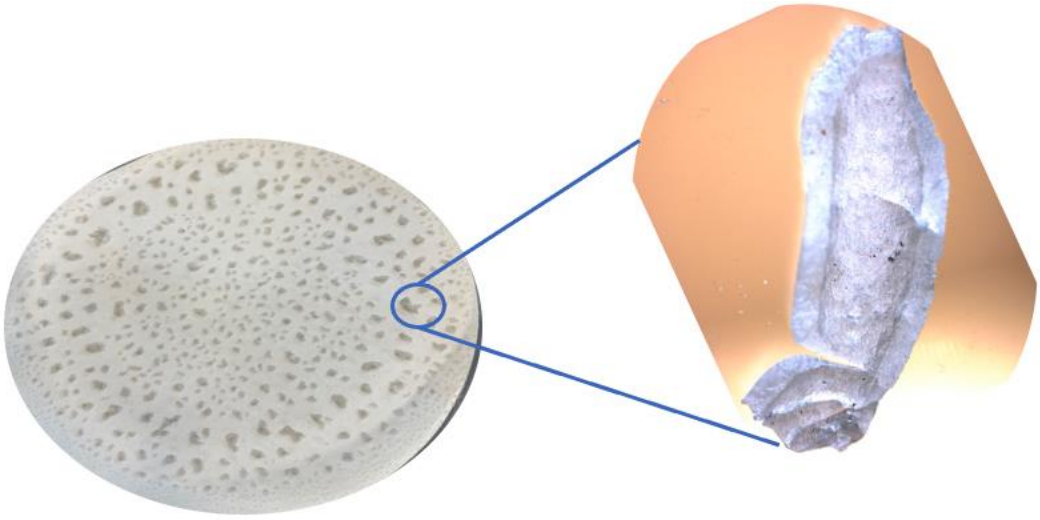

Figure A- 19: Precipitates from carbonation step
Dissolution step parameters: 0.5M citric acid, 72 hours, 30 g/L

Figure A- 20: Ammonium oxalate precipitated during carbonation of oxalic acid extraction solutions, (a) in solution, (b) in filter, and (c) after overnight drying under fume hood

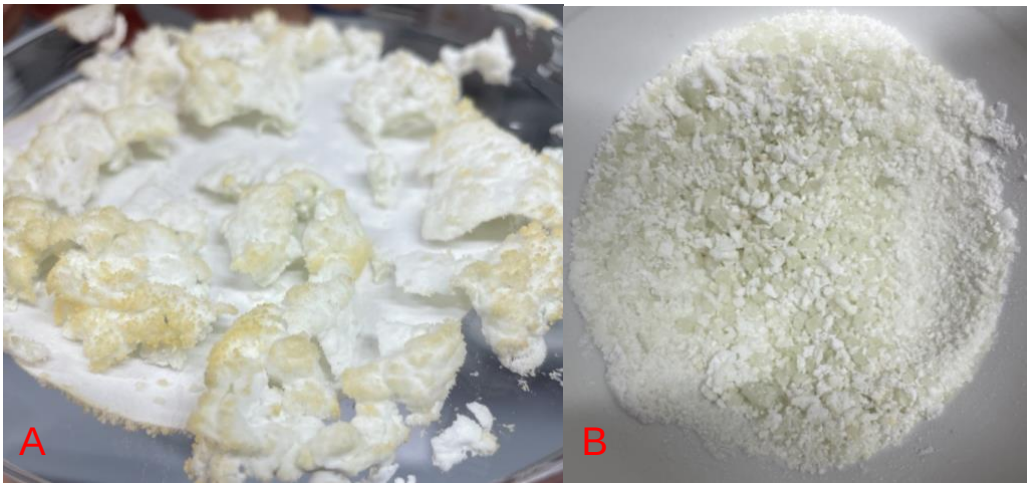

Figure A- 21: Multiple precipitate phases evident after carbonation of extraction solution from 0.5M oxalic acid, 24 hours. Photos taken after (a) overnight drying and (b) partial homogenization in mortar and pestle

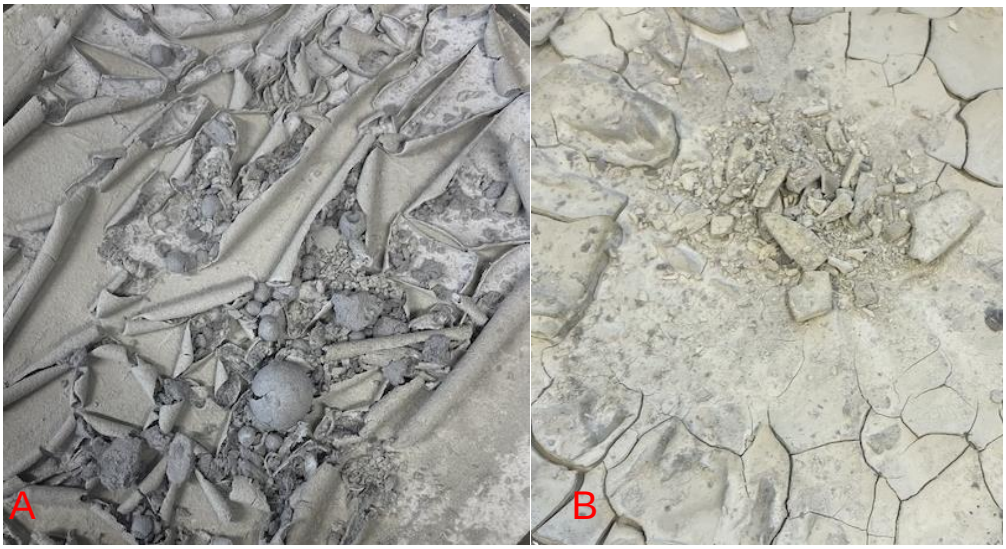

Figure A- 22: Residues from dissolution in (a) citric acid and (b) oxalic acid typically had different appearances. These photos are from 18-day dissolution. Sometimes, residue particles would agglomerate in spheres, as shown in (a).

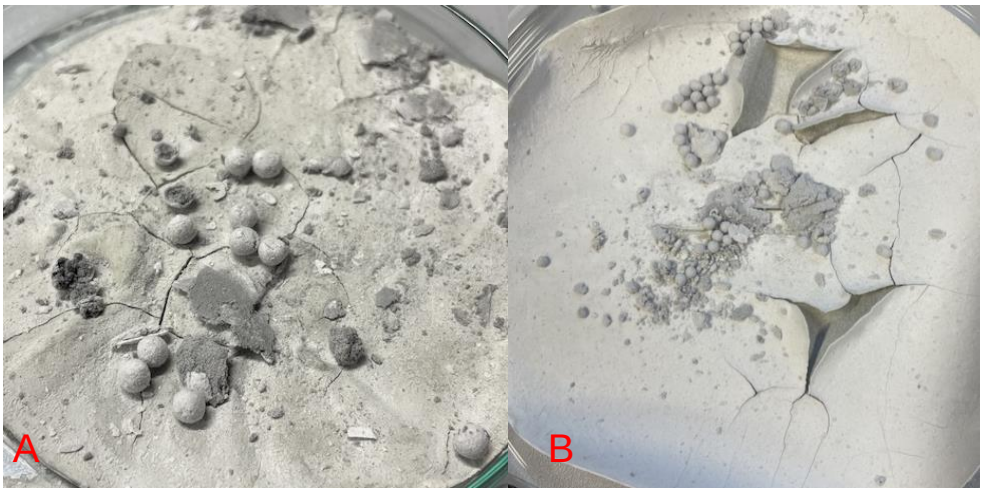

Figure A- 23: Spheres were also generated in some residues of series dissolution. Photos from (a) hydrochloric/oxalic and (b) sulfuric/oxalic 0.1M residues.

Chapter 5

Screenshots of Tool

The following are assorted screenshots from the technoeconomic analysis model presented in Chapter 5. The tool, along with a full user manual, can be found online at https://primecoalition.org/climate-impact/.

Model Control Panel		
	General	
Process Name	AA_450	AA_475
Target CO2 Sequestered (tCO2/yr)	1,000.00	1,000.00
Alkaline Feed	Stillwater Tail 2b	llwater Tail 2b
(Mg wt%)	5.08%	5.08%
(Ca wt%)	9.68%	9.68%
(Suggested Target Cation)	Ca	Ca
Selected Target Cation	Mg	Mg
Feed Particle Size (µm)	60	60
(Size Reduction Suggestion)	Size is sufficient	Size is sufficient
Cost of Alkaline Feed ($/t-feed)	0	0
Cost of CO2 Supply ($/tCO2)	0	0
Target Market Product	Carbonate Product	Carbonate Product
(Target Carbonate Product)	Hydromagnesite (Mg5(CO3)4	Hydromagnesite (Mg5(CO3)4
Product Selling Price ($/t-product)	0	0
Hourly Operation (hr/day)	24	24
Daily Operation (day/yr)	365	365
Project Life (years)	12	12
Project Starting Year	2020	2020

Figure A- 24: Tool Control Panel - General

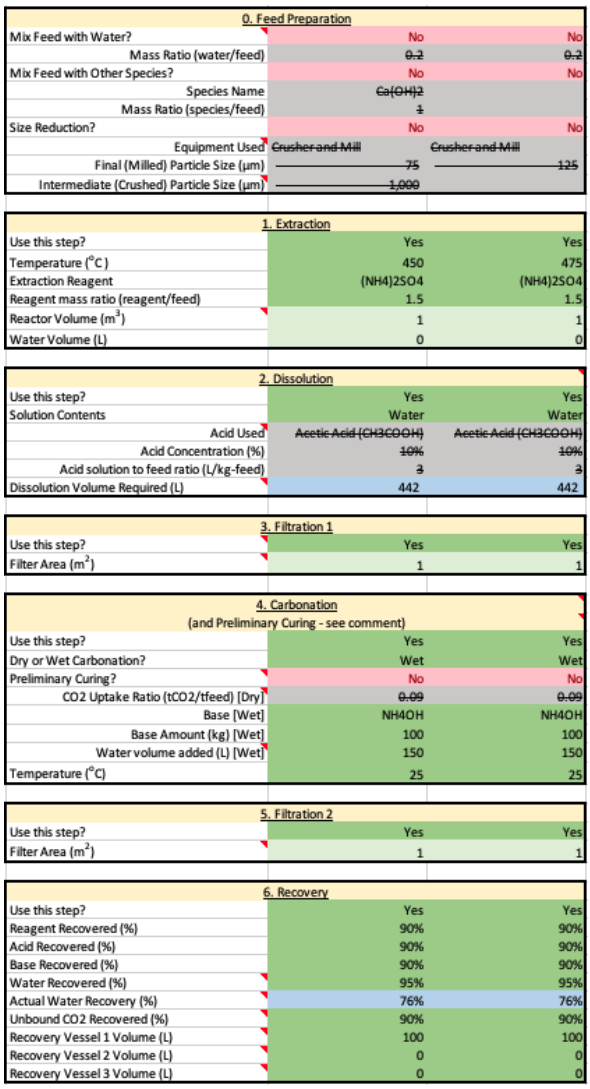

0. Feed Preparation		
Mix Feed with Water?	No	No
Mass Ratio (water/feed)	~~0.2~~	~~0.2~~
Mix Feed with Other Species?	No	No
Species Name	~~Ca(OH)2~~	
Mass Ratio (species/feed)	~~1~~	
Size Reduction?	No	No
Equipment Used	~~Crusher and Mill~~	~~Crusher and Mill~~
Final (Milled) Particle Size (µm)	~~75~~	~~125~~
Intermediate (Crushed) Particle Size (µm)	~~1,000~~	

1. Extraction		
Use this step?	Yes	Yes
Temperature (°C)	450	475
Extraction Reagent	(NH4)2SO4	(NH4)2SO4
Reagent mass ratio (reagent/feed)	1.5	1.5
Reactor Volume (m^3)	1	1
Water Volume (L)	0	0

2. Dissolution		
Use this step?	Yes	Yes
Solution Contents	Water	Water
Acid Used	~~Acetic Acid (CH3COOH)~~	~~Acetic Acid (CH3COOH)~~
Acid Concentration (%)	~~10%~~	~~10%~~
Acid solution to feed ratio (L/kg-feed)	~~3~~	~~3~~
Dissolution Volume Required (L)	442	442

3. Filtration 1		
Use this step?	Yes	Yes
Filter Area (m^2)	1	1

4. Carbonation (and Preliminary Curing - see comment)		
Use this step?	Yes	Yes
Dry or Wet Carbonation?	Wet	Wet
Preliminary Curing?	No	No
CO2 Uptake Ratio (tCO2/tfeed) [Dry]	~~0.09~~	~~0.09~~
Base [Wet]	NH4OH	NH4OH
Base Amount (kg) [Wet]	100	100
Water volume added (L) [Wet]	150	150
Temperature (°C)	25	25

5. Filtration 2		
Use this step?	Yes	Yes
Filter Area (m^2)	1	1

6. Recovery		
Use this step?	Yes	Yes
Reagent Recovered (%)	90%	90%
Acid Recovered (%)	90%	90%
Base Recovered (%)	90%	90%
Water Recovered (%)	95%	95%
Actual Water Recovery (%)	76%	76%
Unbound CO2 Recovered (%)	90%	90%
Recovery Vessel 1 Volume (L)	100	0
Recovery Vessel 2 Volume (L)	0	0
Recovery Vessel 3 Volume (L)	0	0

Figure A- 25: Tool Control Panel – Process Steps

Below the General Tool Control Panel is a control panel for each process step, where the general tool process can be customized to fit the process under evaluation (Figure A- 25). Selecting "Yes" on a step activates related parameters to be controlled, while selecting "No" deactivates them, as shown in **Error! Reference source not found.**. The primary parameters for each step are controlled here, while more advanced parameters can be altered in the "Process" tab of the tool.

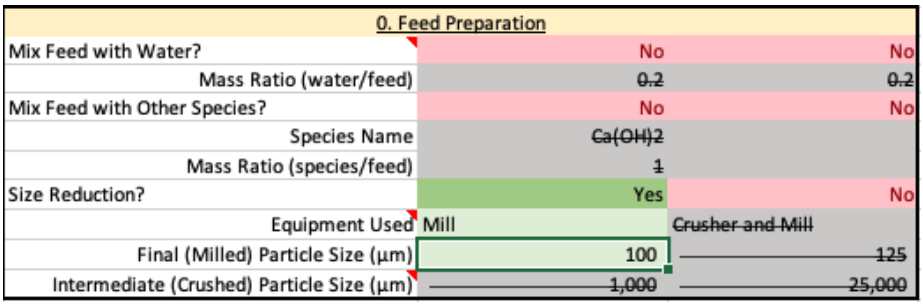

0. Feed Preparation		
Mix Feed with Water?	No	No
Mass Ratio (water/feed)	~~0.2~~	~~0.2~~
Mix Feed with Other Species?	No	No
Species Name	~~Ca(OH)2~~	
Mass Ratio (species/feed)	~~1~~	
Size Reduction?	Yes	No
Equipment Used	Mill	~~Crusher and Mill~~
Final (Milled) Particle Size (µm)	100	~~125~~
Intermediate (Crushed) Particle Size (µm)	~~1,000~~	~~25,000~~

Figure A- 26: Feed Preparation control panel, showing parameter activation upon selecting "Yes" for "Size Reduction?"

The tool has economic outputs based on net present value:

MODEL OUTPUTS		
Process Summary		
Process	Process 1	Process 2
CO2 Sequestration		
Sequestered as Carbonate (tCO2/yr)	25,000.00	25,000.00
Emitted from Process (tCO2/yr)	2,847.67	2,479.63
Emitted from Transport (tCO2/yr)	-	-
Net Sequestered (tCO2/yr)	**22,152.33**	**22,520.37**
Process Economics		
Total Transport Expense ($/yr)	-	$ -
Total Capital Expense ($)	$ 1,992,089.57	$ 1,795,756.67
Total Operating Expense ($/yr)	$ (2,165,688.23)	$ (2,211,931.29)
Project Net Present Value	**$ 21,487,298.92**	**$ 22,040,708.49**

Figure A- 27: TEA Tool Outputs, primary

The upfront cost of equipment, or capital expense (CAPEX), is calculated using bare module costing method.

Capital Expense Summary				
	Process 1		Process 2	
Equipment	Model As:	Cost ($)	Model As:	Cost ($)
0. Feed Preparation				
Mixer (water)	none	$ -	none	$ -
Mixer (other species)	none	$ -	none	$ -
Crusher	none	$ -	none	$ -
Mill	Hammer mill	$ 61,226.51	none	$ -
1. Extraction				
Thermal Reactor	Fired Heater for Molten Salt/Mineral	$ 1,096,559.26	Fired Heater for Molten Salt/Mineral	$ 1,012,149.63
2. Dissolution				
Vessel	Horizontal, CS	$ 184,944.63	Horizontal, CS	$ 167,571.96
3. Filtration 1				
Filter 1	Gravity	$ 55,134.28	Gravity	$ 55,134.28
4. Carbonation				
Curing Chamber	none	$ -	none	$ -
Carbonation Vessel [Dry]	none	$ -	none	$ -
Carbonation Vessel [Wet]	Autoclave (steel, up to 300 psig)	$ 528,473.06	Autoclave (steel, up to 300 psig)	$ 495,255.00
5. Filtration 2				
Filter 2	Gravity	$ 55,134.28	Gravity	$ 55,134.28
6. Recovery				
Recovery Vessel 1	Vertical, CS	$ 10,617.55	Vertical, CS	$ 10,511.52
Recovery Vessel 2	none	$ -	none	$ -
Recovery Vessel 3	none	$ -	none	$ -
Total Capital Expense				
		$ 1,992,089.57		**$ 1,795,756.67**

Figure A- 28: Capital Expense Summary (Tool Output)

Operating Expense Summary						
	Process 1			Process 2		
	Species	Amount (X/yr)	Cost ($/yr)	Species	Amount (X/yr)	Cost ($/yr)
			Products			
Carbonate Product	Magnesite (MgCO3)	47,894.80	$ (3,831,583.73)	Magnesite (MgCO3)	47,894.80	$ (3,831,583.73)
Bulk Cement	none	-	$ -	none	-	$ -
Bulk Concrete	none	-	$ -	none	-	$ -
Other	none	-	$ -	none	-	$ -
Other	none	-	$ -	none	-	$ -
Other	none	-	$ -	none	-	$ -
Other	none	-	$ -	none	-	$ -
	Total Product Revenue ($/yr)		$ (3,831,583.73)	Total Product Revenue ($/yr)		$ (3,831,583.73)
			Raw Materials			
Alkaline Feed	Lizardite (Mg3Si2O5(OH	62,365.40	$ 623,653.99	Lizardite (Mg3Si2O5(OH	62,365.40	$ 623,653.99
Reagent	(NH4)2SO4	9,382.04	$ 731,799.22	(NH4)2SO4	9,378.84	$ 731,549.33
Acid	none	-	$ -	none	-	$ -
Base	NH4OH	31.01	$ 6,201.53	NH4OH	35.13	$ 7,026.00
Water	H2O (liq)	9,755.32	$ 3,195.84	H2O (liq)	9,751.42	$ 3,194.57
CO2	CO2	25,442.46	$ 127,212.30	CO2	25,442.31	$ 127,211.55
Other	none	-	$ -	none	-	$ -
Other	none	-	$ -	none	-	$ -
Other	none	-	$ -	none	-	$ -
	Total Material Costs ($/yr)		$ 1,492,062.89	Total Material Costs ($/yr)		$ 1,492,635.44
			Energy			
	Source	Energy (GJ/yr)	Cost ($/yr)	Source	Energy (GJ/yr)	Cost ($/yr)
Electric	Natural Gas	2,944.42	$ 46,816.30	Natural Gas	-	$ -
Heating	Natural Gas	39,323.94	$ 127,016.31	Natural Gas	39,324.15	$ 127,017.01
	Total Energy Costs ($/yr)		$ 173,832.62	Total Energy Costs ($/yr)		$ 127,017.01
			Total Operating Expense			
			$ (2,165,688.23)			$ (2,211,931.29)

Figure A- 29: Operating Expense Summary (Tool Output)

MODEL OUTPUTS		
Process Summary		
Process	Alternative AA Route	pH Swing
Batch Time (min)	150.00	1,170.00
Batches Required (batch/yr)	3,504.00	449.23
Batch Sequestration Rate (tCO2/batch)	28.54	222.60
CO2 Sequestration		
Sequestered as Carbonate (tCO2/yr)	100,000.00	100,000.00
Emitted from Process (tCO2/yr)	28,169.73	-
Emitted from Transport (tCO2/yr)	-	-
Net Sequestered (tCO2/yr)	**71,830.27**	**100,000.00**
Process Economics		
Total Transport Expense ($/yr)	-	$ -
Total Capital Expense ($)	$ 8,254,244.99	$ 871,122,457.76
Total Operating Expense ($/yr)	$ 9,318,511.49	$ 355,076.71
Project Net Present Value	**$ (47,899,789.18)**	**$ (849,693,919.63)**

Figure A- 30: Tool Outputs Comparing two *ex situ* indirect carbon mineralization processes, with a target of 100 $ktCO_2$ sequestered.